THE UNIVERSITY
of EDINBURGH

THE ASSESSMENT OF MUSCLE WASTING

Alisdair John MacDonald

M.D. Thesis

University of Edinburgh

2015

Supervisors

Prof K.C.H. Fearon, Prof T. Preston

Dedication

To my wife Hannah, son Oliver, my parents, and the memory of Donald and Cathy Kerr

Abstract

Cachexia occurs commonly and is a significant cause of morbidity and up to 20% mortality in patients with cancer. Loss of muscle mass occurs as part of the cachexia wasting process and low muscle mass is a key element of the most recent consensus cachexia definition. Measuring muscle mass and changes in skeletal muscle is important to phenotype cachectic individuals and to monitor response to anti-cachectic treatments. This thesis investigates minimally invasive or burdensome methods of measuring muscle mass and muscle protein kinetics for use in a clinical or research setting.

Quantification of muscle area on routine diagnostic cross-sectional imaging offers a novel and relatively non-invasive method of assessing both regional (and by extrapolation) whole body muscle mass. The need for such a direct measurement of muscle mass was demonstrated by showing that simple anthropometric formulae are unable to predict muscularity accurately (within 25%) when compared with estimates derived from patients diagnostic CT scans.

It may be that qualitative changes in muscle may be more sensitive indices of the wasting process rather than qualitative change. Myosteatosis (infiltration of muscle by fat) is known to occur in both cachexia and age related sarcopenia and can be quantified using the Hounsfield spectrum observed on routine diagnostic CT scans. However, not all patients undergo routine CT scanning and there is a need for a biomarker derived from urine or blood. Consequently, cross sectional imaging was used to phenotype patients in a proteomic analysis of urine with the aim of identifying protein or peptide biomarkers associated with myosteatosis in cancer cachexia. A biomarker model for myosteatosis was developed with good sensitivity (97%) but poor specificity (71%). Many of the potential protein / peptide markers identified had poor associations with known mechanisms of muscle wasting and further study of the identified peptides in an extended cohort would help determine the

validity of the present findings. However, two proteins with potential roles in muscle repair or neuromuscular function (Agarin and Cathepsin C) were identified and these may warrant targeted investigation with evaluation against sequential measures of muscle mass to determine their value in defining muscle loss over time.

As different regional measures of muscularity are available, trunk (L3 CT) and limb muscle (quadriceps MRI) cross sectional measurements were compared with functional assessments to determine the optimal site for measurement. Neither measure proved superior to the other but appeared to reflect different aspects of function. Quadriceps muscle area correlated with quadriceps strength and power whilst truncal muscle area correlated more with complex movements such as the timed-up-and-go test.

Changes in regional muscle area in patients with upper gastrointestinal cancer were assessed by upper and lower limb MRI before and after surgery and by L3 CT cross sectional area before and after neo-adjuvant chemotherapy. No change in limb muscularity was seen at 220 days post operatively compared with pre-op measurements. During neo-adjuvant chemotherapy a significant loss of truncal muscle occurred in the absence of significant weight loss suggesting that sequential cross sectional imaging is capable of detecting changes in body composition that may not be apparent clinically.

Whilst sequential scans may document changes in muscularity, they do not describe the underlying levels of muscle synthesis or degradation that may regulate muscle volume. The final section of this thesis describes the development of a novel tracer method to measure skeletal muscle synthesis and its application in a study of patients with cancer and healthy volunteers. This novel method was able to measure skeletal muscle fractional synthetic rate (FSR) over a longer time-period than previous methods (weeks rather than hours) and reduced the burden on the patient by the use of a single oral tracer dose and single muscle biopsy. Comparison of synthesis rates in quadriceps and rectus abdominis showed higher rates in quadriceps, 0.067% per hour vs 0.058% per hour respectively. Despite a net loss of

muscle as measured by serial CT scans, skeletal muscle FSR appeared to be marginally increased in weight losing patients with cancer compared with weight stable patients and healthy controls. When FSR was combined with measures of muscle mass it was demonstrated that only small differences between synthesis and degradation are required to see the levels of muscle wasting seen in patients with cancer.

In summary, routine cross sectional imaging provides a useful and unique measure of muscularity that is associated with function in patients with cancer Sequential scans can provide additional information about changes in body composition even in the absence of weight loss. There are significant regional variations in both muscle wasting and skeletal muscle fractional synthetic rate. The combination of sequential estimates of muscle mass from diagnostic CT scans along with estimates of FSR allow assessment of the contribution of altered synthesis and degradation to muscle loss. In patients with upper GI cancer it would appear that increased degradation may be more important that altered synthesis. The relative change in either process to account for absolute loss of muscle mass is small. Such findings have implications for the targeted therapy of muscle wasting in cancer patients.

Published and presented work

Publications

Chapter 1

The advantages and limitations of cross sectional body composition analysis

A. J. MacDonald, C. A. Greig, V Baracos

Current Opinion in Supportive & Palliative Care 2011 Dec;5(4):342-9.

Chapter 9

A novel oral tracer procedure for measurement of habitual myofibrillar protein synthesis

A. J. MacDonald, A. C. Small, C. A. Greig, H. Husi, J. A. Ross, N. A. Stephens,

K. C. H. Fearon, T. Preston

Rapid Communications in Mass Spectrometry. 2013, 27, 1769–1777

Chapter 10

Habitual myofibrillar protein synthesis is normal in patients with upper GI cancer cachexia

A.J. MacDonald, N. Johns, N.A. Stephens, C.A. Greig, J.A. Ross, A.C Small, H. Husi,

K.C.H. Fearon, T. Preston

Clinical Cancer Research, Nov 2014, PMID 25370466

Published abstracts

Chapter 3

Can baseline muscle mass be predicted in weight stable patients with cancer?

A. J. Macdonald, N. Stephens, C. Greig, H. Husi, K. C. Fearon, T. Preston

Clinical Nutrition Supplements 2011 Volume 6, Issue 1 , Pages 41-42,

Chapter 7

Upper and lower limb muscle mass in patients undergoing surgery for upper GI cancer

A. J. Macdonald, M. Esposito, C. Gray, N. A. Stephens, C. Greig, K. C. Fearon

Clinical Nutrition Supplements (2011) Volume: 6, Issue: 1, Pages: 42

Chapter 8

Loss of fat free mass occurs during neo-adjuvant chemotherapy for upper GI cancer

A. J. Macdonald, N. Stephens, M. Esposito, J. Ross, L. Wall, C. Greig, V. Baracos, K. C. Fearon

Clinical Nutrition Supplements 2011 Volume 6, Issue 1 , Page 42,

Presentations

Chapter 3

Can baseline muscle mass be predicted in weight stable patients with cancer?

A. J. Macdonald, N. Stephens, C. Greig, H. Husi, K. C. Fearon, T. Preston

Poster Presentation 33rd ESPEN Congress

Gothenburg Sept 2011

Chapter 6

CT derived measures of muscle mass are associated with functional ability but not strength and power in patients with upper GI cancer.

A. J. MacDonald, N. Stephens, C. A. Greig, C. Gray, J. Ross, K.C.H. Fearon

Poster presentation 35th ESPEN Congress

Leipzig Aug 2013

Chapter 7

Upper and lower limb muscle mass in patients undergoing surgery for upper GI cancer

A. J. Macdonald, M. Esposito, C. Gray, N. A. Stephens, C. Greig, K. C. Fearon

Poster Presentation 33rd ESPEN Congress

Gothenburg Sept 2011

Chapter 8

Loss of fat free mass occurs during neo-adjuvant chemotherapy for upper GI cancer

A. J. Macdonald, N. Stephens, M. Esposito, J. Ross, L. Wall, C. Greig, V. Baracos, K. C. Fearon

Poster Presentation 33rd ESPEN Congress

Gothenburg Sept 2011

Chapter 9

A Novel Oral Tracer Technique for Measurement of Habitual Myofibrillar Protein Synthetic Rate

A J MacDonald, AC Small, CA Grieg, H Husi, JA Ross, NA Stevens, KCH Fearon, T Preston

Oral Presentation Joint European Stable Isotope Users group Meeting

Leipzig Sept 2012

Habitual skeletal muscle protein fractional synthetic rate in healthy individuals as determined by a novel oral tracer technique

Alisdair J. MacDonald , Carolyn A. Greig, Holger Husi, Nathan A. Stephens, Jim Ross, Alexandra C. Small, Kenneth C.H. Fearon, Tom Preston.

Poster Presentation 6th Cachexia conference

Milan Dec 2011

Chapter 10

Regional differences in skeletal muscle protein fractional synthetic rate in patients with upper gastrointestinal cancer

A.J. MacDonald, N. Johns, C. A. Greig, H. Husi, J. Ross, K. C. H. Fearon, T. Preston

Oral presentation 35th ESPEN Congress

Leipzig Aug 2013

Habitual skeletal muscle fractional synthetic rate in healthy controls and patients with upper gastrointestinal cancer.

A.J. MacDonald, N. Johns, C. A. Greig, H. Husi, J. Ross, K. C. H. Fearon, T. Preston

ESPEN Fellowship Oral presentation 35th ESPEN Congress

Leipzig Aug 2013

Contents

Figures

Tables

Declaration

The thesis composition herein is my own. Where I have been a member of a research group, I have made a substantial contribution to the work, and this contribution has been asserted clearly in the text. Contributions made by others to the work are stated below and acknowledged in the text. This thesis has not been submitted for any other degree, postgraduate diploma or professional qualification.

Alisdair J MacDonald

Contributions by others

Recruitment of patients and their clinical and functional assessment was performed with the assistance of Dr Carolyn Greig, Mr Nathan Stephens, and Mr Neil Johns.

Surface-enhanced laser desorption/ionization time-of-flight mass spectrometry analysis and subsequent statistical modelling was performed by Dr Holger Husi

Gas Chromatography–Pyrolysis–Isotope Ratio Mass Spectrometry analysis and subsequent calculation of deuterium enrichments was performed by Sandra Small and Prof Tom Preston

Acknowledgements

The work contained in this thesis would not have been possible without the patients and volunteers who gave their time and tissues in the participation of these studies and I am very grateful for their contribution. I am also grateful for the vision and perseverance of my supervisors Profs Fearon and Preston and for the assistance advice and teaching provided by members of the laboratory group Prof Jim Ross, Dr Holger Husi, Dr Iain Gallagher, Kathryn Sangster and Jim Black. I wish to thank Dr Carolyn Greig, Mr Nathan Stephens, Mr Neil Johns and the Department of Surgery at the Royal Infirmary of Edinburgh for their practical advice and contribution. Use of the imaging techniques was made possible by the support and welcome of Prof Vickie Baracos and her team in Edmonton, Canada and also local help by Dr Calum Gray, Dr Tom McGillivray, Janet Christie and PACS managers throughout Scotland.

Abbreviations

ACL	Anterior Cruciate Ligament
Akt	Protein Kinase B
ATFSM	Adipose Tissue Free Skeletal Muscle
ATP	Adenosine Triphosphate
BCM	Body Cell Mass
BIA	Bio-electrical Impedance Analysis
BMI	Body Mass Index
BPS	Biomarker Pattern Software
BSA	Bovine Serum Albumin
Ca2+	Calcuim
CaMKIIβ	Calcium/calmodulin-dependent protein kinase type II Beta
CD	Critical Difference
CI	Confidence Interval
CRUK	Cancer Research UK
CSA	Cross Sectional Area
CT	Computed Tomography
CV	Coefficient of Variation
DNA	Deoxyribonucleic acid
DTT	Dithiothreitol
DXA	Dual X-ray Absorptiometry
ECF	Extracellular Fluids
ECS	Extracellular Solids
EPA	Eicosapentaenoic Acid
FBR	Fractional Breakdown Rate
FFM	Fat Free Mass
FG	Fast-twitch Glycolytic (fibres)
FM	Fat Mass
FOG	Fast Oxidative Glycolytic (fibres)
FOXO	Forkhead box O class transcription factor
FSR	Fractional Synthetic Rate
GC/MS	Gas Chromatography / Mass Spectrometry
GC-P-IRMS	Gas Chromatography-Pyrolysis-Isotope Ratio Mass Spectrometry

GH	Growth Hormone
GI	Gastro-Intestinal
GSK3β	Glycogen synthase kinase 3 beta
HGD	Hand Grip Dynamometry
HR	Hazard Ratio
HU	Hounsfield Units
IAT	Interstitial Adipose Tissue
ICC	Intra-Class Correlation Coefficient
IGF-1	Insulin-like growth factor 1
IKES	Isometric Knee Extensor Strength
IL-1	Interleukin -1
IL-6	Interleukin -2
IMAT	Intermuscular Adipose Tissue
ISAK	International Standards of Anthropometric Assessment
kDa	KiloDaltons
LEP	Leg Extensor Power
LC-MS/MS	Liquid chromatography-tandem mass spectrometry
MAFbx	muscle atrophy F-box or atrogin-1
MEK	Mitogen-activated protein/extracellular signal–regulated kinase kinase
MHC	Myosin Heavy Chain
MIC-1	Macrophage Inhibitory Cytokine-1
MPB	Muscle Protein Breakdown
MPS	Muscle Protein Synthesis
MRI	Magnetic Resonance Imaging
mTOR	mammalian Target Of Rapamycin
MuRF1	Muscle RING Finger-1
NAA	Neutron Activation Analysis
OGJ	Oesophago-Gastric-Junction
p70S6K	p70S6 kinase
PACS	Picture Archiving and Communications System
PAGE	Polyacrylamide Gel Electrophoresis
PCDMS	ProteinChip Data Manager Software
PG-SGA	Patient-Generated Subjective Global Assessment
PI	Prediction Interval

PRT	Progressive Resistance Training
RIS	Radiology Information System
RSMI	Relative Skeletal Mass Index
SAT	Subcutaneous Adipose Tissue
SD	Standard Deviation
SEE	Standard Error of the Estimate
SELDI-TOF-MS	Surface-Enhanced Laser Desorption/Ionization Time-Of-Flight Mass Spectrometry
SO	Slow Oxidative (fibres)
STS	Sit to Stand
TAT	Total Adipose Tissue
TBK	Total Body Potassium
TBW	Total Body Water
TIE1	Tyrosine-protein kinase receptor
TNFα	Tumour necrosis factor α
TUG	Timed Up and Go
UPP	Ubiquitin Proteosome Pathway
USS	Ultrasound Scan
UWW	Underwater Weighing
VAT	Visceral Adipose Tissue
WHO	World Health Organisation
WTCRF	Wellcome Trust Clinical Research Facility
ZAG	Zinc-α2-Glycoprotein

1 Introduction

1.1 Structure and function of muscle.

The ability to make coordinated movements is one defining characteristic of all animals and the common means by which this is achieved is through contraction and relaxation of muscle tissue. The human body, in health is approximately 40% muscle tissue composed of around 600 individual muscles and accounts for 30-45% of whole body protein turnover.

1.1.1 Muscle Ultrastructure

All muscle types in animals and humans have a common basic structure and action and the force generating mechanism is the same throughout. The core elements of this force generating mechanism are the actin and myosin protein filaments making up the thick and thin filaments of muscle. Myosin is the larger of the two and forms the thick filaments. Although myosin is ubiquitous in muscle cells it is not exclusive to them and multiple myosin isoforms exist performing functions such as vesicle transport in non-muscle cells. The Myosin II isoform is the force generating isoform found in muscle, it consists of two large (~200kDa) polypeptide heavy chains and 4 small (~20kDa) polypeptide light chains. Its structure forms a head and tail region with the two heavy chains intertwined to form the tail region and two light chains situated on each of the two heads at one end. Many myosin molecules are bound together to form the thick filament and are orientated with the tail toward the centre of the filament and the heads sticking out toward the ends.

Actin is a 42kDa globular protein found in all eukaryotic cells and a major component of the cytoskeleton. In muscle it forms intertwined helical chains and along with the proteins troponin and tropomyosin make up the thin filaments which are approximately half the diameter of the thick filaments. In skeletal muscle the thick and thin filaments are arranged into a characteristic ordered structure in cylindrical bundles called myofibrils which in turn

are grouped together into muscle fibres or cells. Muscle contractions occur by the interaction of the protruding myosin heads of the thick filaments with the actin of the thin filaments.

The action of muscle movement occurs by the shortening of the muscle through shortening of each of the muscle fibres and their myofibril subunits. These myofibrils are capable of shortening due to their regular structure and the action of myosin on actin. The characteristic structure of the myofibril in skeletal muscle is made up of repeating patterns of sarcomeres. The centre of the sarcomere may be considered the M line, this is a protein disk to which multiple parallel thick filaments are attached. This thick filament dense region is known as the A band. Inter-digitating with the thick filaments are the thin filaments overlapping a portion of the thick filaments, the portion where there is no overlap is known as the I band. The thin filaments end at either end of the sarcomere where they attach to a protein disc known as the Z line. In addition the thick filaments are attached to the Z line by the large elastic protein, Titin (1). Figure 1

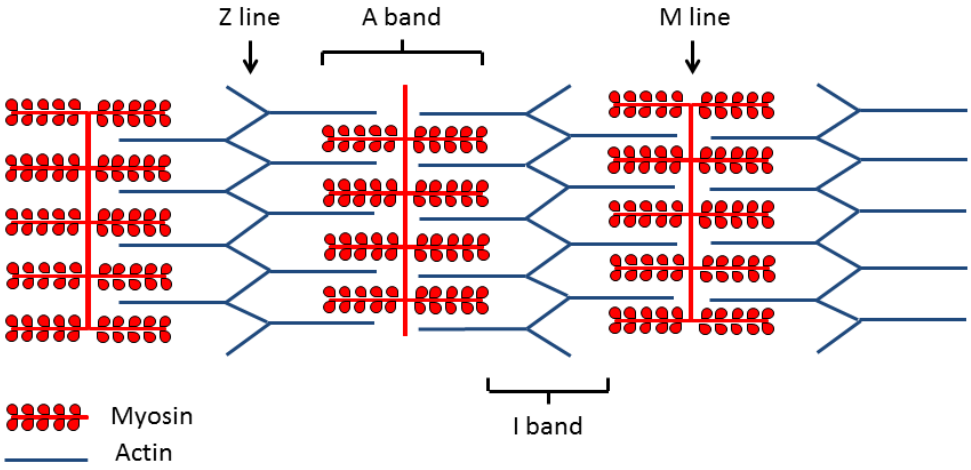

Figure 1 - Skeletal muscle ultrastructure; skeletal muscle consists of inter-digitating actin and myosin fibres

1.1.2 Skeletal muscle force generation

When a muscle shortens, these overlapping thick and thin fibres of the sarcomere move past each other in a movement known as the sliding filament mechanism. This is achieved by the formation of a cross bridge between thick and thin filament by the myosin head binding to actin, the movement of the bound cross bridge and the subsequent dissociation of the cross bridge allowing the process to be repeated. The energy for this process is provided by ATP hydrolysis at the ATPase situated on the head of the myosin heavy chain. The process is regulated by tropomyosin which blocks the myosin binding sites on actin. Binding is allowed by troponin moving the tropomyosin to expose the binding sites and occurs by the action of calcium (Ca^{2+}) on troponin.

1.1.3 The Myofibre

Skeletal muscle cells are arranged as multinuclear myofibres. The myofibre contains many myofibrils within the cytosol, the myofibrils are surrounded by sarcoplasmic reticulum which acts to release Ca^{2+} in response to the muscle action potential in the excitation – contraction coupling process. The whole myofibre is bounded by the cell membrane or sarcolemma which as well as the myofibrils and sarcoplasmic reticulum also contains the nuclei and mitochondria. The sarcolemma has numerous invaginations known as T-tubules which traverse the fibre and transmit the action potential to the sarcoplasmic reticulum to stimulate Ca^{2+} release into the cytosol. As they are single multinucleated cells these skeletal muscle myofibres are extremely large with diameters of 10 to 100μm and lengths of up to 20cm.

1.1.4 Muscle growth and repair

Skeletal Muscle is a highly adaptable tissue undergoing hypertrophy (or hyperplasia) or wasting in response to a range of stimuli. Skeletal muscle differentiation is complete around the time of birth, during this process muscle fibres are formed by the fusion of undifferentiated mononuclear fibroblasts into the multinuclear myofibres. These differentiated myofibres are unable to divide in order to grow new muscle tissue or to repair damage. Instead muscle tissue contains a population of undifferentiated stem cells called satellite cells. The satellite cells are capable of responding to the call for muscle synthesis in two ways. In response to a stimulus (such as specific hormones, strain or injury) the normally quiescent satellite cells undergo mitotic division producing daughter cells that differentiate into myoblasts. The myoblasts will then fuse together to form new myofibres (hyperplasia) or more commonly will fuse with existing myofibres to enlarge or repair them (hypertrophy). As well as being a mechanism for repairing damage, this process occurs as a result of a variety of normal physiological stimuli to muscle growth. Conversely, the plasticity of muscle also means that muscle breakdown will occur in response to opposing (or absent) stimuli. Active muscle atrophy (rather than simply the absence of synthesis) may occur due to an increase in protein degradation.

1.1.5 Role of muscle in whole body metabolism

In addition to its primary role in movement, muscle has a number of additional metabolic functions (2). One of the most important of these is its action as an amino acid store. Muscle is able to be broken down providing glutamine and branched chain amino acids as an energy source (particularly during fasting) and for protein synthetic processes such as the acute phase response to injury. Muscle has a role in thermoregulation, insulin resistance and glucose metabolism. It may also act as a protein and glycogen reserve that can be utilised in

disease or in times of physiological stress and can be an important energy source during starvation (3-5).

1.2 Muscle – adaptation to function.

Whilst the basic elements of muscle are the same throughout, different types of muscle have differences adapting them for specific functions. These differences are most marked when cardiac or smooth muscle is compared with skeletal muscle but variation is also seen in skeletal muscle adapted to specific functions. One key feature of muscle (in particular skeletal muscle) is its plasticity, allowing for an increase and decrease in muscle size as well as changes in fibre type composition that occur as a result of a variety of physiological and pathological influences.

1.2.1 Cardiac Muscle

Cardiac muscle is striated muscle made up of thick and thin filaments in an ordered structure so it is similar to skeletal muscle in its basic elements. However, in contrast to skeletal muscle, cardiac muscle cells are usually mononuclear individual cells linked by intercalated discs and may be branched instead of linear and longitudinal. Each cardiac myocyte is approximately 15μm diameter by 100μm length and is electrically coupled to its neighbouring cells by gap junctions in the intercalated discs. This coupling allows the myocardium to behave as a functional syncytium so the whole myocardium contracts in a coordinated manner in response to a single depolarisation originating at the sino-atrial node. Cardiac muscle may undergo hypertrophy or atrophy but unlike skeletal muscle it has no satellite cells so the potential for regeneration after injury is limited.

1.2.2 Smooth muscle

Smooth muscle is unlike cardiac or skeletal muscle as it lacks the highly ordered arrangement of thick and thin filaments that are characteristic of striated muscle. The contractile elements are made up of actin and myosin arranged into a loose lattice within mononuclear spindle shaped cells. The wide range of functions that smooth muscle performs in different tissues in the body such as gastrointestinal tract peristalsis or maintaining arterial wall tension mean that there are a several configurations of different smooth muscle types.

1.2.3 Skeletal muscle

Skeletal muscle is required to perform a variety of different functions, some muscles such as postural muscles may be required to maintain a constant tone over long periods whereas others may be required to perform rapid brief contractions. To achieve this, different muscles have adaptations in structure dependant on their function. Three basic fibre types exist in skeletal muscle, two fast twitch and one slow twitch, and the proportion of each type determines how a specific muscle will function. Muscle fibres are commonly classified by the myosin ATPase staining classification, which is related to ATPase hydrolysis rates (although the histochemical staining technique is based on pH sensitivity) Type 1 fibres are slow fibres, these muscle fibres contract and relax relatively slowly and the muscle fibres themselves are relatively thin. They are rich in mitochondria and myoglobin, generate ATP mainly by oxidative metabolism of fats and have a rich capillary bed. This makes this fibre type resistant to fatigue. These may also be classified biochemically as slow oxidative (SO) fibres. Type 2 fibres are the fast fibre type and contract and relax rapidly. Two types exist: 2A and 2B. Type 2A fibres generally rely on oxidative metabolism for their energy requirements and utilise glucose or fats as their source of energy, these may be classified biochemically as fast oxidative glycolytic (FOG) fibres. These are relatively thin fibres and are rich in mitochondria and myoglobin so are relatively resistant to fatigue. Type 2B fibres

are more closely related to the biochemical fast-twitch glycolytic (FG) type, these predominantly rely on anaerobic/glycolytic metabolism. They contain few mitochondria and little myoglobin, they are recruited for high intensity muscular activity for short periods and are easily fatigued. Additional human muscle fibres types other than these three classic types also exist by the ATPase staining classification and additional classifications of 1C, 2C, 2AC, 2AB may be used and have intermediate characteristics in a continuum with the three main types. Muscle fibres may also be classified by myosin heavy chain (MHC) identification. Three myosin heavy chain isoforms exist in humans, MHCI, MHCIIa, MHCIIx/d. These correspond to the ATPase classification I, IIa, IIb respectively. MHCIIb does not exist in human muscle although for historical reasons MHCIIx/d and MHCIIb may sometimes be seen with reference to human muscle in the literature. Although an individual muscle may be made up of many different fibre types, each motor unit is predominantly of one type. The plasticity of muscle allows for adaptation of individual muscles through training. Skeletal muscles ability to adapt to specific functions occurs both through an increase in the size of the muscle and also through alteration in the fibre types that the muscle is made up of.

1.3 Physiological and pathological influences on muscle – determinants of synthesis and degradation

Muscle mass changes in an individual as a result of various physiological influences to muscle synthesis and degradation. These influences may occur gradually over decades of life, during development to adulthood or in old age or may be transitory such as the effects of exercise or nutrition. Long term changes are seen in muscle mass as part of normal growth up until around the age of 30 years with muscle mass making up a greater proportion of total body mass with increasing age. After the age of around 30 to 40 years a progressive loss is seen in muscle strength and muscle mass at a rate of approximately 6% per decade even in fit and active individuals (6). Individuals will reach different a different peak muscle mass and will experience different rates of muscle loss or gain at different points in life and in response to particular stimuli such as disease, disuse or training. Net accretion of muscle mass is dependent on the balance of synthesis and degradation both of which fluctuate dependant on different influences, primarily physical activity and diet. These effects occur over much shorter periods of minutes or hours and form a dynamic process. Figure 2

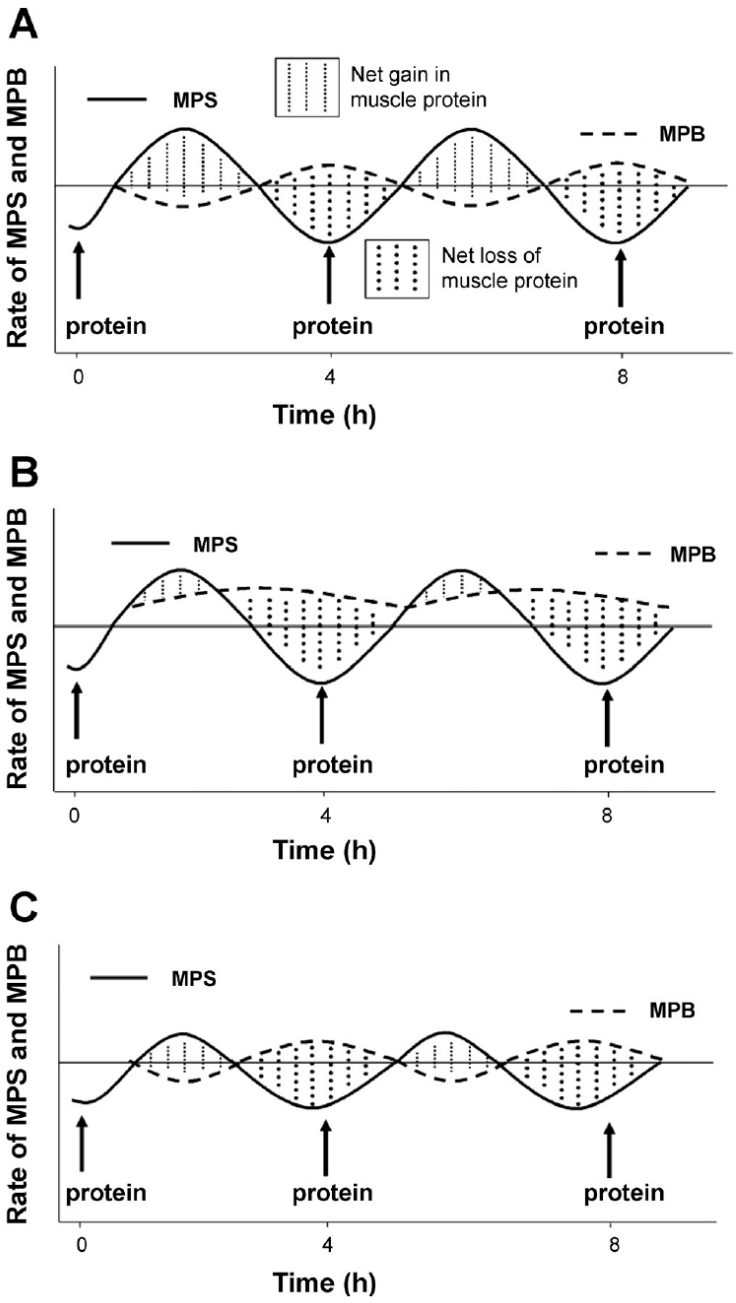

Figure 2 - Net muscle balance is dependent on fluctuating muscle protein synthesis (MPS) and muscle protein breakdown (MPB). A shows a steady state with normal diurnal variation in synthesis and breakdown. B shows a situation of increased breakdown resulting in a net loss of muscle. C shows a situation with normal diurnal variation in breakdown but reduced synthesis leading to net loss of muscle- from Philips et al (7)

1.3.1 Signalling pathways in muscle atrophy and hypertrophy

A number of signalling pathways and transcription factors have been implicated in the atrophy and hypertrophy of skeletal muscle. These catabolic and anabolic pathways may be separate but are closely associated so that a stimulus which activates an anabolic pathway may also inhibit catabolism (8, 9). Figure 3

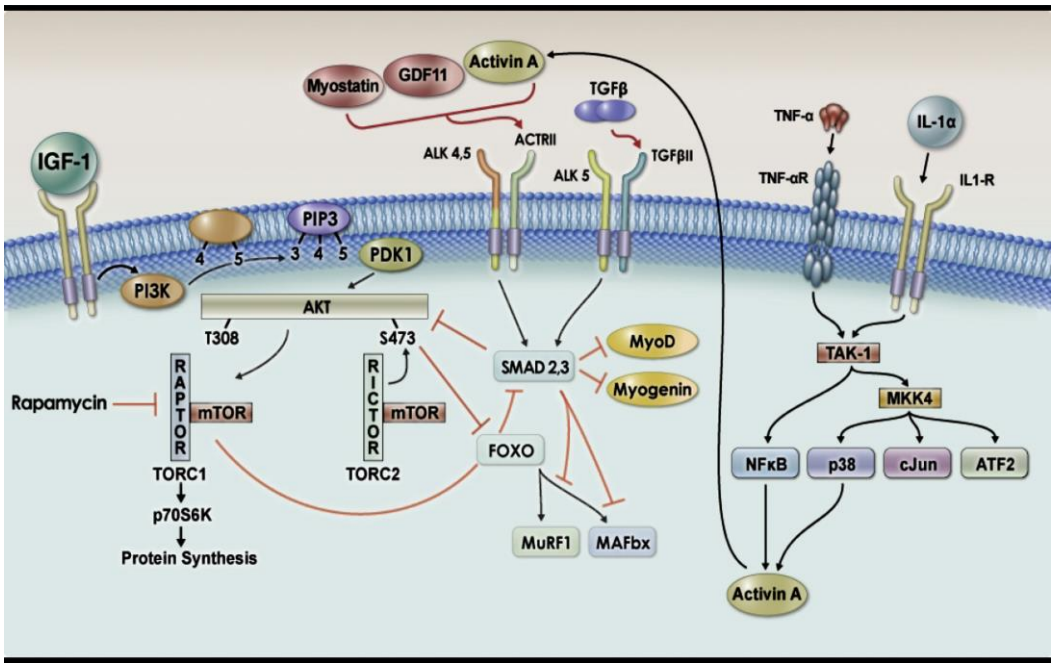

Figure 3 - Key pathways in muscle protein synthesis and breakdown, from Fearon 2012 (10). Activation of the Akt pathway promotes muscle anabolism and inhibits catabolism via inhibition of FOXO and the E3 ubiquitin ligases MuRF1 and MAFbx. Degredative pathways act under the influence of mediators including TNFα, IL-6, IL-1, Myostatin and Activin A.

1.3.1.1 Anabolic pathways

The primary anabolic pathway in skeletal muscle is the PI3K/Akt pathway. Activation of this pathway induces muscle hypertrophy by muscle protein synthesis resulting in an increase in muscle fibre diameter (11) via a variety of downstream mediators including mTOR, p70S6K and GSK3β. In addition, activation of the PI3K/Akt pathway inhibits the effects myostatin which normally acts to inhibit myoblast differentiation (12). The PI3K/Akt

pathway also interacts with muscle degradation pathways via FOXO by blocking the transcriptional up-regulation of the E3 ubiquitin ligases MuRF1 and MAFbx (13).

1.3.1.2 Catabolic pathways

The key catabolic pathways for skeletal muscle include the $Ca2^{+}$ dependant, Caspase dependant, autophagy-lysosomal and the ubiquitin proteasome pathways. The autophagy and the ubiquitin-proteasome pathway are probably the most significant (10).

1.3.1.2.1 Ubiquitin-proteasome

In the ubiquitin proteasome pathway, muscle atrophy occurs via proteolysis by the proteasome. Target proteins are identified for degradation by ubiquitination which in turn is under control of the ubiquitin E3 ligases MuRF1 and MAFbx (14). This pathway is activated by inflammatory cytokines such as TNFα and IL-6. In addition, the degradative pathways may be upregulated by other factors such as myostatin and Activin A, both of which are TGF-β family members and act to suppress muscle synthetic pathways by inhibiting Akt and may promote ubiquitin-proteasome mediated degradation (15-17).

1.3.1.2.2 Autophagy-lysosomal

Mediators such as TNFα which act on the ubiquitin-proteasome pathway may also result in muscle loss via lysosomal autophagic degradation (18). Whilst the UPP acts to rapidly eliminate single proteins or small aggregates, the autophagic system is able to degrade entire organelles (19). Autophagy has been shown to contribute to skeletal muscle degradation in starvation (20), denervation (21) and murine models of cancer cachexia (18). Autophagy also appears to play an essential role in normal muscle homeostasis by the removal of altered organelles, the elimination of protein aggregates, and the disposal of toxic products that may lead to cell death. Normal skeletal muscle remodelling may be dependent on a carefully regulated autophagy flux as autophagy appears to be essential for maintenance of muscle

mass (22) and an increase in initiation and resolution of autophagy and increased expression of autophagy proteins seen after exercise in murine models (23)

1.3.1.2.3 $Ca2^+$ dependant

The $Ca2^+$ dependant system consists of proteases known as calpains, these exert limited proteolytic effects on specific intracellular substrates resulting in deactivation or degradation by other pathways (24).

1.3.1.2.4 Caspases

The caspases are a group of enzymes responsible for the initiation of apoptosis. These proteases may be important in the initiation of myofibrillar degradation (8).

1.3.2 Physical activity

Resistance exercise stimulates an increase in muscle protein synthesis (25). This may occur via induction of muscle production of IGF-1 which activates the IGF1 PI3K/Akt pathway resulting in muscle hypertrophy (26) but may also involve PI3K/Akt independent pathways whereby the mechanical activation of phospholipase D1 and the production of phospatidic acid directly activates mTOR (27). In humans, increased muscle protein synthesis does not occur during resistance exercise (28) but rises after 2-3 hours and may remain elevated for 48 hours after exercise (29-31). This effect can be demonstrated with leucine tracer muscle turnover studies showing an increase in muscle protein synthesis, skeletal muscle FSR may be increased by 40% in response to treadmill exercise (32). This phenomenon can also be demonstrated by a net increase in muscle volume over time as measured by cross sectional imaging, three months of thrice weekly resistance training may result in an increase of 3.1% in thigh extensor muscle volume (33). Aerobic exercise also stimulates muscle protein synthesis as demonstrated by use of a primed constant infusion method (34). Alteration in gene expression following aerobic exercise occurs with an observed decrease in myostatin,

and an increase in proteolytic MuRF-1, Calpain-1 and Calpain-2 (35). The increase in synthesis is part of an increase in muscle turnover as aerobic exercise also induces muscle protein breakdown that balances muscle synthesis (36). This exercise-induced muscle breakdown appears to be an important part of skeletal muscle remodelling. Inhibition of autophagy by deletion of the autophagy gene Atg7 in mice results in muscle atrophy and reduction in force production. This atrophy may result from the accumulation of abnormal mitochondria and subsequent increase in oxidative stress and induction of catabolic pathways (22).

1.3.3 Diet.

Without adequate nutrition net synthesis of muscle is unsustainable and in a severely depleted nutritional state it is inevitable that muscle mass will be lost. It is estimated that a mean protein requirement of 0.89g protein/kg/day is required to maintain a steady state (37). The effect of nutrition on muscle is dependent on overall energy balance, protein balance and essential amino acid availability and is also influenced by the immediate effects of specific nutrients on protein synthesis in the post-prandial phase. Ingestion of carbohydrates may stimulate a net accretion of muscle mass (32) however this effect is relatively minor when compared with the effect of amino acid ingestion (38) where the ingestion of 3g of essential amino acids had an equivalent effect to ingestion of 35g of carbohydrate (39). It appears that the availability of *essential* amino acids are primarily responsible for stimulation of muscle protein synthesis (40), leucine in particular has been associated with an increase in muscle protein synthesis in animal models (41) however this has not been demonstrated consistently in humans (42). In contrast to the effects of exercise, dietary amino acids have a much shorter effect on muscle protein synthesis lasting 1-2 hours after ingestion (43).

The effects of diet and physical activity on muscle synthesis are closely interdependent. Exercise appears to be less effective in achieving a net accretion of muscle in the fasted state.

Oral amino acid supplements may increase muscle protein synthesis four fold but have a transient effect (44) while a combination of amino acids and resistance exercise achieves maximal effect (32).

1.3.4 Ageing

Skeletal muscle is lost after the age of 50 years at a rate of 1-2% per year even in healthy physically active individuals (45) and the resulting relative low muscle mass is known as sarcopenia. The causes and mechanisms of this loss are not clear but a number of factors are proposed. The triggers for development of sarcopenia may be due to age-related hormonal changes such as a decrease in GH and IGF-1 seen in aging (37, 46), reduction in testosterone (47) or impaired insulin resistance. It is also proposed that muscle protein degradation may occur in response to pro-inflammatory cytokines such as TNF-α, IL-1β and IL-6 which may be increased in the elderly and may be detected in elevated plasma levels (37). In addition, behavioural factors such as poor diet (48) and reduced physical activity may contribute (49).

The underlying mechanism resulting in muscle loss in the elderly (sarcopenia) may involve increased degradation via apoptosis of myocytes. As skeletal muscle is multinucleated this apoptosis may occur via myonuclear apoptosis affecting an individual myonuclei and the surrounding portion of sarcoplasm or complete cell death. This apoptosis may occur via a caspase dependant mechanism where a caspase cascade activates effector caspases to carry out proteolysis, or through a caspase independent mechanism via mitochondrial release of mediators causing DNA-fragmentation (50).

Young and old individuals appear to have similar resting rates of muscle protein synthesis and degradation (51). So as an alternative to, or in addition to increased degradation, the possible effect of a blunted response to muscle synthesis stimuli has been investigated. As in young healthy individuals, aging muscle responds to synthetic stimuli such as feeding and exercise. Dietary protein or amino acids stimulate muscle protein synthesis in young and old

in a dose dependant manner up to a plateau reached at 10 grams of oral essential amino acid supplement. At the maximum dose no difference in increased muscle protein synthesis is seen between young and old, however smaller boluses (7g) were associated with a reduced response in older subjects compared with younger subjects (52). Regular training helps maintain muscle function and morphology although there is selective relative atrophy of type II fibres (53). Resistance exercise also simulates muscle protein synthesis in older subjects, this effect may be diminished in older subjects compared with younger or it may be unchanged (52). Several studies looking at combined protein or amino acid ingestion with resistance exercise have shown that there are no age related differences in anabolic response (54-56).

1.3.5 Cancer

Many types of cancer, particularly in the advanced stages are associated with cancer cachexia. Cachexia is a wasting condition that results in weight loss with loss of muscle mass making up an important component of the loss (57-59). In patients with non-small cell lung and pancreatic cancer it has been observed that 47% (60) and 56% (61) of patients had a depleted muscle mass that met the definition of sarcopenia and that this may occur even while the patient remains obese (61). Stable isotope tracer and 3-methylhistidine studies have shown that this loss of muscle mass may be due to a decrease in skeletal muscle synthesis (62, 63), whilst transcriptome analysis of muscle biopsies demonstrates suppression of both anabolic and catabolic pathways in patients with cancer (64). As cachexia is a complex syndrome the exact mechanism of muscle wasting in cancer is uncertain, however, it is believed to be driven primarily by systemic inflammation (65). One aspect of systemic inflammation is the acute phase response. This acute phase response places a high nutritional demand on the patient. Due to the different amino acid composition of muscle and acute phase response proteins (synthesised in the liver), there is an imbalance in essential amino

acids and it is estimated that 2.6g of muscle must be catabolised to produce 1g of fibrinogen (66) using muscle as an endogenous store of accessible amino acids. Pro-inflammatory cytokines such as IL-6, IL-1 and TNF-α appear to exert an effect directly on skeletal muscle acting to cause a net loss of skeletal muscle protein. In addition these cytokines cause anorexia further exacerbating the nutritional deficit in cancer cachexia. Although low grade inflammation has been implicated in sarcopenia of old age, it appears that this exuberant inflammatory response sets muscle loss in cancer apart from that seen in aging and starvation (67). It should be recognised, however, that some cancer patients lose weight and yet have no evidence of systemic inflammation and therefore other mechanisms must be involved.

1.4 The clinical importance of muscle

Human activity, physical and mental well-being is dependent on our ability to move. Skeletal muscle function is essential for life, from the unconscious movements of breathing to the complex movements necessary for communication, work or self-expression. Disability in the form of paralysis or weakness is associated with adverse health (68) emotional (69, 70) and economic outcomes (71). In conditions where there is a global reduction in muscle mass, weakness or fatigue such as in aging or in cancer cachexia the potential for adverse outcome exists. Recognition of this potential has led to specific definitions of muscle wasting in particular clinical scenarios namely Myopenia, Sarcopenia and Cachexia.

1.4.1 Myopenia

The term myopenia first appears in the medical literature in 1987 to describe low muscle mass in patients with rheumatoid arthritis (72). Having gone unused over the last 2 decades, the word has recently been proposed as a new universal term for muscle wasting (73).

Myopenia describes “the phenomenon of a patient having lost enough skeletal muscle mass to have decreased quality of life or increased morbidity or mortality sufficient to merit therapeutic intervention” (73). The term is not specific to any disease and is not defined by any particular values of muscle mass or loss of muscle mass. The key element in the concept of myopenia is that the loss in muscle mass should have clinical significance and it is recognised that this may mean a different absolute muscle mass or loss in muscle mass in each condition, age or ethnic group.

1.4.2 Sarcopenia (Muscle loss in Aging)

The progressive loss of muscle mass and function in aging is now well recognised and although may be more a physiological than pathological process, sarcopenia has been shown to be associated with pathological outcomes (74). The term sarcopenia has endured a plethora of evolving definitions since its conception in 1989 (75). Having originally been used to describe muscle loss in aging, the name has been applied to low muscle mass caused by a number of conditions including cancer cachexia, chronic kidney disease, rheumatoid arthritis, immobility and starvation. Recent opinion reverts sarcopenia towards its original definition as a description of a syndrome of “sarcopenia with limited mobility” which should “not be attributable to the direct effect of specific disease” but is not necessarily restricted to use in older persons (76). This definition restricts its use to muscle atrophy that occurs with aging but distinguishes it as a pathological syndrome rather than a simple observation of physiological aging by the inclusion of a statement that the muscle loss should have a functional impact.

In aging, loss of muscle mass occurs at a rate of about 6% per decade over the age of 45 years and is seen in both active and sedentary individuals (77). Muscle loss will vary between individuals as they age and the peak muscle mass from which they lose muscle will be different from person to person. In order to account for these differences in starting

points, low muscle mass is commonly defined by reference to a young, healthy (therefore, non-sarcopenic) population, with a value below 2 Standard Deviations of the mean being regarded as sarcopenic. The first large study using this definition was performed by Baumgartner et al in 1998 using DXA and anthropometric measurement in a north American white and Hispanic population (78). This paper found the prevalence of sarcopenia to be >50% in people over 80 years old and showed that this new definition was associated with self-reported disability. The values for sarcopenia defined in this paper as an index, in terms of kg muscle mass per metre height^2, when applied to other populations do not always give a similar prevalence of sarcopenia. Analysis of 7518 French women found the prevalence to be 10.9% in a 86-95 year old age group (79). It is not clear whether this is due to the difference in the ethnicity of the defining (North American) healthy group but perhaps illustrates the importance of using specific cut offs for the region, ethnicity or sex of the population being studied. However, the principle applied by Baumgartner of a definition 2SD below a healthy mean appears valid when applied in numerous other studies where the association of low muscle mass to physical disability is explored further.

The clinical implications of reduced muscle mass in aging are now well known and have been demonstrated using a variety of techniques for muscle mass estimation. Muscle strength and power decrease with age (80) and this loss appears to be due to a reduction in muscle mass as age is unrelated to muscle strength when corrected for muscle mass(81). This relationship translates to functional impairment for specific tasks, leg muscle mass as measured by DXA is inversely related to lower extremity performance as measured by repeated chair stands (82), quadriceps sarcopenia measured by CT is associated with postural instability by one leg standing time (83).

Difficulty with specific tasks has an influence on overall functional ability in terms of activities of daily living. There are observed associations between sarcopenia and physical disability. These associations appear particularly strong amongst women over 60 years with

a skeletal muscle mass index less than 2SD below the sex-specific mean for young adults. Here, 78% reported difficulty stooping/crouching/kneeling, 49% difficulty climbing 10 stairs and 38.5% difficulty performing home chores (84). These findings of impairment in functional status are not consistent across all studies however with some failing to demonstrate this association (85, 86). Sarcopenia has been demonstrated to be associated with falls in older people. Baumgartner, reported an odds ratio of 1.42-4.73 for falls for men with sarcopenia compared with those without. A more recent study has confirmed the association between muscle mass and falls in men but not in women(87).

Of greatest clinical importance is the association of low muscle mass with morbidity and mortality. Sarcopenia is associated with increased length of hospital stay (88), and increased risk of nosocomial infection in care of the elderly (89). Sarcopenia presents a slightly increased risk of hip fracture (90, 91), however measures of muscle quality in terms of fatty infiltration of the muscle (myosteatosis) are more strongly predictive (90). This measure of muscle quality is also associated with an increased risk of hospitalisation in older people (incidence rate ratio 1.24-1.73%) (92) where no relationship with muscle mass is seen. Despite this, there appears to be little evidence for increased mortality associated with low muscle mass. Large studies using robust measures of muscle mass such as appendicular DXA or CT have failed to demonstrate a significant association of absolute muscle mass with increased mortality in multivariate analyses (93-95). Whilst absolute muscle mass does not appear to be a good predictor of mortality, the rate at which muscle is lost does predict all-cause mortality. In a study of 715 men with muscle mass assessed over a 7.5 year period, those losing more than 264g per year had a higher mortality (HR 1.19-4.33) compared with those losing less than <144g per year. As such, loss of muscle mass may be more a marker of the underlying disease/comorbidity rather than a cause of mortality itself.

In summary, the critical measures of muscle in aging are functional. In *aging*, muscle mass is less useful as a surrogate measure as it is closely associated with function, appears to add

little additional value to functional assessments and does not convincingly appear to be associated with significant additional risk (in terms of morbidity or mortality) unrelated to function.

1.4.3 Cancer cachexia

Like sarcopenia, cachexia has also undergone a series of evolving definitions (96) leading towards a clinically applicable and relevant definition used today. Cancer cachexia is defined as "a multifactorial syndrome characterised by an on-going loss of skeletal muscle mass (with or without loss of fat mass) that cannot be fully reversed by conventional nutritional support)" (97). The precise definition from this recent consensus paper requires weight loss >5% over past 6 months, or BMI <20 and any degree of weight loss >2%, or appendicular skeletal muscle index (or equivalent measure of muscle mass) consistent with sarcopenia and any degree of weight loss >2%. This new definition is based on the understanding that previous definitions based on non-specific cut off for weight loss alone did not reflect the functional impairment seen in cancer cachexia and may fail to identify at risk individuals with significant low muscle mass but little weight loss. During weight loss in cancer cachexia there is evidence to suggest that there is a dissociation between loss of skeletal muscle and weight loss with a more severe loss in skeletal muscle mass (98-100) than in total body weight or fat mass. However, this is not universally true as this finding was not seen in all cancer types (98) and in selected studies fat loss has been found to be greater than muscle loss (101). It is also recognised that this definition of cachexia fits into a spectrum of disease ranging from pre-cachexia where there may be early clinical and metabolic changes with minimal weight loss through to refractory cachexia associated with low performance status (WHO score 3 or 4) and a life expectancy of less than three months. Figure 4

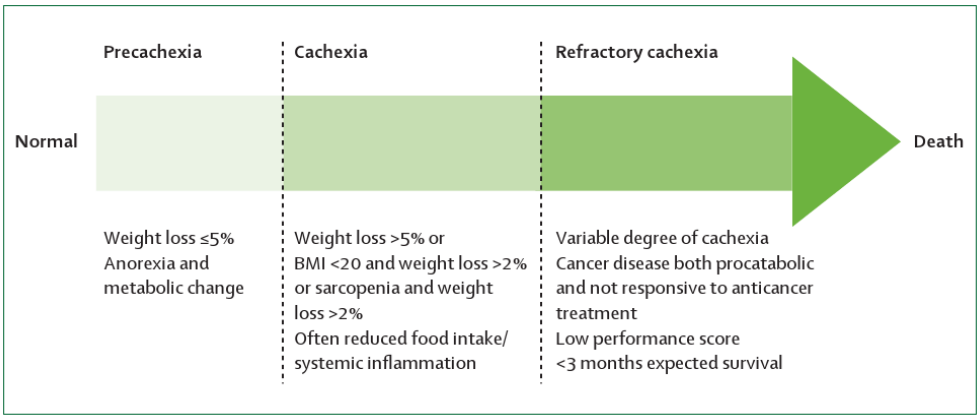

Figure 4 - The cachexia spectrum from Fearon et al (59). Clinically apparent cachexia represents one stage on a spectrum of disease leading from metabolic change without altered body composition to severe loss of weight, muscle and function.

The rationale for basing the new definition around loss of muscle in cancer cachexia comes from the understanding of the clear clinical (102) and functional implications (103) of low muscle mass for patients with cancer. Little evidence exists directly describing the effect of muscle loss in cancer on limb strength and power in cancer. However, the muscle mass / strength relationship appears to be maintained across several disease states with strength per unit (e.g., cm^2 CSA) of muscle being unchanged in cancer (103). It may therefore be assumed that muscle wasting in cancer is associated with loss of muscle function. This translates into a strong relationship between muscle mass and muscle strength. In a study of 35 patients undergoing surgery for upper GI cancer, exercise capacity was related to skeletal muscle mass measured by DXA pre-operatively and in the recovery phase 6 and 12 months post-operatively with correlation coefficients r = 0.6 to 0.7 respectively (104). Changes in muscle mass by DXA explained one third (r^2=0.33) of the change in exercise capacity over the same period. This relationship was true for both men and women and was seen in both weight stable and weight losing patients. In addition, a muscle mass measured by CT equivalent to Baumgartner's definition of sarcopenia was associated with low functional

status (as measured by PG-SGA questionnaire) in 47% of obese patients with cancer (termed sarcopenic obesity) compared with 26% without low muscle mass (105).

Further support for the key role of low muscle mass in defining cancer cachexia is the impact on survival of cancer-associated low muscle mass. CT based body composition studies have shown reduced survival associated with low skeletal muscle mass. In patients with solid tumours of the respiratory and gastrointestinal tracts, sarcopenic obesity was associated with a reduced median survival of 21.6 months compared with 11.3 months HR 2.4 [1.5-3.9](105). These findings have been reproduced in patients with pancreatic cancer (61). Low muscle mass also has implications for the treatment of patients with cancer, sarcopenia determined by lumbar CT is associated with increased risk of toxicity to anti-cancer chemotherapy and with a reduced time to tumour progression in metastatic breast cancer for both capceitabine (102) and 5-fluorouracil-based chemotherapy (106). These findings suggest that skeletal muscle mass may be a better predictor of chemotherapy toxicity than simple body mass. Compounding the risk of low skeletal muscle mass in chemotherapy is the finding that muscle mass continues to fall during chemotherapy (107, 108).

1.5 Interventions in myopenia

1.5.1 Sarcopenia of aging

1.5.1.1 Exercise

A number of studies have examined the possibility for reversing or slowing the progressive loss of muscle mass with aging by dietary, nutritional and pharmacological methods. These studies aim to assess an effect either on muscle loss itself or on the consequences of sarcopenia. A Cochrane review on physical therapy in the elderly found that progressive resistance strength training (PRT) has a small but significant effect on improving physical function, a small to moderate effect on decreasing some impairments and functional

limitations, and a large effect on increasing strength, and concluded that "Doing PRT two to three times a week can improve physical function in older adults, including reducing physical disability, some functional limitations (i.e., balance, gait speed, timed walk, timed 'up-and-go', chair rise; and climbing stairs) and muscle weakness in older people." (109). Resistance type exercise over a 12 week period in men aged 65-85 has been shown to reduce body fat mass and increase quadriceps CSA by 8.8% and relative increase in type II fibre type (110) and similar findings have been seen by other groups (111-113). There is currently no long term longitudinal evidence that physical activity produces a sustained increase in muscle mass (114).

1.5.1.2 Dietary supplements

Protein and amino acid supplementation has been shown to increase muscle protein synthesis (40, 115) and muscle mass (116). However this effect has not been seen with long term supplementation (48).

1.5.1.3 Pharmacologic treatment

Testosterone supplementation, given to frail elderly men increases knee extensor strength and lean body mass. However, due to concerns over safety, it is undesirable to remain on testosterone supplements in the long term and the beneficial effects disappear with withdrawal of treatment (117). Other hormone treatments have a less clear effect on muscle mass with studies of growth hormone supplementation in men and women and oestrogen supplementation in women yielding both positive and negative results (118, 119).

1.5.2 Myopenia of cachexia

1.5.2.1 Exercise

Good quality studies of resistance exercise in patients with cachexia are difficult to perform due to issues of patient fatigue, symptoms arising from the cancer or from on-going cancer therapy. A review of those studies currently available (predominantly in breast cancer) suggest that exercise therapy may have some beneficial effects on quality of life and psychological wellbeing (120).

1.5.2.2 Dietary supplements

Dietary supplementation with eicosapentaenoic acid (EPA) present in fish oil may reduce the production of pro-inflammatory cytokines such as IL-6, IL-1 and TNF in cancer and act to reduce weight loss in pancreatic cancer (121, 122) and increase lean body mass and quality of life (123). More recently, eicosapentaenoic acid supplementation has been shown to result in increased muscle mass in non-small cell lung cancer with 69% of patients gaining or maintaining muscle mass compared with 29% with standard treatment (124). This finding has not been seen in all studies with a number reporting no change in body weight or lean mass (125, 126) and a Cochrane review concludes that there is no advantage of EPA enhanced nutritional supplements over non EPA supplements in pancreatic cancer (127). Specially formulated nutritional supplements containing protein with added leucine increases skeletal muscle FSR but did not improve lean mass compared with simple casein protein (128).

1.5.2.3 Pharmacologic treatment

Pharmacological and neutraceutical interventions have been shown to be effective in cancer cachexia to increase appetite, physical activity and muscle mass using a combined treatment with megestrol acetate, eicosapentaenoic acid, L-carnitine and Thalidomide (129) and with combined treatment of carnitine and celecoxib (130). Other promising combination

treatments such as fomoterol/megestrol and novel therapies such as Ghrelin analogues, anti IL-6 and anti myostatin antibodies are currently under development and entering phase II/III clinical trials (131, 132).

1.5.2.4 Design of intervention trials

Cachexia intervention trials are bedevilled by heterogeneity of the population. Recent efforts have sought to focus on a patient's low skeletal muscle mass. However, patients may have low levels of muscularity due to their congenital stature, old age or co-morbidity rather than cancer specific loss. One route round this would be to identify patients on the basis of current active loss of muscle. However, this requires a baseline predicted level of muscularity to establish active muscle loss at the time of cancer diagnosis. Equally, it may be possible to identify a biomarker for change in the quality or quantity of muscle to identify patients undergoing cancer related muscle wasting.

1.5.3 Biomarkers in muscle wasting

The National Institutes of Health Biomarkers Definitions Working Group defines a biomarker as "A characteristic that is objectively measured and evaluated as an indicator of normal biological processes, pathogenic processes, or pharmacologic responses to a therapeutic intervention" (133). Biomarkers may be a diagnostic tool for the identification of patients with a disease or abnormal condition, a tool for staging of disease or classification of the extent of disease, an indicator of disease prognosis or for prediction and monitoring of clinical response to an intervention.

Whilst established cancer cachexia is well defined (97) and usually clinically apparent there is currently no method for detecting the presence of an early or "pre-cachectic" phase. It is hypothesised that the cachectic process may be more likely be reversible as a result of intervention in this early stage thus the identification of biomarkers of cachexia that are valid

throughout the cachexia process might be a great advance. In cancer cachexia biomarkers may include signalling molecules, metabolites of fat or muscle breakdown or may be seen in a specific phenotype by body composition analysis. Previous investigations for cachexia biomarkers have analysed skeletal muscle, proposing calcium/calmodulin-dependent protein kinase type II Beta (CaMKIIβ) and Tyrosine-protein kinase receptor (TIE1) as potential markers (134). Serum or urinary markers may also exist and serum myoglobin has been proposed as one potential marker of muscle wasting (135). Existing biomarkers for muscle mass are direct and indirect measures of muscle mass/volume including CT, Magnetic Resonance Imaging (MRI), Bio-electrical Impedance Assessment (BIA) and DXA. Although identification of low muscle mass has prognostic significance these measures may not be specific for cancer cachexia related muscle wasting. Isotope labelling methods of muscle synthesis measurement may be considered a biomarker for changes in cancer related muscle synthesis. However, these methods are currently burdensome for the patient and do not provide an integrated measure compatible with measurement in a patients home or during normal activity (136).

1.6 Body composition analysis

Cachexia, Myopenia and Sarcopenia are syndromes based on risk stratification by means of body composition analysis. Several concepts of human and animal body composition exist and these different models or concepts have often been developed as the technology to define each body component has developed. Body composition may be measured by a variety of different methods and may be considered according to different models. Wang's 5 level model describes how the body's constituents may be considered according to different tissue types or anatomy (137). In practice, body composition methods usually describe composition according to a compartmental model where the body is described as consisting of 2 or more compartments e.g. fat and fat free mass in a 2 compartment model or water, protein, mineral and fat in a 4 compartment model (138).

1.6.1 Body composition methods

A range of methods exist for evaluating body composition, the choice of method used will depend on the degree of precision required, the design of the study whether longitudinal or cross sectional, the size and nature of the study population, the facilities available and the convenience and tolerability of the test involved for participants and researchers. Any method selected is likely to involve a degree of compromise.

1.6.1.1 Anthropometric measurements.

Body composition descriptions by anthropometric measurements are one of the simplest assessments of body composition that can be made in the field. There are 10 standard types of measurement:

1) Stature, a simple measure of body height.

2) Segment lengths such as lower extremity length or thigh length.

3) Body breadths, less commonly used measures of frame size.

4) Circumferences such as mid upper arm circumference or abdominal circumference used in assessment of adiposity or head circumference used in clinical assessment of neonatal growth.

5) Skinfold thickness measured at specific anatomical locations such as abdominal, triceps or subscapular. These are also used to give measures of adiposity or may be combined with others (e.g. mid arm circumference and triceps skin fold thickness) to give estimates of muscle mass).

6) Body surface area may be used to estimate basal metabolic rate of FFM.

7) Body volume (used to estimate body density). This is more complex to asses and requires specialist techniques such as water displacement.

8) Body weight, the simplest crude measure of growth, obesity or wasting in conditions such as cachexia.

9) Body mass index (BMI), body weight/height^2 is considered a crude measure of adiposity. This is the most widely used measure of body composition worldwide and was first described in 1832 by Adolphe Quetelet and termed the Quetelet Index (139). The relationship of BMI to total body adiposity was first examined in 1972 (140) in 7424 'healthy' men in 12 cohorts in five countries and termed body mass index. Whilst the correlation between body mass index and fat mass is strong, BMI alone accounts for only 25% of the difference in body fat percentage between individuals as measured by a four compartment model (141).

10) Body density, calculated from body weight and volume and may be used to derive molecular level estimates of fat and fat free mass.

Most anthropometric measures such as height, weight and skinfold thickness are simple and easy to use, making them quick, cheap and reproducible. As a result they are most suitable for large scale population studies. At their simplest level the data itself (or a combination of measurements) such as weight (or weight loss) or BMI are used as body composition measures and can be used to stratify risk in particular groups. The ability of these measures

to give accurate body composition estimates is limited. Simple two compartment models (fat and fat free mass) may be derived from height weight, circumference and skin fold measures however the equations from which these estimates are made are highly dependent on the population in question and as a result over 100 skin fold thickness prediction equations exist (142). Such prediction equations may also be inaccurate in specific disease states such as chronic heart failure (143).

1.6.1.2 Air / Water displacement methods

The relatively consistent density of the fat components of the body allow for 2 compartment models to be calculated using underwater weighing, water or air displacement methods. In the hydrodensitometry method the volume of water displaced and/or the subject's weight underwater are combined with their weight to calculate the density of the whole body (D_b). These measures are combined with assumed densities for fat (D_{FM})and fat free (D_{FFM}) mass to calculate total body fat (FM) and fat free mass (FFM) in a two compartment model. The equation governing this relationship is $1/Db = FM/D_{FM} + FFM/D_{FFM}$(138) and an example of an equation for its use in calculating body fat is %body fat =((4.57/body density)-4.142) x 100 (144). One drawback of this method is that a number of assumptions need to be made including allowance for estimated lung and gastrointestinal volume and may add an additional 3-4% to the error in the measurement of fat mass (138). This effect is reduced in air displacement plethysmography. However, both methods rely on assumptions of density and hydration of fat and fat free mass. It is known that the density of fat free mass is not necessarily constant and that its composition varies with gender, physical activity and aging (142). It is likely, particularly in disease, that variations in the water and mineral fractions of fat free mass exist that make densitometry measures alone unreliable and unsuitable as a reference method in heterogeneous populations (138). As a result displacement methods are robust for healthy individuals but may be more variable in altered body composition. Methods based in body density and volume have an estimated cumulative error for body

fatness of 3-4% (138, 145, 146). Despite their similar methodologies, water and air displacement methods may differ when compared directly even in healthy populations with air displacement plethysmography overestimating body fatness in men and underestimating in women by around one per cent compared with water displacement (147). Differences between the two methods of ~2% are also seen in lean individuals although not in those of average fat mass (148). The underwater weighing method has limited use in practice due to the need for total immersion in water which may be unacceptable to approximately one third of middle aged women (149).

1.6.1.3 Isotope dilution

Isotope dilution methods provide body a measure of composition at an atomic (150) and molecular level. The principle of the dilution method is to determine the size of a compartment by adding a known quantity of a measurable isotope and then measuring its concentration in the compartment of interest (151). Total body water may be measured in this way by adding deuterated ($^{2}H_2O$), tritiated ($^{3}H_2O$) or ^{18}O labelled ($H_2{}^{18}O$) water. The measurement of total body water (TBW) using this method has an accuracy and precision of 1-2% although it is still dependant on an assumed value for the amount of H or O exchanged with molecules other than water (such as hydrogen atoms associated with carboxyl, hydroxyl, and amino groups and oxygen associated with carboxyl and phosphate groups) termed non-aqueous hydrogen exchange. This non-aqueous hydrogen exchange is in the order of 4% for tritium and deuterium This measure of total body water is used to provide an estimate of fat free mass based on the assumption of the relatively constant water content of fat free mass being 0.732 L per kg (152). This value appears to be very consistent in a number of mammals. The data for humans is based on examinations of 9 cadaveric dissections in individuals including one with advanced malignancy and one with extreme cachexia. It is also consistent with the hydration data underpinning the 5 level system of body composition (137, 152). The range of reported values for TBW:FFM is 0.686 to 0.808

(152) and includes severely dehydrated and oedematous subjects. This 15% difference in hydration between individuals will lead to inaccurate estimates of fat free mass when using a mean value for hydration in individuals with different disease states. Although these values are extremes and are unlikely to be relevant in analysis of relatively healthy cohorts, their possible range should be considered in studies of patients who potentially have seriously disordered body composition such as may be seen in cachexia, sepsis or the post-operative state. More complex body composition models may be developed using dilution methods which can measure hydration while estimating body composition at the cellular level (138). The addition of sodium bromide enables measurement of the extracellular water component as it mixes with this compartment and the intracellular water volume can be calculated when total body water is known. Four compartment models require the addition of other body composition measures in combination with the dilution method (153).

1.6.1.4 Bio-impedance

The bio-impedance (BIA) method is closely related to body water measures in that the resistance across a region of the body is proportional to the body's fluid volume in that region (138). The measurement is made by attaching electrodes at the wrist and/or ankles and passing a weak current through the body, measuring the voltage drop. The impedance index ($height^2/R$) is assumed to be proportional to the volume of TBW (154). The bio-impedance method is widely used due to its safety, low cost, speed, reproducibility and ease (155). There are a number of factors that affect the accuracy of the method such that BIA calculations of body fat may vary by 10% of body weight (155) and so limiting its use. Indeed, its accuracy may be no better than anthropometry (156). Some of the assumptions made by BIA for the estimation of TBW and fat free mass include an assumption that the human body can be approximated to a cylinder for the use of the $height^2/R$ equation and assumption of consistent uniform hydration (155). Even within the same individual BIA measurements are susceptible to changes caused by posture, hydration, fed or fasting state,

physical activity, sweating and menstrual cycle (157). A large number of prediction equations exist and are specific to the populations in which they were defined. The coefficient of variation in one large series for race specific equations over a wide age range (12-94 years) was 6% for FFM and 8% for TBW (158). Errors are smaller in healthy normal weight individuals (standard error of estimation) (SEE 1.8 to 3.9 kg) compared with overweight individuals (SEE 8.8 kg) (154). Similar errors are seen in disease (1.6 to 4 kg) provided that population specific equations are used (157).

The main role for bio-impedance may be in screening large populations. Its role for assessing individuals or small groups is limited. It is unable to be used in individuals with BMI <16 or >34 kgm^2, it cannot detect changes in FFM, FM or TBW less than its limit of precision of 1.5 – 2 kg and although reproducibility in weight stable individuals is good (159) some authors consider the measurement of longitudinal changes when significant weight loss occurs controversial because of physiological changes (157, 160, 161). Newer multi-frequency BIA instruments have more promise in that they can measure both body water and extracellular space. However, their accuracy in specific groups should be validated against a reference (4C) model.

1.6.1.5 Total Body Potassium (K)

Total body K methods of body composition are based on the natural abundance of radioactive ^{40}K which emits 1.46 MeV ɣ radiation at a constant rate. Body cell mass can be estimated from measures of ^{40}K which is present in human tissue at 0.0118% of total body potassium. As 97% of potassium is intracellular, TBK can be used to estimate body cell mass which in turn can estimate FFM. The measurement of total body ^{40}K is generally performed by large multi-detector arrays which must be housed in a shielded room (such as 15cm thick steel(138)) or a 'shadow shield' of 10cm lead (162) to exclude background radiation. Scans may take 15mins to an hour depending on the efficiency of the scanner. The accuracy of the method is considered to be 1-5% for adults(138). The measurement of ^{40}K using this

technique is extremely precise. However the conversion to BCM and FFM relies on assumptions of some constant relationships which may limit its accuracy. Conversion to BCM is by the ratio established in 1963 by Moore et al of BCM (kg) = 0.00833 x TBK (mmol). The factor relating TBK to BCM has recently been revised (163). Conversion to FFM is based on a TBK/FFM ratio of 68.1 mmol kg^{-1} from whole body human cadaver analysis. This value ranges across studies with different methodologies from 52.0 to 66.0 in females and 60.0 to 68.1 in males. The TBK/FFM ratio also decreases with age(138). Total body potassium counting has the disadvantage of being an installed facility that is not widely available, however it has the significant advantage that its use in the measurement of BCM is robust even in the face of fluid shifts which occur predominantly in the extracellular space (58). TBK counting is considered a gold standard measure of body cell mass although not of FFM unless included with TBW measurement in a multi-compartment model.

1.6.1.6 Neutron Activation Analysis (NAA)

In vivo neutron activation analysis is a term that describes a number of related techniques that have the ability to acutely measure a number of specific elements in the human body. The principle of the method is a controlled neutron irradiation which induces release of ɣ radiation with element specific detectible energies. Typical protocols may take between 30 and 60 mins to complete and have a coefficient of variation (CV) of 2.8% for Nitrogen or 3% for Carbon (150). The primary disadvantage is that these methods are costly and require considerable expertise in addition to a small radiation dose approximately equivalent to a routine chest x –ray (138). This method is considered the gold standard for measurement of nitrogen (164) which in turn is directly proportional to body protein mass (protein=6.25 x Total Body Nitrogen) (163). NAA can also measure total body Ca, P, Cl and Na.

1.6.1.7 Dual Energy X-ray Absorbometry (DXA)

DXA (or DEXA) has become a widely used modality for skeletal muscle mass estimation. The ready availability of DXA scanners (for assessment of bone mineral density) make this a relatively fast, cheap and safe method to measure lean mass. DXA was originally conceived as a method to measure bone mineral density for which it should be regarded as a primary measure. The principle behind the technique was first developed in 1963 and involves the passage of a photon beam through the body tissues and measuring its attenuation with a photon detector. Different elements exert different effects on the photon beam and knowledge of the typical constituents of bone, fat mass and fat free mass make it possible to determine the type of tissue that the beam is passing through. In DXA, photon beams of two different energies are used in order to take advantage of the different levels of attenuation exerted by different elements on beams of different energies. In the human body (and in animal studies) the determination of tissue mass is complicated by the fact that at any point the beam may be passing through two or three tissue types. Where two tissue types are present (e.g. fat and fat free mass) the DXA scanner may be calibrated using a phantom consisting animal soft tissues and lean and fat soft tissue mass determined by measurement of the ratio of attenuation of the two photon energies. In the presence of bone, the soft tissues are estimated using the ratio of attenuations at either side of the bone. The DXA method relies on assumptions of constant elemental proportions of fat, lean and bone mineral components (150) and are based on mathematical models to estimate the mass (or volume) of specific tissues. DXA values of body composition may be given as whole body fat and fat free mass (which includes viscera), appendicular lean and fat mass (which is ~75% of skeletal muscle mass) or as estimated cross sectional area of thigh. Studies in which the focus has been on skeletal muscle mass typically use CT or MRI measures as the gold standard against which DXA is compared. Whole body DXA or DXA truncal adiposity may be a very reproducible measure with a CV of 2% for fat free mass and 0.8% for fat (165),

although the algorithms used by different scan manufacturers may mean that values from different scanners are not comparable (138).

1.6.1.8 Computed tomography and Magnetic Resonance Imaging

CT or MRI give measures at the tissue system level (150). They provide measures of muscle mass as defined by muscle volume rather than protein content. Measures obtained using MR and CT imaging may be classified as Total Adipose Tissue (TAT), Subcutaneous Adipose (SAT), Visceral Adipose Tissue (VAT) and Intermuscular or Interstitial Adipose Tissue (IMAT or IAT) although numerous abbreviations exist. Visceral adipose may be further divided into retroperitoneal and intra-peritoneal adipose although this is rarely done in human studies (166, 167). In both CT and MRI skeletal muscle may be compartmentalised into individual muscles or muscle groups. It may also be described as anatomical muscle which includes both contractile muscle tissue and IMAT or more commonly Adipose Tissue Free Skeletal Muscle Tissue (ATFSM) which excludes IMAT (57, 168). These measurements are often attributed a high quality, for the reasons of their specificity and precision. The separate determination of subcutaneous, intra-abdominal and intra-organ adipose tissues is a good example of specificity which is only possible with these approaches. Thus the clinical implications of excess intra-abdominal adipose (169, 170) and conditions of hepatosteatosis (171) and myosteatosis (90, 172, 173), have been revealed by MR and CT image analyses. In addition, magnetic resonance spectroscopy may be used to obtain a direct measure of intramyocellular lipids using ^{1}H-MR spectroscopy (174). Other, non-image-based methods lack tissue specificity, are dependent on prediction equations or assumptions of tissue density or distribution (150). As a result CT is capable of detecting changes in muscle mass in response to resistance training which are undetectable using DXA (175), BIA, total body water or in vivo neutron activation (176). CT and MRI for determination of tissue cross sectional area (CSA) fit the description of an in vivo reference

method as they are not a derived measure so are often regarded as the gold standard measure for *in vivo* body composition (177).

1.6.1.8.1 Reliability and Repeatability

Error in cross sectional imaging measurements may be related to the technical error associated with the process of scanning, such as patient positioning or equipment, and/or the observer error associated with analysis of the resulting image (173). To quantify error researchers report repeatability and inter- and intra- operator reliability. Inter and intra-operator reliability do not give a complete picture of the repeatability of the test as they do not account for error associated with image acquisition. Repeatability describes the differences between consecutive separate scans in the same individual and is most relevant to real practice as it determines the ability of the technique to observe true differences between individuals or between time points.

Error is reported in several ways. For practical purposes, the limits of agreement, critical difference (CD) and prediction interval (PI) indicate the limits of the technique to measure tissue area or volume in an individual. The coefficient of variation (CV), confidence interval (CI) of the prediction and standard error of the estimate (SEE) indicate the limits of the technique to define the true mean of the group. The coefficient of variation is proportional to the limits of agreement in normally distributed data. Tables 1-3 summarise measurement error estimates previously reported in the literature.

Author	year	Disease	Region	Software	technique	Modality	CSA / Volume	ATFSM	Anatomic SM	SAT	VAT	IMAT
Keller (173)	2002	low back pain	paraspinal L3-4 L4-5		Manual delineation	CT	CSA		CV 2 - 2.5%, CD 5.5-7%			
Strandberg (178)	2010	ACL injury	thigh	Image J	HU and manual delineation	CT	CSA	CV 0.93% [1]				
Hicks (179)	2005	Elderly	L4-5			CT	CSA	CV <5%				
Mitsiopoulos (180)	1998	Cadaver	Thigh and arm			MRI	Vol	0.34 ±1.1%, 2.0% ± 1.2% [2]				
Gallagher (181)	2004	Healthy	whole body (40 slices)	Tomovision	HU and manual delineation	MRI	CSA	1.40%		1.70%	2.30%	5.90%
Gray(57)	2011	cancer	quads	Analyse	k means, Manual segmentation	MRI	CSA/VOL		Max Error 0.40%			
Irving (182)	2007	Healthy	abdomen	Tomovision	HU & manual delineation	CT	CSA			CV 0.4 - 1.5%	CV 0.8 - 2.5%	
Irving (182)	2007	Healthy	abdomen	Image J	HU & manual delineation	CT	CSA			CV 0.7 - 1.4%	CV 1.1-1.6%	
Irving (182)	2007	Healthy	Thigh	Tomovision	HU & manual delineation	CT	CSA	CV 0.2 - 1.7%				
Irving (182)	2007	Healthy	Thigh	Image J	HU & manual delineation	CT	CSA	CV 0.4 - 3.5%				

Table 1 – Previously published inter-observer error estimates in cross sectional imaging body composition measures. (ACL Anterior Cruciate Ligament, L Lumbar vertebra, CSA Cross Sectional Area, Vol Volume, CV Coefficient of Variation, CD Critical Difference, HU Hounsfield Units, SAT Subcutaneous adipose tissue, ATFSM adipose tissue free skeletal muscel, SM skeletal muscle, VAT Visceral adipose tissue, IMAT Intermuscular adipose tissue)

[1] Method unclear, possibly not true ATFSM
[2] Between labs

Author	year	Disease	Region	software	technique	modality	CSA / Volume	ATFSM	Anatomic SM	TAT	SAT	VAT	IMAT
Strandberg (178)	2010	ACL injury	Thigh	Image J	HU and manual delineation	CT	CSA	CV 1.61% [3]					
Mitsiopoulos (180)	1998	Cadaver	Thigh and arm			MRI	CSA	r=0.99 SEE 7.9cm (2.6%)			r=0.99 SEE 6.5cm (3.3%)		
Mitsiopoulos (180)	1998	Cadaver	Thigh and arm			MRI	VOL				.-2.9 ± 1.2%		
Positano (168)	2009	Healthy	Thigh	Hippofat	Semi-automated	MRI	VOL	CV 0.49%			CV 1.12%		CV 1.69%
Gray (57)	2011	cancer	Quads	Analyse	k means	MRI	CSA/VOL		Max Error 0.40%				
Irving (182)	2007	Healthy	Abdomen	Tomovision	HU & manual delineation	CT	CSA				CV 1%	CV 2%	
Irving (182)	2007	Healthy	Abdomen	Image J	HU & manual delineation	CT	CSA				CV 2.1%	CV 2%	
Irving (182)	2007	Healthy	Thigh	Tomovision	HU and manual delineation	CT	CSA	CV 0.9 - 1.2%					
Irving (182)	2007	Healthy	Thigh	Image J	HU & manual delineation	CT	CSA	CV 2.8 - 2.9%					
Gronemyer (183)	2000	Healthy	Umbilicus	Photoshop	Intensity threshold	MRI	CSA			2.8%	0.2%	10.8%	

Table 2 – Previously published values for intra-observer error in cross sectional imaging body composition analysis. (ACL Anterior Cruciate Ligament, L Lumbar vertebra, CSA Cross Sectional Area, Vol Volume, CV Coefficient of Variation, CD Critical Difference, HU Hounsfield Units, SAT Subcutaneous adipose tissue, ATFSM adipose tissue free skeletal muscel, SM skeletal muscle, VAT Visceral adipose tissue, IMAT Intermuscular adipose tissue)

[3] Method unclear, possibly not true ATFSM

Author	year	Disease	Region	software	technique	modality	CSA / Volume	ATFSM	Anatomic SM	TAT	SAT	IMAT
Berker (184)	2010	Healthy	L4-5	CT software	HU & manual delineation	CT	CSA	CV 2%†				
Boettcher (185)	2009	Healthy	Lower limb	MATLAB	Thresholding (semi-automated)	MRI	CSA	CV 1.3 ± 0.9%			CV 2.2 ± 1.5%	CV2.8 ± 0.8%
Verdijak (110)	2009	Elderly	quads	IMPAX	HU &manual delineation	CT	CSA		CV 0.6%			
Val-Laillet (167)	2010	Diet modification (pig)	t13, l2	Image J	Histogram of HU	CT	CSA			SD 1.1cm2 ‡		
Prado (105)	2008	Cancer	L3-4	Tomovsion	HU & manual delineation	CT	CSA	CV 1.54% *				
Mourtzakis (186)	2008	Cancer	L3-4	Tomovsion		CT	CSA		CV 1.6% *	CV 2.3% *		
Keller (173)	2002	low back pain	paraspinal L3-4 L4-5		manual	CT	CSA		CV 3.6-5.8% CD 10-16%			
Mitsiopoulos (180)	1998	Cadaver	Thigh and arm			MRI	CSA	r=0.99 SEE 8.8cm (2.9%)			r=0.99 SEE 6cm (2.5%)	r=0.96 SEE 1.7cm
Mitsiopoulos (180)	1998	Cadaver	Thigh and arm			MRI	VOL	1.8 ± 0.6%			1.5 ± 1.5%	
Beneke (187)	1991	Healthy	Quads (anthropometric landmarking)	MOP (Kontron)	Manual delineation	MRI	CSA	1.6%**				
Beneke (187)	1991	Healthy	Quads (MRI determined landmarking)	MOP (Kontron)	Manual delineation	MRI	CSA	0.7%**				
Hudash (188)	1985	Healthy	Quads		Manual delineation	CT	CSA		2 cm2 ($p<0.05$) *††			

Table 3 – Previously published estimates of repeatability in cross sectional imaging body composition analysis 4. (ACL Anterior Cruciate Ligament, L Lumbar vertebra, CSA Cross Sectional Area, Vol Volume, CV Coefficient of Variation, CD Critical Difference, HU Hounsfield Units, SAT Subcutaneous adipose tissue, ATFSM adipose tissue free skeletal muscel, SM skeletal muscle, VAT Visceral adipose tissue, IMAT Intermuscular adipose tissue)

[4] (*Variance between adjacent slices on same scan, † same observer, ‡on a mean CSA of 95.3 cm2, ** Prediction error, ††Mean difference

A number of studies address the repeatability of C-S imaging in body composition (173, 184, 185, 187, 188) and report good agreement between repeated measurements using either MRI or CT for both fat and muscle. The greatest CV for muscle was 5.8% with a CD of up to 16% (173), however this study used manual delineation of the paraspinal muscles and attributed more than half the error to the observer rather than technical error. Most studies report the CV to be between 1-2%. The technical error associated with patient positioning and slice selection is illustrated by the variation of between 1.5 and 2.5% between adjacent abdominal slices in the same individual (105, 186) and by a reduction in total measurement error by 50% when positioning was performed based on MRI land-marking rather than surface anthropometric based skin marking (187). Furthermore, repeatability may not be equivalent across individual muscles or muscle groups; possibly due to difficulties in visual discrimination. Beneke et al attained a PI of 0.7% in the quadriceps muscle group but 6.0% when measuring rectus femoris alone (187).

Because of the differences in methodology and reporting of results between studies, no meta-analysis of error in cross sectional imaging is possible to date. Using the data reported in Tables 1-3 an impression of broad estimates for total repeatability can be made. ATFSM CSA of quadriceps or thigh using CT or MRI would be expected to have a maximum error of ~2% for an individual or ~0.7% for the true mean of a group. Values for SAT are slightly higher around ~4% and ~1.5% with IMAT being the least precise measure with errors of around ~4.7% and ~1.7%. These values assume careful land marking, patient positioning and use of a semi-automated image analysis technique without which the error in the method may double. In the abdomen CT has broadly similar errors as MRI for measures of muscle and SAT with limits of agreement around ~5% and CV ~2%. Similar errors are seen for VAT on CT. Estimation of visceral adipose is difficult particularly in MRI (189) and the CV may increase to ~10%. Poor reproducibility can occur due to incorrect land marking or slice selection so image analysis protocols should use specific bony landmarks rather than soft

tissue. These values for repeatability are important for development of study design. The error term and the estimated effect size are used to calculate the sample size (n) required to detect a given difference. When studying change over time, the summed intra-observer error of the measurement at two time points limits the magnitude of change that can be detected.

1.6.1.8.2 Comparison between CT and MRI

CT and MRI measurements are comparable with regard to SAT CSA values in the abdomen with a SEE of 4.4cm^2 and CV% of 4.4%. However, VAT CSA compares less favourably with a SEE of 8.3cm^2 and CV% 12.8% which is probably due to the lower reproducibility of MRI measures of VAT. In the thigh ATFSM and SAT are comparable between CT and MRI r=0.97, SEE 3.9cm^2, CV 10.1%, r=0.99 SEE 2.4cm^2, 5.5% (180). In the lower limb agreement between CT and MRI also appears to be strongest around the belly of the muscle than at a joint such as knee or ankle (190) although this is likely due to the error associated with measuring small areas rather than any specific characteristic of MR or CT.

1.6.1.8.3 Limitations associated with tissue identification and segmentation methods

Segmentation of different tissue types using CT is achieved using defined Hounsfield Units (HU) for specific tissues in conjunction with manual correction. In this context variations in the image analysis software appear to exert little influence on measurements of CSA (182, 191). For MRI these defined values do not exist and a variety of different approaches to segmentation are used. The most commonly used segmentation techniques include those based upon signal intensity using either a pixel intensity histogram (181) or by a clustering approach such as fuzzy c-means (168, 189, 192) or k-means (57). Fully automated analysis methods may be quicker and more reproducible than methods dependant on manual delineation (193) but may under- or over-estimate fat measures (using expert manual segmentation as the standard) by 11% (189, 193) and is currently not possible for specific

muscles or muscle groups. Combination of automated MRI analysis and manual correction may reduce the CV (SAT<0.5%, ATFSM <0.5%, IMAT <2%) (168) while improving the speed of analysis.

1.6.1.8.4 Use of single slice cross sectional imaging to predict regional or whole body values

In many publications data are reported using directly determined units of tissue cross-sectional area (cm^2) from a single image (107, 124). However, several authors have worked to find the single image which is most representative of whole-body organ volumes (i.e for muscle and adipose tissues) (194, 195). The intention of this has been to estimate values for total body fat, fat free mass, skeletal muscle mass or regional volumes such as thigh muscle or visceral adipose, while limiting the time taken for analysis. As a result cross sectional data are often used as a surrogate for these measures, since they are linearly related to whole body or regional measures. For example, thigh CSA at the mid-femur point is highly correlated with thigh muscle mass r^2=0.72 ($p<0.01$) (195). For specific muscle groups however the strength of association is variable and may be most strongly correlated at different anatomical locations in the thigh (196, 197). Conventionally the mid-thigh level is used for the measurement of muscle mass by a single cross sectional image, however a more proximal location may be preferred in order to detect changes in response to resistance training and this may be even more sensitive a measure than thigh volume (33). Lee et al (195) demonstrated using 41- slice whole body MRI in 387 volunteers that a single slice CSA measurement at mid-thigh explained 77% (SEE 2.14kg, 6.5%) and 79% (SEE 1.56kg, 7.4%) of the variability in total body skeletal muscle in men and women respectively. However, the same study also reported the variability explained by an abdominal slice 10cm above L4-5 as 74% (SEE 2.29kg, 6.9%) and 67% (1.95kg, 9.2%) (43). Using a similar protocol in 327 volunteers Shen et al (194) showed an optimal linear relationship between a slice 5cm above L4-5 and whole body skeletal muscle with r^2 =0.855 (95% CI ±5.190 litres)

and adipose r^2 =0.927 (95% CI ±6.170 litres). Importantly, these relationships were maintained over a range of body composition (muscle or fat mass 10-60kg) (194) and in cancer, obesity and sarcopenic obesity (186). Comparison of abdominal ATFSM CSA with DXA indicates that whole body fat free mass may be estimated to within ±3kg (186) although systematic differences between CT and DXA may mean that values obtained using these measures are not interchangeable (198).

The standard error and the mean residual error of the estimates of whole body volume based on single image assessments are considerable, and thus the use of a single cross sectional image to accurately predict total body composition is better suited to groups rather than individuals. For example, in the study described above, the minimum detectable difference in whole body adipose tissue volume between individuals was between 10.4 and 12 litres. Whole body estimates based on a single image however, are useful when used to illustrate the approximate magnitude of a difference in tissue area; for example Shen's regression suggests that 14 cm^2 of total adipose tissue at a lumbar vertebral landmark equates to 1 kg of whole body adipose tissue.

1.6.1.8.5 Hounsfield units

One particular advantage of CT is that it provides a reproducible measure of skeletal muscle X-ray attenuation in the form of Hounsfield units (HU). In skeletal muscle this measure has been shown to be directly related to the degree of intramyocellular lipid, of which an abnormal accumulation is termed myosteatosis (199). The HU measure is reproducible to within 1% (200, 201) and corresponds to approximately 1 HU change per 1% increase in lipid concentration. This is best performed by averaging the whole of the muscle area of interest, since sampling appears to result in unacceptably high variability (173). Myosteatosis has been shown to be associated with pain (173) and lower limb function and risk of hip fracture (90, 172), obesity and insulin resistance (202) and therefore appears to reflect the

pathological process observed in muscle wasting. It also responds to muscle preserving interventions in a similar way to muscle mass (124).

1.6.1.8.6 Practical limitations of cross sectional imaging

The limitations of this method are related to cost (MRI), exposure to ionising radiation (CT), the potential sources of error, and the accessibility of the measurements to the researcher and clinician (MRI and CT). Potential pitfalls include errors in patient positioning, technical errors, movement, slice selection and image interpretation including identification of specific muscles (previously described) and also within the abdominal cavity where the peritoneum may be incorrectly marked (203) or intestinal contents identified as anatomical adipose (204). In addition MRI has specific technical considerations with regard to patient suitability and tolerance, scan sequence type (205), artefact (190, 206) and non-linearity of scale away from the centre of the scan (207, 208).

1.6.1.8.7 Conclusion

Cross sectional imaging is the only technique that can reliably measure muscle and fat distribution in the trunk and can discriminate between the intra-abdominal organ and muscle component of fat free mass. Although this technique can precisely track changes within an individual, the use of a single slice has limited ability to distinguish true differences in *total* body composition between individuals. Despite these limitations, CS imaging offers significant advantages over other methods for body composition analysis in patients with cancer cachexia due to its convenience for both the patient and researcher and tissue specificity.

1.6.2 Body composition models

Body composition may be considered at many different levels and at varying degrees of complexity. Models may describe the body according to tissue type, chemical composition or anatomical distributions and may be divided into 2, 3, 4 or more compartments. These considerations give rise to the 5 level model of body composition and the description of body compartments when used in practice.

1.6.2.1 Five level body composition model

Body composition models may be described according to the five levels of human body composition (137). These are atomic, molecular, cellular, tissue system (functional) and whole body. Figure 5

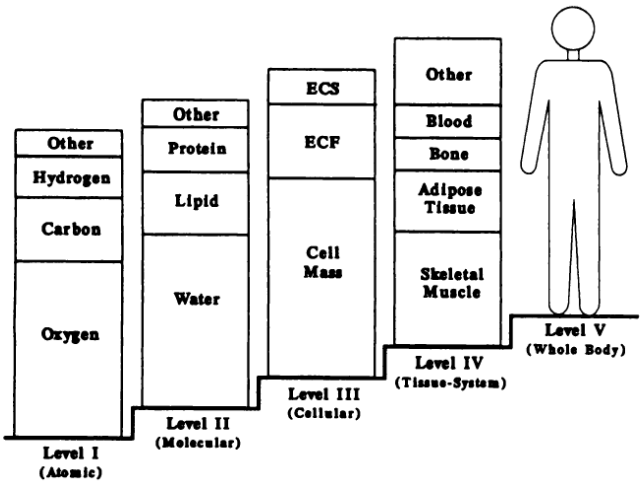

FIG 1. The five levels of human body composition. ECF and ECS, extracellular fluid and solids, respectively.

Figure 5 – Five levels of human body composition, from Wang et al (137)

The component of interest will determine which body composition level is used, the particular method or methods used for measurement will determine which component or groups of components are described within each model. For example four components may

be described according to the molecular level model but the method used may only be capable of quantifying the components as fat or fat free mass.

1.6.2.1.1 Level I: Atomic

Techniques exist to measure all 50 of the elements that are found in the human body, four of these Oxygen (O), Carbon (C), Hydrogen (H) and Nitrogen (N) account for 95% of body mass, and the addition of Sodium (Na), Potassium (K), Phosphorous (P), Chlorine (Cl), Calcium (Ca), Magnesium (Mg) and Sulphur (S) make up 99.5% of total body mass (150). Clearly, whole body direct atomic level measures are not possible with *in vivo* body composition analysis, however a number of elements may be estimated using knowledge of the exchangeable compartment of an element – its volume of distribution. These elements may be measured with a radioisotope or using an exogenously administered element with similar properties as a difficult to measure endogenous element e.g., bromide for chloride distribution. These atomic level measurements may be used to estimate body components of more biological interest such as nitrogen used to estimate protein, where established stoichiometric relationships exist between the atomic and higher level component. Other examples include total body potassium counting and in vivo neutron activation.

1.6.2.1.2 Level II: Molecular

Molecular level analysis is commonly used in body composition research. Here there are five main components; lipids, water, proteins, carbohydrates and minerals (137). Body composition may be described by simple division of these components into two groups (two compartment model: fat and fat free mass) or into more complex multi-compartment models (138). Furthermore, each component may be divided into sub-fractions. Lipids may be divided into essential and non-essential lipids. Non-essential lipids are the triacyglycerols and are referred to as fats these represent the energy storage compounds and are equivalent

to “fat mass”(150). The essential lipids are those required for cell structure, biochemical and physiological processes and include lipids of cell membranes and would usually be included in the “fat free mass” body component depending on the measurement technique used. Water may be considered as extracellular or intracellular and extracellular fluid may be further subdivided into interstitial and vascular components, plasma, connective tissue, bone and gastrointestinal tract components. Protein may be considered as total protein or as muscle and non-muscle proteins. The carbohydrate component is almost entirely glycogen, present in liver (~1% wet weight) and skeletal muscle (~2% wet weight). Finally, the mineral component includes bone and soft tissue mineral. The methods used to measure molecular level components include isotope dilution, densitometry and DXA methods.

1.6.2.1.3 Level III: Cellular

There are three components at the cellular level: body cell mass (BCM), extracellular fluid (ECF) and extracellular solids (ECS). The component generally of most interest here is the cell mass. Extracellular solids consist of bone minerals, collagen, reticular and elastic fibres. Extracellular fluid consists of extracellular water and the soluble electrolytes and proteins dissolved in it, making extracellular fluid a slightly larger component than extracellular water (by 2%). The volume of the extracellular fluid compartment and its plasma content can be directly measured by dilution methods. There is no direct measure of extracellular solids *in vivo* although can be estimated by measurement of total body calcium (TBCa) by neutron activation analysis where ECS=TBCa/0.177 (137). Alternatively, bone mineral can be estimated by DXA. The cell mass component may be estimated using total body potassium (TBK) where body cell mass (BCM) = 0.00833 x TBK. BCM excludes intracellular fat as the model can be written as body weight = fat + BCM + ECF + ECS. The methods used to measure cellular level components include isotope dilution, total body potassium (or bromide space) and DXA or NAA.

1.6.2.1.4 Level IV: Tissue system

The tissue system level comprises different functional or anatomical tissue components. These are adipose (subcutaneous, visceral, yellow marrow and interstitial), skeletal muscle, bone, visceral organs and brain. Assessment of body composition at this level is highly relevant in clinical research as it distinguishes components that have distinct physiological and anatomical functions. Precise tissue level assessments can be made from dissection of cadavers but imaging techniques are used to determine different tissue types in vivo. These include computer tomography (CT), magnetic resonance imaging (MRI) and to a lesser extent DXA and ultrasound scanning (USS). Non-imaging techniques can also be used to distinguish particular tissue types such as the use of 24-h urinary creatinine and 3 methyl histidine for estimation of muscle mass.

1.6.2.1.5 Level V: Whole body

The whole body level includes a general description of the physical properties of the body as a whole and concerns body size, shape and physical characteristics. These include measurement of height, weight and body density along with a variety of other specific anthropometric measurements. Alterations in body components measured by other models are reflected in changes in these anthropometric measurements and some inferences as to alteration in tissue, cellular or molecular changes can be made although these are imprecise. Different physical characteristics (such as BMI) are also often considered as specific risk factors in populations. These measurements are generally easy to perform and are most often used in large scale population studies.

1.6.2.2 Multi-compartment body composition models

1.6.2.2.1 Two compartment model

The simplest body composition model describes two body compartments. These are fat (fat mass, FM) and non-fat tissues (fat free mass, FFM). This typically requires a single measurement such as TBW measurement, TBK, anthopometry, BIA or hyrodensitometry. The measurement on these examples measures the fat free mass and the fat mass is calculated from knowledge of whole body mass. Apart from the crude mature of the description, these methods rely on assumptions of constant tissue compositions such as fat free mass hydration of potassium concentration which could be disturbed in certain populations or diseases.

1.6.2.2.2 Three compartment model

Addition of a second measure allows expansion of the model to a 3C model. For example addition of TBW to underwater weighing or TBK can provide a measure of body water, fat and fat free solid mass. This model relies on the same assumptions made in the 2C model.

1.6.2.2.3 Four (or multi) compartment model

There are two basic 4C models, the Fuller model corresponding to the molecular level in Wang's 5 level model and the Wang model corresponding to the cellular level in the 5 level model. The first method incorporates body weight, underwater weighing or air displacement plethysmography with TBW and DXA to provide a measure of water, protein, mineral and fat.

The Wang 4C model measures body cell mass (BCM), extracellular fluids (ECF) and extracellular solids (ECS) in addition to weight. BCM is measured by whole body K counting, ECF by measuring TBW and subtracting ICW (derived from BCM) and ECS by DXA. Fat mass is then whole body mass – (BCM+ECW+ECS).

The principal difference between 2C and 4C models is the latter's ability to account for hydration changes. For all ages and conditions, the 4C model should be regarded as the reference point however potential errors still exist as the measurement errors may propagate.

As the ECS/mineral compartment is minor in both 4C model variants, it can be assumed to be a fixed portion of FFM.

1.7 Measuring protein dynamics / balance in skeletal muscle

Skeletal muscle comprises around 30-40% of adult body mass in men and 20-30% in women. The turnover rate is relatively low at around 1% per day but the large quantity of protein within skeletal muscle in an individual make this rate a significant component of whole body protein metabolism. In an average male with 24kg of skeletal muscle this equates to 240g per day, as a result, pathological changes to the balance between synthesis and degradation may rapidly result in significant alteration of whole body lean mass (136). As discussed in the previous section, muscle mass and change over time may be quantified via a variety of body composition methods. However, skeletal muscle mass and change in muscle mass is determined by a balance of synthesis vs degradation which are not adequately explored by measuring body composition alone. Each of these processes (synthesis or degradation) may be up or down regulated by a variety of physiological or pathological processes acting through complex and incompletely understood mechanisms. In situations where synthesis exceeds degradation an increase in muscle mass will be observed and where degradation occurs faster than synthesis muscle wasting will result. In diseases of muscle wasting such as cachexia the overall net loss of muscle may be a result of a fall in muscle synthesis or an increase in degradation or a combination of both. It is important to determine the extent to which a reduction in muscle protein synthesis is responsible for falling muscle mass in conditions such as cachexia and aging. Currently, research into the mechanisms of muscle loss in cancer has focussed on degradation pathways, however, a depression of muscle synthesis may be an equally or more important factor (62). It is therefore important to be able to measure accurately skeletal muscle synthesis and its response to stimuli in a variety of research and clinical settings. If an accurate picture of

skeletal muscle protein synthesis is given in combination with measurements of muscle mass, then muscle protein breakdown can be derived by balance.

1.7.1 Measures of skeletal muscle synthesis

Skeletal muscle synthesis is typically determined by the measurement of the rate of incorporation of a labelled tracer into muscle tissue. In human in vivo research the tracer takes the form of an essential amino acid (such as leucine, valine or phenylalanine) labelled with a stable isotope such as ^{15}N, ^{13}C or ^{2}H (209). It is required to be absorbed and distributed in the body in a predictable manner so it is administered by intravenous infusion and given in a suitable dose over a reasonable timeframe compatible with the rate of muscle synthesis in order that detectable amounts may be found in a muscle biopsy taken at the end of the protocol. The fractional synthetic rate (FSR) may be estimated from the change of abundance of the tracer incorporation of the labelled amino acid into the muscle protein relative to the labelling of the pool from which the amino acid is incorporated into the protein (210). Some practical problems exist with the technique. These include difficulty in measuring the precursor pool (amino-acyl tRNA pool), ensuring that there is adequate incorporation of tracer into muscle protein over the time period of interest and the possible influence of amino acid tracers on protein metabolism. Two commonly used variations on the technique exist (the flooding dose method or primed constant infusion) with advantages and disadvantages present in each (210-212).

1.7.1.1 Flooding dose

The flooding dose method utilises a single large dose of a labelled (and unlabelled) amino acid administered over seconds or minutes. This approach saturates the uptake of amino acids by the tissue minimising the labelling gradients between plasma and tRNA bound amino acids. The major advantage of this is that this enables amino acid labelling in the plasma pool to be used as a precursor (213, 214). One of the main features of the technique

is that it allows measurements of tissue protein synthesis to be made over short periods of time, typically 30 minutes to 2 hours. This means that rapid measures can be made to assess the influence of acute interventions, is more convenient for participants as it does not require a prolonged infusion and also is less sensitive to non-steady state conditions. A major criticism of the flooding dose approach is the observation that large doses of amino acids may perturb normal amino acid transport and metabolism and influence the synthesis of muscle protein. The extent to which this occurs appears to be dependent on the amino acid tracer used, the protein undergoing analysis and the physiological state of the subject. In human skeletal muscle protein, the tracer ^{13}C-leucine given by the flooding dose method in a fasted state provides an estimate of fractional synthetic rate that is twice that seen using a primed constant infusion. A similar although less dramatic difference is seen in individuals in a fed state (211). This increase in the estimate of fractional synthetic rate seen with flooding dose protocols can also be demonstrated using a constant infusion method to estimate the effect of the amino acid flood (215-217). Using this experimental design a flooding dose of either leucine or valine increases the rate of labelling (a higher rate of muscle protein synthesis) by either phenyalanine or valine administered as a primed constant infusion.

1.7.1.2 Primed constant infusion

The primed constant infusion method aims to minimise the stimulation of protein fractional synthetic rate by giving a slow infusion of labelled amino acid tracer at a lower dose, aiming to achieve labelling in the free plasma pool of 5-10% - a level which is believed not to influence amino acid metabolism (218). The use of this approach introduces practical problems with the administration and measurement of the labelled amino acid tracer. The issue arises from the need for a prolonged intravenous infusion. The lower concentration of amino acid tracer in the precursor pool requires longer protocols, particularly when measuring slow turnover proteins such as in skeletal muscle in order to ensure adequate

tracer incorporation over the timeframe of the study protocol. Labelling periods may typically be of 4-14 hours (219), during which time participants are required to remain attached to an intravenous infusion and conform to strict feeding/fasting regimes or physical activity protocols.

1.7.2 Measures of skeletal muscle degradation

1.7.2.1 3-methylhistine excretion

3- methylhistidine is an amino acid formed by methylation of peptide bound histidine. It is present in actin and myosin and is excreted in the urine when these protein are broken down (220). It is not reused for protein synthesis and if given intravenously more than 95% is excreted unchanged by 48 hours (221). As a result, urinary 3-methylhistidine can be used as a measure of muscle breakdown. This is usually achieved via 24 hour urine collections and may be combined with a urinary creatinine estimate of muscle mass to give a fractional catabolic rate. The primary disadvantage of this method is the need for a meat free diet. The use of urinary 3-methylhistidine may be inaccurate in individuals with very low muscle mass where non muscle sources may begin to contribute a measureable proportion of excreted 3-methlyhistidine. This difficulty may be largely overcome by the use of serum 3-methylhistidine for the measurement of flux in a single limb (this is the arterio-venous difference times blood flow (63)).

1.7.2.2 Tracee release method

This method is the reverse of the tracer methods used for measuring muscle FSR. It involves infusing a stable isotope tracer intravenously to reach an equilibrium and then observing its decay in the arterial blood and muscle intracellular pool. The calculation of fractional breakdown rate FBR is based on the rate at which tracee released from breakdown dilutes the

intracellular enrichment using a modified precursor-product equation. This method requires a constant infusion protocol and a muscle biopsy to determine the plateau intracellular enrichment and takes around three hours to perform (222).

1.7.3 Measuring muscle protein balance.

1.7.3.1 A-V difference methodology

Individual measures of rates of skeletal muscle protein synthesis or degradation do not correspond with changes in net protein balance (32). As a result Wolfe et al developed a method to allow the "simultaneous measurement of both muscle protein synthesis and breakdown and therefore a measure of net muscle protein balance" (32). This is the A-V balance method. In this method a constant arterial infusion of labelled amino acid is administered into a limb and levels measured in the venous outflow. Net synthesis and breakdown is measured from the difference, which represents the incorporation of the tracer rather than by muscle biopsy. This method has some significant limitations in practice as it requires steady state conditions, particularly with respect to infusion rates and blood flow that prevents its use during exercise. It also provides a measure of limb (including skin, fat and bone) rather than muscle protein turnover (223).

1.7.4 Heavy water methodology

The measures of muscle protein metabolism described above are short term, are invasive, require carefully controlled conditions including those of diet and exercise and perform best in steady state conditions. The use of the stable isotope deuterium (^2H) could make it possible to develop a measure of skeletal muscle synthesis that reduces or avoids these disadvantages as well as minimising concern over measurement of the precursor pool (224). Deuterium has been used to measure metabolism of different tissue types in a variety of settings. Administered in the form of heavy water (^2H_2O) deuterium equilibrated in body

water in humans throughout all tissues in the body in around one hour and eliminates from the body with a half-life of around one week. Endogenous labelling of nonessential amino acids occurs rapidly which are then incorporated into proteins via tRNAs. The stable C-H bonds do not exchange hydrogen with body water and so make $^{2}H_2O$ a good label for measuring protein synthesis (224).

Previous studies have used $^{2}H_2O$ in experiments of body water turnover, glucose, carbohydrate, liver protein, lipid metabolism and nucleic acid synthesis in healthy humans and as doubly labelled water in energy expenditure study in patients with cancer (225). This has no adverse effects other than nausea and vertigo which may occur if the percentage in total body water is increased too rapidly. In animals oral $^{2}H_2O$ dose has been used to measure skeletal muscle protein fractional synthetic rate. These protocols have involved high doses typically with an initial peritoneal bolus (226) or labelling beginning in utero (224). Enrichment is then maintained with 4% or 8% $^{2}H_2O$ in drinking water to maintain a plateau similar to that seen in the primed constant infusion method. At the end of the experimental protocol the animal may be sacrificed and protein synthesis in any tissue examined. Gas chromatography / mass spectrometry (GC/MS) analysis of protein-bound ^{2}H-alanine enrichment in mice is then used to calculate skeletal muscle fractional synthetic rate and in mice may be in the region of 0.27% hr^{-1} (226).

$^{2}H_2O$ may be safely given to humans at a rate to increase ^{2}H labelled body water by not more than 0.5% per day. This has been used increasingly widely in high turnover proteins such as liver protein synthesis and other metabolic pathways. Currently two studies have attempted to measure skeletal muscle synthesis with a $^{2}H_2O$ tracer in man (227, 228). Robinson et al compared skeletal muscle synthesis in aerobic training vs control participants over 6 weeks. Total body water $^{2}H_2O$ was raised to 1.5 – 2.5% with the administration of multiple regular doses beginning with a one week priming week and then twice daily dosing over the

subsequent 5 weeks. Fractional synthetic rate was calculated using alanine enrichment measured by GC/MS. In addition DNA synthesis was calculated in a similar manner. The older exercise group had higher rates of muscle protein synthesis compared with a younger sedentary group (7.4±1.0 vs 5.54±1.0%/wk) and also showed skeletal muscle DNA synthesis of 4% over the training period compared with zero in the sedentary group. This study shows that the method can be used to measure muscle synthesis over long time period compatible with interventions in humans. The disadvantages of this protocol are in the repeated dosing, multiple muscle biopsies and use of mixed muscle protein. Compared with animal studies where the animal may be sacrificed at the end of the protocol, human studies have access to limited amounts of tissue of ranging from 20 to 150mg as they are usually restricted to needle biopsy specimens. The dosing in animal studies also allows for the animals total water consumption to consist of $^{2}H_2O$. These two factors combined with the low turnover of skeletal muscle protein result in very small amounts of detectable enriched amino acid such that it may be insufficient for accurate measurement (224). The study by Robinson overcame this with a long period of repeated dosing. A consequence of this was the need for two biopsies to be performed as baseline muscle protein alanine had to be measured after the priming week as body $^{2}H_2O$ reached the plateau phase. Additionally mixed muscle protein synthesis was measured, presumably to minimise losses from sample processing.

In studies of muscle wasting conditions a multiple dose, multiple biopsy protocol is undesirable as patients with these conditions may be unable or unwilling to comply, particularly if also undergoing treatment or intervention for their condition. It may also be desirable to measure myofibrillar rather than mixed muscle protein synthesis. Differences in the protein fraction measured may contribute to the current variability in measurement of muscle protein synthesis (219) and intervention may alter one fraction differently to another, Gasier et. al. noted a 20% increase in myofibrillar FSR compared with mixed protein FSR in response to resistance exercise using a $^{2}H_2O$ labelling protocol (227). A single dose, single

biopsy protocol, measuring myofibrillar FSR could be developed using the known predictable kinetics of body $^{2}H_2O$ and utilising the increased sensitivity of Gas Chromatography-Pyrolysis-Isotope Ratio Mass Spectrometry (GC-P-IRMS) (229). A further advantage of a single dose is that accurate estimates of body composition can be made simultaneously by isotope dilution.

1.8 Thesis aims

The overall aim of the thesis is to explore the benefits, limitations and results obtained by the use of different technologies to measure muscle mass and muscle protein dynamics in both health and muscle wasting conditions such as sarcopenia of old age and cancer cachexia.

i. To determine the need for, and limits of, routine clinical imaging and other cross sectional imaging to define abnormal muscle mass and quality (Chapters 3,4,5)

ii. To use cross sectional imaging techniques to assess altered distribution of body muscle mass and to describe changes in regional muscle mass with time. (Chapters 6,7,8)

iii. To develop a novel protocol for the measurement of myofibrillar protein synthesis that places a limited burden on the patient. (Chapter 9)

iv. To evaluate the use of this novel measure in patients with cancer assessing regional differences in muscle synthetic rate and muscle synthetic rate in patients with cancer vs healthy individuals. (Chapter 10)

2 Methods

2.1 Participant Groups

Data from patient and volunteer participants in this thesis was drawn from four sources. One previous study in healthy individuals in Edinburgh and Aberdeen, one on-going study of patients with upper GI cancer in Edinburgh, a pilot study of healthy individuals initiated and completed as part of this thesis and a follow on comparison of healthy individuals and patients with cancer initiated and completed as part of this thesis. Each study received approval from the regional ethics committee.

i. Muscle and aging study – A previous study of young and elderly volunteers from the Royal Infirmary of Edinburgh and Aberdeen Royal Infirmary undergoing functional assessment, biopsy and MRI of quadriceps (n= 63 older volunteers, n=33 young volunteers)[5].

ii. CRUK cancer biomarker study – An on-going study of patients with upper GI cancer at the Royal Infirmary of Edinburgh undergoing functional assessment, MRI quadriceps, CT scan, blood, urine and muscle sampling. (n=121 patients with cancer)[6].

iii. Oral tracer pilot study - Healthy volunteers recruited prospectively in the oral tracer pilot study performed primarily as part of this thesis. (n=5 male healthy volunteers)

iv. Habitual skeletal muscle synthesis in health and in cancer study - Healthy volunteers and patients with upper GI cancer at the Royal Infirmary, recruited prospectively as part of this thesis. (n=6 healthy volunteers, n=15 patients with cancer)[7].

[5] I acknowledge Dr Carolyn Greig who recruited and tested volunteers for this study
[6] I acknowledge Dr Carolyn Greig and Mr Nathan Stephens who recruited and tested volunteers for this study
[7] I acknowledge Mr Neil Johns who assisted with recruitment and biopsy of patients in this study

2.2 Participant recruitment

2.2.1 Healthy volunteers

2.2.1.1 Muscle and aging study

Data was analysed from participants previously recruited to studies of muscle mass and function in healthy elderly and young individuals, taking place at the University of Edinburgh and University of Aberdeen. Participants were recruited via local advertisement and completed a screening health questionnaire (230).

2.2.1.2 Oral tracer pilot study (muscle protein synthesis)

Healthy volunteers were approached via email advertisement circulated within the University of Edinburgh Little France site. Interested participants were sent a participant information sheet and a health questionnaire (appendix 1). This was intended to exclude any individuals with significant co-morbidity and was modified from a health questionnaire designed to screen healthy elderly individuals (230).

2.2.1.3 Habitual skeletal muscle synthesis in health and in cancer – healthy volunteer group

Healthy volunteers were approached via email advertisement circulated within the local university site, by advertisement in local free advertising websites and local community magazines and also by poster advertising in the University of Edinburgh and NHS at the Royal Infirmary of Edinburgh. These individuals also completed a screening health questionnaire

2.2.2 Patient volunteers

2.2.2.1 CRUK biomarker study (cancer cachexia)

Patients with gastric, oesophageal and pancreatic cancer undergoing staging investigations for potentially curative surgery at the Royal Infirmary of Edinburgh were recruited as part of an on-going CRUK funded study into cancer cachexia biomarkers. Patients were identified at the Upper gastrointestinal MDT and recruited during outpatient clinic attendance. Not all patients subsequently went on to have curative surgical resection.

2.2.2.2 Habitual skeletal muscle synthesis in health and in cancer – patient group

Patients with gastric, oesophageal and pancreatic cancer booked for potentially curative surgery at the Royal Infirmary of Edinburgh were recruited the study skeletal muscle protein synthesis measured using and oral tracer in patients with cancer and healthy volunteers. Patients were identified at the Upper gastrointestinal MDT and recruited during outpatient clinic attendance. All patients subsequently went on to have curative surgical resection.

2.3 Study Protocols

2.3.1 CRUK biomarker study protocol

Patients were identified at the upper Gastrointestinal MDT and approached at their routine pre-operative clinic appointment and patient information sheets provided. Formal written consent, MRI scans and functional assessments were performed during a dedicated visit at the Wellcome Trust Clinical Research Facility (WTCRF) during the week prior to surgery. Quadriceps biopsy was obtained at the time of surgery. Follow up visits were scheduled for repeat MRI and function at approximately 3 monthly intervals post operatively. Patient data was prospectively collected with CT scans being obtained retrospectively.

2.3.2 Oral tracer pilot study protocol

Ethical approval for the study was obtained from the South East Scotland Research Ethics Committee, co-sponsored by the University of Edinburgh and NHS Lothian Health Board. Participants were recruited by local advertising. Interested participants were provided with an information sheet and completed a health assessment questionnaire. The initial visit was made at the WTCRF where formal written consent was obtained. Height and weight were recorded and a baseline blood sample taken. The tracer dose was taken in a single bolus as 70g of deuterium diluted with tap water to a final volume of 100mls. The participant returned on three further occasions staggered over the course of 2 weeks for further blood sampling. On each of these subsequent post-dose visits a percutaneous quadriceps biopsy was taken Figure 6. No specific dietary or exercise instructions were given and volunteers were encouraged to maintain their normal regimen.

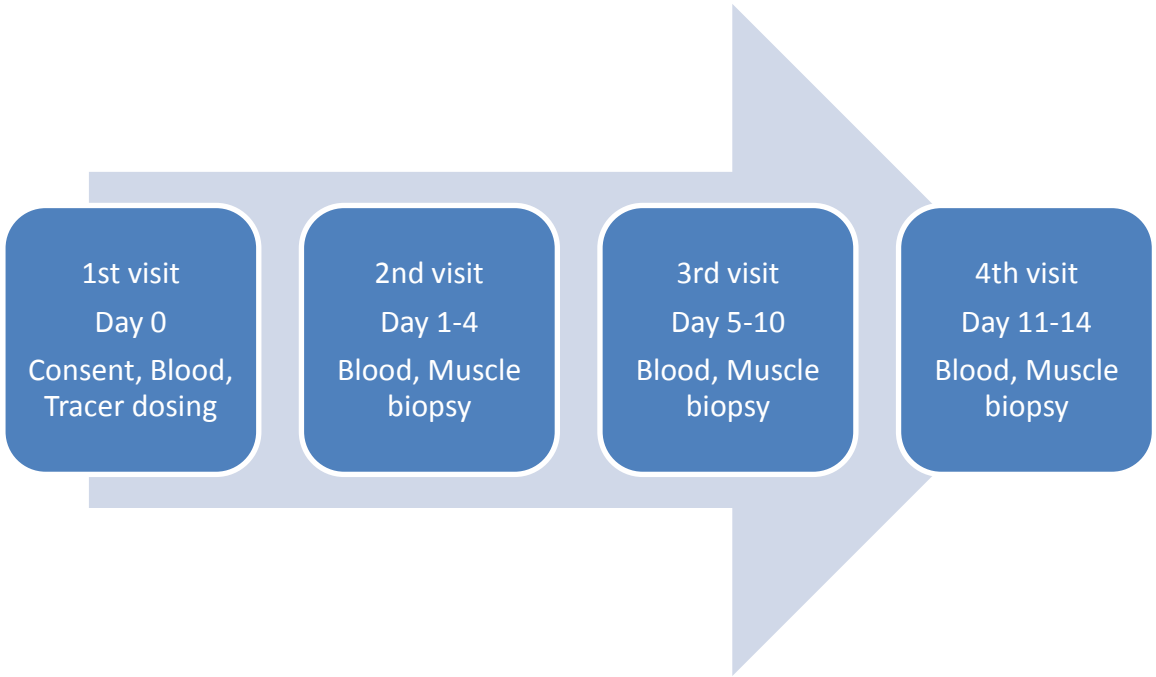

Figure 6 - Oral Tracer Pilot Study Protocol for measurement of protein synthesis in skeletal muscle.

2.3.3 Habitual skeletal muscle synthesis in health and in cancer study protocol

2.3.3.1 Healthy volunteers

Ethical approval for the study was obtained from the South East Scotland Research Ethics Committee, co-sponsored by the University of Edinburgh and NHS Lothian Health Board. Healthy volunteers attended the WTCRF where formal written consent was obtained. Height and weight were measured and a baseline blood and urine sample taken. The tracer was taken as a single dose of 90g of deuterium oxide, diluted in tap water to a total volume of 135mls. Volunteers returned approximately 24 hours later for a second blood and urine sample. A container was given to volunteers to collect a urine specimen at home. A final visit was arranged between 7 and 14 days after dosing for blood sampling, urine sample and quadriceps muscle biopsy, the patients self-collected urine sample was handed in a this visit (Figure 7). No specific dietary or exercise instructions were given and volunteers were encouraged to maintain their normal regimen.

2.3.3.2 Patient volunteers

Patient volunteers were initially approached at the surgical out-patient clinics where they were given a patient information sheet and health questionnaire. A follow up phone call was made 24 hours later and patients expressing an interest were enrolled. The initial visit was made in the patient's own house. Formal written consent was obtained, blood and urine sampling was performed and the tracer taken as a single dose of 90g of deuterium diluted in tap water to a total volume of 135mls. A second visit was made in the patient's house, blood and urine samples were taken and a specimen container provided for a self-collected urine. The final meeting with the patient occurred when they attended for surgical resection of their cancer at approximately 6-14 days after dosing. The self-collected urine sample was handed in, height and weight information was gathered from the pre-operative assessment. A catheter specimen of urine was taken after induction of anaesthesia and blood sampling taken

either during insertion of intravenous catheter or as a sample from an arterial line. Quadriceps muscle biopsy was taken in the anaesthetic room whilst under general anaesthetic. Rectus muscle biopsy was obtained by sharp dissection by the operating surgeon from the abdominal wound (Figure 7). No specific dietary or exercise instructions were given and volunteers were encouraged to maintain their normal regimen.

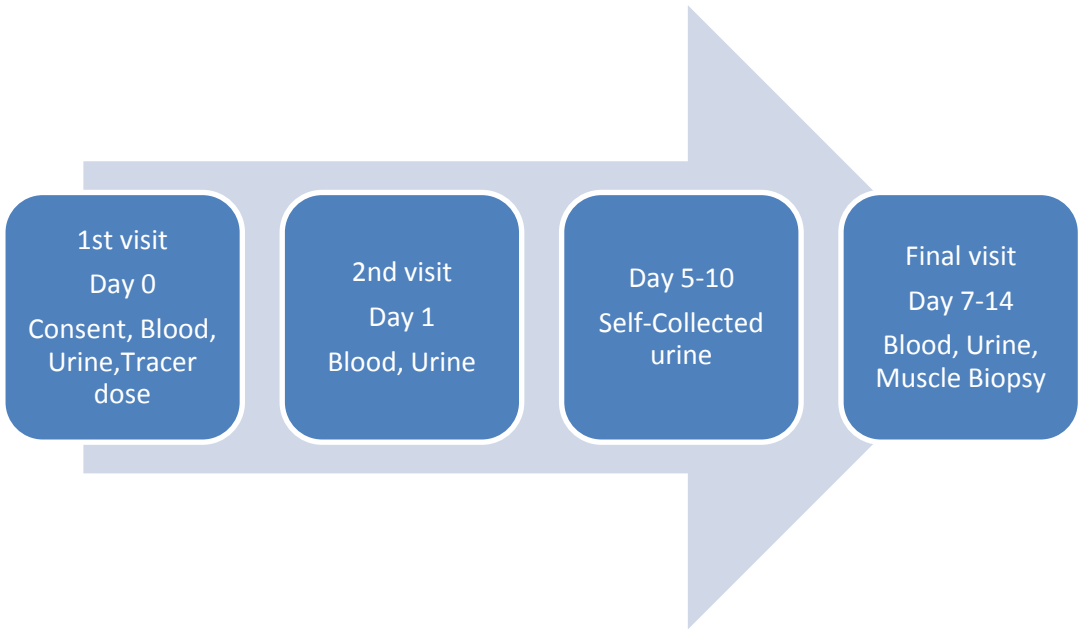

Figure 7 - Protocol for Oral tracer study of the comparison of skeletal muscle synthesis in healthy volunteers and patients with cancer

2.4 Muscle mass measurement by cross sectional imaging

2.4.1 Computed Tomography (CT) body composition analysis

2.4.1.1 CT scan identification and location

CTs were either retrieved from current computerised records (PACS) at RIE, from peripheral hospital or from historical records a variety of sites.

2.4.1.1.1 Current CTs at Royal Infirmary of Edinburgh

Patients routine diagnostic and staging CT scans were analysed for muscle mass assessment. Recent CTs performed at the Royal Infirmary of Edinburgh were easily identified from the electronic clinical record (TrakCare, InterSystems Corporation, Cambridge Massachusetts). CTs could then be found on the PACS (Picture Archiving and Communications System) electronic x-ray viewing system.

2.4.1.1.2 Current CTs at peripheral hospitals

As the RIE is a tertiary referral centre for the East of Scotland a number of patients had CT scans performed at peripheral hospitals not fully integrated into the national PACS archive. These scans were not recorded on the local TrakCare system. It was possible to obtain a number of these CT scans by liaison with the local radiology or PACS manager in order to transfer the scans to the National Archive.

2.4.1.1.3 Historical CTs

CTs performed prior to implementation of the PACS and TrakCare system were obtained from magneto-optical discs stored in the department of radiology. The Radiology Information System (RIS) previously used to record radiological examinations was consulted to identify the date of CT scans. This information was then cross referenced to the paper log for the CT scanner on the date of the scan to identify the ID code for the magneto-optical disc on which the CT scan was stored. This disc was then located from storage and uploaded

to the PACS system. During the course of this study a replacement of the CT scanning equipment resulted in the loss of equipment to read the magneto-optical discs. CT scans were then read with a Plasmon 520 magneto-optical drive connected to a laptop via a SCSI adapter. Read-o-matic and DICOMatic software (Tomovision, Canada) was used to read the discs and convert the images from proprietary to the DICOM format.

2.4.1.2 Slice selection and preparation

Two cross sectional images were located at the level of the third lumbar vertebra (L3) on abdominal CT scans. L3 was identified by locating the lowest thoracic vertebra (the lowest vertebral body with ribs) and counting vertebra in a caudad direction. The slice with both transverse processes visible was taken as the first slice. Cross sectional images were saved in the DICOM format and anonymised with DicomWorks software (Philippe Puech). Quality control was performed at this stage noting the presence of abdominal wounds (on post-operative scans), extensive tissue oedema, oblique cross sections and scans with portions of the abdominal wall lying outside the scan area.

2.4.1.3 Tissue segmentation

Muscle CSA was measured with SliceOmatic V4.3 software (Tomovision, Canada) according to a previously established protocol (186)

Tissue segmentation was performed using Hounsfield unit ranges -29 to +150 for muscle, -190 to -30 for subcutaneous adipose, -190 to -30 for intermuscular adipose, -150 to -50 for visceral adipose. Each tissue type was manually delineated using the region growing tool. Care was taken to exclude intestinal contents and abdominal viscera such as pancreatic, renal and hepatic tissue where present. Muscle groups included were Quadratus lumborum, Erector spinae, Psoas major and minor, Internal abdominal oblique, Transversus Abdominus, External abdominal oblique and Rectus abdominus Figure 8.

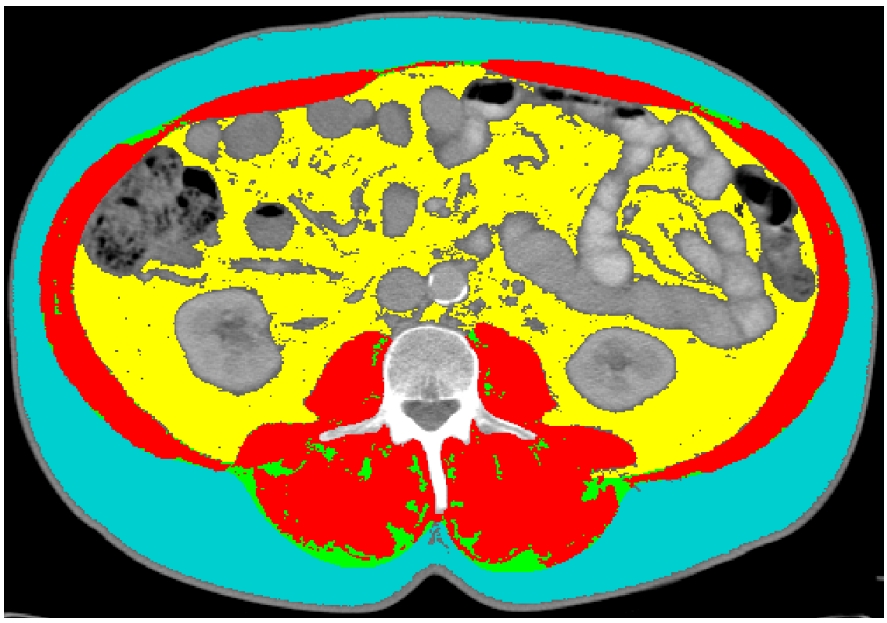

Figure 8 - Segmented L3 CT cross sectional image. Red = Skeletal muscle, Blue = Subcutaneous adipose, Yellow = Visceral adipose, Green = Intermuscular adipose

The software outputted data as a cross sectional area in cm^2 and a mean Hounsfield unit value for each tissue. Cross sectional area of muscle and adipose was expressed as cm^2 adjusted for height.

2.4.2 Magnetic Resonance Imaging (MRI) body composition analysis

2.4.2.1 MRI acquisition

The mid-point of the upper arm and mid-femur point were land-marked prior to the scan according to International Standards of Anthropometric Assessment (ISAK) guidelines 2001). Mid-points were marked for future identification by securing a cod liver oil capsule to the skin, this proved to be the most reliable technique as the marker was then clearly visible on the MRI images. Participants lay supine within the 1.5 –T Phillips GyroscanIntera with the isocentre of the magnetic field located at the mid-femur point for the first series of thigh taken in a single acquisition or in two sequential acquisitions of upper and lower thigh and a

second series taken with the isocentre located at the mid-point of the upper arm. T1-weighted axial images were prescribed from the proximal border of the patella to the anterior iliac spine. Imaging parameters were: slice thickness 10 mm; acquisition matrix 512 x 512; echo time (TE) 15 ms; repetition time (TR) 425 ms; and flip angle 90°. The number of slices acquired ranged from 38-45 depending on thigh length. Total scan time was 6 minutes.

2.4.2.2 Muscle cross sectional area manual delineation

The cross sectional area (CSA) of muscle in each image was quantified off-line using ANALYZE 8.0 (Mayo Clinic, Rochester, USA) by a manual delineation technique.

2.4.2.2.1 Biceps

Biceps group were identified on a single cross sectional MRI image on the slice marked with the oil capsule

Figure 9. Muscle borders were outlines by the placement of movable splines. The region within this area was the highlighted with the fill tool and an output given in mm^2. This was corrected for height and expressed as cm^2/m^2.

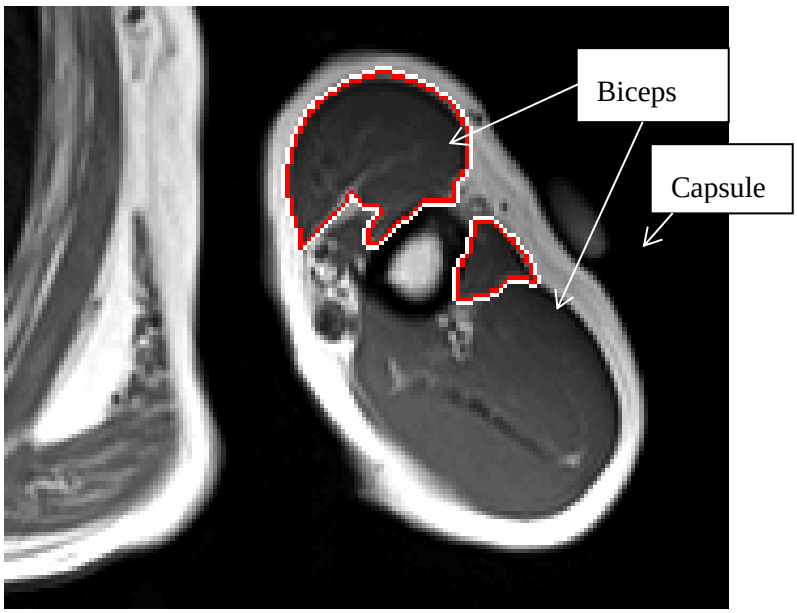

Figure 9 - Biceps group manual delineation by MRI. Figure shows biceps cross section (outlined) and oil capsule marker.

2.4.2.2.2 Quadriceps

Quadriceps group comprising Rectus femoris, vastus laterralis, Vastus medialis and Vastus intermedius were outlined around the facial boundary of the whole muscle group (Figure 10) in a similar manner to biceps to give a cross sectional area corrected for height in cm^2/m^2. This process was repeated for the all slices throughout the length of quadriceps. The area at the marked midpoint was noted. Muscle volume data was automatically calculated using all slices from measured slice area and known slice thickness. Images were carefully inspected to exclude overlapping slices which could occur around the midpoint when MRI of whole thigh was obtained in 2 acquisitions.

Figure 10 - Quadriceps manual delineation on MRI. Figure shows quadriceps at mid femoral point (outlined) and capsule marker

2.4.2.3 K-means muscle segmentation

An identical procedure was performed for both Quadriceps and Biceps. An automated in house programme based on k-means clustering was applied to the manually segmented image (57). The purpose of this was to exclude areas of fat lying within the muscle or between muscle groups to provide an objective measure of healthy muscle tissue. Careful examination of each individual slice processed was performed. The K-means processing was observed to fail on a number of scans, this occurred either due to low contrast across the scan as a whole or due to contrast gradients on individual slices. This did not occur across all slices of an individual scan and so it often was possible to obtain a mid-point k-means CSA when the k-means volume failed.

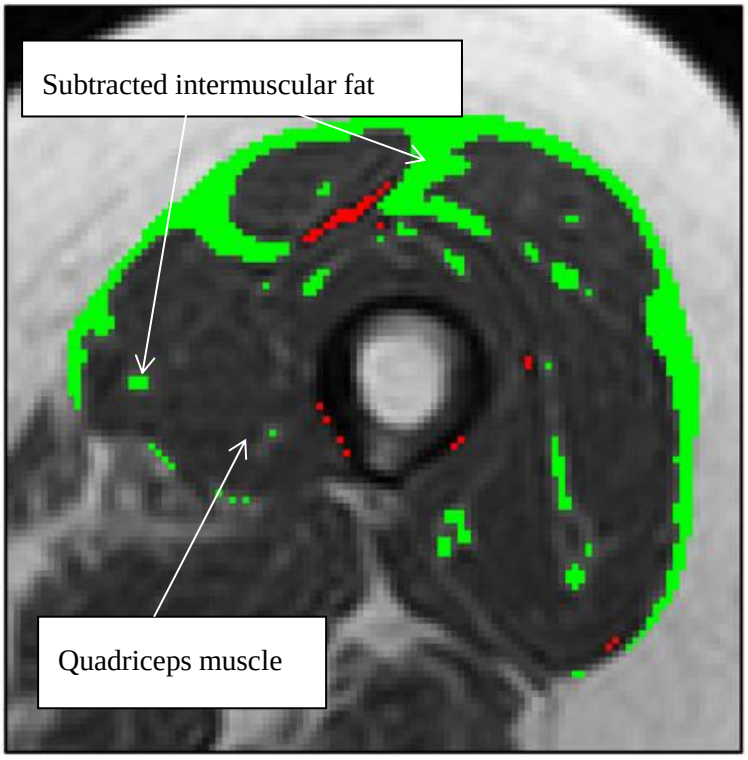

Figure 11 – MRI semi-automated k-means fat subtracted quadriceps muscle. Intermuscular fat highlighted in green is identified by the K-means method and subtracted from the manually delineated gross quadriceps area.

2.5 Functional measures

2.5.1 Sit to stand

Sit to Stand times (STS) (231, 232) were measured by two observers as the initial part of the timed up and go test using a digital stopwatch. The participant began seated with their arms by their side and feet placed on the floor in front of the chair. Following instruction the participant rose to a standing position. Timing began with the first movement forward and ended with a standing position. The sit to stand test is associated with coefficient of variation for repeated tests of between 6.8% (healthy volunteers) and 14% (elderly) (231).

2.5.2 Timed up and go

Timed up and go (TUG) (233) was measured in conjunction with the sit to stand test and timed by two observers using a digital stopwatch. The participant began seated in a straight backed chair. They were instructed to rise from the chair walk at their normal walking pace around a marker placed three metres away, return to the chair and sit down. The TUG test is recognised as a reliable and reproducible test with an inter-rater reliability intra-class correlation coefficient (ICC) of .99 and an intra-rater ICC of .98 (234).

2.5.3 Isometric Knee Extensor Strength

Maximum Isometric Knee Extensor Strength (IKES) (235) was measured with the participant seated in an adjustable straight-backed chair with the pelvis secured and the knee flexed at 90^{o}. A cuff was placed around the ankle and attached via an inextensible chain to a strain gauge and data acquisition system (Powerlab, AD instruments, UK). Following instruction, the participant made a maximum voluntary contraction which was held for 5 seconds. Three separate measurements (Newtons) were obtained for each limb and the highest value from the dominant limb used in subsequent analysis. The coefficient of variation for IKES is 6.9% for a single session and 10% across sessions occurring over several days (236).

2.5.4 Maximum Leg Extensor Power

Maximum Leg Extensor Power (Nottingham Power Rig) (LEP) was measured using the Nottingham Power Rig. The participant was seated on the rig with the seat position adjusted so that in full extension the footplate was fully depressed. The participant pushed as hard and as fast as possible against the footplate to accelerate the fly wheel. The final velocity of the flywheel was used to calculate the average power output (Watts) during a single maximal

thrust of the lower limb. The process was repeated five times with each limb and the highest value from the dominant limb used in subsequent analysis. The coefficient of variation for repeated tests of leg extensor power measured using the Nottingham power rig in healthy individuals 8.7% (237).

2.5.5 Hand grip dynamometry

Hand grip dynamometry (HGD) Patients were seated with the shoulder relaxed and the elbow flexed at 90º. Hand grip strength was measured using a hydraulic dynamometer (Fabrication enterprises inc., USA). Three measurements were obtained for each side and the highest value (kg) used in further analysis. Repeat measurements were performed following a rest of at least 2 min. Reproducibility assessed by repeated measurements demonstrates a coefficient of variation of 11.4% (237).

2.6 Tissue sampling

2.6.1 Muscle biopsy

Muscle biopsies were taken under local anaesthetic in the WTCRF for healthy volunteers. Biopsies in patients with cancer were taken in the anaesthetic room under general anaesthetic.

2.6.1.1 Quadriceps (vastus lateralis) biopsy

The participant lay in the supine position with the thigh exposed and the procedure was performed under aseptic conditions. The skin of the thigh was prepared with Betadine skin prep. Five to ten mls of 1% lignocaine (Lidocaine; Hameln Pharma Ltd., Gloucester, UK) was infiltrated into the skin and fascia and a small transverse incision (~5mm) made on the anterior aspect of the thigh at approximately the midpoint where the bulk of the muscle was

apparent. A Bergstom needle was passed through the skin incision aiming lateral to the femur to biopsy vastus lateralis with gentle suction applied. A number of earlier biopsies yielded only small sample and so in later participants a second passage of the needle was performed to improve sample size. Gentle pressure was applied after the procedure to ensure haemostasis, the wound was cleaned and steri-strips applied to close the wound. In patients with cancer the procedure was performed under general anaesthetic so the application of local anaesthetic was omitted. In a number of these patients Hartmann-conchotome forceps were used to obtain muscle the quadriceps biopsy in place of the Bergstom needle. Muscle biopsies were snap frozen in liquid nitrogen prior to storage at -80°C.

2.6.1.2 Rectus muscle biopsy

Rectus muscle was obtained in patients with cancer at the time of abdominal surgery. A sample approximately 0.5 to 1cm^2 of rectus abdominis muscle was obtained by the operating surgeon using sharp dissection avoiding the use of diathermy. Samples were blotted briefly on a swab to remove excess blood before bring snap frozen in liquid nitrogen and stored at -80°C.

2.6.2 Blood sampling

Venous blood samples were taken using 2 x 9ml serum Monovette tubes (Sarstedt, Nümbrecht, Germany). Samples were centrifuged at 4°C at 15 000 x g for 15 mins, plasma withdrawn with a pasteur pipette, divided into 1ml aliquots and frozen at -80°C prior to processing.

2.6.3 Urine sampling

Random urine samples were collected, specimens taken at any time of day other that the first voiding in the morning were considered suitable. Urine samples obtained in the presence of the patient were collected into plain sample containers, divided into 20ml aliquots and frozen

at -40°C prior to analysis. Self-collected patient urine samples were collected into 100ml containers containing 0.5g boric acid, divided into 20ml aliquots and frozen at -40°C ~24 to 48 hours after collection. Patients were instructed to record the date and time of self-collected sample collection.

2.7 Skeletal muscle biopsy processing

The objective of skeletal muscle processing was to produce a myofibrillar fraction and a sarcoplasmic fraction. The myofibrillar fraction could be further processed to isolate myosin and the sarcoplasmic fraction further processed to isolate free intracellular amino acids Figure 12.

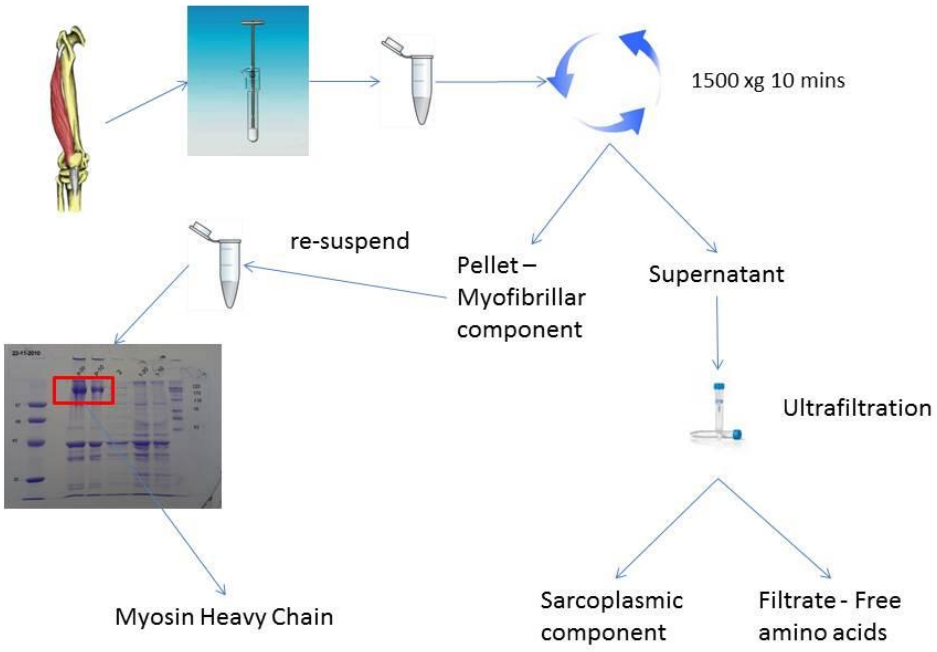

Figure 12 - Muscle processing schematic for estimation of protein synthesis using 'heavy water' protocol.

2.7.1 Homogenisation

Quadriceps biopsies were homogenised in a glass-glass hand homogeniser in 1ml of homogenisation buffer (250mM sucrose, 100 mM KCl, 20 mM imidazole, 5 mM EGTA,2 mM $MgCI_2$) at 4°C. Larger rectus biopsies were homogenised in 10mls of an identical buffer with an electric hand homogeniser.

2.7.2 Myofibrillar pellet isolation

The myofibrillar component was isolated by serial washes in Trition X-100 in a modification of the protocol by Solaro et al (238). Homogenates were centrifuged at 2500 x g for 20mins. The supernatant was withdrawn and retained as the sarcoplasmic fraction. The pellet was re-suspended in a buffer containing Triton X-100 (60 mM KCI, 30 mM imidazole, 2 mM $MgCI_2$, 0.1% Triton X-100) centrifuged at 2500 x g for 10 mins and the supernatant discarded. This was repeated two further times. The pellet was then re-suspended in wash buffer (150 mM KCl, 20 mM imidazole), centrifuged at 2500 x g for 10 mins and the supernatant discarded. The final was stage was repeated, a 10µl aliquot was withdrawn for verification of the fraction protein contents prior to final centrifugation, the remaining supernatant was discarded and the pellet frozen at -80°C prior to processing for GC-P-IRMS.

2.7.2.1 SDS-Page minigel verification

Protein samples were separated by 1D SDS / polyacrylamide gel electrophoresis (PAGE) on a 10 % Tris-HCl gel (Bio-rad) (239). The myofibrillar pellet was suspended in 1ml of homogenisation buffer and a Bradford protein assay (240) performed. 10µg of protein from both the sarcoplasmic fraction and myofibrillar suspension underwent denaturing at 95°C for 5 minutes in sample loading buffer and loaded into 33µl wells along with high and low molecular weight markers (Biorad). Gels were run at 200mV until the bromophenol blue marker reached the bottom of the gel. Protein bands were visualised by Coomassie staining.

Gels were incubated in Coomassie blue for 25 minutes, washed briefly with water and de-stained with a 20% methanol, 10% acetic acid solution in three washes of one hour duration each before being photographed over a light box.

2.7.2.2 Western blotting protocol

Myofibrillar and sarcoplasmic fractions were run on SDS / polyacrylamide gel electrophoresis as per (2.7.2.1). After gel running the gels were placed in a wet transfer system (Biorad) with a PVDF membrane and transferred at 0.1A for 30 mins followed by 0.3A for 30 mins. Transfer was performed with continuous stirring on ice in the cold room. The membrane was blocked with 1% bovine serum albumin (BSA) overnight in the cold room and then washed with TBS/Tween solution three times for 5 minutes each. The primary anti-myosin antibody (Sigma) was incubated at a concentration of 1:10000 for 2 hours at room temperature. A further three washes in 1% BSA were performed and the secondary goat-anti-mouse antibody (Sigma) incubeated at 1:5000 dilution at room temperature for 2 hours. Three washed in TBS/tween solution were performed. Chemo-luminescence solution was applied and film was exposed for 6 seconds in the darkroom.

2.7.3 Myosin isolation

Myosin was isolated for mass spectrometry analysis by SDS/ polyacrylamide gel electrophoresis (241). The myofibrillar pellet from a 30mg mouse muscle sample was re-suspended in 1ml of homogenisation buffer (2.7.1). Bradford protein assay was performed (240). 500µg of myofibrillar protein in 520µl was denatured at 95°C for 5 mins in 130µl of sample loading buffer containing 1mM Dithiothreitol (DTT). This was loaded into a 1.5mm thick 6% SDS PAGE mini-gel (Bio-rad) (consisting of one 33µl well and a second single large well) along with a high molecular weight marker (Bio-rad). The gel was removed and placed in a wash of colloidal Coomassie blue (Fisher) for 25 minutes at room temperature.

The gel was removed and washed in water three times for 30 minutes each time or until protein bands were clearly visible. The 200 kDa band was cut from the gel macerated with a sharp blade and placed into a 10ml vial. Gel pieces underwent further washing in water until colourless. Gel pieces were then dehydrated by serial washes in 100% acetonitrile and dried at room temperature.

2.7.4 Free intracellular amino acid isolation

The retained sarcoplasmic fraction was processed for free amino acids by a series of ultrafiltration steps. Initial small quadriceps biopsies were processed in 2-5ml filtration tubes while the later larger rectus biopsies were processed in 20-50ml filtration tubes, otherwise the process was identical for all sets of samples. Supernatant from the initial homogenate (2.7.1) was passed through 0.45µm and then 0.2µm filters using a syringe into 10ml or 50ml tubes as appropriate. The resulting filtrate underwent ultrafiltration in a 10kDa filtration tube (Vivaspin, GE Healthcare) in a centrifuge at 3000 x g for approximately 1-2 hours until run dry. The retentate was discarded and the filtrate frozen at -40°C until GC-P-IRMS analysis. 10µl aliquots were taken at each stage and run on SDS PAGE as per (2.7.2.1) to verify the success of each step.

2.8 Measurement of ^{2}H enrichment in body water, serum albumin alanine, free intracellular and myofibrillar alanine.[8]

2.8.1 Preparation of muscle biopsies

The washed myofibrillar protein pellet (the product of paragraph 2.7.2) was freeze-dried prior to acid hydrolysis. To avoid the need for additional biopsies to determine basal ^{2}H

[8] I acknowledge Sandra Small and Prof Tom Preston who performed this analysis at the Scottish Universities Environmental Research Centre, East Kilbride

abundance in protein-bound alanine, albumin was extracted from each basal serum sample by differential solubilisation in ethanol (242). Albumin and myofibrillar protein pellet samples were freeze dried prior to acid hydrolysis. Samples of ~2 mg protein were aliquotted into 4 mL glass vials (Chromacol, Welwyn Garden City, UK) where 4 at a time, they were placed in a PTFE cylinder. 0.5 mL 6M HCl was added to the cylinder. Oxygen was excluded by gassing the container with nitrogen before it was sealed within a steel pressure vessel (Parr, Moline, IL, USA). Samples were hydrolysed by gas phase acid hydrolysis at 150^{o}C for 4 hours (243).

Nor-leucine internal standard (300 nmoles) was added to each hydrolysis vial and the amino acids were dried in a vacuum desiccator over NaOH pellets. Amino acids were derivatised as ethoxy carbonyl ethyl esters. Briefly, 0.4 mL of solvent (60:32:8, deionised water:ethanol:pyridine) was added and the sample was swirled to dissolve. Ethyl chloroformate (0.02 mL) was added. The tube was swirled to facilitate reaction and CO_2 release. Dichloromethane (3 mL) and sodium bicarbonate were added (0.75 mL, saturated). Sample tubes were shaken to allow the phases to separate. Once the phases had separated, the upper phase was discarded and the lower phase was dried by addition of granular anhydrous Na_2SO_4. The residual solvent was blown off and the derivatised amino acids were re-dissolved in 0.3 mL hexane. They were transferred to 1.5 mL 'wineglass' GC vials for analysis and freezer storage. No independent protein analysis was undertaken as sample amino acid concentration could be estimated by comparison with the internal standard. Following GC analysis (see below) some samples contained insufficient sample and were rejected from the analysis. This was most likely due to a combination of low protein content in the original biopsy and processing yield.

2.8.2 Preparation of serum samples

Two mL serum samples were thawed for analysis. One ml (3 x 0.3 mL replicates) was used for analysis of ^{2}H enrichment in body water by continuous flow IRMS following gaseous equilibration with 20% H_2 in He in the presence of a platinum catalyst (20-22, SerCon, Crewe, UK) (225). Each sample batch included working standards calibrated against international reference waters. Gravimetric dilutions of each subject's dose were analysed against the same standards to facilitate total body water estimation. One mL of each serum sample was processed for analysis of free amino acid enrichment by cation exchange. Briefly, nor-leucine (300 nmoles) was added as internal standard. The samples were ultrafiltered to remove proteins and diluted to 8 mL with deionised water. Samples were acidified to pH 2 and amino acids were loaded onto 2ml bed volume columns of Dowex 50WX8-200 cation exchange resin and eluted with 5mL 2M NH_4OH and 5mL deionised water to purify. After vacuum drying into 4 mL vials, samples were divided into two equal aliquots and derivatised as ethoxy carbonyl ethyl esters, exactly as protein hydrolysates.

2.8.3 Gas Chromatography – Pyrolysis – Isotope Ratio Mass Spectrometry (GC-P-IRMS) of amino acids

An Agilent 7890 GC with a heated injector and split/splitless injection was used. The GC oven temperature programme was: start at 50^{o}C and hold for 1 minute; ramp at 25^{o}C/min to 150^{o}C; ramp at 2.5^{o}C/min to 200^{o}C; ramp at 1^{o}C/min to 220; ramp at 7.5^{o}C/min to 250 with a 1 minute hold. A constant carrier flow of 1.6 mL/min helium was used with pressure a programme. The GC was fitted with a capillary flow technology Dean's switch (Agilent, UK) which, under computerised pressure control, diverted the sample flow to a flame ionisation detector (FID) or a 1350^{o}C capillary pyrolysis furnace (Nu Instruments, UK) to convert analytes to H_2 gas prior to the IRMS open/split. It was activated after 26 minutes and again after 44 minutes to cause peaks eluting between these times to be diverted towards the

IRMS. The pyrolysis furnace consisted of a 320 mm length of 0.5 mm ID alumina tubing, loosely filled with alumina wool. It was conditioned with 1µL injections of hexane each time it was replaced and at the start of each analytical 'campaign'. The pyrolysis tube connected directly to the IRMS open/spilt via a short length of 0.32 mm ID silica tubing.

2.8.3.1 IRMS conditions

The mass spectrometer used was a Horizon (Nu Instruments, UK) which was controlled by proprietary software. The ion source was operated at 950 µA trap current and the tuning parameters were optimised to provide flat-topped *m/z* 3/2 ratio traces with low and stable H_3^+ contribution. The latter was typically 7 ppm/nA. All analyses were performed by comparison to a pure H_2 reference gas. In addition, *m/z* 3/2 ratios of neutral amino acids in the region of the chromatogram selected for analysis by IRMS were compared with that of the internal standard, nor-leucine. The amino acids were alanine, valine, iso-leucine, leucine, glycine, nor-leucine and proline (Figure 13) *M/z* 2 peak areas <1 nA were rejected as being too low for accurate ratio analysis. Iso-leucine peak areas were frequently below this threshold. Above 1nA major peak area, precision was routinely close to 1 ppm ^2H (δ^2H = 6 ‰) in samples near natural abundance.

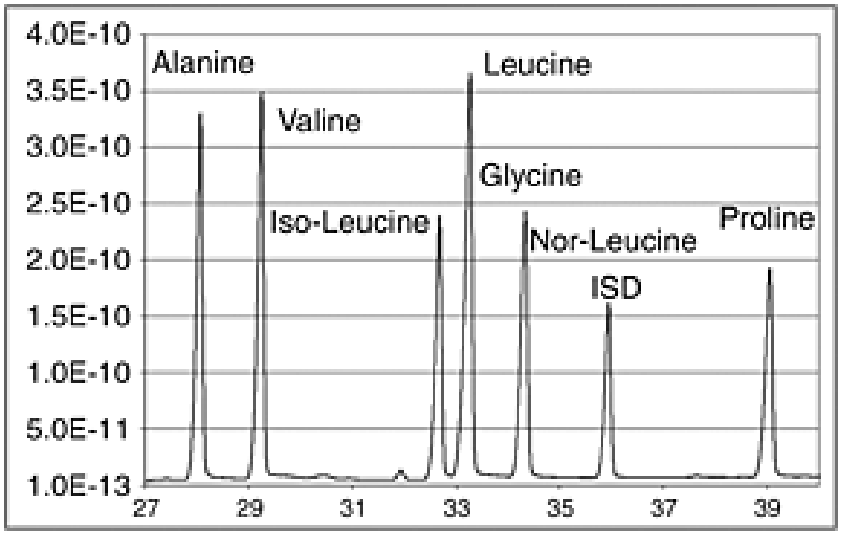

Figure 13 - Ion chromatogram (m/z 2) of neutral amino acids

A number of precautions were taken to maximise sensitivity: the choice of the column bore and phase ratio were made in order to maximise loading without compromising resolution; the ion source was operated at high trap current and tuned according to the manufacturer's recommendations; helium carrier flow was minimised to increase hydrogen gas concentration while not compromising separation; the pyrolysis furnace was operated at high temperature to ensure high conversion yield and minimal fractionation; sample loading was optimised to ensure intense peaks while not compromising separation due to column overload. These precautions were necessary as ^{2}H natural abundance is low and analytical precision worsens with decreasing peak area. In contrast to ^{13}C analysis, compound-specific ^{2}H analysis requires more attention to these details as in practice, dynamic range is often less. Sample loading of the order of 1 nmole analyte injected produced peak areas above 1nA. Peak shape and resolution deteriorated due to 'fronting' when more than 10 nmole of an analyte was injected. Increasing injection volume improved the situation with low concentration samples. Nevertheless, some samples in particular protein hydrolysates, failed to give sufficient peak area for accurate analysis.

As an independent test of the system's performance, a series of ^{2}H-alanine standards was created, encompassing the full range of enrichment from natural abundance, through low enrichment protein-bound amino acids to high enrichment free amino acids. This was constructed by gravimetric dilution of a commercial ^{2}H-alanine ($^{2}H_4$-L-alanine 99 Atom % ^{2}H, CDN Isotopes, Quebec, Canada) with natural abundance L-alanine (Sigma, Poole, UK). The whole curve was constructed from 10 individual solutions ranging from natural abundance to 5,400 ppm ^{2}H excess ($\delta^{2}H$ = 38,000 ‰) in H_2 as analysed, where 4/15 of the hydrogen atoms in the alanine derivative were labelled. The maximum enrichment that IRMS can measure is governed by sample size, the dynamic range of head amplifiers and the analyte. Head amplifier gain is often determined by ^{13}C analysis at natural abundance, with

100-fold difference between the major and minor beam feedback resistors. In practice with modern amplifiers operating at 50V, analysis of a far greater range of enrichments is possible than is generally appreciated, without resorting to altering amplifier gain. Indeed, for H_2 analysis the limitation is more likely to be imposed by the fact that H_2 analysis is conducted on dual collector instruments, where above 33 Atom % ^2H, when for a diatomic species major and minor beam intensity are equal, a triple collector capable of analysing all H_2 isotopomers would seem more suitable. However, the latter is not feasible when using low resolution continuous flow IRMS to measure H_2 with helium as carrier. 33 Atom % ^2H excess equates to 330,000 ppm ^2H excess. As a maximum of 4/15 hydrogen atoms in the alanine derivative used can become labelled, the maximum possible enrichment is 267,000 ppm ^2H excess. IRMS is quite capable of analysing the full range of conceivable enrichments. Additional limitations may be imposed if the mass spectrometer is run by a research group that usually measures stable isotope natural abundance, due to understandable but surmountable concern over cross-contamination.

As with unknown samples, the alanine gravimetric series included nor-leucine as internal standard. These standards were derivatised and analysed as ethoxy carbonyl ethyl esters in the same manner as the samples. Data was expressed as a raw delta (ratio) by the IRMS software by comparison with a reference gas. Once transferred to a spreadsheet, raw ratios in delta notation were normalised to the internal standard ratio and converted to ppm ^2H excess by subtraction of the basal value. The slope of the resulting curve of measured versus calculated enrichment was 0.94, the intercept was not different from zero and the Pearson correlation coefficient was 0.98. Thus, this exercise revealed that the combination of GC, pyrolysis and IRMS was capable of performing well over a range of ^2H enrichments that exceeded by tenfold the expected maximum enrichment in this protocol. Insertion of enriched samples before natural abundance samples to test for memory, revealed the system

to be memory free over this range. Furthermore, the problem of sensitivity alluded to above diminishes as the minor peak area increases with increasing enrichment.

2.9 Surface-enhanced laser desorption/ionization time-of-flight mass spectrometry (SELDI-TOF-MS) analysis of urinary proteome.[9]

2.9.1 SELDI-TOF-MS

SELDI-chips (CM10 and IMAC30) were prepared for sample application according to the manufacturer's recommendations and as previously reported [21538913]. Briefly, IMAC30 chips were loaded with 0.1M CuSO4, washed with water, neutralised with 0.1M NaAc pH4 and washed with water, followed by two washes with 0.1M NaHPO4, 0.5M NaCl, and CM10 chips were washed twice with 0.1M NaHPO4 pH4.0. All chips were processed in a bioprocessor-assembly by incubating 0.1ml urine and 0.1ml binding buffer (CM10: 0.1M NaHPO4 pH4.0; IMAC30: 0.1M NaHPO4, 0.5M NaCl) for 1 hour at room temperature with vigorous shaking, followed by three washes with 0.2ml binding buffer for 5 minutes each at room temperature with vigorous shaking and two washes with 0.2ml water at room temperature with vigorous shaking, air-dried and 2 times 1μl energy absorbing matrix (SPA, in 50% ACN, 0.5% TFA) was added. Air-dried chips were analysed in a PCS4000 SELDI-TOF instrument (Bio-Rad, Hemel Hempstead, UK) by measuring the 1000 to 25000 Da range with a laser setting of 2.5 μJ and spectra were exported as '.xml' files. The SELDI instrument was calibrated using the ProteinCip All-In-one peptide standard (Bio-Rad, Hemel Hempstead, UK). Source voltage was 25000 V, detector voltage was 2946 V. Quality control

[9] I acknowledge Dr Holger Husi who performed this analysis at the Tissue Injury and Repair Group, University of Edinburgh

and consistency was ensured by using one random pool of urines on one spot per chip each. Spectral alignments of all quality controls ensured consistency of all spectra.

2.9.2 Data processing

ProteinChip Data Manager Software (PCDMS) version 4.1 with integrated Biomarker Wizard cluster analysis (Bio-Rad, Hemel Hempstead, UK) was used for analysis. SELDI-TOF-MS traces were split into two groups, control and myosteatosis. The baseline was subtracted from individual m/z traces and profiles were normalised using total ion current, followed by identification of peak clusters using the cluster analysis tool. Peaks were selected in the first pass where the signal to noise (S/N) ratio is greater to 5, a valley depth of at least 3, and in the second pass S/N was 2 and the valley depth of 2. The cluster mass window was set to 0.2% of mass. Clustered peaks were only included if they occurred in at least 10% of all spectra. The resulting p-values, ROC areas, average and median m/z values, and intensities of the clustered peaks were exported and saved as '.csv' files and used for model building. Heat-maps using Pearson's correlation and principle component analysis (PCA) plots were calculated to assess global group divisions (i.e. myosteatosis and control). A two-sample t-test was used to compare mean normalized intensities between the case and control groups. The p-value was set at 0.05 to be statistically significant.

2.9.3 Model building and validation

Clustered peak lists were analysed with the Biomarker Pattern Software (BPS) (Bio-Rad, Hemel Hempstead, UK). m/z versus intensity matrices were analysed using decision tree-analysis, selecting the standard error rule of minimum cost-tree regardless of size, and the method used was Gini. V-fold testing was set to 1000. 20 myosteatosis samples and 20 control samples were randomly chosen and used as the learning and testing dataset. The

remainder of 15 samples was used as the validation dataset for blind-testing. Sensitivity was defined as the probability of predicting myosteatosis cases, and the specificity was defined as the probability of predicting control samples.

2.9.4 Peak isolation and identification

Peaks observed in the CM10 and IMAC30 chip-types which show marked expression differences between control and myosteatosis samples, or are branching points in the models were further investigated. 0.5ml urine from positive or negative samples in relation to specific peaks was added to 30µl CM10 or IMAC30 spin column resins (Bio-Rad, Hemel Hempstead, UK) and 0.75ml binding buffer (0.1M NaHPO4 pH4.0 for CM10 resins, and or 0.1M NaHPO4 pH7.0 including 0.5M NaCl for IMAC30 resins) and incubated for one hour at room temperature under constant agitation. Unbound material was removed and the resin washed four times with 0.3ml binding buffer. Bound material was separated by electrophoresis on a 16.5% Tris-Tricine gel (Bio-Rad, Hemel Hempstead, UK), and gel bands in the region of 2 to 10 kDa were excised after Coomassie staining (BioSafe Coomassie, Bio-Rad, Hemel Hempstead, UK). Positive and negative samples were both chosen on the presence and absence of a specific m/z peak to be identified based on SELDI-TOF-MS analysis. Proteins and peptides from gel bands were digested in situ with trypsin, the resulting peptides eluted with ACN, and analysed by LC-MS/MS as described [21538913]. Fragmentation spectra were then processed by Xcalibur and BioWorks software (Thermo Fisher Scientific, Loughborough, UK) and submitted to the Mascot search engine (Matrix Science, London, UK) using UniProt/SwissProt (release July 2010, Homo sapiens, 18055 sequences) as the reference database. Mascot search parameters were: enzyme specificity trypsin, maximum missed cleavage 1, fixed modifications cysteine carbamidomethylation, variable modification methionine oxidation, precursor mass tolerance +/-3Da, fragment ion mass tolerance +/- 0.4Da. Only Mascot hits with a false discovery rate

of less than 0.05 were taken into consideration. Proteins with at least two peptide matches were then analysed by pattern matching based on SELDI-TOF-MS measured expression levels of peaks of interest (expected abundance in selected samples) and observed presence of proteins. Peptide distribution of identified peptides within a protein as well as calculated molecular mass of identified proteins was also used to assess whether breakdown products are likely to account for mass variances between the expected mass and the molecular weight of the full length protein.

2.9.5 Mascot-SELDI matrix matching

Observed proteins with at least two peptide matches from the LC-MS/MS analysis were then further analysed by pattern matching based on SELDI-TOF-MS measured expression levels of peaks of interest (expected abundance in selected samples). This was done using software written in-house, which compares observed protein expression patterns in a pre-defined set of samples (LC-MS/MS results) against a matrix of peak patterns (SELDI-TOF clustered peak intensities, where estimated peaks are set to null) in the same set of samples. The scoring is based on sensitivity (percent observed over expected) and specificity (percent not observed over not expected), and results are presented in descending order of cumulative scores.

3 The need for direct measures of muscle mass: limitations of prediction of whole body muscle mass from simple anthropometry

3.1 Introduction

Cancer cachexia is currently defined by the presence of weight loss >5% or by weight loss >2% in the presence of a low muscle mass (44) or low BMI. This definition focusses on active loss of body mass more than the presence of low body mass alone. Similarly, although an absolute low muscle mass is associated with worse outcome in patients with cancer (244) it may be that an active on-going decrease in muscle mass is of greater significance. Determining the dynamics of loss of skeletal muscle mass in patients with cancer is not possible as a pre-illness measure of skeletal muscle mass is unlikely to be available. Most patients are able to report reliably a pre-illness weight or amount of weight loss (184) but no equivalent exists for the estimation of change of muscle mass. The use of clinical imaging (in the form of routine diagnostic CT scans) is now commonplace for the determination of body composition in cancer cachexia research (185). These scans can give an accurate measure of body composition at diagnosis (and follow up) (141). Measures of muscularity in the form of cross sectional area may be converted to estimates of whole body muscularity by established prediction equations (186, 194, 195). If a method were available to estimate pre-illness muscularity then change in muscle mass could be estimated using this and the measured value from the diagnostic CT-determined value of muscle mass just as a measured weight and patient estimated pre-illness weight can be used to determine the dynamics of weight loss.

Such pre-illness muscle mass estimation could be derived from simple anthropometric measurements. In health, muscle mass may be relatively predictable in individuals of average build and could be estimated by measures of height and weight. If this is a valid proposition then it should be possible to estimate an individual's pre-illness muscularity from a self-reported pre-illness weight. From routine CT scans an actual measure of muscularity can be taken, allowing the identification of patients in whom there is a loss of muscle mass that is disproportionate to overall weight loss. The aim of this study was to determine whether prediction equations for muscularity derived from healthy volunteers or patients with limited weight loss could accurately predict muscularity in a relatively weight stable cohort of patients with upper GI cancer.

3.2 Aim

To compare new and existing prediction equations for muscle mass with estimates of muscle mass derived from measured values in non-cachectic patients with cancer.

3.3 Patients and methods

In a cohort of patients recruited at the Edinburgh Royal Infirmary, comparisons were made between whole body muscle mass estimated from established prediction equations calculated from measured muscle cross sectional area and established anthropometric prediction equations from the literature Figure 14. A second comparison was made between measured muscle cross sectional area in the same Edinburgh cohort and predicted cross sectional from a new equation derived from a Canadian cohort of weight stable patients with cancer Figure 15.

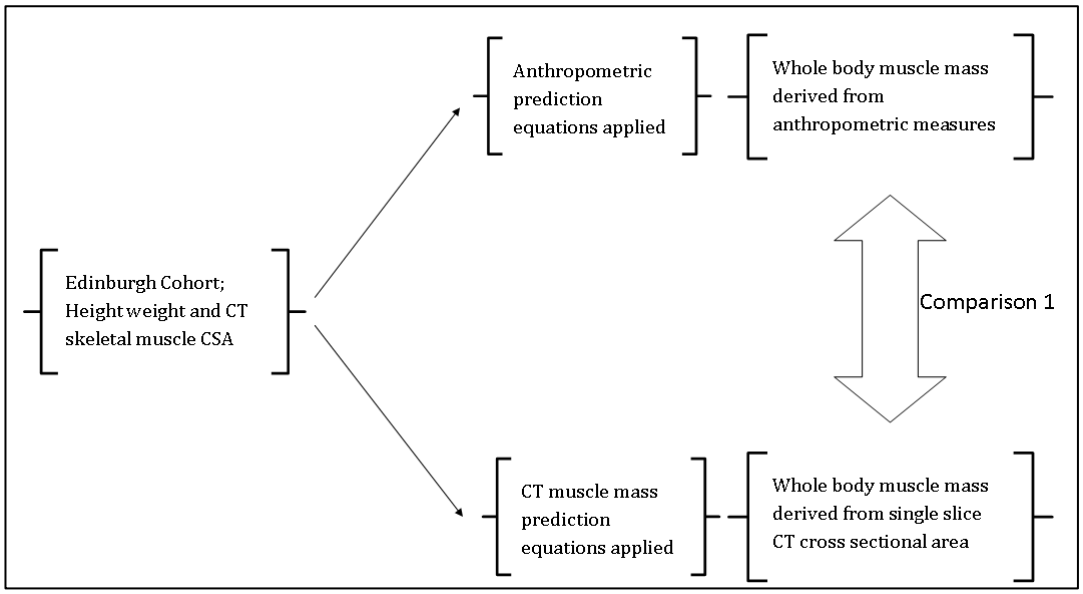

Figure 14 - Comparison 1; literature derived anthropometric predictors of muscle mass vs CT derived whole body muscle mass.

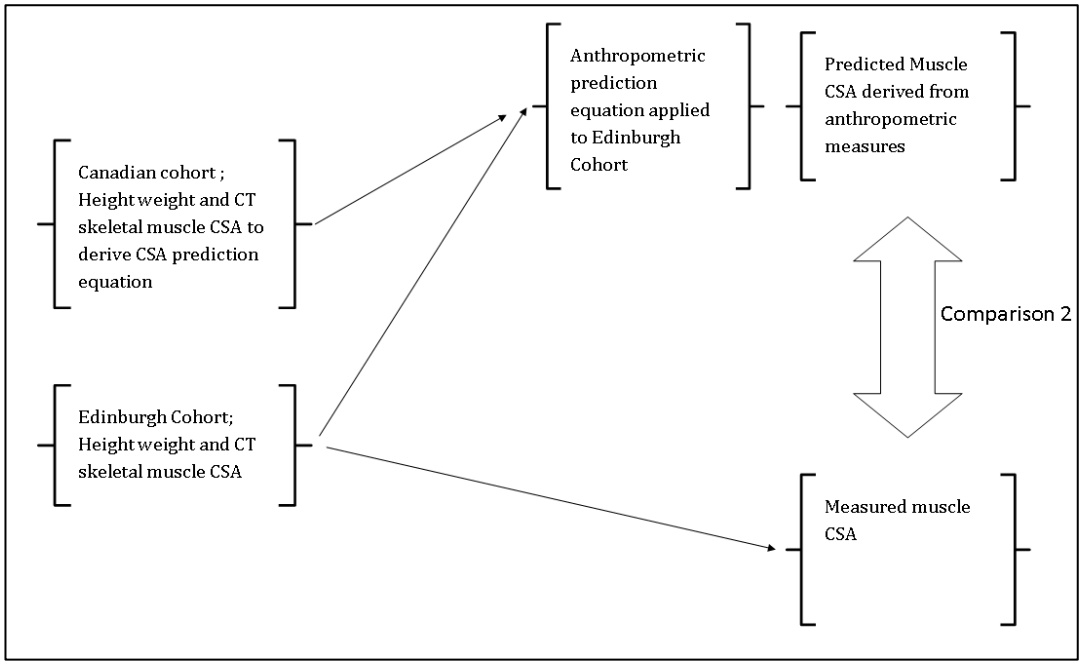

Figure 15 - Comparison 2; Predicted skeletal muscle cross sectional area vs measured cross sectional area

3.3.1 Patients

3.3.1.1 Edinburgh Cohort

In Edinburgh, data was gathered prospectively for patients with gastric, oesophageal and pancreatic cancer undergoing staging investigations for potentially curative surgery between 2000 and 2005 (CRUK biomarker study, chapter 2.1). Of 60 patients recruited who had pre-operative CT scans available, 31 were considered weight stable without cachexia (self-reported weight loss less than 5%) and included for analysis. These were 26 male, 5 female. The site of the cancer was oesophagus 13, Oesophago-Gastric-Junction (OGJ) 7, gastric 7, pancreas 3, duodenum 1. The patient characteristics are shown in Table 4.

	Minimum	Maximum	Mean	Std. Deviation
Age	43	83	65.7	9.0
Weight (kg)	56.0	133.0	81.1	18.3
Height (cm)	153	191	173	9.0
BMI (kg/m^2)	18.7	43.9	27.6	5.4
% wt loss	-10.4	5.0	0.2	3.5

Table 4 - Patient characteristics of Edinburgh cohort (n=31)

3.3.1.2 Canadian Cohort

Data was extracted from a cohort of Canadian patients in the province of Alberta who were part of an existing study (245). These patients had gastrointestinal and lung cancer and had previous diagnostic or staging CT scans available, a total of 797 patients were identified for inclusion as being weight stable (<8% weight loss).

3.3.2 Method

3.3.2.1 Data collection

In the Edinburgh cohort, height, weight age, sex and self-reported weight loss were recorded for the weight stable upper GI cancer patients. All patients included had a pre-operative staging CT scan performed prior to surgery. Skeletal muscle Cross sectional Area (CSA) was measured from an single CT slice at the level of L3 using Slice-o-matic as per the established protocol (methods 2.4.1) (186). Muscularity was expressed in cm^2 of muscle cross sectional area. In the Canadian cohort similar data was collected and CT's were analysed by an identical method. A novel prediction equation for muscularity was derived from these weight stable patients with cancer. This regression equation predicts muscularity, defined as a cross sectional area of muscle in cm^2 and was based on gender age and weight. L3 muscle area (cm2) = 115.536 + -38.096(gender male=0, female=1) + 0.943(weight kg) + -0.491(age years) Table 5.

	B	SE B	β
Step 1			
Constant	161.200	1.096	
Gender	-52.056	1.665	-0.74*
Step 2			
Constant	81.090	3.761	
Gender	-37.302	1.479	-0.53*
Weight (kg)	0.974	0.045	0.46*
Step 3			
Constant	115.536	5.283	
Gender	-38.096	1.414	-0.54*
Weight (kg)	0.943	0.043	0.45*
Age (years)	-0.491	0.055	-0.16*

Table 5 - Linear regression to predict L3 CT muscle area (cm2), in n=797 patients from Edmonton, Canada with <8% weight loss. NOTE: R2 step 1 = 0.52; R2 step 2 = 0.67; R2 step 3 = 0.70 *p<0.001, height (m2) was not a significant predictor of L3 muscle area

3.3.2.2 Group Comparison

3.3.2.2.1 Comparison 1

In order to allow comparison with anthopometrically derived measures of muscle mass, the cross sectional area was also expressed as total body muscle mass using the equation of Shen (194) based on MRI CSA skeletal muscle 5 cm above L4-5.

Whole body skeletal muscle = 0.166 * CSA + 2.142

Comparison of measured and predicted muscularity for the Edinburgh group was made with prediction equations from total body potassium from Larsson et al (246) and Boddy et al (162) and with prediction equations from NAA, Slater et al (156) and tritium dilution, Hume et al (247) Table 6. FFM was converted to SMM via the ratio of Wang et al. SMM/FFM ratio 0.528 ± 0.036 for men and 0.473 ± 0.037 for women (248). TBK was converted to SMM by the ratio of Wang et al SMM (Kg) = TBK x 0.0085 (249).

Study	**Sex**	**Anthropometric prediction equation**
Larsson (246)	Males	TBK = -12.04 x Age +34.67 x Weight + 1375 x Height -449.6
	Females	TBK = -13.37 x Age +18.55 x Weight + 1897 x Height -810.4
Boddy (162)	Males	TBK = 23.96 x Weight + 3515 x Height -12.09 x Age -3762
	Females	TBK = 14.76 x Weight +2207 x Height -9.05 x Age -1669
Slater (156)		FFM = 7.4 x Height^3 / 0.732
Hume (247)	Males	FFM= (19.48 x Height+0.2968 x Weight-14.01) /0.732*1/1.041*0.94
	Females	FFM= (34.54 x Height + 0.1838 x Weight-35.27)/0.732*1/1.041*0.94

Table 6 - Equations from the literature; TBK, NAA and Tritium dilution derived prediction equations.

The five literature derived equations used to derive measures of muscle mass consisted of individuals of a range ages and health status in predominantly Caucasian populations. Volunteer characteristics from established prediction equations are shown in Table 7.

Study	Location	Age (yrs)		Weight (kg)		n		Health status
		Male	Female	Male	Female	Male	Female	
Larsson	Sweden	49.3 ± 6.9	49.0 ± 6.8	80.7± 9.4	66.6 ± 10.0	164	205	Healthy
Boddy	Scotland	18 to 77		43.1 to 93.3		49	54	Healthy
Slater	Scotland	3 to 87		BMI 18.5 to 29.9		135	126	Healthy, HIV, Cancer, Obese, Diabetes
Hume	Scotland	35 to 71	33 to 84	Not reported		30	30	Obese, CVA, MI, Bronchitis, Osteoarthritis
Shen	USA	41.6±15.8	47.8± 18.7	81.3 ± 12.0	70.0 ± 15.4	123	205	Healthy

Table 7 - Patient and volunteer characteristics in prediction equation studies

3.3.2.2.2 Comparison 2

Comparison of a direct measure of muscle mass in the form of skeletal muscle cross sectional area (cm^2) was made with a prediction equation derived from CT cross sectional areas from the Canadian Group. A prediction equation was derived from the Canadian weight stable cancer patients for skeletal muscle CSA using height, age, weight and sex: L3 muscle area (cm2) = 115.536 -38.096(gender male=0, female=1) + 0.943(weight kg) - 0.491(age years). This was applied to the Edinburgh weight stable upper GI patients to give a predicted measure of muscularity in cm^2, which was then compared with measured muscularity in the Edinburgh group (cm^2).

3.3.3 Statistical Analysis.

3.3.3.1 Edinburgh Cohort CT derived measures of muscle mass vs anthropometry derived measures of muscle mass.

The regression equation of Shen was applied to the measured CSA of skeletal muscle from CT to give a CT-derived estimate of whole body skeletal muscle mass. The anthropometric derived estimates from Larsson, Boddy, Slater and Hume were compared with the CT-derived estimates. A Bland-Altman analysis performed to assess agreement, the mean difference determines the presence of bias, the SD of the differences between the 2 muscle mass values is calculated and the limits of agreement determined as 2SD either side of the mean difference. Bland-Altman plots were charted to reveal variation in the differences with increasing total muscle mass.

3.3.3.2 Edinburgh cohort CT measures of muscle area vs predicted muscle area (Canadian cohort derived prediction equation)

A similar analysis was performed comparing the measured CT CSA with the anthropometry-derived predicted CT CSA. The mean difference and limits of agreement were calculated.

3.4 Results.

3.4.1 Comparison 1: CT derived estimates of whole body muscle mass vs anthropometrically derived estimates of muscle mass in the Edinburgh cohort.

3.4.1.1 Muscle mass estimates in Edinburgh cohort as derived from prediction equation studies.

When the muscle mass prediction equations were applied to the weight stable Edinburgh cohort a spread of up to 7 kg was observed in the estimated mean muscle mass between prediction equations (Table 8)

	Mean	Minimum	Maximum	Std. Deviation
Larsson (TBK) prediction equation	32.15	19.31	49.31	7.52
Boddy (TBK) prediction equation	28.45	17.10	41.21	6.66
Slater (TBW) prediction equation	25.36	16.45	35.90	4.72
Hume (Tritium) prediction equation	25.60	16.31	38.93	5.67
Shen equation from measured muscle CSA	25.9	16.6	41.2	5.1

Table 8 - Muscle mass characteristics of Edinburgh cohort patients as estimated by muscle mass literature derived prediction equations. Muscle Mass in kg

3.4.1.2 Bland-Altman comparison of prediction equations.

The predictive equation using anthropometric data based on tritium dilution (Hume) measure of FFM converted to skeletal muscle mass had the least bias with a mean difference of 0 compared with the direct CT-based estimate of muscle mass (Shen). This pairing also had the smallest limits of agreement (Table 9). These limits of agreement indicate that the predicted whole body muscle mass by anthropometric assessment will lie within ±4.97 kg of the CT based estimate of whole body skeletal muscle mass. The same data is presented as a Bland-Altman plot in Figure 16. The comparisons for the other equations (Larsson, Boddy

and Slater) are shown in Figure 17, Figure 18 and Figure 19 respectively. There was evidence of heteroscedasticity in the Shen vs Larsson comparison with an increasing difference with increasing muscularity indicated by a downward sloping distribution of points (Figure 16).

	Mean difference	Upper limit	Lower limit
Shen - Larsson	-6.56 (-7.88, -5.24)	0.47 (-1.81, 2.75)	-13.59 (-15.87, -11.31)
Shen - Boddy	-2.86 (-4.09, -1.63)	3.73 (1.59, 5.86)	-9.45 (-11.58, -7.31)
Shen – Slater	0.23 (-1.23, 1.69)	8.05 (5.39, 10.70)	-7.58 (-10.24, -4.93)
Shen - Hume	-0.00 (-0.93, 0.93)	4.97 (3.36, 6.58)	-4.97 (-6.58, -3.36)

Table 9 - Bland-Altman analysis of CT derived whole body muscle mass (Shen) vs anthropometric muscle mass prediction equations (Larsson, Boddy, Hume, Slater). Values in kg with 95%CI

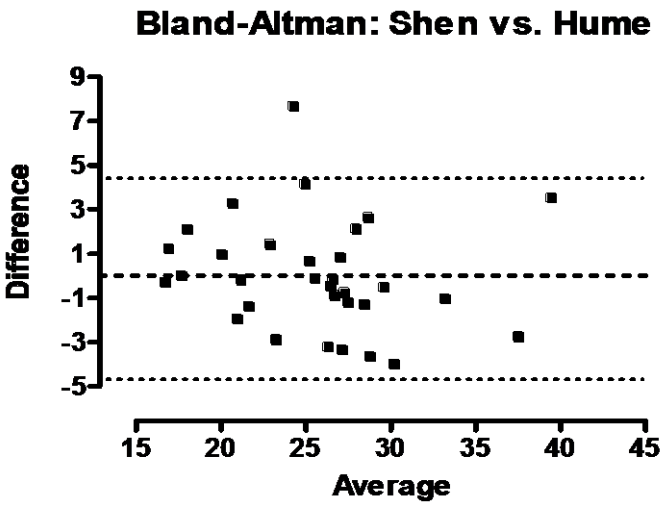

Figure 16 - Bland Altman plot of Shen vs Hume equations for whole body muscle mass (mean difference 0.00, upper limit 4.97, lower limit -4.97)

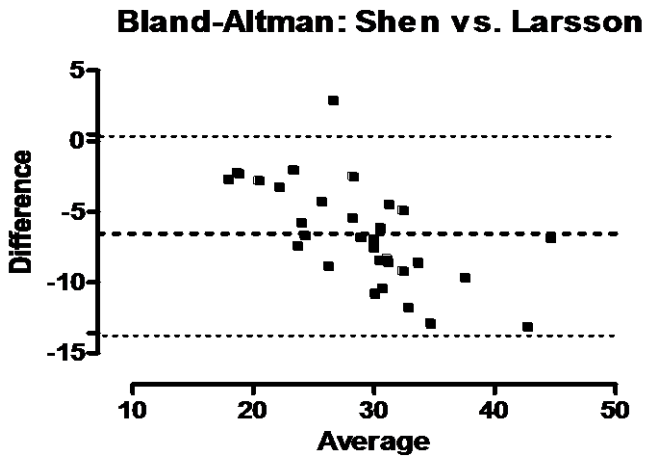

Figure 17 - Bland Altman plot of Shen vs Larsson equations for whole body muscle mass (mean difference -6.56, upper limit 0.47, lower limit -13.59)

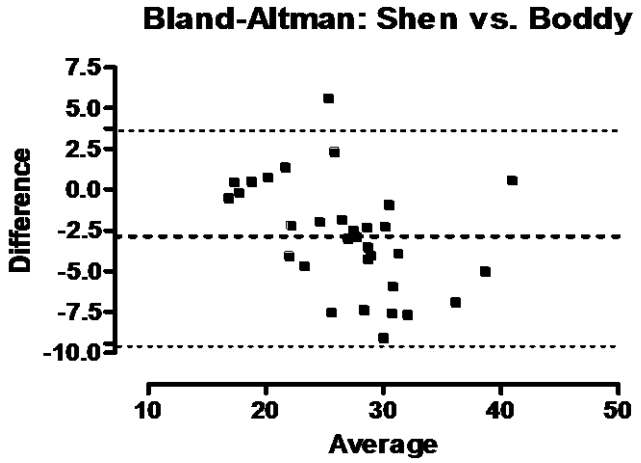

Figure 18 - Bland Altman plot of Shen vs Boddy equations for whole body muscle mass (mean difference -2.86, upper limit 3.73, lower limit -9.45)

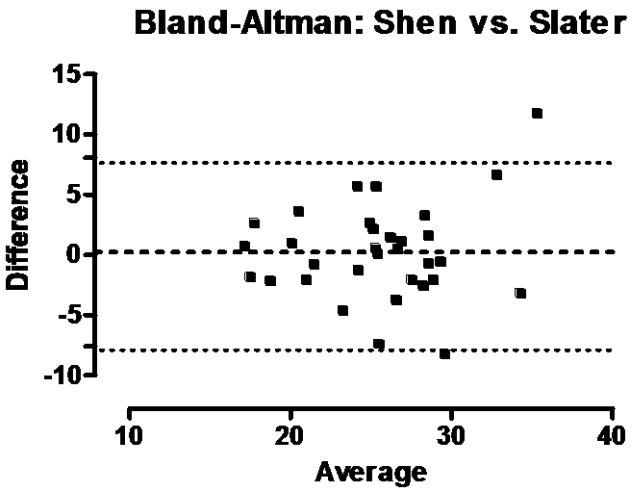

Figure 19 - Bland Altman plot of Shen vs Slater equations for whole body muscle mass (mean difference 0.23, upper limit 8.05, lower limit -7.58)

3.4.2 Comparison 2: Measured CT muscle CSA vs predicted muscle CSA applied to Edinburgh cohort.

The anthropometric-based prediction equation for skeletal muscle CSA derived from the Canadian cohort was applied to anthopometric data in the Edinburgh cohort to obtain a predicted skeletal muscle CSA. The measured value was compared with the predicted value. The distribution of estimated and measured L3 skeletal muscle cross sectional area is described in Table 10.

	Minimum	Maximum	Mean	Std. Deviation
Canadian prediction equation	94.9	209.2	153.6	26.6
CT measured CSA	86.9	235.3	142.8	31.0

Table 10 - Muscle area characteristics for the Edinburgh cohort for measured values and CSA prediction equation expressed as CSA in cm2

	Mean difference	Upper limit	Lower limit
Predicted – measured CSA	10.74 (5.79, 15.68)	37.16 (28.60, 45.73)	-15.68 (-24.25, -7.11)

Table 11 - Bland-Altman analysis of predicted vs measured CT CSA; mean difference and limits of agreement

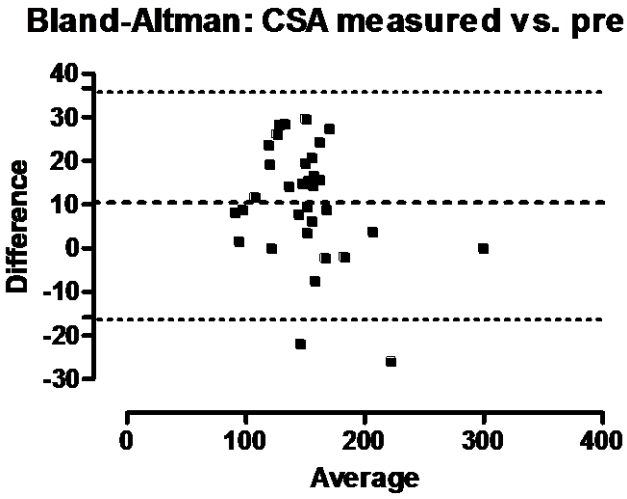

Figure 20 - Bland Altman plot of muscle CSA from measured CT CSA vs CSA prediction equation

3.5 Discussion

The Hume prediction equation performed best with no bias and the smallest limits of agreement, although all prediction equations gave broadly similar results. The two total body potassium derived equations (Larsson and Boddy) showed evidence of bias with the mean differences significantly different from zero and the limits of agreement broad. This bias was less evident in the two FFM derived equations (Slater and Hume) where both equations had mean differences around zero. The limits of agreement were broad in the prediction equations from both TBK and FFM, these were equivalent to a difference in the region of 25% of the mean estimated muscle mass, an amount much greater than would be considered acceptable for use in assessment of change of muscle mass, where the change expected may be in the order or 2 – 10%. The prediction equation for CSA derived from the Canadian cohort also performed poorly, a bias was shown which gave estimates of muscle cross sectional area over $10cm^2$ greater than the measured value. Broad limits of agreement were seen with a difference of up to 37.16 cm^2 where the mean CSA is 142.8 cm^2 . Whichever model is considered, it appears that the wide variation in body composition in healthy populations does not allow accurate prediction of specific body compartments from simple anthropometric measurement as demonstrated by the wide limits of agreement. This finding is consistent with previous evaluations of anthropometric measures. Greater accuracy in anthropometric estimates of muscle mass could be achieved with the addition of other measures (250) such as sub scapular or triceps skin fold thickness and waist or hip circumference. However, these measurements would not be available for the pre-illness state. The Larsson equation is the poorest performing prediction equation here. This predictor is the only one not to include age at any stage and possibly highlights the importance of this as a known determinant of muscle mass (251).

Several of the prediction equations appear to overestimate muscle mass compared with the measured mass in Scottish weight-stable patients. The Canadian CSA prediction equation gave estimates of muscle mass that were higher than measured values. This suggests that the Canadian group in which the equation was derived appear to be more muscular than the Edinburgh group for their weight. There are three possible explanations for this. The first may simply be due to the fact that 2 different populations were used and that the Canadians are more muscular for their weight than the Edinburgh group. Alternatively it could relate to the difference in weight loss definitions between the two groups. At the time that the CSA prediction equation was derived both 5% and 10% cut offs for weight loss were used in the scientific literature for cancer cachexia definitions and the 8% cut off for a weight stable group in the Canadian cancer cohort was used as it was shown to be associated with a threshold of increased risk of mortality/morbidity (245). In contrast, the Edinburgh cohort were included on the basis of the most recent cachexia definition of 5% weight loss. If the Canadians with greater weight loss (albeit below 8%) experienced a greater loss of fat mass to muscle mass this could give the impression of increased muscularity in that group. Finally, the present findings could reflect a difference in the way the equations were derived. The CSA prediction equation was derived using a multiple regression model and is heavily influenced by a large constant modified by gender, age and weight with height adding nothing to the model. Similar to the CSA prediction equation, the mean difference seen when comparing the healthy Larsson and Boddy cohorts to the Edinburgh weight stable cancer cohort suggests that the two groups may have different muscle mass after age, weight height and sex are taken into consideration. As a result it could be suggested that patients with upper GI cancer with little or no weight loss appear to have a loss of muscle mass out of proportion to their total weight loss. This finding would be consistent with the theory that muscle wasting may occur early in the cancer cachexia spectrum (97).

Newman et al (252) developed an alternative sarcopenia definition where measured muscle mass was expressed relative to ideal muscle mass based on weight, height and sex called the residuals method which when compared with the standard definition of sarcopenia (78), was found to have a stronger association with lower extremity function. Although the present study has shown that it is not possible to predict an individual's muscle loss, it could be possible by this method to classify groups of patients by difference in muscle mass from a predicted healthy muscle mass in a manner similar to Neuman's method. This in turn could be used to better define a pre-cachexia cohort of patients. Further research to determine the clinical significance of sarcopenia (and pre-cachexia) defined in this way in patients with cancer would be required.

Whilst it was not possible to predict pre-illness muscle mass or CSA from height, weight, age and sex for individuals the method may still be of use in large groups of patients. Using the Hume equation where no bias exists, the group mean muscle mass should be approximately the same as a group mean muscle mass derived from a CT cross sectional area. If it is assumed that these two mean values are equally valid then it should be possible to detect a "measured" difference in the group means using illness CT muscle mass estimation and pre-illness prediction despite our inability to determine muscle loss or gain in an individual. A sample size calculation based on means and SD from the Hume and Shen group characteristics (Table 8) using a paired t-test with α=0.05 and 1-β=0.8 indicate that a minimum of 37 patients would be required to ensure that a 10% difference in pre-illness to cachectic muscle mass was reliable (253). A simple linear regression of the Hume predictor against the Shen predictor gives an R^2 of 0.76 and standard error of estimation of 2.8. These values are slightly poorer but comparable with measures of muscle mass from 24-h Urinary 3-methylhistidine and BIA which have r^2 0.77 and 0.86 and SEE of 2.3 and 2.7 respectively.

Simple anthropometric estimation of pre-illness muscle mass cannot be used to classify an individual as muscle losing or gaining unless the change is greater than ± 4.97 kg, though the

Hume equation could be used to describe the mean muscle mass change in a similar cohort of patients provided the sample size is adequate.

3.6 Conclusion

Known prediction equations are not able to provide a reliable estimate of muscle mass in weight stable patients with cancer. It was not possible to derive a better estimate based on raw cross sectional muscle area. The variation in muscle mass between individuals requires a the use of a direct measure to determine muscularity.

4 Low muscle mass: Quadriceps MRI versus appendicular skeletal muscle mass as an index of sarcopenia in the elderly.

4.1 Introduction

Age-related loss of muscle mass (sarcopenia) is inevitable. Unlike other muscle wasting syndromes (e.g. cachexia related to acute/chronic illness, denervation atrophy) sarcopenia may occur without specific underlying pathology. However, sarcopenia is associated with several adverse outcomes including increased frequency of falls (74, 254) with attendant morbidity and mortality (95, 255), poor prognosis and higher risk of failing to regain full function following illness or surgery (256), increased risk of dependency, including institutionalisation and adverse metabolic sequelae, such as increased insulin resistance (257). In an ageing population sarcopenia is an increasingly serious public health problem (71).

An operational definition of sarcopenia is important in order to obtain comparable measures of prevalence, determine relative risk, target patients for therapeutic intervention, set treatment goals and monitor outcome. Defining sarcopenia has been the subject of much debate for over 20 years. The most widely reported definition of sarcopenia is based upon dual X-ray absorptiometry (DXA) measurement of appendicular skeletal muscle mass standardised for height squared (termed the 'relative skeletal mass index', RSMI). Sarcopenia is defined as an RSMI of greater than 2 standard deviations below a healthy reference population (78).The original study provided thresholds for men and women of 7.26 $kg.h^{-2}$ and 5.45 $kg.h^{-2}$ respectively from which the prevalence of sarcopenia among the white and Hispanic populations of New Mexico was calculated as 13 – 24% for men and women

aged 65–70y and greater than 50% in those aged more than 80y.

While both the DEXA-based method of determining sarcopenia and the use of the cut-offs described above is widespread, there are recognised limitations. Firstly, DEXA does not estimate directly muscle mass and secondly, the precision of the cut-offs is limited by the use of predictive reference population data with population values being established using anthropometric measures (78) rather than normative reference data (258). Magnetic resonance imaging (MRI) is increasingly used to determine muscle mass in healthy volunteers due to its precision, reproducibility and safety and is increasingly recognised as a gold standard measure of skeletal muscle in studies of body composition. Whilst whole body or whole limb MRI quantification of skeletal muscle is the gold standard measure (180, 259), this process is costly and time consuming. As a result, single slice regional measures are commonly used as these are known to be closely correlated with whole body (194) or whole muscle volumes (196). A measure of MRI quadriceps or thigh muscle CSA is often used as it is relatively easy to obtain and analyse (57), is reproducible and is believed to be of relevance to performance measures (83). The most recent definition of sarcopenia recognises the loss of muscle mass as part of a clinical syndrome of reduced muscle mass associated with limited mobility (76). The definition recognises that there may be multiple modalities for muscle mass measurement but establishes a common consensus of a value 2 SD below the mean of a healthy population 20-30 years old. This definition implies that different measures should be interchangeable, however values are likely to be both population and modality specific. This chapter compares cut off values for lower limb sarcopenia measured by MRI developed in a Scottish population with established DXA-based values where the equations used to calculate appendicular skeletal muscle mass were developed originally in a North American population.

4.2 Aim

This work aims to determine gender specific cut-offs for sarcopenia using MRI as a direct estimate of muscle mass in a cohort of healthy young individuals and applying this value to healthy elderly men and women. These cut offs are defined as two standard deviations below the mean in the healthy young group as established in previous DXA and abdominal CT based definitions of sarcopenia. Comparison will be made between MRI and DXA definitions in the elderly group.

4.3 Materials and Methods

4.3.1 Volunteer participants[10]

47 older men (median age 72y, range 65-84y), 16 older women (median age 78y, range 75-85y), 20 young men (median age 22.5y, range 19-25y) and 16 young women (median age 25.5y, range 19-30y) participated in the study (Table 12) (Muscle and aging study chapter 2.1). They were defined as healthy after applying previously published health selection criteria (230) to the responses to a questionnaire. None was engaged in any form of physical training. All procedures received local ethical committee approval. Informed consent was obtained from the volunteers prior to their participation in the study. The study conformed to the standards set by the Declaration of Helsinki.

4.3.2 MRI

MRI scans of quadriceps muscles were analysed as described in the Methods c

Chapter 2.4.2. The assumption that a single slice CSA of quadriceps at mid-thigh is representative of whole muscle volumes was tested by correlating quadriceps CSA and

[10] I acknowledge Dr Carolyn Greig who recruited patients for this study

volume in 52 scans in both young and older participants.

4.3.3 DXA

A subset of 28 older participants (14 men and 14 women >75y) undertook body composition measurement using DXA (Hologic QDR 4500A). The data were analysed to derive the following components: total fat mass (FM), percentage of fat, lean body mass, appendicular skeletal mass (ASM) and total skeletal muscle (TSM). Two whole body scans were performed, and the average of two scans was used in subsequent analysis. Data was normalised for height^2 (RSMI)

4.3.4 Definitions of sarcopenia

Sarcopenia was defined according to MRI quadriceps CSA <2SD compared with the mean obtained from the young group. This was compared in a subgroup (n=30) with the established Baumgartner definition based on DXA measurement of RSMI below 7.26 kg.h^{-2} and 5.45 kg.h^{-2} for men and women.

4.3.5 Statistical analysis

Group data are presented as means and standard deviations for parametric data and as median and range otherwise. Group comparisons were by Student's t test or non-parametric equivalent where appropriate. SPSS v15.0 statistical software was used for data analysis. The Kolmogorov-Smirnov test of normality was applied to all the data. Statistical significance was set at a p value of <0.05. Data analysis was sex specific.

4.4 Results

Men were both taller and heavier than women within both the younger and older groups. Older men and women were shorter in stature than their younger counterparts. BMI was similar between groups (older men slightly overweight, other groups within normal range) (Table 12). Mid-thigh quadriceps CSA was closely correlated with quadriceps volume R^2=0.94 (Figure 21). Left quadriceps CSA standardised for stature ($cm^2.m^{-2}$) was significantly greater in men than in women ($p < 0.01$) and was significantly greater in the younger than the older cohort ($p < 0.01$) (Table 12).

Cohort	Young		Old	
	Men (n=20)	Women (n=16)	Men (n=47)	Women (n=16)
Age (y) (median range)	22.5 (19-25)	25.5 (19-30)	72 (65-84)	78 (75-85)
Height (m)	1.77 ± 0.07	1.67 ± 0.08*	1.72 ± 0.06 †	1.57 ± 0.06 *†
Weight (kg)	75.5 ± 9.1	64.3 ± 8.6*	74.5 ± 9.2	58.5 ± 8.1*
BMI (kg/m^2)	24.0 ± 2.5	22.9 ± 2.5	25.3 ± 2.9	23.8 ± 3.0
CSA (cm^2/m^{-2})	28.9 ± 3.7	22.4 ± 2.5*	22.2 ± 2.8†	17.1 ± 2.7*†
Quadriceps Sarcopenia	0%	0%	47%	56%

Table 12 - Characteristics of subjects in MRI study. Data are shown as mean +/- SD except where indicated. * = Gender difference $p < 0.005$, † = $p < .05$. Abbreviations – CSA = cross sectional area, BMI = body mass index.

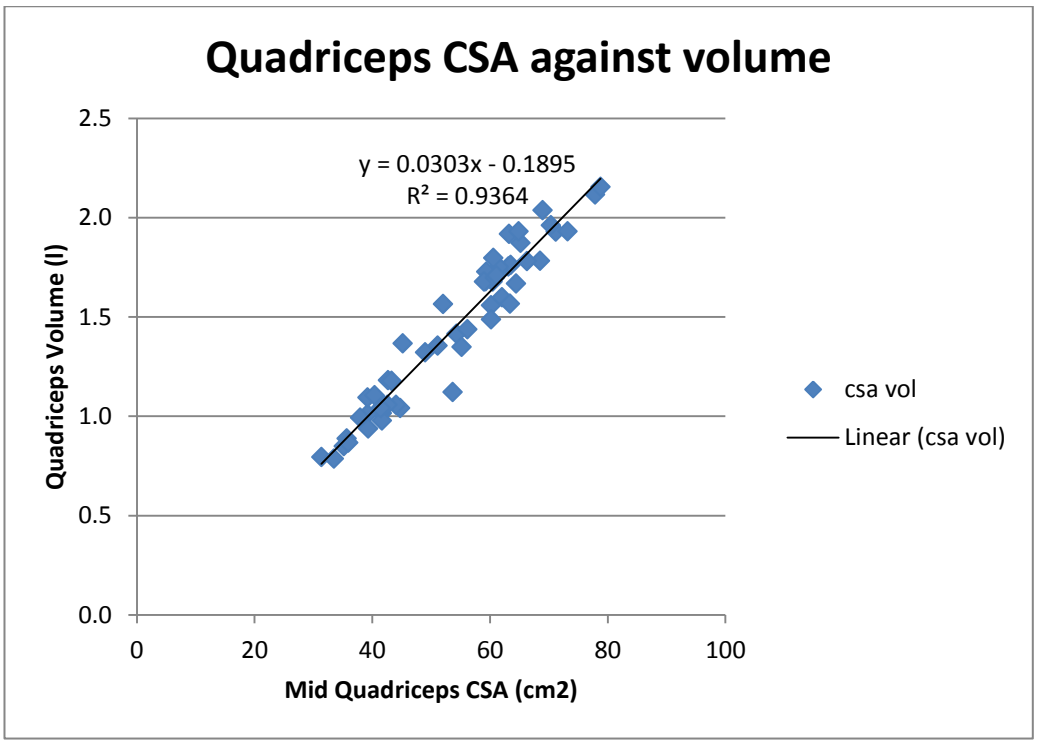

Figure 21 - Quadriceps CSA vs Quadriceps volume. There is a close correlation between cross sectional area on a single slice and whole quadriceps volume.

In younger men the mean (SD) CSA for the left leg was 28.9 (3.7) $cm^2.m^{-2}$ giving rise to a sarcopenia cut-off 2 SD below this as 21.5 $cm^2.m^{-2}$ for males. In younger women the mean (SD) CSA for the left leg was 22.4 (2.5) $cm^2.m^{-2}$ giving rise to a sarcopenia cut-off of 17.4 $cm^2.m^{-2}$ for females (Figure 22).

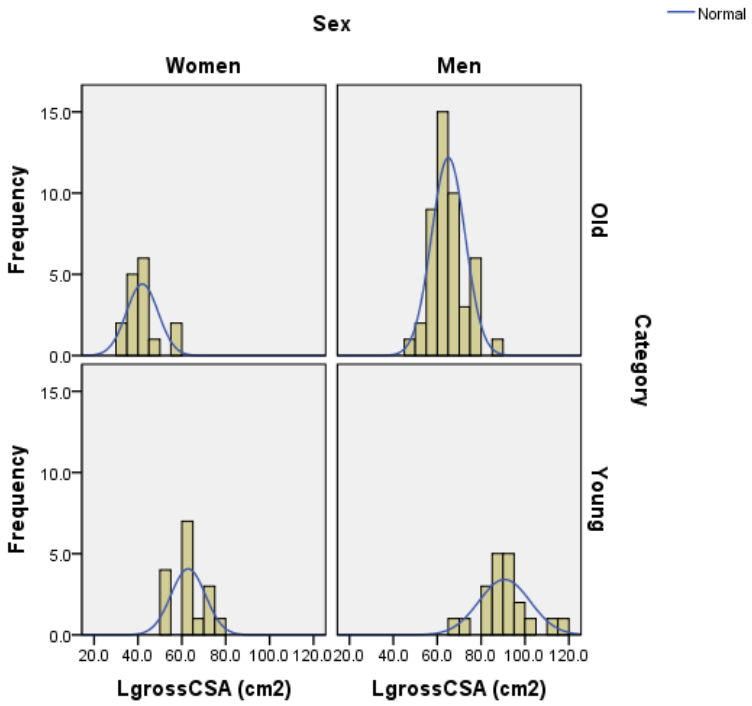

Figure 22 - Distributions of quadriceps CSA measures by sex and age group. Sex specific values for sarcopenia were defined as values 2SD below the mean in the young groups.

These gender specific definitions were applied to the mean quadriceps CSA in the older cohort resulting in the classification of 47% (n=22/47) of the older men and 56% (n=9/16) of the older women as sarcopenic (Table 13). Sarcopenic men were significantly older and taller than those classified as non-sarcopenic and they demonstrated significantly less standardised quadriceps CSA ($p < 0.05$, mean difference 4.8 $cm^2.m^{-2}$). There were no differences in age or stature between the female groups. Sarcopenic women had significantly less quadriceps CSA ($p < 0.05$, mean difference 4.1 $cm^2.m^{-2}$).

	Men		Women	
	Sarcopenic (n=22)	Non-sarcopenic (n=25)	Sarcopenic (n=9)	Non-Sarcopenic (n=7)
Age (median - range)	75 (65-84)*	70 (65-79)	78 (76-85)	78 (75-85)
Weight kg	73.9 ± 7.9	75.0 ± 10.3	59.0 ± 3.2	57.9 ± 8.9
Height m	174.3 ± 5.6*	169.1 ± 4.3	157.3 ± 6.2	155.6 ± 6.1
BMI	24.30 ± 2.0*	26.2 ± 3.3	23.9 ± 3.5	23.8 ± 2.5
CSA $cm^2.m^{-2}$	19.6 ± 1.2†	24.4 ± 1.8	15.3 ± 1.5†	19.4 ± 2.1

Table 13 - Characteristics of elderly subjects divided by presence / absence of MRI sarcopenia. Data are shown as mean +/- SD except where indicated. Students t-test was used to compare parameters between sarcopenia classes within gender. * $p<0.05$, † $p<0.005$

For a subset of 28 subjects (14M/14F) DEXA derived data was available for calculation of skeletal muscle mass. Using the relative skeletal muscle index (RSMI) measure of muscle mass and population reference values (78) to classify sarcopenia we found a lower proportion of both men and women classified as sarcopenic compared with using MR derived quadriceps CSA data (Table 14). Of the 14 female subjects who had muscle mass assessed by DXA, 2 (14%) were classified as sarcopenic using reference values whilst 9 (64%) were classified as sarcopenic using MRI based muscle mass assessment. For male subjects 8 out of 14 were sarcopenic using the MRI based cut-off whereas DXA and population reference values again classed only 2 (14%) as sarcopenic. No individual classified as sarcopenic according to the DXA based RSMI was classified as non-sarcopenic using the MRI estimates of CSA. (Table 14)

	Older	
	Men (n=14)	Women (n=14)
Age (median (range))	78.5 (75-84)	78 (75-85)
Height m	1.70 ± 5.9	1.57 ± 5.8
Weight kg	74.3 ± 11.8	59.6 ± 8.1
BMI	25.4 ± 3.9	24.1 ± 3.2
RSMI.Height^{-2} kg.m^{-2}	7.9 ± 1.0	6.2 ±0.72*
DEXA sarcopenia (%)	14%	14%
Quadriceps CSA sarcopenia (%)	57%	64%

Table 14 - DXA subgroup characteristics. Data are shown as mean +/- SD except where indicated. Students t-test was used to compare parameters across gender. * p-value< 0.05. RSMI = relative skeletal mass index, CSA= Cross Sectional Area.

Significantly more patients were classified as sarcopenic by quadriceps classification than by DXA (Table 14). Male p= 0.0461, female p=0.0183 (Fishers exact test)

4.5 Discussion

In this study we directly estimated quadriceps muscle mass in young and older men and women in order to generate muscle cross sectional area (CSA) cut-offs from normative data and define MRI quadriceps sarcopenia. The MRI-based technique utilising our own reference values categorised approximately half of the older cohort (men 46%; women 56%) as sarcopenic compared with 14% for both genders when applying Baumgartner's DEXA-based definition and population reference limits (78). These differences in classification derived from MRI or DEXA data highlight the problem of designation of sarcopenia based upon predicted population values rather than normative values even when the same definition (i.e. 2 SD below reference values) is applied. In using 2 standard deviations from

normative values as a cut-off for sarcopenia we are following convention in the field and conform to the current consensus definition (76). None of the patients classified as sarcopenic by the MRI definition were non-sarcopenic by Baumgartner's DXA definition suggesting that the reference MRI population are more muscular relative to the elderly population than Baumgartner's healthy cohort. This difficulty demonstrates the importance of using a population specific reference group when defining sarcopenia as highlighted by the current consensus definition. The upper age limit in the young reference group in this study was 30 years and is consistent with the current recommendations that a reference group should be healthy persons between the age of 20 and 30 years. Baumgartner's reference population was drawn from the Rosetta study of non-hispanic white man and women of 18 to 40 years. This may explain some of the apparent difference in muscularity between the reference populations as muscle mass may already begin to decline from the age of 30 (76). True reference population values can be difficult to define due to the requirement to recruit and analyse large numbers of individuals to minimise sampling error. For studies involving MRI quantification of muscle mass this is impractical and a limitation of this study is the relatively small number of individuals recruited to define the reference group.

4.5.1 Conclusion

The use of the young healthy population in this study did not result in similar stratification as established DXA values, caution should be exercised when comparing the results of studies using different modalities for measurement of muscle mass particularly where performed in populations other than those in which the reference values were defined.

5 Biomarker discovery for altered muscle quality: proteomic identification of potential markers of myosteatosis in cancer patients urine

5.1 Introduction

Chapter 3.6 described the development of a quadriceps definition of low muscle mass and found that the new MRI value categorised a healthy elderly population differently to alternate DXA methods. This variation between populations in combination with the known variation within populations means that it is likely that muscle mass alone, measured in small groups of elderly, co-morbid patients is unlikely to identify accurately the presence of cachexia associated muscle loss. Alternate measures of muscle quality (such as fat infiltration) have the potential to provide a more biologically relevant measure of muscle disease. Other measures of muscle wasting (rather than muscle mass) might include a measurement of the breakdown products of muscle degradation. This chapter investigates the use of an alternate measure available from cross sectional imaging that provides a measure of muscle quality which could be related to the presence of pathological processes in skeletal muscle. It investigates the urinary proteome (i.e. a matrix that contains a mix of muscle derived peptides / proteins) as a biomarker for muscle wasting that is a potentially more biologically relevant, practical and less burdensome alternative to cross sectional imaging methods.

5.2 Background

Cancer cachexia is a syndrome of muscle and fat loss leading to progressive functional impairment (97, 260) due to complex and variable host-tumour interactions (10, 261) mediated largely by pro-inflammatory cytokines and other factors acting as lipokines and myokines such as zinc-α2-glycoprotein (ZAG) (262) and macrophage inhibitory cytokine-1 (MIC-1) (263). Whilst the classic cachexia phenotype is of a wasted, underweight patient, due to the increasing prevalence of obesity in the general population it is now well recognised that the pathological process underlying cachexia may occur in overweight individuals leading to a situation where muscle or fat wasting may be difficult to recognise (61). Currently, cachexia is defined by the presence of weight loss greater than 5% or greater than 2% in the presence of low muscle mass or low BMI (97). This definition also introduces the concept of the pre-cachectic phase as yet undefined but which may be a stage at which intervention is best targeted. By relying on weight loss, the current cachexia definitions rely on relatively crude measures to identify cachexia by the visible effect on the phenotype rather than by identifying the presence of the underlying pathological process. Weight loss (often self-reported) as a measure may be difficult to determine accurately and, even when accurately reported, may be complicated by factors which act to increase body mass such as fluid accumulation or fat gain as a result of chemotherapeutic or hormonal treatment. The detection of low muscle mass is known to be associated with adverse outcome particularly in the presence of obesity (61). However, the use of low muscularity as a component of the classification of cachexia is hampered by the fact that a measure of muscle mass is only available generally as a single measure without reference to loss or gain. As a result, individuals with a low starting muscle mass in health risk being included along with those with severe cachexia. One alternative to measuring the *quantity* of fat and muscle tissue in body composition is to measure the tissue *quality*.

Intramyocellular lipid accumulation occurs in a number of pathological processes such as diabetes, obesity, aging and cancer cachexia (103, 199) and is associated with the severity of weight loss in cancer cachexia (264). This process is also known as myosteatosis. Myosteatosis is also associated with increased levels of circulating inflammatory mediators in elderly Caucasian and African-American individuals (265). Despite demonstrable subcutaneous and visceral lipolysis during cancer cachexia, myosteatosis and sequestration of fat into skeletal muscle might also be a key component of the cachexia syndrome (264).

Intramyocellular lipid concentration has previously been measured using Computed tomography scanning in individuals without cancer and is directly related to the radiological density as measured by the Hounsfield units (200, 266). The measurement of mean Hounsfield units of tissue on CT is precise to within 1% and may be more reproducible than tissue volumes. As such, measurement of the mean Hounsfield units of muscle gives a measure of progression of the dynamic process of muscle deterioration that cannot be estimated by measurement of muscle volume alone. Intracellular lipid as measured by Hounsfield units is associated with decreased functional capacity (172, 267-269), pain (179, 270) and hospitalisation (92).

As stated, early recognition of cachexia and assessment of its progression or regression may be difficult with the common measures used to diagnose cachexia. Assessment of muscle quality may provide a means of doing this although CT assessment for clinical purposes is generally performed only sporadically and is unsuitable for monitoring response to anti-cachectic treatments.

Assessment of the urinary protein profile to determine metabolites which may act as biomarkers is one potential method for diagnosing or monitoring disease. Urine is an ideal sample source for the clinical setting, as it can be obtained easily, is relatively stable and collection of samples is non-invasive. In addition, urine contains a relatively small number of proteins typically present at low concentrations compared with serum or plasma and so is a

simpler matrix for detecting proteins (271). Despite the relative simplicity of urine this method is complicated by the difficulty in standardising urine samples across individuals to determine the clinically relevant concentration of any particular urinary biomarker. One solution to this is to look at the whole urine protein and peptide profile with SELDI-TOF-MS mass spectrometry (MS) and identify potential biomarkers from a urinary proteomic "fingerprint" of multiple peaks corresponding to the urinary metabolites of a potential marker. Previous studies have found the technique of SELDI-TOF-MS ideally suited for urine analysis, with a combination of high throughput, speed and relatively low cost (272). The main drawback of SELDI-TOF-MS is the comparatively medium resolution of the spectra obtained. However this is adequate to resolve peaks in the 1000 to 25000 Da range from spectra with less than 500 peaks. The presence or absence of myostetotoic muscle is predicted by a decision tree model consisting of the presence or absence of multiple urinary protein/peptide peaks.

SELDI-TOF MS is an established technique for peptide/protein biomarker discovery (273). This method has been successfully performed in a recent study where SELDI-TOF MS was capable of identifying diagnostic markers of upper gastro-intestinal cancer in the urine of the same patients investigated in this Chapter (274). As excess or abnormal skeletal muscle protein breakdown or synthesis is likely to result in the presence of metabolites in the urine just as cancer associated markers appear in urine, an identical methodology should be suitable for detection of protein/peptide markers for the presence of myosteatosis.

5.3 Aim

The aim was to discover a urinary protein/peptide biomarker fingerprint for muscle wasting in cancer cachexia using myosteatosis as a measure of reduced muscle quality. The identity of such markers may offer insights into the development of myosteatosis and provide evidence to support its existence as an active pathological metabolic process in cancer cachexia. It may also identify high-risk groups amongst individuals with cancer-associated weight loss and potentially provide a novel non-invasive method for detecting and monitoring cancer cachexia during clinical trials of novel therapeutics.

5.4 Materials and methods

5.4.1 Patients[11]

Patients included were from the CRUK biomarker study group (Methods Chapter 2.1) who had available urine and CT scans.

5.4.2 Materials.

All buffers, gels and SELDI chips were from Bio-Rad (Hemel Hempstead, UK), and all other chemicals were obtained from Sigma-Aldrich (Gillingham, UK).

5.4.3 Sample collection.

Morning random urine samples were collected via a urinary catheter in the operating theatre immediately prior to surgery from patients with upper gastrointestinal (GI) cancer undergoing resection. All procedures were approved by the local research ethics committee. Written informed consent was obtained. The study conformed to the standards set by the

[11] I acknowledge Mr Nathan Stephens and Dr Carolyn Greig who recruited patients for this study

Declaration of Helsinki. All urine samples were stored at -40◦C. Long term storage of samples (>1 month) was at -80◦C.

5.4.4 Myosteatosis stratification.

A single cross sectional slice at the level of L3 was obtained from participants routine CT scan performed in the preoperative period. Tissue segmentation was performed according to the established protocol (Methods Chapter 2.4.1). A mean HU value for skeletal muscle was produced by the slice-o-matic programme for each patient (186). Myosteatosis was defined by the mean Hounsfield units for skeletal muscle. No established cut off value for myosteatosis exists, therefore an estimate was derived from the literature based on values two standard deviations below a normal healthy cohort (275). Values below 39.5 HU were regarded as myosteatotic.

5.4.5 Peptide identification and prediction model building[12]

5.4.5.1 SELDI-TOF-MS.

Mass to charge (m/z) peaks relating to potential peptides of interest were identified using SELDI-TOF-MS (methods chapter 2.9) SELDI-TOF-MS utilises a binding surface as a separation step prior to laser ionisation and time of flight mass spectrometry. Two binding resins (cationic and anionic) are used in this analysis to allow for the potential for different target peptide characteristics. Those used were CM10, a positive ion exchange resin and Immobilized metal ion affinity chromatography IMAC30 cation metal binding surface.

[12] I acknowledge Dr Holger Husi who performed this analysis

5.4.5.2 Model building and validation.

Model building was performed for prediction of myosteatosis from clustered peak lists using decision tree-analysis (methods chapter 2.9.3). 20 myosteatosis samples and 20 control samples were chosen randomly and used as the learning and testing dataset. The remainder of 15 samples was used as the validation dataset for blind-testing. Sensitivity was defined as the probability of predicting myosteatosis cases, and the specificity was defined as the probability of predicting control samples.

5.4.5.3 Peak isolation and identification.

Peaks observed in the CM10 and IMAC30 chip-types which show marked expression differences between control and myosteatosis samples, or were branching points in the models were further investigated to identify the peak of interest. Urine from positive or negative samples in relation to specific peaks was added CM10 or IMAC30 spin column resins before being washed and separated by gel electrophorseis (Methods Chapter 2.9.4). Resulting peptides and proteins were eluted from gel bands and analysed by Liquid chromatography-tandem mass spectrometry (LC-MS/MS) (274). Fragmentation spectra submitted to the Mascot search engine for protein identification (Matrix Science, London, UK) using UniProt/SwissProt (release July 2010, Homo sapiens, 18055 sequences) as the reference database.

5.4.5.4 Mascot-SELDI matrix matching.

Observed proteins with at least two peptide matches from the LC-MS/MS analysis were then further analysed by pattern matching based on SELDI-TOF-MS measured expression levels of peaks of interest (expected abundance in selected samples). This was done using software written in-house, which compares observed protein expression patterns in a pre-defined set of samples (LC-MS/MS results) against a matrix of peak patterns (SELDI-TOF clustered peak intensities, where estimated peaks are set to null) in the same set of samples. The

scoring is based on sensitivity (percent observed over expected) and specificity (percent not observed over not expected), and results are presented in descending order of cumulative scores.

5.5 Results

55 patients (mean age 64 yrs) with upper GI cancer were stratified according to the presence or absence of myosteatosis with 24 being regarded as non-myosteatotic (Table 15). All data exception of CRP had a normal distribution. The Non-myosteatotic control group were significantly shorter, lighter and older than the Myosteatotic group but had similar BMI and weight loss (students t test) and similar CRP (Mann-Whitney U).

	Control n=24	**Myosteatosis n=31**	**Entire cohort n=55**
Mean age	60 (10)	67 (7)*	64 (9)
Male : Female	18:6	27:4	45:10
Height	168.7 (8.3)	174.8 (7.3)*	
Weight	72.6 (16.5)	82.9 (14.8)*	78.4 (16.3)
Weight loss	-6.7 (8.8)	5.3 (6.9)	5.9% (7.7%)
BMI	25.4 (4.7)	27.2 (4.6)	26.4 (4.7)
CRP	1.5 (144)	3 (171)	2 (171)
Skeletal muscle mass			
Mean HU	45.9 (4.6)	33.5 (4.6)*	39.0 (7.7)

Table 15- Demograpics of the cohort (n=55) of patients with upper GI cancer in the study of the urinary proteome. Myosteatotic and non-myosteatotoc. Data is Mean (SD) or Median (range) for CRP. *=p<0.05 Myosteatois vs control (student's t test, Mann-Whitney U).

Four peak clusters in the IMAC30, and 8 in the CM10 datasets showed statistically significant p-values < 0.05, which indicates a potentially significant difference in expression levels for a particular protein or peptide cluster.

Decision-tree modelling using the Biomarker Pattern software (BPS) of peak clusters of 20 random samples of each cohort was validated by the remainder of the entire cohort (4 control and 11 myosteatotic samples). Decision tree models are shown in Figure 23A and Figure 23D. The IMAC30 chipset-based model (Figure 23A) showed a sensitivity of 100% and a specificity of 25% for the validation data-set, and application of the derived model to the entire cohort showed a sensitivity of 97%, specificity of 71%. Application of the CM10 chipset-based model (Figure 23D) to the validation dataset gave a sensitivity of 73%, specificity of 25%, and for the entire cohort the values are 77% sensitivity, 67% specificity.

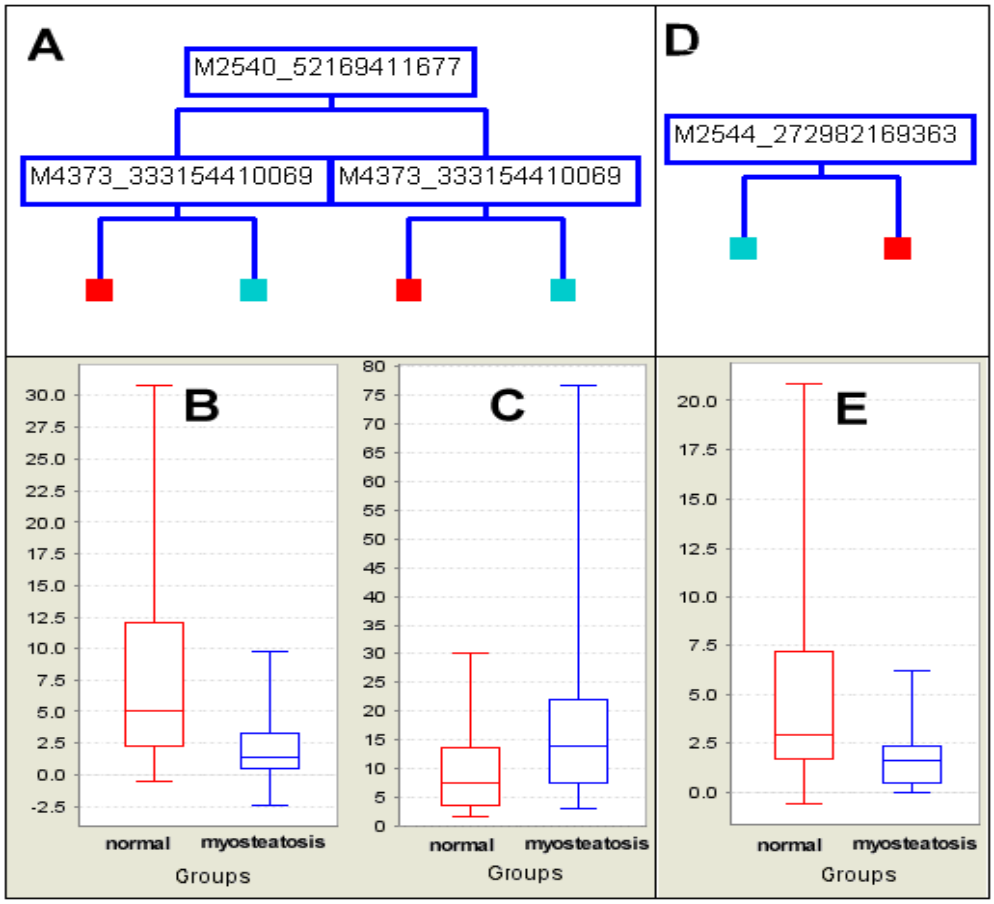

Figure 23- Decision tree-analysis models and expression profiles of potential biomarker peaks. Cluster-peaks implicated in the tree-analysis model using the IMAC30 chip-type (panel A) or the CM10 chip-type (D) stratifying myosteatosis (blue) and control (red) were plotted according to their normalized intensity values (B, C and E, y-axis) for peak clusters of m/z 2540 (B), 4373 (C) and 2544 (E).

Statistical analysis of the m/z cluster peaks implicated in the models and potential marker peaks showing low p-values are shown in Table 16. Peaks of interest were analysed by m/z clustering with a window of 0.2% of mass in 55 urine samples on both IMAC30 and CM10 chip-sets. Both average m/z and intensities with standard errors are included. P-values were calculated using the Mann-Whitney nonparametric test, and the receiver-operating characteristic (ROC) area with myosteatosis as the positive group. The average and median fold change was calculated using intensity values of individual peak clusters from the control and myosteatotic groups. Frequency % describes the likelihood of a particular peak to be found in a specific group by peak-clustering using a S/N of 5. Sensitivity and specificity values were calculated by computational decision-tree modelling using the peak in question as the sole predictor, and the SELDI normalised cut-off values are the associated mass spectrometric intensity values where the reported sensitivity and specificity levels are met. The model score is derived from the tree-analysis modelling and describes the importance of a peak within the model.

chip-type	p-value	ROC area	m/z average	m/z STD	Intensity average	Intensity STD	average fold change in myosteatosis	% found in control	% found in myosteatosis	sensitivity	specificity	SELDI normalized intensity cut-off	model score
IMAC30	**<0.001**	**0.249**	**2540.6**	**0.656**	**4.710**	**6.798**	**0.25**	**29**	**6**	**77**	**67**	**3.796**	**57**
IMAC30	**0.010**	**0.692**	**4374.1**	**2.053**	**15.006**	**15.331**	**1.92**	**33**	**52**	**90**	**46**	**5.330**	**100**
IMAC30	0.031	0.677	3293.3	1.211	2.959	3.632	2.03	13	23	97	38	0.187	50
IMAC30	0.038	0.633	4022.5	3.849	15.242	14.390	1.82	58	87	23	100	23.359	40
CM10	0.004	0.278	3935.1	3.023	8.794	11.684	0.44	42	23	61	83	4.010	46
CM10	**0.013**	**0.293**	**2544.2**	**0.734**	**3.120**	**3.819**	**0.37**	**21**	**3**	**100**	**33**	**6.248**	**100**
CM10	0.032	0.337	3905.1	1.346	11.689	20.742	0.40	29	23	68	63	4.555	0
CM10	0.035	0.367	19135.9	4.947	1.174	1.325	0.50	42	35	100	25	2.631	0
CM10	0.038	0.323	8872.9	8.216	6.644	6.701	0.68	79	45	48	88	2.734	0
CM10	0.040	0.352	9972.8	5.235	8.391	6.251	0.77	33	29	77	63	7.948	0
CM10	0.045	0.648	7271.1	3.684	3.358	6.625	1.12	17	23	42	92	2.372	0
CM10	0.049	0.633	22341.0	34.548	0.995	1.077	1.80	38	61	48	88	1.024	0

Table 16 - Expression profiles of potential biomarker peaks identified in decision tree-analysis models and cluster analysis. Peaks included from the model building are highlighted in bold.

Of the four peak clusters in the IMAC30-based dataset which had either high model score values, or showed p-values below 0.05, three were up-regulated and one down-regulated myosteatosis (see e.g. m/z 2540 in Figure 23B and m/z 4373 in Figure 23). The CM10-based chipset showed eight peak clusters of interest, of which one was up-regulated, six down-regulated and one unchanged in myosteatosis (see e.g. m/z 2544 in Figure 23E). All of these clustered peaks, which showed statistical significance from both the IMAC30 and CM10 dataset, were further investigated by enrichment of urinary proteins from 14 (IMAC30) and 22 (CM10) samples each, and excision of gel bands after electrophoresis and LC-MS/MS downstream processing, followed by Mascot searching and identification of proteins contained within the samples as described earlier (274). All lead m/z clusters have p-values below 0.05.

All potential markers in this study were identified by Mascot-SELDI pattern matching. This was done using a dataset of 600 proteins identified for the IMAC30 chip-type from 14 urine samples, and 950 proteins for CM10 chips from 22 urine samples, in the region between 2 and 10 kDa, and each individual identification was based on Mascot scores greater than 16 and consisting of at least 2 peptides each. The scores were calculated as a percentage of the expected pattern in the Mascot-identified protein list compared with the measured pattern of peaks found by SELDI-TOF above the base-line (sensitivity), thereby setting all estimated peaks as null values, which were used to calculate the specificity. Table 17 lists all molecules found by this approach.

m/z peak	regulation	Protein ID	Protein name	mass [Da]	Mascot score	average number of peptides	Mascot-SELDI matrix matching scores
2540	down	GELS_HUMAN	Gelsolin precursor	85698	118	6.9	60 // 77
		MASP2_HUMAN	Mannan-binding lectin serine protease 2 precursor	75702	65	9.3	60 // 77
4022	up	MASP2_HUMAN	Mannan-binding lectin serine protease 2 precursor	75702	65	9.3	50 // 100
3934	down	CATC_HUMAN	Dipeptidyl-peptidase 1 precursor / Cathepsin C	51854	105	3	66 // 76
		AGRIN_HUMAN	Agrin precursor	214846	45	8.7	55 // 76
2544	down	ARSA_HUMAN	Arylsulfatase A precursor	53588	25	2	50 // 94
		GFAP_HUMAN	Glial fibrillary acidic protein	49937	61	4	50 // 88
8874	down	A2GL_HUMAN	Leucine-rich alpha-2-glycoprotein precursor	38178	90	7.9	66 // 100
9971	down	CYTB_HUMAN	Cystatin-B	11197	77	7.4	100 // 100
7271	-	H2AV_HUMAN	Histone H2AV	13509	30	2.3	100 // 100

Table 17 - List of potential biomarkers identified in this study. Mascot-identified protein expressions in 14 samples for the IMAC30 chipset, and 22 samples in the CM10 chip-type in the 2 to 10kDa range were compared with the expected expression pattern found by SELDI in the same samples. The regulation refers to the measured differences of peak intensities (up: up-regulation; down: down-regulation; -: not significant). The Mascot-SELDI matrix matching scores were calculated as percentages for sensitivity and specificity.

Both the m/z 3293 and 4373 from the IMAC30 screen and m/z 3905 from the CM10 chip-set data could not be matched to observed expression patterns, and m/z 19136 and 22355 from the CM10 chipset were too far removed from the gel-analysed mass range to assign them to observed protein patterns. Both the m/z 2540 and 4022 clusters from the IMAC30 dataset matched Mannan-binding lectin serine protease 2 precursor (MASP2), and the m/z 2540 peak also matched the expression pattern of Gelsolin (GSN). The observed expression patterns of both Agrin (AGRN) and Dipeptidyl-peptidase 1, also known as Cathepsin C (CTSC), matched the m/z 3934 peak cluster. The down-regulated m/z cluster at 2544 matched to both arylsulfatase A (ARSA) and glial fibrillary acidic protein (GFAP) expression profiles. The down-regulated m/z 8874 peak cluster expression profile matched Leucine-rich alpha-2-glycoprotein precursor (LRG1). The m/z 9971 cluster was associated with Cystatin-B, and the observed Histone H2AV (H2AFV) expression correlated with the m/z 7271 peak. None of the peak clusters show any significant age-or sex-related expression differences

The m/z distribution of individual peaks within a peak cluster shows the expected pattern of a heterogeneous population of urinary molecular species. However, this does not exclude that some peak clusters might consist of more than one unique protein or peptide.

5.6 Discussion

In the present study approximately 42% of patients with upper GI cancer were found to have myosteatosis. One potential limitation of this study is that no previously established definition of myosteatosis exists. Here a value 2 SD below the mean in a healthy population was used in a similar manner to definitions for sarcopenia and were selected from values stated in one small study (275). The populations described in other similar studies of skeletal muscle attenuation in healthy individuals are also small however, and different (although

similar) values could be obtained depending on the series chosen (276, 277). Skeletal muscle attenuation in the form of HU has recently been demonstrated to be associated with adverse outcome in patients with gastrointestinal and lung cancer (245) independent of BMI, Skeletal muscle mass or weight loss. Values obtained for increased risk were <33 for individuals with BMI>25 or 44 for those with BMI<25 and so are not dissimilar to the value of 39.5 chosen for all participants as a cut off for this study. Using this definition, HU values divided the cohort into two groups that had similar characteristics in terms of BMI, weight loss and CRP, implying that there was no difference between them in conventional measures of cachexia severity (59). The non-myosteatotic group were slightly older although the difference of seven years is unlikely to be clinically significant.

In this cohort SELDI-TOF-MS was able to analyse and screen urine from upper GI cancer patients for prospective myosteatosis biomarkers and to establish a proteomic fingerprint pattern which potentially can be used in clinical diagnostics.

It was found that both IMAC30 and CM10 are useful chip-types for the analysis of human urine (274), and models based on the analysis of 55 samples were generated from cancer patients. The samples were measured on CM10 and IMAC30 chips, and using the tree-analysis method, statistical models were established with overall sensitivities of 97% (IMAC30) and 77% (CM10) and specificities of 71% (IMAC30) and 67% (CM10) across the entire datasets. Using expression pattern matching, it was possible to assign several proteins identified in urine to the proposed biomarkers.

Cystatin-B is described as a protein which is able to stimulate cancer cell growth both in vitro and in vivo (278). However, this molecule has no known association with skeletal muscle wasting. Mannan-binding lectin serine protease 2 precursor (MASP2) matched the m/z 2540 and 4022 clusters from the IMAC30 dataset, however m/z 2540 was shown to be down-regulated, and the m/z 4022 up-regulated. It is a possibility that this could be an indicator that fragmentation states are altered in myosteatosis by e.g. lower quantities of

other proteases, such as Cathepsin C a lysosomal protease associated with proteolysis after muscle trauma (279), which we found to be associated with the down-regulated m/z 3934 cluster peak. Exercise injuries in mouse models have shown an up-regulation of Cathepsin C in skeletal muscle (280), and our observed down-regulation of the associated m/z cluster might indicate a dysfunction in muscle repair. The down-regulated m/z peak of 2540 also matched the expression pattern of gelsolin, which is an actin-filament modulating protein and can be found in smooth and skeletal muscle cells, as well as a secreted form in plasma (281). However, reported down-regulation of gelsolin in breast cancer cells, ovarian carcinomas, melanomas suggests that this molecule acts as a tumour suppressor (282), and so is unlikely to be a potential indicator of muscle-loss.

Agrin (AGRN), which also matched the same m/z cluster as cathepsin C is a component of the basal lamina on the surface of muscle fibers of the neuromuscular junction, and defects in this gene perturbs the maintenance of the neuromuscular junction (283), whereas an over-expression in a laminin-deficient mouse model increases muscle integrity and regenerative capacity (284). The observed down-regulation in the CM10-chipset based model could be related to a dysfunction of muscle regeneration. Conflicting with the down regulation observed here, however, is the finding that the Agrin fragment (CAF) has recently been identified as being elevated in the serum of a series of 73 older volunteers with sarcopenia compared with age matched controls (285). It is possible that this could reflect different mechanisms of wasting in aging and cancer whereby muscle regenerative ability is diminished in cancer but maintained in aging. CAF appears to be elevated in a group of sarcopenia patients that are potentially affected by an over-activity of neurotrypsin which leads to NMJ destruction with subsequent loss of muscle mass and function.

The down-regulated m/z cluster at 2544 matched to both arylsulfatase A and glial fibrillary acidic protein expression profiles. Mutations in arylsulfatase A can cause demyelination and

glial fibrillary acidic protein is associated with central nervous system disorders (286) and chronic neuropathies (287).

The down-regulated m/z 8874 peak cluster expression profile matched Leucine-rich alpha-2-glycoprotein precursor (LRG1), which is a secreted protein and has been postulated as a biomarker of ventricular dysfunction and heart failure (288). The reported up-regulation associated with heart disease is in contrast with our observed down-regulation of this marker, and its role in myosteatosis remains unclear. Histone H2AV expression correlated with the m/z 7271 peak. Some members of the histone H1 family have been reported to be involved in cell survival in breast cancer cells and H1.2 was identified as an apoptogenic factor (289). The measured SELDI-MS based slight up-regulation could be an indication of elevated apoptosis in general, and a specific role in muscle function, cancer or fat infiltration remains unclear.

With the exception of Agrin and Cathepsin C, the poor associations of some of these markers with known mechanisms of muscle wasting casts some doubt over the specificity of these results to changes in muscle quality in terms of intramyocellular lipid. One possibility is that some of the markers listed above might also be associated with other factors, such as cancer type. The cohort here included patients with cancers of both oesophagogastric and pancreatic origin and the presence of unrecognised specific markers for these cancer types might skew any interpretation of the results.

Additional potential limitations are that there may be effects on skeletal muscle HU other than intracellualr lipid. A clear association between intramyocellular lipid and Hounsfield units has been demonstrated in healthy individuals (200) but this has not been repeated patients with cancer. It is possible that tissue oedema could represent an additional influence on mean Hounsfield unit of skeletal muscle in patients with cancer that would not be present in healthy volunteers. Whilst a number of potential markers indicated such as Cathepsin C, Agrin and arclsulfatase A may be associated with muscle or neuromuscular wasting several

of these proteins are non-specific or cancer specific. This may indicate that the models are describing both muscle wasting and additional factors, potentially including cancer progression or nutritional states unrecognised or not assessed in this cohort. The potential influence on mean Hounsfield units in patients with cancer by factors other than intramyocellular lipid also requires to be explored further.

5.7 Conclusion

In conclusion, stratification and pattern matching allowed a search for specific myosteatosis-related potential biomarkers in urine using SELDI-TOF mass spectrometry. A down-regulation of a fragment of cathepsin C in myosteatosis was observed and this might relate to in muscle repair. Down-regulation of fragments from agrin, arylsulfatase A and glial fibrillary acidic protein were observed. These proteins have described functions in neuromuscular junctions and the central nervous system, and might indicate a systemic denervation of muscle tissue. Further study including an extended cohort would help determine the validity of the present findings.

6 Which index of muscle mass (trunk or limb) best reflects muscle function in cancer patients

6.1 Introduction

Chapter 5 attempted to develop a marker for muscle wasting / altered quality by proteomic analysis. Whilst this produced results that were consistent with the hypotheses (of the existence of myosteatosis-associated changes in the urinary proteome) the strength of the associations was weak and further work will be required. As currently there are no suitable surrogate markers for muscle wasting, evaluation relies on direct measurement of muscle mass. Typically these measures are of the limbs by DXA or MRI of or of truncal muscles from CT cross sectional area. These muscle groups may have different biological responses to cancer cachexia and may make different contributions to how patients are able to function physically. This Chapter explores the association between regional measures of muscle mass and measures of physical function.

Muscle mass may be measured in muscle wasting as a marker of disease severity, progression or response to treatment. However, perhaps the most important clinical aspect of muscle wasting as a measure in cancer cachexia or aging is the contribution its makes to the functional ability of the patient. Studies of muscle size and function typically assess strength or power along with muscle CSA and volume in specific muscle groups. This relationship is well studied in healthy individuals (290, 291) and in aging (268) with a clear correlation seen between muscle mass and strength (81).

In health a significant correlation is seen between muscle cross sectional area of the thigh and quadriceps strength measured by CT (292). Despite a strong correlation, there is

significant variation in muscle strength / power between individuals not explained by simple differences in sex or lean mass (292) . This variation has been extensively studied in aging where age-related changes in muscle quality may contribute to changes in muscle function in terms of strength and power (277). Although cross sectional area of skeletal muscle is commonly reported in assessment of cancer cachexia, the relationship of muscle area or volume with strength or power is not well described in this patient group. This is of particular importance as pain (293), fatigue, symptoms associated with cancer or cancer treatment as well as alterations in muscle quality will all affect the functional performance of these patients. The commonly studied muscle groups include the muscles of the lower limb, thigh and quadriceps or upper limb biceps area or forearm muscles involved in hand grip strength. These muscles or muscle groups are chosen as they are known to be functionally important in common actions such as rising form a chair or climbing stairs or may contribute to clinically significant event e.g. quadriceps weakness contributes to risk of falls in the elderly. Additionally, simple functional task measures such as timed up and go and sit to stand times are related to both muscle function and to disability, risk of falls and hospitalisation. These measures of function may be considered in a spectrum of complexity (Figure 24) whereby “simple” measures aim to assess the function of a single muscle or muscle group such as isometric knee extensor strength. Dynamic measures such as Leg extensor power where the limb moves during the measure are more prone to recruit additional muscle groups and may provide a less “pure” measure of an individual muscle group. The sit to stand measure is a more complex functional measure of muscle strength and power that also involves coordination of lower limb and truncal muscles and the timed up and go is more “complex” still involving both muscle strength, power, coordination and balance. Recently, lumbar skeletal muscle cross sectional area has become a commonly reported measure of muscularity in a variety of settings including cancer cachexia (294-296). However, it is not known how truncal muscularity relates to the strength and power of different muscle groups. In studies in patients with cancer it is not always practical or

appropriate to undertake extensive investigation for clinical research that adds to the burden of investigation or treatment of their cancer, particularly with regard to measures requiring significant exertion on the part of the patient or participant. Use of routine diagnostic CT scans is cheaper, quicker, reduces patient burden and also allows for retrospective analysis. This modality is now extensity used but has not been validated against function, limb strength and power in patients with cancer.

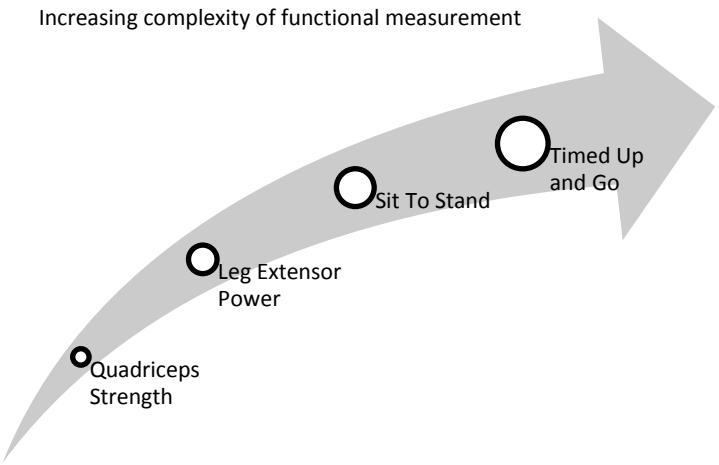

Figure 24 - Functional measures range from assessment of a single muscle groups to complex functional measures

6.2 Aim

The aim of the present chapter was to describe the relationship between trunk (L3) muscle cross sectional area CSA with lower limb strength and power sit to stand times (STS) and Timed up and go (TIG) and to compare these with the relationship between lower limb (quadriceps) CSA and the same measures in patients with pancreatic and upper GI cancer.

6.3 Method

Data was extracted from an existing cohort of patients, recruited prospectively, undergoing assessment for surgery for pancreatic and oesophago-gastic cancer as part of the CRUK biomarker study (Chapter 2.1) (297). Routine demographic and clinical data were gathered.

Maximum Isometric Knee Extensor Strength (strain gauge) (IKES), Maximum Leg Extensor Power (Nottingham Power Rig) (LEP), sit to stand time and timed up and go test were measured as described in Methods (Chapter 2.5)[13]. Muscle cross sectional area was measured on CT at the truncal level L3 Methods chapter 2.4.1) and MRI for quadriceps (Methods Chapter 2.4.2). Skeletal muscle CSA was measured from routine CT scans performed within 42 days of function measurement and prior to any surgical intervention. MRI was performed on the day of functional assessment.

6.3.1 Statistical analysis

Linear regression analysis was performed for height adjusted skeletal muscle CSA as a predictor for each measure of function. Strength, power, Sit to stand time and timed up and go were correlated with variables known to be associated with function: muscle cross sectional area, mean Hounsfield units for muscle, CRP, weight, height and weight loss (267). Statistical significance was set at a two-tailed p value of ≤ 0.05. Associations are described with r^2 values and uncorrected p values for each comparison. P values required for significance after Bonferonni correction for multiple comparisons are displayed for each analysis.

[13] I acknowledge Dr Carolyn Greig and Mr Nathan Stephens who recruited patients and performed functional assessments

6.4 Results

44 (16 female) patients underwent functional assessment. Due to patient availability / frailty IKES was unavailable in three patients, MRI quads in 14, MRI biceps in 30, CT in 10, STS and TUG in 4. Characteristics of the overall group are described in Table 18. All data were normally distributed Table 19.

Descriptive Statistics

	N	Minimum	Maximum	Mean	Std. Deviation
Age	44	39.00	88.00	63.34	11.03
Height M	44	1.52	1.90	1.70	.09
Weight (kg)	44	48.80	121.70	74.26	15.94
Self reported weight change %	44	-43.8	10.9	-6.7	9.3
CRP (mg/L)	44	1	172	20	40
IKES (N)	41	91.5	548.0	262.9	95.0
LEP (W)	44	39.0	270.0	101.5	49.0
STS (s)	40	0.30	0.98	0.63	0.17
TUG (s)	40	4.21	12.53	7.02	1.64
Quads CSA (cm2/m2)	30	12.59	25.62	18.35	3.37
Quads k-means CSA (cm2/m2)	25	9.00	23.97	15.38	3.44
L3 muscle CSA (cm2/m2)	35	34.38	58.40	44.51	6.10
Muscle mean HU	35	20.12	55.06	39.42	8.39

Table 18 - Group characteristics for patients with upper GI cancer undergoing cross sectional imaging and functional assessment.

One-Sample Kolmogorov-Smirnov Test

	IKES	LEP	HGD	STS	TUG	Quads CSA (cm2/m2)	Quads k-means CSA (cm2/m2)	Biceps CSA (cm2/m2)	biceps k-means CSA (cm2/m2)	Muscle mean HU	L3 muscle CSA
Asymp. Sig. (2-tailed)	.836	.169	.851	.850	.561	.797	.977	1.000	.922	1.000	.756

Table 19 - Kolmogorov-Smirnov test for normal distribution of data. No data group demonstrated a distribution that was significantly different from the normal (parametric) distribution ($p<0.05$)

Functional measures were compared with patient characteristics by simple linear regression. P=0.001 was considered significant to account for multiple comparisons after Bonferroni correction. Height and weight were significantly related to function in terms of quadriceps power while only weight was associated with quadriceps strength. These associations are expected and provide the rationale behind correction of these measures of strength and power for stature where they are used independently of other body composition measures (297). Age, CRP and weight-loss showed weak associations with function but with the exception of TUG and age, lost significance after correction for multiple comparisons. (Table 20)

	Height (m)		Weight (Kg)		Age (yrs)		CRP (mg/l)		Weight change	
	R^2	p	R^2	p	R^2	P	R^2	p	R^2	p
IKES (n=41)	0.049	0.166	0.287	***<0.001***	0.001	0.861	0.113	0.032	0.116	0.029
LEP (n=44)	0.225	***0.001***	0.199	0.002	0.091	0.049	0.051	0.140	0.061	0.106
STS (n=40)	0.003	0.748	0.000	0.983	0.101	0.045	0.050	0.163	0.087	0.065
TUG (n=40)	0.003	0.740	0.000	0.941	0.268	***0.001***	0.162	**0.010**	0.000	0.891

Table 20 - Regression analysis of patient characteristics with functional measures. Significant at p=0.001 (IKES = Isometric Knee Extensor Strength, LEP = Leg Extensor Power, STS = Sit To Stand time, TUG = Timed Up and Go)

Height corrected ($1/m^2$) truncal muscle (L3) CSA as measured estimated from routine CT was not related to measures of quadriceps function (significance at $p \leq 0.025$ for multiple comparisons) (IKES, LEP) (Table 21) but had significant association with more complex functional measures (Table 22) (significance at $p \leq 0.025$ for multiple comparisons). No relationship was seen with any functional measure and CT derived skeletal muscle mean Hounsfield units (Table 21, Table 22).

Quadriceps muscle strength and power	Truncal (L3) Muscle CSA (cm/m2)		Truncal (L3) Muscle HU	
N=31	R^2	p	R^2	p
Dominant IKES	0.068	0.150	0.032	0.325
Dominant LEP	0.081	0.103	0.014	0.509

Table 21 - Association of height adjusted CT measures of L3 muscle with quadriceps (Isometric Knee Extensor Strength and Leg Extensor Power) function. Significant at p=0.025

Complex function	Truncal (L3) Muscle CSA (cm/m2)		Truncal (L3) Muscle HU	
N=31	R^2	p	R^2	p
STS	0.234	***0.006***	0.006	0.672
TUG	0.175	***0.019***	0.103	0.078

Table 22 - Association of height adjusted CT measures of L3 muscle complex function (Sit to Stand, Timed Up and Go). Significant at p=0.025

Both gross and fat-subtracted measures of quadriceps muscle mass (from MRI imaging) were significantly correlated with quadriceps strength and power (Table 23). No association was seen with the more complex functional measures (Table 24). (significance at p=0.025)

Quadriceps muscle strength and power	Quads Muscle CSA (cm/m2) N=30		Quads K-means muscle (cm/m2) N=25	
	R^2	p	R^2	p
Dominant IKES	0.399	***<0.001***	0.412	***0.001***
Dominant LEP	0.242	***0.006***	0.346	***0.002***

Table 23 - Association of height adjusted MRI measures of quadriceps muscle cross sectional area with quadriceps function (Isometric Knee Extensor Strength, Leg Extensor Power). Significant at p=0.025

Complex function	Quads Muscle CSA (cm/m2) N=30		Quads K-means muscle (cm/m2) N=25	
N=28	R^2	p	R^2	p
STS	0.024	0.436	0.069	0.227
TUG	0.026	0.409	0.160	0.058

Table 24 - Association of height adjusted MRI measures of quadriceps muscle cross sectional area with complex function (Sit to Stand, Timed Up and Go). Significant at p=0.025

6.5 Discussion

Measures of muscle mass from quadriceps MRI and L3 CT both appear to relate to muscle function although measures from the two different anatomical locations appear to reflect different functional abilities in this group of patients with cancer.

As might be expected, MRI estimated quadriceps size, corrected for stature correlates with quadriceps strength and power. This appears to be true whether measures of total quadriceps CSA or the fat-subtracted area is used. This finding is consistent with known relationships between quadriceps strength and CSA in healthy individuals where cross sectional area of quadriceps correlates with knee extensor strength in healthy young men (r=0.59) and women (r=0.51) (292). The data presented in this chapter suggests that fat subtracted CSA could possibly be a more relevant measure as it appears that similar or greater variance (r^2) is described by the fat subtraction method despite smaller numbers in this group (25 vs 30 in the gross CSA group) and would be consistent with the principle that muscle quality (as described by fat infiltration) is an important influence on muscle function (267). However this finding was not reproduced when using HU as a measure of muscle quality. This measure differs from MRI fat-subtracted muscle area in that macroscopic adipose is already excluded during analysis of CT scans leaving only microscopic or intramyocellular deposits (264). Skeletal muscle HU have previously been shown to correlate with muscle function in terms of mobility limitation in healthy older people (267), this finding has not been reproduced here in terms of strength, power or simple tests of mobility. It is possible that other factors such as gross alteration in hydration status may be present in patients with cancer that influence skeletal muscle HU and diminish the strength of this association.

MRI of quadriceps CSA did not correlate with outcome in simple tests of mobility (i.e. Sit to stand and timed p and go). This finding is surprising as these tests are predominantly tests of quadriceps function with quadriceps strength normally the strongest predictor of Sit to stand

times in healthy individuals (298). However even in community dwelling older people knee extensor strength explains only 16.5% of the variance in the sit to stand test (298) with other factors such as visual contrast sensitivity, lower limb proprioception, peripheral tactile sensitivity, reaction time, and scores on the Short-Form 12 Health Status Questionnaire pain, anxiety, and vitality scales also contributing. In addition, strength training does not improve Sit to stand performance in older adults (299) and in heart failure, muscle size and strength are weaker predictors of exercise capacity in patients with cardiac cachexia vs non-cachectic individuals (300).

The measures of truncal skeletal muscle by L3 CT differed from the measures of quadriceps by MRI in their associations with function. As thigh muscle cross sectional area and L3 muscle cross sectional area both correlate strongly with whole body muscularity (195) it might be assumed that they should correlate directly with each other and therefore also equally with quadriceps strength and power. This was not found to be the case in this dataset. In contrast, lumbar skeletal muscle was a predictor of STS and TUG. Both the STS and TUG tasks require the use of a combination of lower limb and trunk motion initiated by *erector spinae* and involving *rectus abdominis* in addition to quadriceps and gluteal muscles (301). Trunk muscles also make a significant contribution to balance and coordination when weight is shifted, the trunk responds to counteract the change in the centre of gravity, maintaining postural control. Effective trunk muscle function is essential for balance, transfers, gait, and the range of activities in daily living (302). Trunk muscle fatigue impairs balance and functional task performance (303) and makes an equal or greater contribution than limb muscle strength (304). As a result, in disease states with muscle wasting, skeletal muscle measures at L3 from CT may be a better surrogate measure of functional impairment and disability than quadriceps CSA

6.6 Conclusion

Both CT of truncal musculature and MRI of quadriceps are potentially valid markers of muscle function. However, these measures appear not to be interchangeable as they reflect different aspects of functional ability. The mass of trunk muscles may play a different role in complex movements compared with the mass of lower limb muscles. Consideration of these differences is essential when selecting measures of muscle mass or function for use in definitions of muscularity in wasting conditions, or for use as outcome measures in studies of wasting conditions.

7 Regional changes in muscle mass following cancer surgery: a pilot study of patterns of change following resectional surgery for cancer

7.1 Introduction

In the previous chapter the apparent dissociation between regional measures of muscle mass and measures of function raised the possibility that cancer cachexia may exert different effects on muscle groups in different regions of the body. This chapter looks at changes in muscularity after surgery for cancer and investigates whether there is evidence of greater or less change in muscle mass in different regions of the body as a result of cancer cachexia and surgical trauma.

Muscle mass is lost in cancer cachexia (60) and the resulting low muscle mass is associated with increased morbidity during cancer treatment and poor survival. A number of treatments for cancer including chemotherapy (107) and surgery (305, 306) also result in muscle loss and the combined effect of cancer and its treatment may leave patients in a profoundly myopenic state. In curative surgery for cancer, removal of the tumour removes the driver of cachexia and resulting weight gain in the months or years postoperatively is regarded as an encouraging clinical finding. Persistent body weight loss >5%, beyond 6 months after gastrectomy for gastric cancer is associated with a 20% reduction in survival compared with non-weight losing individuals (307). After resection for upper GI cancer two thirds of patients have not regained their pre-operative weight by 6 months due to inadequate caloric intake. This model of semi-starvation does not preclude recovery of muscle mass. There is limited evidence examining recovery of muscle mass after surgery. A small non-randomised study of recovery after colonic surgery suggests that femoral muscle mass may decrease by

2% 8 days after surgery but increase by 7% 8 days after surgery in those undergoing a multimodal recovery programme (308). Post-operative whole body protein loss may also be demonstrated over a similar period after abdominal surgery by a cumulative negative nitrogen balance which occurs despite nutritional supplementation (309). Over longer periods muscle mass may not be regained; in a study of 72 patients undergoing abdominal surgery a loss of muscle mass was observed using mid-arm circumference over an 18 months follow up (310). After total hip arthroplasty muscle wasting occurs and is not regained at 5 months postoperatively despite active physical rehabilitation (311). This suggests that there may be a limited ability for regeneration after muscle atrophy from trauma or disuse in older patients. Conversely examination of the transcriptome from quadriceps biopsies taken before and after curative surgery for upper GI cancer shows that pathological processes in skeletal muscle of patients with cancer are no longer present after cancer resection and that the transcriptome becomes indistinguishable from that seen in muscle of normal healthy volunteers (64). This suggests that after upper GI cancer resection recovery of muscle mass should be possible as the suppression of skeletal muscle accrestion secondary to cancer cachexia has been removed.

There is limited longitudinal data assessing regional measures of muscle mass in cancer cachexia. While regional measures of muscle mass are associated with whole body muscle mass at a single point in time in a variety of settings, it is not known whether changes in muscle mass occur at the same rate in different regions of the body during muscle wasting in cancer cachexia. There is some evidence to suggest that upper and lower limb and trunk muscle or lean mass is altered at different rates in cancer cachexia. DXA measurement of regional lean mass in cancer patients who are recieving palliative care have shown that gain in lower limb mass may be observed concurrently with loss of upper limb lean mass during cancer cachexia (312). The current consensus cachexia definition includes low muscle mass

in its definition and quantifies this in terms of a low appendicular skeletal muscle mass consistent with sarcopenia (males <7.26 kg/m2; females <5.45 kg/m2) on DXA and any degree of weight loss >2% (97). Alternative methods of measuring muscle mass exist and the definition allows for any measure of low muscle mass placing absolute muscularity below the 5th percentile. Examples of these values are given and include, mid upper-arm muscle area by anthropometry (men <32 cm2, women <18 cm2); appendicular skeletal muscle index determined by dual energy x-ray absorptiometry (men <7.26 kg/m2; women <5.45 kg/m2) (78); lumbar skeletal muscle index determined by CT imaging (men <55 cm2/m2; women <39 cm2/m2) (106); whole body fat-free mass index without bone determined by bioelectrical impedance (men <14.6 kg/m2; women <11.4 kg/m2)(84). Each of these definitions quantifies muscle in a different region of the body using different techniques. If muscle mass is lost preferentially from one region compared with another then patients may be more or less likely to classified as cachectic dependent on the measure of muscle mass used rather than on the progression of disease. Cross sectional imaging allows for a direct measure of muscularity in different regions of the body and its excellent reproducibility means that it is ideally suited for monitoring longitudinal change in muscle mass (186). MRI can be used to measure muscle cross sectional area in upper or lower limbs and has no radiation dose so is suitable for use where repeated measures are required.

7.2 Aim

The pattern of regional change in muscle mass (arms versus legs) is poorly characterised in cancer cachexia. The aim of this work was to examine change in muscle mass in patients upper and lower limbs 7 months after Upper GI Surgery for cancer.

7.3 Methods

Patients undergoing curative surgery for oesophageal, gastric and pancreatic cancer were recruited (from the CRUK biomarkers study, chapter 2.1) and underwent MRI of upper arm (biceps) and thigh (quadriceps) pre-operatively and on one or more occasions in the year following surgery where possible.

7.3.1 MRI

MRI of biceps and quadriceps was performed pre-operatively and at intervals postoperatively according to the previously described method (Methods Chapter 2.4.2)

7.3.2 Statistical analysis

Descriptive data is described as mean and standard deviation (SD). Paired t-tests were used to assess change in muscle mass between baseline and follow up scans in both biceps and quadriceps. Additionally, paired t-tests were used to compare rates of change in biceps vs quadriceps in patients where both scans were present.

7.4 Results

12 patients (6 male, 6 female) were recruited and had MRI scans performed pre-operatively. Mean age was 61.6 (9.3) years and BMI 25.6 (5.8) at the time of surgery. Two patients had gastric cancer undergoing subtotal gastrectomy, 5 patients had oesophageal cancer undergoing an Ivor Lewis procedure, 4 patients had cancer of the pancreas or duodenum undergoing Whipple's procedure and one had cancer of the pancreas undergoing a distal gastrectomy. No patient developed clinical or radiological evidence of recurrence in the interval to follow up scan, 5 patients subsequently developed recurrence at a mean of 424

(88) days post operatively. Self-reported Pre-op weight loss was 10.3% (9.9) with 9/12 patients losing weight >5% (Figure 25). Weight loss from surgery to follow up scan was 3.7% (13.1) with 7/12 losing weight >5%. Weight measured at the time of surgery was lower than pre-illness self-reported weight p=0.007 but weight at follow up was not significantly lower than at the time of surgery p=0.215 (Table 25) suggesting that weight loss had been arrested by surgical intervention. No patient had returned to their pre-illness stable weight by 7 months after surgery.

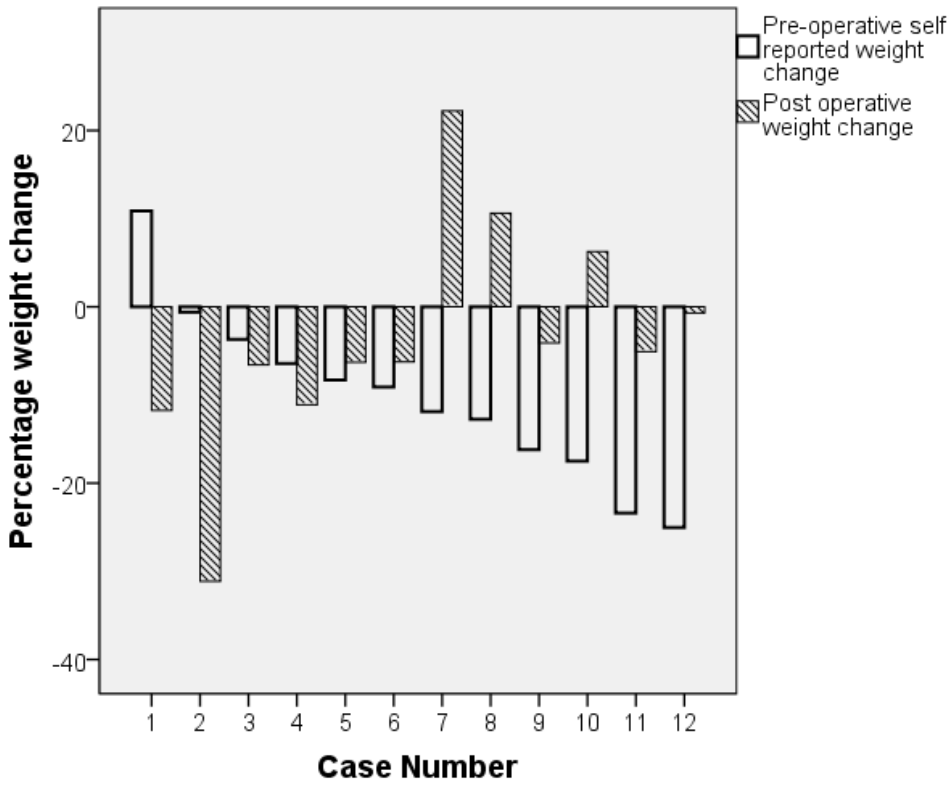

Figure 25 - Percentage pre-operative self-reported weight change and post operative (mean 220 days) measured weight change by case.

A first MRI scan was performed immediately prior to surgery with a second scan after surgery at mean of 220 (52) days. All patients had baseline and follow up quadriceps MRI. One patient did not undergo an initial biceps scan and four patients declined to have a follow up biceps scan. Immediately before surgery mean CSA in quadriceps was 51.2cm^2 (11.33) and 54.2 cm^2 (13.3) at follow up p=0.131. Immediately before surgery mean Biceps CSA was 10.5cm^2 (3.2) in 8 patients and was 11.2 cm^2 (3.4) at follow up p=0.370 (Table 25). There was no significant difference in the percentage change in arms and legs in individual patients Quadriceps +3.4% (8.9) and Biceps +8.9% (19.0) p=0.486. 4/12 patients lost quadriceps muscle CSA during the follow up period with the remaineder gaining muscle, 3/8 patients lost biceps CSA over the follow up period with the remainder gaining muscle (Figure 26).

	Weight (kg)	Quadriceps CSA cm^2	Biceps CSA cm^2
Pre-illness	81.64 (22.2)	-	-
At Surgery	72.92 (20.8)*	51.2 (11.33)	10.5 (3.2)
Follow up	68.30 (11.9)*†	54.2 (13.3)†	11.2 (3.4)†

Table 25 - Weight and muscularity in patients undergoing upper GI cancer resection at pre-operative, time of surgery and post-operative periods. Mean scan to scan interval 200 days (* p≤0.05 compared to Pre-illness time point, † p≥0.05 (not significant) compared to At surgery time-point)

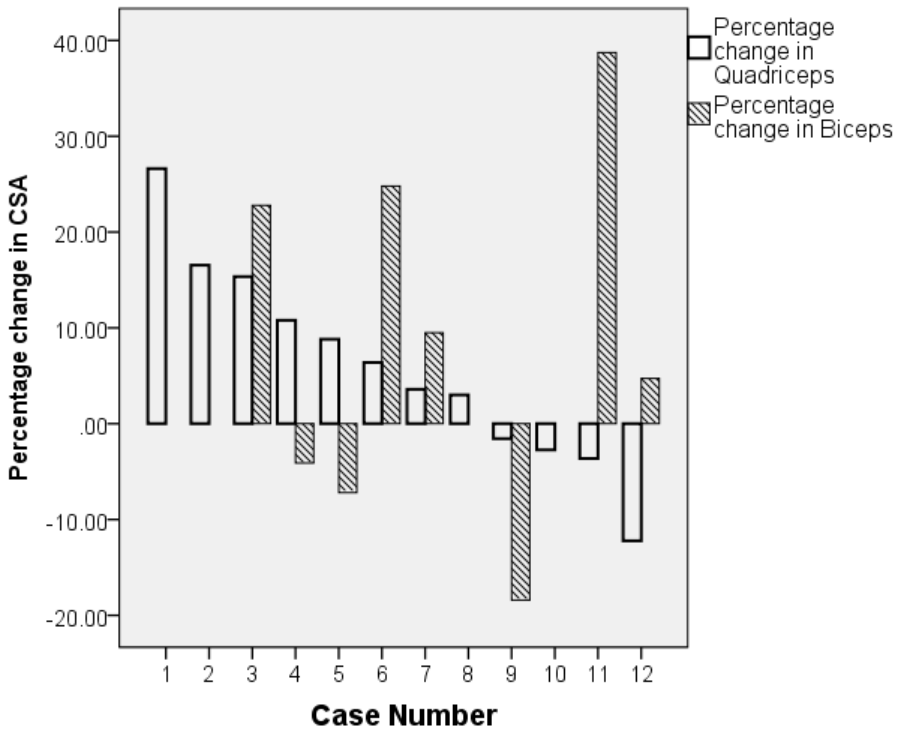

Figure 26 - Percentage change in muscle CSA in Biceps and Quadriceps after surgery for upper GI cancer with mean scan to scan interval 220 days.

7.5 Discussion

In this cohort of patients there was no detectable significant change in body weight or muscularity between the time of surgery and follow up at 7 months. Three quarters of the patients had cancer cachexia pre-operatively with overall substantial significant weight loss as a group pre-operatively. Despite the additional trauma of surgery and disruption of the normal anatomy of the upper gastrointestinal tract the rate of weight loss decreased significantly so that just over half could be considered cachectic at follow up and as a group there was no significant difference between weight at surgery and weight 7 months later. Measurement of muscle mass showed a similar pattern with no significant change in muscle mass overall. These results are somewhat consistent with a previous series by Liedman and

co-workers measuring body weight, fat and muscle mass via total body potassium (TBK) (101). In this later study there was no fall in muscle mass at either 6 or 12 months after surgery for gastric cancer although a fall in total body weight was noted. Leidman and co-workers hypothesised that the effects of surgery cause a reduction in body weight by a fall in fat mass only. Weight loss post operatively was less marked in the current group of patients, this may reflect the nature of the surgery with only 2 patients undergoing subtotal gastrectomy and the inclusion of a single patient who had a distal pancreatectomy and who experienced a 22% increase in body weight between surgery and follow up. After pancreatic surgery patients have been shown to lose weight up until 6 months and only begin to gain weight after this point (313). An alternative hypothesis to Leidman's would suggest that by 7 months after surgery any catabolic effect of surgery has been overcome by the patients' recovery after removal of their cancer. This would appear more likely given the known effects of trauma and reduced mobility on muscle mass. However, it would also imply that skeletal muscle mass begins to recover earlier than fat mass if overall body weight takes more than 6 months to increase after surgery. Although not statistically significant the data in the present study suggests a trend for on-going weight loss or incomplete recovery of body weight at 7 months after surgery coupled with static or slightly improved measures of muscle mass. If these alterations in body composition were true it would imply on-going nutritional deficit resulting in low body weight through fat mass depletion with recovery of muscle mass through removal of the cancer (and therefore cancer cachexia). This pattern would be consistent with the assumption that cancer cachexia acts to reduce both fat and fat free mass while inadequate caloric intake acts primarily to reduce fat mass.

There are a number of limitations to this study, the number of patients assessed is small and the failure to identify a difference in any measure between the two time-points may represent a type II error. The small numbers reflect the difficulty of performing prospective

longitudinal studies in patients undergoing surgery for poor prognosis cancer. Although non-invasive, additional MRI scanning is a time consuming, inconvenient and often claustrophobic additional burden of examination for a patient already attending surgical clinics, pre-operative clinical imaging and assessment prior to surgery and in the months following it. This group was drawn from a larger cohort of patients and represents patients who were able or willing to attend on multiple occasions for assessment and therefore the results may be subject to selection bias. This limitation highlights the importance of focussing on routine clinical imaging (e.g. CT skeletal muscle CSA) for body composition measurements. In Edinburgh, the clinical policy is that patients with cancer of the upper GI tract CT do not routinely undergo CT in the post-operative period except where recurrence is suspected so this modality was unsuitable for longitudinal study in this group of patients. Moreover, it was not possible to compare truncal L3 muscle CSA before and after surgery.

The choice of upper and lower limb CSA of biceps and quadriceps was made as these are associated with the functionally important movements of elbow flexion and knee extension. Single slice measures of quadriceps are known to correlate very closely with whole muscle measures (see chapter 4). However, biceps CSA is less well evaluated. Observations in this series give a mean % change in biceps of 8.9% but with extremely wide variability seen by a standard deviation of 19%. This could mean that biceps is subject to great variability in synthesis or catabolism between individuals dependant on nutrition, lifestyle and the effects of cancer and surgery. Alternatively it could represent poor reproducibility of this measure. Slice selection was made based on established anthropometric land-marking of the midpoint of the arm. It is possible that more accurate land-marking could be achieved by adjustment of the selected slice based on anatomical landmarks on the MRI scan at the time of analysis (314). Alternatively a different regional measure could be used such as truncal muscle as

seen on cross sectional imaging of the abdomen which although may be less well associated with specific muscle strength and power is a known reproducible measure of muscle mass.

The question of whether there are true regional differences in muscle wasting during recovery from cancer cachexia remains unanswered. This question is important as the cachexia definition allows for any regional measure to define the presence of cachexia and so regional susceptibility to this systemic condition may result in falsely classifying individuals as cachectic or non-cachectic depending on the muscle mass measure chosen. The principles of the study design in this chapter are appropriate to answer this question although with some modifications. The gold standard investigation for evaluation of muscle mass would be whole body MRI scan, however this is costly and time consuming for the researcher. The use of a single slice in this study has resulted in doubt over the validity of the biceps measurement and so a compromise of whole muscle volume assessments of biceps and quadriceps would provide a more time consuming but robust measure and reduce the number of patients required for the study by eliminating error associated with single slice estimation. It would also be possible to obtain a measure of trunk CSA during the same scan with minimal additional resource. This present analysis was performed on data collected as part of the larger CRUK biomarker study and so required additional investigations to be performed on the participants. The patients underwent blood, urine and muscle biopsy at each visit in addition to undergoing MRI scans. They were also asked to complete three separate health questionnaires and to undergo physical activity monitoring and perform tests of physical ability such as strength, power and complex functional tests. This resulted in a demanding protocol which may reduce compliance and appeared to influence attendance at follow up investigations. Future study would ideally limit investigation to MRI measures of body composition and simple clinical data. This reduction in burden to the patient would allow for repeated measures of body composition. An ideal protocol would involve 4 serial

MRI scans. An initial scan at diagnosis would determine baseline muscle distribution. A follow up scan immediately prior to surgery would allow measurement of regional patterns of muscle loss with cancer. Subsequent MRI at one month would demonstrate the effect of surgery on regional patterns of muscle loss and a final scan around 8-12 months post operatively would demonstrate the reversibility of the initial changes with removal of the cancer and sufficient time to recover from the effects of surgery.

7.6 Conclusion

There was no net change in arm or leg muscle mass 7 months after upper GI surgery. By this time-point the catabolic effects of surgery appear to have been balanced by the benefits of cancer resection.

8 Trunk changes in muscle mass following neo-adjuvant chemotherapy for upper gastrointestinal cancer.

8.1 Introduction

Chapter 7 showed, in patients with cancer cachexia a period of initial weight loss followed by stabilisation after surgery and no regional differences in muscle mass in the post-operative period. Investigation of changes prior to surgery was not possible by this method due to the absence of pre-operative MRI scans. Weight loss and body composition change in the pre-operative phase may, however, be more relevant to the investigation of cancer cachexia. This Chapter looks at the use of routine clinical CT scans performed in the pre-operative phase to asses body composition change prior to surgery.

Body composition change is the key defining characteristic of cancer cachexia (97). Weight loss in cancer is predictive of outcome in terms of survival and loss of lean mass is independently predictive of functional impairment (84), increased duration of hospital stay (88) decreased survival (61) and delayed recovery after surgery (256). These body composition changes may also confer additional risk to individuals undergoing treatment for cancer as low muscle mass predicts chemotherapy toxicity and time to tumour progression in metastatic breast cancer (102) and 5-fluorouracil-based chemotherapy toxicity in colorectal cancer (106). In addition to the effects of cancer on muscle mass, treatment such as chemotherapy could also result in net skeletal muscle catabolism either through a direct action to reduce skeletal muscle protein synthesis/breakdown or indirectly via inadequate nutrition secondary to nausea and poor appetite. This has previously been shown to occur during sorafenib chemotherapy for patients with renal cell cancer. Sorafenib appears to act to reduce skeletal muscle mass by a proposed mechanism indirectly suppressing Akt and

mTOR, which are key mediators in activating muscle protein synthesis by amino acids (107). This may not be true of all anti-cancer chemotherapy however and one recent phase II study of the mitogen-activated protein/extracellular signal–regulated kinase kinase (MEK) inhibitor Selumetinib in patients with cholangiocarcinoma demonstrated skeletal muscle anabolism as a side-effect of therapy (315) which may be explained by its effect as an inhibitor of Il-6. In upper GI cancer the impact of neo-adjuvant chemotherapy on patients nutritional status as assessed by changing body composition is not known.

8.2 Aim

The aim of this study was to evaluate changes in body composition by the use of routine CT scans during neo-adjuvant therapy for upper GI cancer.

8.3 Methods

Patients undergoing pre-operative assessment for curative surgery for cancers of the stomach and oesophagus were recruited as part of the CRUK Biomarkers study (methods chapter 2.1). Clinical data including height, weight, pre-illness weight, surgery and disease stage were recorded. Recorded weights taken during chemotherapy visits were extracted from the oncology case record and routine CT images taken at the time of diagnosis and post-chemotherapy prior to surgery were retrieved. Chemotherapy regimens varied acoording to pathology and included cisplatin, 5FU, capecitabine and epirubicin. Change in muscle and fat mass was obtained from 2 consecutive pre-op CT scans performed before and after neo-adjuvant chemotherapy. The cross-sectional area (CSA) of skeletal muscle and fat was measured on a single image at the level of the third lumbar vertebrae (L3) by a single observer with SliceOmatic V4.3 software (Tomovision, Canada) according to the established

protocol (methods chapter 2.4.1) (186). Short scan intervals (<50 days) were excluded. Muscle and Adipose were expressed in cm2/m2 and analysed as a cross sectional measure. Estimates of whole body fat (FM) and fat free mass (FFM) were made using the regression equations of Mourtzakis et al (186) [FFM= (0.3Xmuscle CSA) +6.06, FM=(0.042XFatCSA) + 11.2] to give clinical context to the magnitude of the changes observed and expressed as percentage change per 100 days to consider rates of change (61). Patients were categorised as sarcopenic, obese and sarcopenic obese according to established cut offs of 52.4cm2/m2 for men and 38.5cm2/m2 for women, overweight BMI>25, obese BMI >30 (105). Data are expressed as mean ± SD, differences between paired observations were determined by students' paired t-test performed on uncorrected values.

8.4 Results

22 patients 19 male, 3 female were identified with suitable pre-operative scan intervals. At the time of surgery mean age (SD) was 62.2 years (SD 9.8), height 1.73 metres (0.08) and weight 82.99 kg (15.6). Proportion of normal/overweight/obese by BMI were 7 (31.8%)/9 (40.9%)/6 (27.3%). The mean time between CT scans was 81 days (18.0). Fat CSA was excluded for 3 patients as a portion of the fat mass was outside the scan area.

	Pre-illness (self-reported)	Initial CT scan	Post chemotherapy CT scan	Significance (p) *
Weight kg (SD)	86.5 (16.5)	84.2 (16.2)	82.99 (15.6)	0.149
Muscle CSA cm2/m2		52.0 (10.3)	48.9 (9.3)	<0.0001
Fat CSA cm2/m2 (n=19)		134.4 (54.2)	128.0 (54.5)	0.309
Fat Free Mass kg		52.9 (10.6)	50.1 (9.6)	
Fat Mass kg (n=19)		28.1 (6.9)	27.3 (7.1)	
Obesity (BMI > 25)	8 (36%)	7 (32%)	6 (27%)	1
Sarcopenic (CT CSA)		10 (45%)	14 (63%)	0.125
Sarcopenic obesity		1 (4.5%	2 (9.1%)	

Table 26 - Changes in weight and body composition in upper GI cancer patients (n=22) undergoing neo-adjuvant chemotherapy. * Initial vs post chemotherapy CT (mean scan interval 81days)

There was significant change in weight between self-reported pre-illness weight and both weight at initial scan time-point p=0.049 and the pre-operative post chemotherapy scan time-point p=0.029. Weight loss between scans (during chemotherapy) did not reach significance p=0.149. Compared with pre-illness self-reported stable weight, 11 patients lost weight >5%, 9 patients were weight stable and 2 patients were heavier than their recalled healthy weight at the time of assessment. There was a significant loss of muscle mass as expressed by cross

sectional area of skeletal muscle p<0.0001 but no significant loss of fat cross sectional area p=0.309. Although nearly 20% more patients appeared sarcopenic after chemotherapy this apparent difference did not reach statistical significance (McNemar's test) p=0.125. There was no change in categories of obesity (McNemar's test) p=1.

There was considerable variation in the rates of change of fat mass when expressed as percentage change per 100 days with 6 patients appearing to have fat mass gain (>2%) (Figure 27).

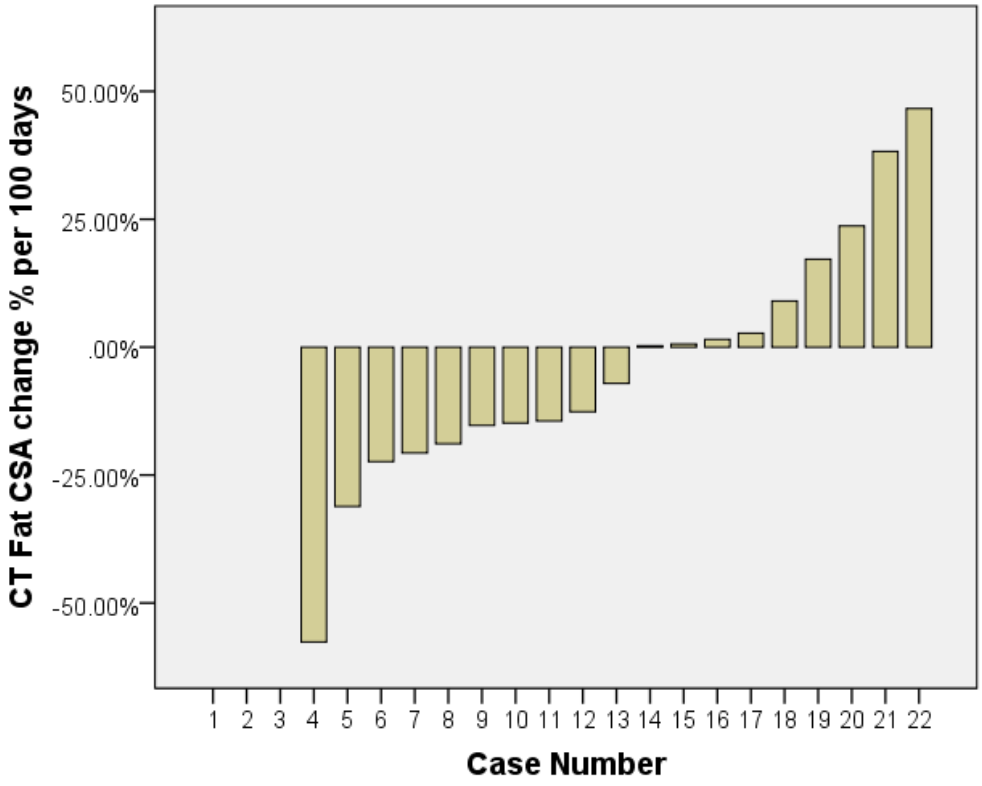

Figure 27 – Waterfall chart: Change in CT measured Fat CSA during neo-adjuvant chemotherapy in patients with upper GI cancer (n=22)(percent change per 100 days).

Changes in lean mass were more consistent with only one individual appearing to gain muscle mass Table 27. As expressed by cross sectional area, muscle area increased in one patient, was static in 3 patients and fell by at least 2% in the remaining 18 (Figure 28).

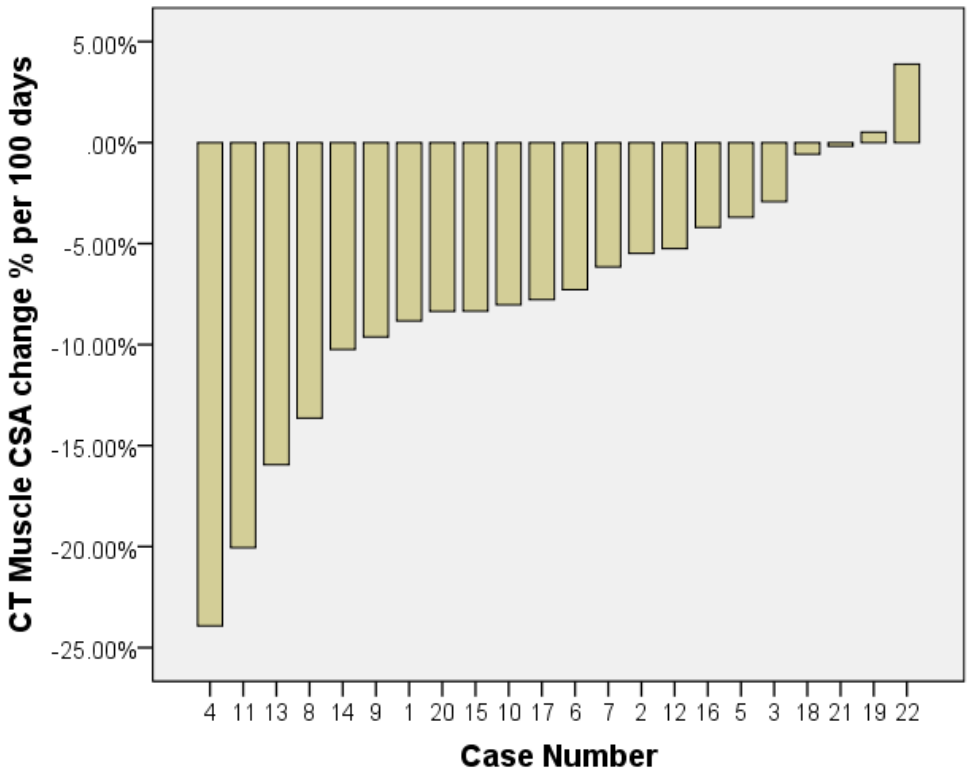

Figure 28 - Waterfall chart: Change in CT measured Muscle CSA during neo-adjuvant chemotherapy for upper GI cancer (percent change per 100 days)

	Minimum	Maximum	Mean	Std. Deviation
Pre op lean mass change % per 100 days	-20.62%	3.29%	-6.69	5.81
pre op fat mass change % per 100 days	-39.37%	24.31%	-3.37	13.87

Table 27 - Rate of change of whole body lean mass and fat mass in patients undergoing neo-adjuvant chemotherapy

8.5 Discussion

8.5.1 Muscle mass

These data confirm that sequential cross sectional imaging can detect changes in body composition within the clinical setting in small groups of patients. This data shows that neo-adjuvant chemotherapy is associated with loss of truncal skeletal muscle without loss of fat and in the absence of significant weight loss. There was a high prevalence of sarcopenia prior to commencing chemotherapy and significant loss of muscle mass during treatment in most patients. This finding of a high prevalence of sarcopenia is consistent with studies using cross sectional area measurements in lung and renal cancer where (60, 107) there appeared to be a trend for an increase in the prevalence of sarcopenia post-chemotherapy although the number of patients in this cohort is small and this may represent a type II error.

8.5.2 Fat mass

No loss of fat mass was seen during the same time interval. There was a wide variation in changes in adipose cross sectional area during the study period with percent change per 100 days ranging from 39% loss to 24% gain. Fat mass loss is a well-established phenomenon in patients with a variety of different types of cancer (99) and is clearly demonstrated in patients with advanced lung and gastrointestinal cancer (316, 317) where accelerated loss occurs in the 7 months prior to death. This appears to be in contrast with the current finding. However, a similar recent study of CT assessed body composition change in patients undergoing Serafanib chemotherapy for renal cancer also noted wide variation in fat mass change (107). Here 50% of patients experienced an initial gain in adipose and as a group only demonstrated a loss of adipose after one year of follow up. Possible explanations include; 1) Changes in fat mass have not been described using serial assessments with modern precise imaging techniques in early cancer and it is possible that significant loss of

fat mass does not occur without cancer progression. This explanation may be supported by the observation that patients undergoing neo-adjuvant chemotherapy have reduced levels of physical activity and energy expenditure (318) and so may deposit fat whilst losing muscle. 2) Assessment of total body adipose using a single cross sectional image is less precise than for estimation of muscle mass (259). No adequate studies of reproducibility exist for adipose tissue measured in this way and it is possible that wide variability could result from real changes in body fat distribution or from inconsistency of CT slice selection and patient positioning in the CT scanner.

8.5.3 Weight

50% of the patients were cachectic by measure of >5% weight loss and significant weight loss was noted prior to beginning chemotherapy in the group as a whole. No significant weight loss was observed during neo-adjuvant chemotherapy. This finding highlights the importance of body composition measures in patients undergoing treatment or assessment for cancer as the underlying loss of lean mass in these patients is not apparent in simple assessment of body weight.

8.6 Conclusion

Patients undergoing neo-adjuvant chemotherapy for oesphago-gastric cancer have a high prevalence of cancer cachexia prior to treatment. During chemotherapy significant loss of muscle mass occurs which is not apparent by measurement of weight loss alone and is not matched by loss in adipose tissue. Such changes may impact on the functional recovery of patients who subsequently undergo upper GI resection (256).

9 Measurement of muscle protein dynamics in free living subjects: development of a novel oral tracer technique for measurement of habitual skeletal muscle protein fractional synthetic rate and evaluation in a pilot group of healthy volunteers.

9.1 Introduction

The preceding Chapters have evaluated the use of cross sectional imaging in the assessment of muscle wasting. Cross sectional imaging is able to observe changes in muscle mass but is reliant on serial measurements and gives no insight into the mechanisms of muscle loss. This Chapter describes the development of a novel measure of muscle change.

Muscle wasting occurs commonly in a number of diseases including cancer cachexia, chronic obstructive pulmonary disease, cardiac failure, HIV-AIDS, and renal failure. It is believed that the body's normal mechanisms for muscle growth and repair are impaired in these conditions. Some doubt remains over whether this net muscle wasting is caused primarily by reduced muscle synthesis or increased muscle degradation. Both processes appear to occur in muscle wasting, the catabolic and anabolic signalling pathways appear to be interdependent and as a result suppression of degradation may also promote synthesis and vice versa (319). Previous intervention studies attempting to modify muscle mass through suppression of the inflammatory response and therefore reducing skeletal muscle net loss have resulted in limited success, either producing mixed results or requiring complex regimes to demonstrate differences in muscle mass between intervention and control arms (129). Promising novel therapies are currently undergoing evaluation in patients including oral β-agoniststs (320) and anti-myostatin antibodies (321) which aim to promote net skeletal

muscle protein anabolism. These interventions require robust measures of muscle mass accretion to demonstrate their efficacy. It is therefore important to be able to assess muscle synthesis accurately in order to develop a greater understanding of the pathophysiology of muscle wasting in these conditions and also to monitor response to proposed treatments in clinical trials.

Although cross sectional imaging is capable of assessing longitudinal changes in muscle mass it has a number of practical limitations which restrict its use (259). Primarily these problems are related to the requirement for multiple measures, as described in chapters 3 to 8. Difficulties arise either from the need for multiple additional assessments in the case of MRI or rely on coinciding clinical assessments out-with the control of the researcher in the case of CT. In addition these modalities may have difficulty in reliably detecting the small accumulations or losses of muscle mass which occur over the medium timescale relevant to evaluation of novel interventions in cancer cachexia. The alternative to evaluation of change in muscle mass by multiple sequential static measures is the use of a single dynamic measure of muscle synthesis by the use of tracers to calculate skeletal muscle fractional synthetic rate (FSR). The measurement of muscle FSR is also of interest in other situations such as in sarcopenia (the process of muscle atrophy seen in aging), muscle atrophy seen during prolonged bed rest or spaceflight, and in sports physiology where there is increased muscle synthesis during athletic training. Skeletal muscle FSR is measured by the administration of a labelled tracer, the incorporation of which can be measured in skeletal muscle biopsies. Conventional methods for this involve the administration of amino acids such as leucine, phenylalanine, labelled with stable isotopes such as ^{15}N, ^{13}C or ^{2}H. Many other stable isotope labelled amino acids have been applied for specific biological and analytical reasons (e.g., glycine, valine, proline, lysine). These protocols require the administration of the labelled amino acid to be given by intravenous infusion either as a large bolus (flooding dose

protocol) or a longer infusion (primed constant infusion protocol). There are a number of disadvantages. a) the administration of amino acids is known to influence protein synthesis so use may alter the variable of interest. b) the use of an infusion requires the protocol to be completed in a controlled study environment, places additional burden on the patient/participant and may limit their normal levels of activity. c) The infusion protocols are performed over short time periods and are unable to measure the cumulative effects of disease such as cancer cachexia, treatments or response to training that usually occur over a time period of several weeks. d) There are technical difficulties with the estimation of the precursor pool as it must be assumed that there is a constant gradient between plasma and tRNA bound amino acids within the cell.

One solution to these difficulties is use of a deuterium tracer which may be administered orally and endogenously label the amino acid of interest with ^{2}H . A protocol of this kind avoids excess amino acid administration and can allow administration of the tracer in the patient/participants own home. As the labelling of free amino acids should be faster than the rate of incorporation of amino acids into muscle protein, the plasma $^{2}H_2O$ may be used as the precursor in calculation of skeletal muscle FSR. This endogenous labelling has previously been demonstrated in non-essential amino acids including alanine where four hydrogen atoms come into rapid equilibration with body water via pyruvate (Figure 29) (224).

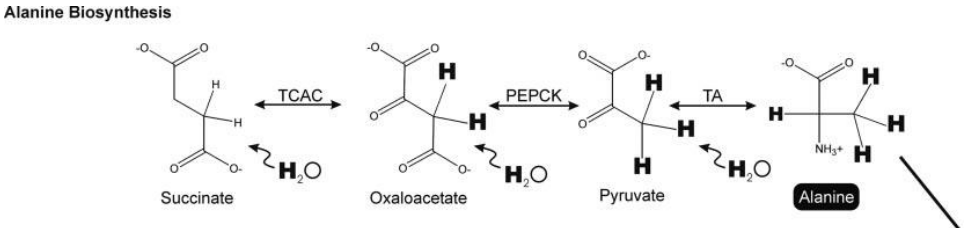

Figure 29 - Alanine biosynthesis (From Gardner et al. (322) Deuterium (H) is incorporated from heavy water. Alanine (Ala), a non-essential amino acid is synthesised from abundant metabolic precursors from the tricarboxylic acid cycle (TCAC), phosphenol pyruvate carboxykinase (PEPCK), and transaminase activity (TA), incorporating four H into alanine yielding C–H bonds.

This method of endogenous labelling by oral deuterium tracer has been used previously in studies of skeletal muscle synthesis on animal models and in studies of plasma and liver proteins as well as glucose and carbohydrate metabolism in humans and animals (323, 324). These studies have been able to achieve relatively high concentrations of labelled product in the tissue, protein or molecule of interest by measuring fast turnover proteins or giving high dose or repeated doses of oral, intravenous or intraperitoneal deuterium. In clinical studies in humans it is necessary due to potential side effects of deuterium dosing to use a low dose protocol (ie ~0.5 mole per cent excess per day). In order to ensure good compliance with the protocol and to maximise the potential benefits of reduced participant burden a single oral dosing regime is desirable. This factor combined with the low turnover of skeletal muscle (FSR ~1% per day) results in a very low level of ^{2}H incorporation in the protein of interest. To overcome this requires the use of highly sensitive GC-pyrolysis-IRMS as proposed by Gasier et al (229).

Previous investigators have described wide variation in the range of human skeletal muscle FSR. This variability may be related to the choice of tracer used, experimental conditions such as exercise or feeding/fasting and the protein fraction analysed. Myosin is the main force generating component of skeletal muscle and would be the preferred cellular component for assessment of muscle specific FSR. Protocols exist for isolation of myosin however these are not widely used as the most widely described method of protein electrophoresis is both costly and time consuming taking 13-16 hours per sample (325). Commonly whole muscle lysates or myofibrillar components are analysed for muscle FSR. Whole muscle protein FSR may be associated with variability due the presence of different protein fractions including sarcoplasmic, mitochondrial, and myofibrillar proteins and gives

a significantly greater FSR than myofibrillar/myosin heavy chain FSR values (219). The myofibrillar component consisting of myosin, actin, tropomyosin, and troponin may be a more robust and clinically relevant fraction for analysis as it represents the "mechanical" fraction of skeletal muscle while minimising losses due to sample processing. A simple method for myosin isolation has been described using separation on SDS minigel although this has not been used for preparation of human skeletal muscle for assessment of FSR in this setting where high yield is essential (326).

9.2 Aim

This study examined the feasibility of a protocol to measure skeletal muscle fractional synthetic rate in free living healthy volunteers over a two week period using a single oral deuterium tracer dose. The specific objectives were

i. To determine the feasibility and acceptability of developing a protocol requiring a single deuterium dose and single muscle biopsy

ii. To verify the distribution and elimination characteristics of total body water ^{2}H.

iii. To verify the extent of endogenous ^{2}H labelling of alanine.

iv. To reproduce a protocol for myofibrillar isolation.

v. To investigate the feasibility of myosin isolation in small samples using animal skeletal muscle prior to human sample processing.

vi. To determine whether intramuscular free alanine enrichment is in equilibrium with that in the plasma free alanine pool?

vii. To determine whether intramuscular free alanine enrichment is in equilibrium with body water ^{2}H enrichment?

viii. To determine whether muscle protein incorporates the tracer with time in a steady linear fashion that can be measured with sensitivity and accuracy?

ix. To compare estimates of muscle protein FSR with published values?

9.3 Method

9.3.1 Human protocol

Healthy male volunteers were recruited to the study designed to measure habitual skeletal muscle fractional synthetic rate as described in Methods for the oral tracer pilot study (Chapter 2.2.1.2). Participants were fit and active individuals recruited via email or local advertising and were assessed against previously published exclusion criteria (230). Serial serum samples and muscle biopsies were collected after administration of a single oral bolus of deuterium oxide. Time-points for sample collection were staggered between subjects in order to give a range of muscle biopsy sample times relative to dosing Figure 6. No specific instructions were given to participants who were encouraged to continue their regular diet and activity patterns over the course of the two week protocol. Procedures are described in full in sections 2.2.1.2, 2.3.2, 2.6.1.1, 2.6.2, 2.6.3.

9.3.2 Preparation of serum samples

One ml of serum was used for analysis of ^{2}H enrichment in body water by continuous flow IRMS. One mL of each serum sample was processed for analysis of free amino acid enrichment by cation exchange. Basal deuterium abundance in protein-bound alanine from serum albumin was measured (242) and assumed to be equal to basal abundance in skeletal muscle.

9.3.3 Preparation of skeletal muscle biopsies

9.3.3.1 Myofibrillar component separation

Skeletal muscle biopsies were processed to isolate the myofibrillar component from sarcoplasmic proteins by serial triton x-100 washes as described in 2.7.2. An aliquot was removed for Western blotting for myosin and actin at stages during processing to confirm the presence of myosin.

9.3.3.2 Myosin isolation

Myosin separation by protein electrophoresis on SDS minigels according to the protocol by Hasten et al (326) was trialled initially in samples of skeletal muscle from healthy mice. Muscle samples of between 20 and 50mcg were homogenised in buffer A using a glass hand homogeniser. Protein concentration was measured by the Bradford assay (240). Samples were denatured in the sample loading buffer at 95° for 5 mins before loading into 6% and 7.5 % minigels at various concentrations to determine the maximum practical loading concentration with bands visualised using Coomassie blue staining. Subsequently, larger samples were loaded onto single well 6% minigels (as per methods chapter 2.7.3). The myosin band was identified with colloidal Coomassie stain, cut out, de-stained, macerated and dehydrated with serial alcohol washes.

9.3.3.3 Free intracellular amino acid separation

After homogenisation of skeletal muscle biopsies and centrifugation the initial supernatant was processed for separation of free intracellular amino acids by ultrafiltration as described in Methods Chapter 2.7.4. An aliquot of the filtrate was run on a SDS page minigel and stained with Coomassie blue to confirm removal of proteins.

9.3.4 Preparation of Albumin and myofibrillar pellet samples[14]

Albumin and myofibrillar protein pellet samples were freeze dried prior to acid hydrolysis at 150^{o}C for 4 hours gas phase acid (243) the derivatised amino acids were re-dissolved in 0.3 mL hexane and transferred to 1.5 mL 'wineglass' GC vials for analysis and freezer storage. Following GC analysis (see below 9.3.5) some samples contained insufficient sample and were rejected from the analysis. This was most likely due to low protein content in the original biopsy.

9.3.5 GC-pyrolysis-IRMS of amino acids[15]

An identical procedure was performed to determine ^{2}H enrichment of amino acids in serum albumin, the free intracellular pool and the myofibrillar component as described in Methods Chapter 2.8.3. In basic outline; the amino acids derived from sample hydrolysis were added to the gas chromatograph stage separating amino acids, with amino acid peaks identified using a flame isolation detector. Sample flow was diverted to a 1350^{o}C capillary pyrolysis furnace to convert analytes to H_2 gas. Finally the atom fraction ^{2}H was determined by the isotope ratio mass spectrometry stage. As an independent test of the systems' performance, a series of deuterated alanine standards was created, encompassing the full range of enrichment from natural abundance, through low enrichment protein-bound amino acids to high enrichment free amino acids. This was constructed by gravimetric dilution of a commercial deuterated alanine ($^{2}H_4$-L-alanine 99 atom %, CDN Isotopes, Canada) with natural abundance L-alanine (Sigma).

[14] I acknowledge Sandra Small who performed this preparation
[15] I acknowledge Sandra Small and Prof Tom Preston who performed this analysis

9.3.6 Calculations

Fractional synthetic rate (FSR; % day^{-1} or % $hour^{-1}$) was calculated as:

$$FSR = \frac{\text{Change of myofibrillar protein-bound alanine enrichment with time}}{\text{Average free alanine enrichment}}$$

Alternatively,

$$FSR = \frac{\text{Change of myofibrillar protein-bound alanine enrichment with time}}{\text{Alanine enrichment estimated from average body water enrichment}}$$

Average free alanine or body water enrichment over each specific period was calculated from the area under the curve of the log transformed elimination plot.

Absolute synthetic rate of myofibrillar protein (ASR; g day^{-1}) was calculated as:

$$ASR = FSR/100 \times SMM \times 1000 \times 12.4/100$$

9.4 RESULTS

Five healthy non-smoking physically active males were recruited. One volunteer dropped out after the first biopsy due to discomfort at the biopsy site and results were excluded from analysis. No side effects of deuterium dosing were noted. Median (range) age was 37 (24-52), BMI 24.9 (22-26.4). All other subjects completed all sample collections at the

predetermined staggered time-points Figure 30. Median biopsy weight was 35mg, biopsies less than 20mg subsequently proved to be inadequate for analysis.

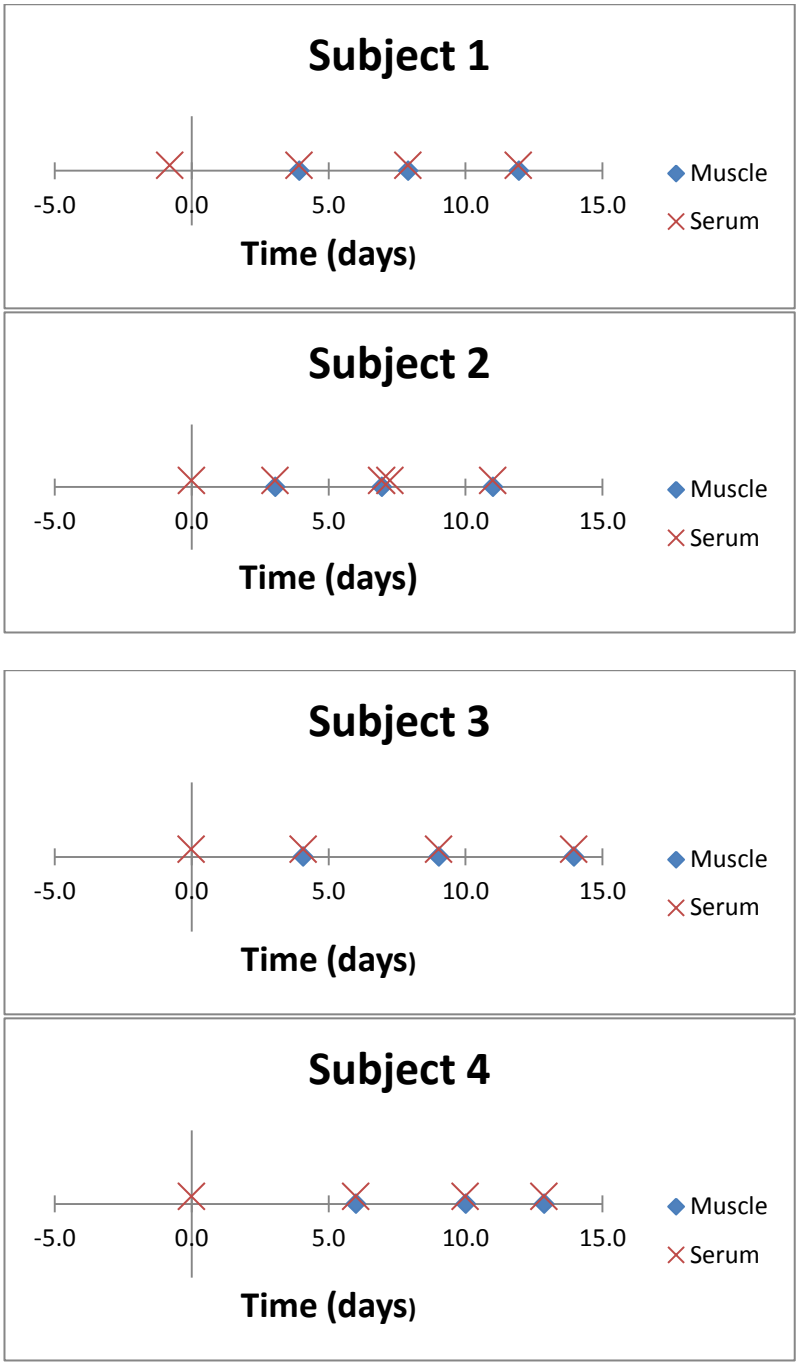

Figure 30 - Specimen collection time-points relative to deuterium dosing for each of the four subjects

9.4.1 Myofibrillar separation.

The centrifugation protocol successfully separated high (myofibrillar pellet fractions) and low molecular weight proteins with a negligible 200kDa band remaining in the supernatant (sarcoplasmic fraction) Figure 31.

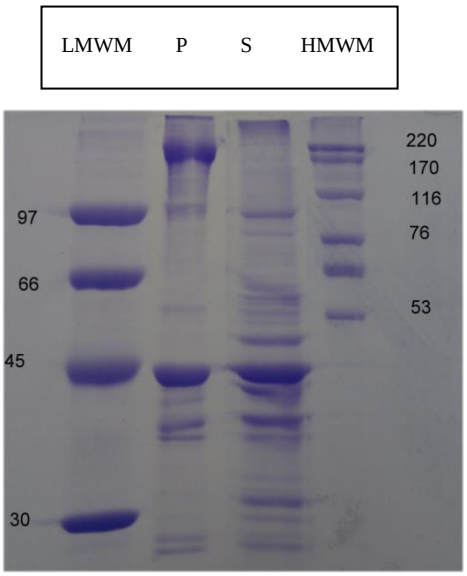

Figure 31 – SDS PAGE gel electrophoresis of myofibrillar pellet and supernatant fractions showing separation of the ~200kDa myosin band into the pellet fraction (P – myofibrillar pellet, S – supernatant, LMWM – low molecular weight marker, HMWM – High molecular weight marker)

Western blot analysis with anti-myosin antibody demonstrated a strong myosin band at 200kDa in the myofibrillar pellet fraction with a reduction in the supernatant fraction (Figure 32). There were visible bands produced at a number of molecular weights, this was thought either to represent non-specific binding or fragmentation of the myosin protein.

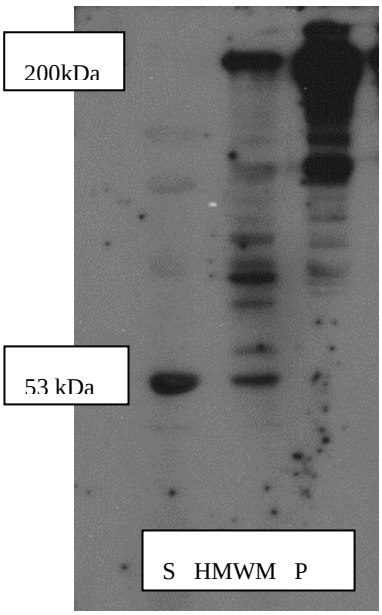

Figure 32 - Western blot analysis for myosin of myofibrillar P (pellet) and sarcoplasmic S (supernatant) fractions (HMWM, High molecular weight marker). There appears to be effective isolation of myosin into the pellet fraction.

9.4.2 Myosin Isolation

Trial protein samples were run on 6% and 7.5% 1mm thick gels demonstrating that the 6% gel was superior and that a maximum of 100ug of protein could be loaded into a 80ul well to achieve well defined myosin bands with minimal smearing. (Figure 33, Figure 34)

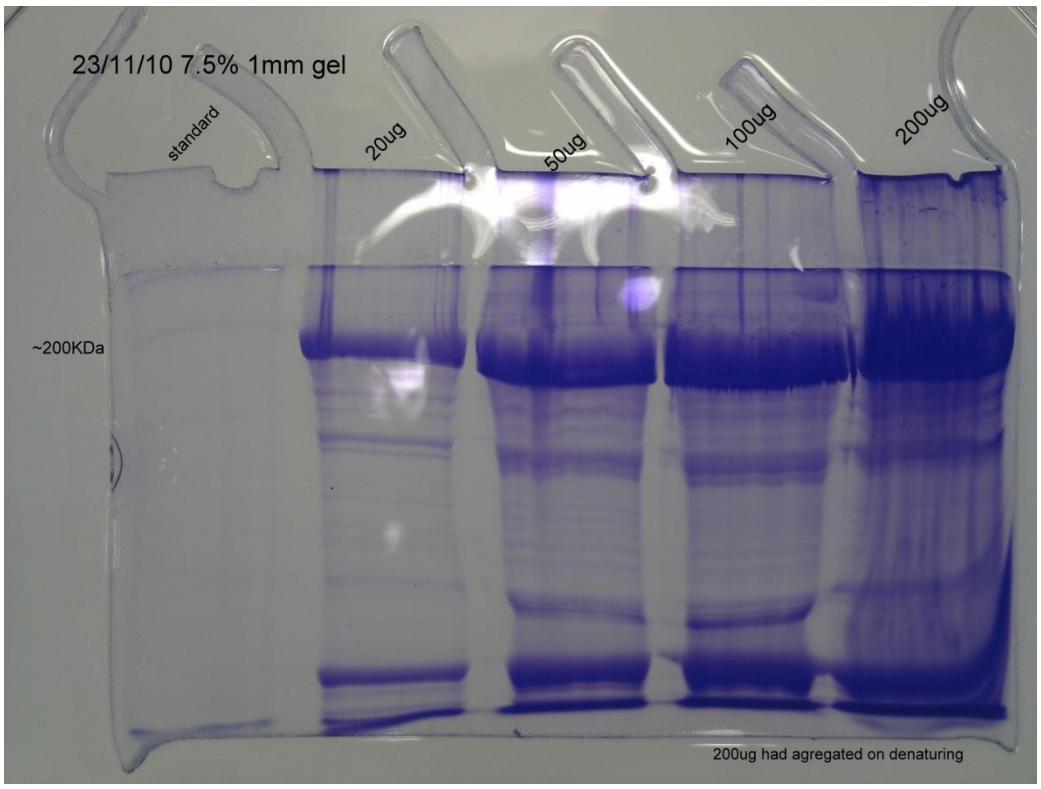

Figure 33 – Myofibrillar protein pellet loading concentration trial 7.5% gel. Protein quantities of 20, 50, 100 and 200µg.

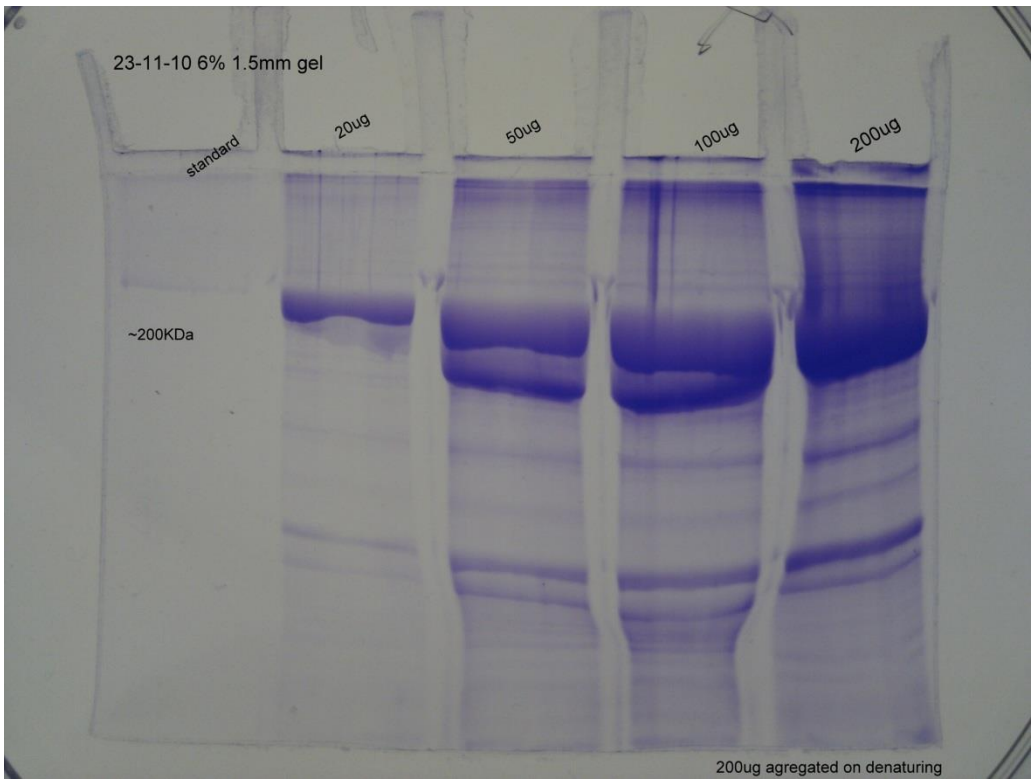

Figure 34 – Myofibrillar protein pellet loading concentration trial 6% gel. Protein quantities of 20, 50, 100 and 200µg.

Further trial samples were processed on a single well mini-gel and the myosin band isolated by cutting the band from the gel (as described 2.7.3) before presenting it for analysis of alanine enrichment (Figure 35). The final total protein concentration was subsequently found to be inadequate for GC-P-IRMS analysis of deuterated alanine in the isolated myosin band.

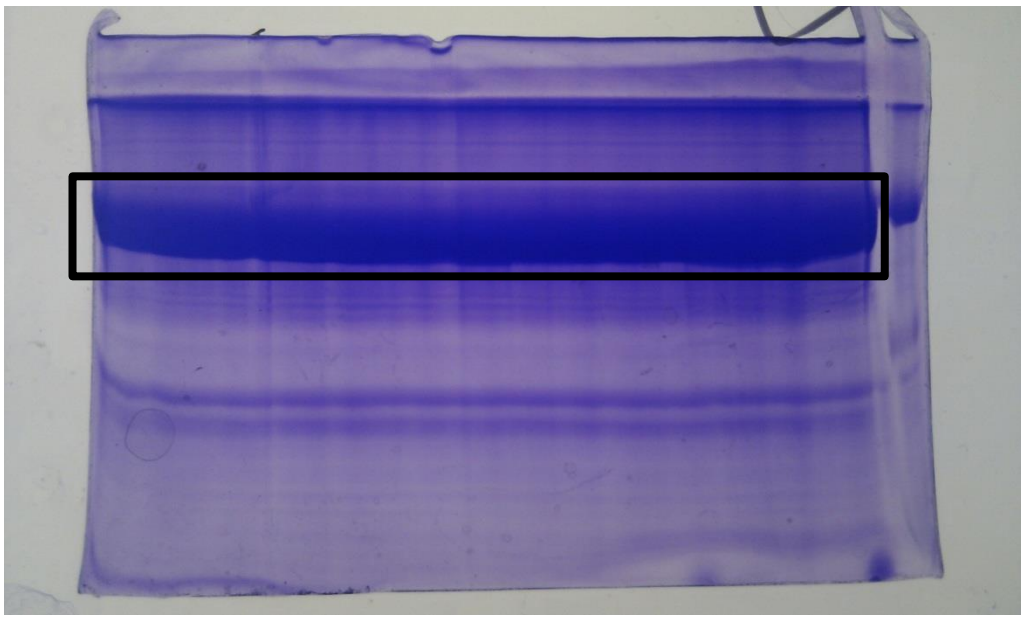

Figure 35 - Myosin isolation by mini-gel protein electrophoresis. Myosin band (black rectangle) subsequently cut-out, dried and washed for GC-P-IRMS analysis of deuterated myosin amino acids.

9.4.3 Intracellular free alanine

Isolation of free intracellular amino acids (from protein bound amino acids) was attempted by a series of ultrafiltration steps. No detectable protein bands were present following 10kDa ultrafiltration Figure 36. Amino-acid concentration was insufficient for analysis of intracellular deuterated alanine.

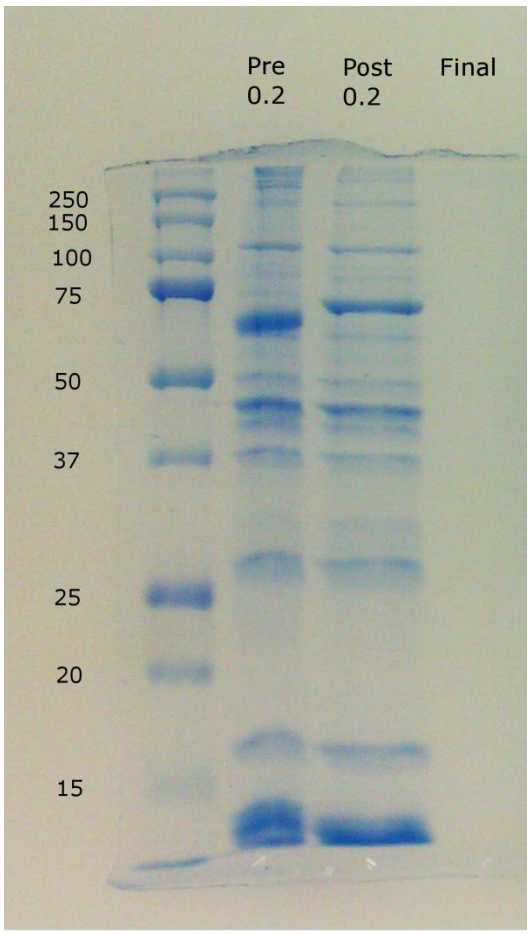

Figure 36 – SDS PAGE gel separation of intracellular (supernatant) component stained with coomassie blue. Free amino-acid isolation (1st lane = protein standard, Pre 0.2 = Initial supernatant, Post 0.2 = after 0.2µm filtration, Final = after 10kDa ultrafiltration

9.4.4 Total body water and serum alanine $^{2}H2O$ enrichment

With a single oral dose, Body $^{2}H_2O$ enrichment increased to 1514 ppm ^{2}H excess (1435-1582) and elimination half time was 8.3 days (7-10). These values being the enrichment at the time the dose was taken, calculated from the intercept of the elimination plot. Serum alanine enrichment kinetics mirrored those of body water (Figure 37). Average maximum measured enrichment in free alanine was 333 ppm ^{2}H excess (301-356 ppm excess).

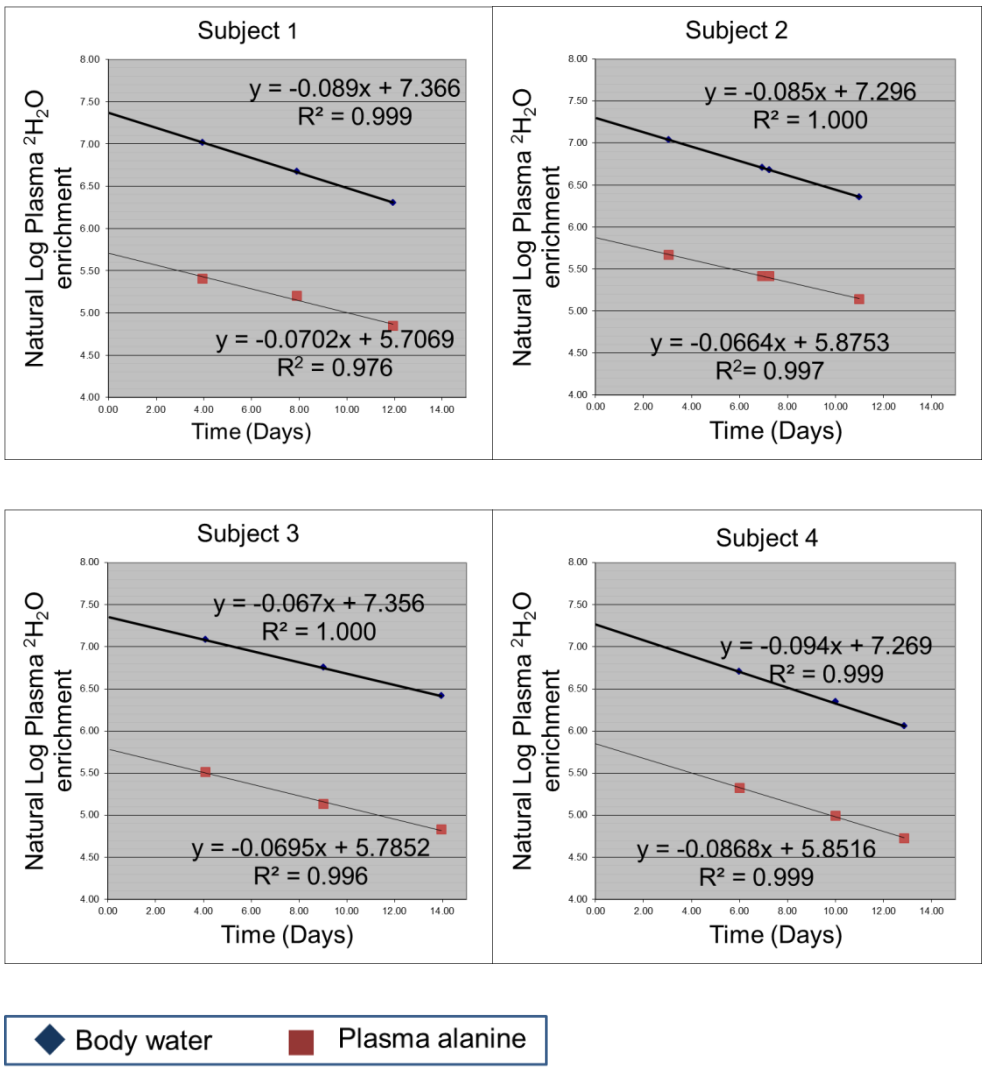

Figure 37 - Body water and serum alanine enrichment in four healthy subjects given an oral dose of deuterated water at time 0.

Alanine, the principal analyte, elutes first and is clearly resolved from other neutral amino acids. Nor-leucine was used as internal standard allowing concentration and isotopic calibration. Measured deuterium abundance were normalised to this (327).

Figure 38 shows all free pool data from each subject showing the enrichment of serum alanine relative to body water over time. This is expressed as the ratio of free alanine enrichment to that of body water after correction of the free alanine term by the factor 15/4,

as a theoretical maximum of 4 of the 15 hydrogen atoms in the analyte can come into equilibrium with body water. Should the theoretical number of hydrogen atoms became labelled, this plot should show a constant value of 4. There was no significant trend with time indicating that alanine came rapidly into isotopic equilibrium with body water and remained in equilibrium over the period of study. Elimination rate of deuterated free alanine mirrored that of body water (Figure 37). The average number of hydrogen atoms in alanine that become labelled was 3.64, indicating that circulating free alanine reached 91% of the maximum theoretical enrichment.

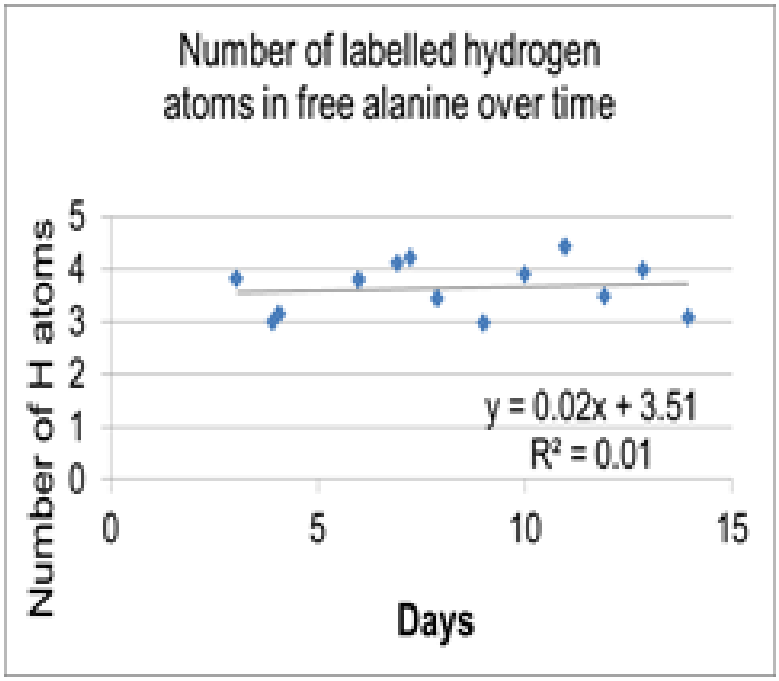

Figure 38 - Alanine enrichment in total body water in all participants over time after oral deuterium dosing

The deuterium enrichment of other free neutral amino acids in the circulation was measured. Free glycine showed an average of 1.6 hydrogen atoms become labelled compared with a theoretical value of 2 (322). Valine showed a value of 1.07 compared with 1.0. Leucine showed a similar degree of labelling to Valine. Free isoleucine was of too low concentration

for accurate analysis. In contrast, proline showed that on average only 0.88 labelled atoms compared with a maximum theoretical value of 5. The hydrogen atom on the alpha carbon (C2) of free branched chain and other essential amino acids equilibrates rapidly with body water during transamination (243). In contrast, it appears that proline acts as a non-dispensable amino acid, its free pool deriving from the diet and protein breakdown with little coming from *de novo* synthesis (328, 329).

Habitual myofibrillar protein FSR ranged from 1.0-2.1 % day-1 with an average of 1.18% day-1 (Table 28). Body composition analysis allowed estimates of absolute myofibrillar protein synthesis to be made. Habitual myofibrillar ASR ranged from 36.6-74.5 g day^{-1} with an average of 49.9 g day^{-1}.

Subject	Interval (days)	Average precursor ppm ^{2}H excess	Myofibrillar protein ppm ^{2}H excess	Myofibrillar protein FSR % day^{-1}
1	4	262.1	22.2	2.1
1	12	197.8	40.4	1.7
2	3	321.8	12.8	1.3
2	7	282.8	19.7	1.0
3	9	237.8	31.7	1.5
4	13	198.7	25.3	1.0

Table 28 - Habitual myofibrillar protein fractional synthetic rate in 4 healthy adult males

9.5 Discussion

We have developed a new protocol that allows habitual rates of myofibrillar protein synthesis to be measured whilst placing a minimal burden on the subject. Rates of protein synthesis compare with those in the literature (219). Our average rate of 1.18 % day^{-1} (0.049% $hour^{-1}$), compares well with the mean value of 0.044 % $hour^{-1}$ for the 8 studies

discussed by Smith et al (219). Smith and co-workers noted the wide variation of reported values, quoting a range of 0.31-0.61 % $hour^{-1}$, and discussed a number of factors that might influence results, including protocol duration and the uncertainty of the precursor enrichment in addition to there being considerable inter-subject variability. The heavy water protocol described here allows much longer study periods, thus overcoming some of the issues relating to short study periods. No obvious trend was seen with measurement period over 3-13 days, as a result this method may allow for a flexible protocol whereby a single biopsy can be taken at any time over the following two weeks. This may reduce difficulty in coordinating protocol timings in patient volunteers undergoing additional clinical investigations or treatments. The two subjects with repeat biopsies showed FSR within 13% of the mean, but as reported by Smith, the range of FSR showed considerable inter-subject variability, even in this small pilot study. Analysis of the samples in this pilot study required the commissioning of new GC-P-IRMS machinery and the ability of this equipment to successfully analyse low abundance ^{2}H was one test of the new protocol. Technical improvements should be possible with increasing experience to improve the precision of the equipment.

There are many benefits of an extended tracer protocol: habitual rates describe the true integrated response of skeletal muscle protein to anabolic stimuli such as food, activity and hormones while the negative effects of fasting, inactivity, inflammatory mediators and other disease-related factors are also integrated; short term variability such as diurnal cycles are damped by longer measurement periods; reduced impact of precursor contamination on the accurate estimation of protein-bound tracers is a technical benefit of prolonged measurement periods (330). Questions relating to acute effects on skeletal muscle protein synthesis may still be addressed within the framework of this protocol as it does not compromise the ability to conduct a short term infusion of, say ^{13}C-leucine to examine of specific stimuli, such as a single meal.

Our finding that on average, 3.64 hydrogen atoms in free alanine come from body water compares with the MIDA analysis of plasma proteins in adult rats after long term labelling, where 3.6-3.7 alanine hydrogen atoms were shown to come from body water (224). This may reflect incomplete labelling in the β hydrogen atoms (i.e., at C3) rather than the α position (C2), which was observed through isotopomer analysis using GCMS (324). It is possible that these observations can allow for prediction of precursor enrichment from body water. However, we measured plasma free alanine (in addition to body water enrichment) to reduce assumptions of the degree of labelling from body water and to facilitate greater measurement accuracy through using the same instrument for analysis both precursor and product. Unfortunately two of the original objectives – comparison of body water enrichment and plasma free alanine enrichment with intracellular free alanine – were not met due to undetectable levels of free intracellular alanine, this is likely to be due to the small biopsy size yielding very small quantities of intracellular fluid. Future extension of this approach to larger surgical biopsies of abdominal wall muscle, may confirm this point as larger samples of intracellular fluid should be accessible allowing the deuterium enrichment in serum alanine to be compared with that of intramuscular free alanine. Likewise, estimation of 2H enrichment in the myosin fraction to estimate myosin specific FSR was not possible. The method selected for myosin isolation (326) was chosen as it was believed that it would minimise protein losses and for its speed and simplicity. This method proved to be unsuitable in this protocol. One problem appeared to be difficulty solubilising myosin, after initial homogenisation and centrifugation re-suspension of the myofibrillar component produced a suspension rather than a solution which would then suffer further aggregation/clumping during denaturing. As a result much of the protein content may not enter the gel and the resulting gel band contained insufficient protein for analysis. Solubility of myosin may be improved with increasing salt concentration of the buffer used to around 3 time that used in this protocol, potentially resolving this issue. This myosin separation protocol has not been widely used in the literature, the most common alternative used the column electrophoresis

method by Balagopal et. al. (325). This method is costly and time consuming, taking around 13 hours per sample but would be the most appropriate method for a future study comparing myosin and myofibrillar fractional synthetic rate.

A single oral bolus of approximately 1g ^2H_2O/kg body weight was used in the present study. The recent 6 week study by Robinson et. al. (228) used 5 kg ^2H_2O per subject. In our group of healthy adult males, a dose of 70g ^2H_2O raised body water to a maximum of 1514 ppm ^2H excess, falling exponentially with time as water was eliminated with a half time of 8.3 days. There were no reported side effects of deuterium dosing at this level in our subjects. A future increase in dose to achieve a target of 2000 ppm ^2H excess or greater in body water could be trialled in future to improve in measurement sensitivity giving the potential in future studies to measure smaller protein samples as the smallest samples in this study were insufficient for analysis.

The protocol was well tolerated by the study subjects despite the repeated muscle biopsies and blood sampling. There were no issues with the deuterium dosing itself although one subject did drop out due to discomfort during the first muscle biopsy. This is potentially an issue for future studies in patients. However, experience within the Department of Surgery in Edinburgh with quadriceps biopsy suggests that this is an unusual event as over 100 elderly volunteers and patients with cancer have had single and serial biopsies with no significant reported complications. The protocol permits use of a single biopsy, as serum albumin was used to give basal protein-bound alanine abundance and future studies would use a protocol with only a single biopsy to minimise the discomfort related to muscle sampling. In future, urine samples may substitute blood samples as these have sufficient alanine and glycine for analysis, potentially reducing the required serum samples for this procedure to a single sample for the analysis of basal alanine abundance in albumin further reducing the burden on the patient or volunteer. Urine is also a very suitable for analysis of deuterated water (225) in

place of body water enrichment from plasma. An endpoint within an elective surgical procedure would further reduce the impact of the protocol on frail subjects as it may then simply require a basal blood sample, a single oral tracer dose with a series of urine samples, ending when a biopsy is taken during surgery.

9.6 Conclusion

In summary, the application of GC-pyrolysis-IRMS facilitated the implementation of a new protocol to measure skeletal muscle protein synthesis over longer periods with minimal burden on the subjects.

10 Use of a novel oral tracer technique to compare habitual skeletal muscle fractional synthetic rate in healthy individuals and patients with cancer.

10.1 Introduction

Chapter 9 investigated the feasibility of measuring skeletal muscle fractional synthetic rate using a single oral tracer protocol. This enabled the initiation of a study to compare habitual skeletal muscle fractional synthetic rate in healthy individuals and patients with cancer described here.

The loss of skeletal muscle mass in cancer is well described (60, 245, 331-333) and is one defining characteristic of cancer cachexia (97). The mechanisms by which muscle wasting may occur are also well studied (10). However, the relative importance of each pathway is unknown. This uncertainty extends to the relative contributions of the synthetic or degradative pathways, with decreasing muscle mass resulting either from a fall in skeletal muscle synthesis, increase in degradation or a combination of the two (334). Cancer cachexia may act to increase whole body protein synthesis and turnover in patients with lung and colorectal cancer compared with controls measured by 24-h infusion of [^{15}N]glycine (335). Other small studies (n=5) in humans have shown whole body protein turnover to be unchanged when compared with controls (62) or have shown no difference in whole body protein synthesis and breakdown rates in patients (n=11) before and after resection of colorectal cancer (336). Studies of skeletal muscle protein synthesis have demonstrated both reduced (62) and unchanged (333) FSR in patients with cancer compared with controls. The more recent of these studies (333) also assessed myofibrillar FSR in both the fasting and the post-absorptive state. The expected increase of FSR with feeding was observed in the control subjects but was lost in patients with cancer. This finding highlights the importance of considering the intermittent effects of normal stimuli to protein synthesis when estimating

the overall impact of cachexia on muscle synthesis over time. The novel protocol developed in Chapter 9 provides a method by which habitual skeletal muscle protein synthesis may be measured. This allows comparison of skeletal muscle FSR in healthy volunteers and patients with cancer in a way that accounts for the normal variations (or loss of variation) seen during feeding and fasting states. It is hypothesised that habitual FSR will be significantly reduced in patients with cancer compared with controls as a result of the cumulative effect over several days of a blunted anabolic response to normal stimuli.

An additional benefit of the new method is the limited burden it places on the patient owing to the need for only a single biopsy. To further reduce the discomfort it is possible to recruit patients with cancer undergoing resectional surgery allowing for the biopsy to be taken under a general anaesthetic. It may also be possible to further reduce patient discomfort by calculating body water / alanine enrichment from urine rather than serum samples (337).

In Chapter 9 an attempt was made to confirm that body water, serum alanine and intracellular alanine enrichment were equivalent to reduce concern over the use of serum measurements as estimates of the precursor pool. This was unsuccessful due to the small biopsies taken during this protocol. The use of a protocol where biopsies are taken under general anaesthetic allows larger biopsies of rectus abdominis to be taken which should allow measurement of intracellular alanine and the checking of one of the assumptions underlying the method. Comparison of rectus and quadriceps muscle will also allow for comparison of regional differences in muscle synthetic rate as may be expected from the results of Chapter 6 and 7. As the deuterium dosing was well tolerated during the pilot phase it should be possible to increase the deuterium bolus dose. This should increase the final myofibrillar enrichment, this along with technical refinements in the GC-P-IRMS machinery and software should improve the sensitivity and accuracy of the measure. This may be particularly important in measurement of patients with cancer where there may be reduced muscle FSR leading to reduced myofibrillar enrichment.

An added benefit of performing a study in patients with cancer undergoing surgery is the availability of pre-operative cross sectional imaging. This allows for estimation of muscle mass, and in those patients undergoing neo-adjuvant chemotherapy and subsequent pre-operative re-staging it also allows for measurement of muscle mass change. Additional body composition measures may be obtained from total body water measured by deuterium dilution with no alteration to the protocol.

10.2 Aim

This Chapter aims to compare skeletal muscle fractional synthetic rate in healthy volunteers and patients with cancer. Secondary aims are to compare quadriceps FSR with rectus abdominis FSR in patients with cancer and to compare FSR in patients with cancer with or without weight loss and muscle loss.

10.3 Methods

10.3.1 Human Protocol

Healthy volunteers and patients with upper gastrointestinal cancer were recruited, Habitual skeletal muscle synthesiswas measured in health and in cancer as described in Methods 2.2.1.3 and 2.2.2.2. A single oral dose of 133g 70 atom% of deuterium oxide was administered with serial blood and urine samples being taken at baseline and during the study protocol. A final quadriceps biopsy was taken in healthy volunteers and a quadriceps and *rectus abdominis* biopsy was taken at surgery in the patients. The full protocol is described in methods chapter 2.3.3.

10.3.2 Preparation of serum samples

One ml of serum was used for analysis of ^{2}H enrichment in body water by continuous flow IRMS. One mL of each serum sample was processed for analysis of free amino acid enrichment by cation exchange. Basal deuterium abundance in protein-bound alanine from serum albumin was measured (242) and assumed to be equal to basal abundance in skeletal muscle.

10.3.3 Preparation of skeletal muscle biopsies

10.3.3.1 Myofibrillar component separation

Rectus and quadriceps skeletal muscle biopsies were processed to isolate the myofibrillar component from sarcoplasmic proteins by serial triton x-100 washes as described in 2.7.2.

10.3.3.2 Free intracellular amino acid separation

Rectus abdominis muscle was additionally processed for recovery of free intracellular amino acids. After homogenisation and centrifugation the initial supernatant was processed for separation of free intracellular amino acids by ultrafiltration as described in Methods Chapter 2.7.4.

10.3.4 GC-pyrolysis-IRMS of amino acids

An identical procedure was performed to determine ^{2}H enirchment of amino acids in serum albumin, the free intracellular pool and the myofibrillar component as described in methods chapter 2.8.3. In brief; the amino acids derived from sample hydrolysis were derivatised and injected into a gas chromatograph stage separating amino acids, with amino acid peaks identified using a flame isolation detector. Sample flow continued into a 1350^{o}C capillary

pyrolysis furnace to convert analytes to H_2 gas. Finally the ^2H abundance and concentration of individual neutral amino acids was determined by on-line isotope ratio mass spectrometry.

10.3.5 Body composition

Deuterium dilution space was calculated from the intercept of the elimination plot divided by the dose, following the methodology as used in the doubly-labelled water protocol (IAEA Human Health Series #3) (338). Total body water (TBW) was calculated from deuterium space assuming non-aqueous hydrogen exchange factor of 1.041. Fat free mass was calculated from TBW by assuming FFM hydration was 73.2% (339). Skeletal muscle mass (SMM; kg) was estimated from FFM using the MRI-validated equations of Wang (249) which describe the ratio of SMM:FFM with gender and age. A myofibrillar protein content of 12.4% SMM was assumed (Reference Man; ICRP 1973).

10.3.6 CT measures of body composition

Cross sectional measures of muscularity were taken from routine CT scans in patients in the pre-operative period according to the previously described method in chapter 2.4.1. Where more than one scan was available (e.g. pre and post neo-adjuvant chemotherapy) both were analysed and an interval change calculated. Values were adjusted for height and expressed as cm^2/m^2. Low muscularity was defined as a skeletal muscle index measured from CT <55.5 cm^2/m^2 for men and 38.9cm^2/m^2 for women (60). Myosteatosis was defined as mean HU<41 for BMI<25 or HU<33 for BMI≥25 (295). In order to provide clinical context and to allow comparison with total body water measures of body composition, cross sectional measurements were converted to whole body estimates of FFM using the formula of Mourtzakis et. al (186). Where a single time-point CT scan was used this was the immediate pre-op scan.

10.3.7 Calculation of Fractional Synthetic Rate and Fractional Breakdown Rate

Fractional synthetic rate (FSR; % day^{-1} or % $hour^{-1}$) was calculated as:

$$FSR = \frac{\text{Change of myofibrillar protein-bound alanine enrichment with time}}{\text{Average free alanine enrichment}}$$

Average free alanine or body water enrichment over each specific period was calculated from the area under the curve of the log transformed elimination plot.

Whole body estimates of myofibrillar synthesis and breakdown were made assuming that quadriceps FSR is similar to skeletal muscle FSR in all muscles.

Absolute synthetic rate of myofibrillar protein (ASR; g day^{-1}) was calculated as:

$$ASR = FSR/100 \times SMM \times 1000 \times 12.4/100$$

Fractional breakdown rate (FBR) was estimated from measured CT net muscle loss assuming Net change in muscle mass = FSR – FBR.

10.4 Results

10.4.1 Group characteristics

A total of 21 patients and volunteers were included for analysis. Six new healthy volunteers were recruited and analysed along with replicate samples from one age-matched volunteer from the pilot phase. Fifteen patients with upper GI cancer were recruited with one patient dropping out after deuterium dosing without giving a reason. Patient characteristics are described in Table 29. Two patients experienced mild symptoms of vertigo around 2 hours

after dosing. The patient group was stratified into cachectic and non-cachectic groups by weight loss of ≥5%, group characteristics are described in Table 30. Visual inspection indicated that all data was not normally distributed and because sample size was small, non-parametric tests were used for comparison of groups. Groups were well matched with the exception of age in the weight-losing cancer group who were slightly older (Table 30). Results are expressed as median and range or interquartile range unless otherwise stated.

Patient	Site	Pathology	NAC	Comorbidity
1	Oesophagus	ypT3N2 Poorly differentiated ACC	Cis / 5FU	None
2	Oesophagus	ypT1bN0 Poorly differentiated ACC	None	None
3	Oesophagus	ypT2N1 Poorly differentiated SCC	Cis / 5FU	None
4	Gastric	ypT3N0 Poorly differentiated ACC	Cap	None
5	Gastric	ypT3N1 Poorly differentiated ACC	Cis / 5FU	COPD
6	Gastric	ypT1bN1 Poorly differentiated SCC	None	Angina
7	Oesophagus	ypT1N1 Poorly differentiated SCC	Cis / 5FU	Smoker, alcohol excess
8	Gastric	ypT3N0 Poorly differentiated ACC	Epi/Cis/Cap	None
9	Oesophagus	ypT3N0 Poorly differentiated ACC	None	Breast cancer, Renal cell carcinoma, hip fracture
10	Oesophago-gastric junction	ypT3N3 Poorly differentiated ACC	Cis / 5FU	None
11	Oesophagus	ypT3N2 Poorly differentiated ACC	Cis / 5FU	None
12	Gastric	ypT4aN2 Poorly differentiated ACC	Epi/Cis/Cap	Coeliac disease, mild asthma
13	Oesophagus	ypT3N1 Poorly differentiated ACC	Cis / 5FU	Alcohol excess
14	Oesophago-gastric junction	ypT3N2 Poorly differentiated ACC	Cis / 5FU	None

Table 29 - Pathology and Neo-adjuvant chemotherapy (NAC) in patients with upper GI cancer included in habitual muscle synthesis study (cis=cisplatin, 5FU = 5 Fluorouracil, Cap = capecitabine, Epi = epirubicin)

		Median	IQR	P*
Control (n=7)	Age (yrs)	52.1	51.5-53.1	
	Weight (kg)	70.4	67.1-80.8	
	Height (m)	1.68	1.65-1.71	
	BMI (kg/m^2)	25.5	24.7-26.4	
	Sex M:F	3:4		
Weight-stable cancer (n=6)	Age (yrs)	62.5	57.0-70.3	0.051
	Weight (kg)	85.3	78.0-93.3	0.073
	Height (m)	1.78	1.74-1.78	0.101
	BMI (kg/m^2)	27.2	25.7-29.8	0.295
	Sex M:F	4:2		
	Weight loss (%)	0	0-0	
Weight-losing cancer (n=8)	Age (yrs)	63.4	61.5-66.3	0.009
	Weight (kg)	70.0	62.9-72.3	0.463
	Height (m)	1.7	1.65-1.75	0.613
	BMI (kg/m^2)	23.5	20.9-26.2	0.397
	Sex M:F	4:4		
	Weight loss (%)	10	7.6-12.1	

Table 30 Descriptive characteristics of groups by weight loss category with comparison of control participants vs weight stable patients with cancer and controls vs weight losing patients with cancer. p values calculated vs control group (Mann-Whitney U)

10.4.2 Urine, serum and intracellular alanine enrichment

Free intracellular alanine enrichment was measured in 11 rectus samples with matching serum samples. Results were not available from all patients due to technical difficulty measuring amino acid deuterium enrichment in the intracellular samples. Median enrichment was 366 ppm in free intracellular alanine from rectus and 325ppm in serum. Intracellular alanine and serum alanine enrichment were strongly correlated with a correlation coefficient 0.734 (Spearman's rho p=0.01). Total body water enrichment was measured in serum and urine samples. A total of 43 pairs of urine and serum samples were available across all patients and time-points. Urine and serum enrichment was significantly correlated r^2=0.998 p=<0.0001, (Figure 39).

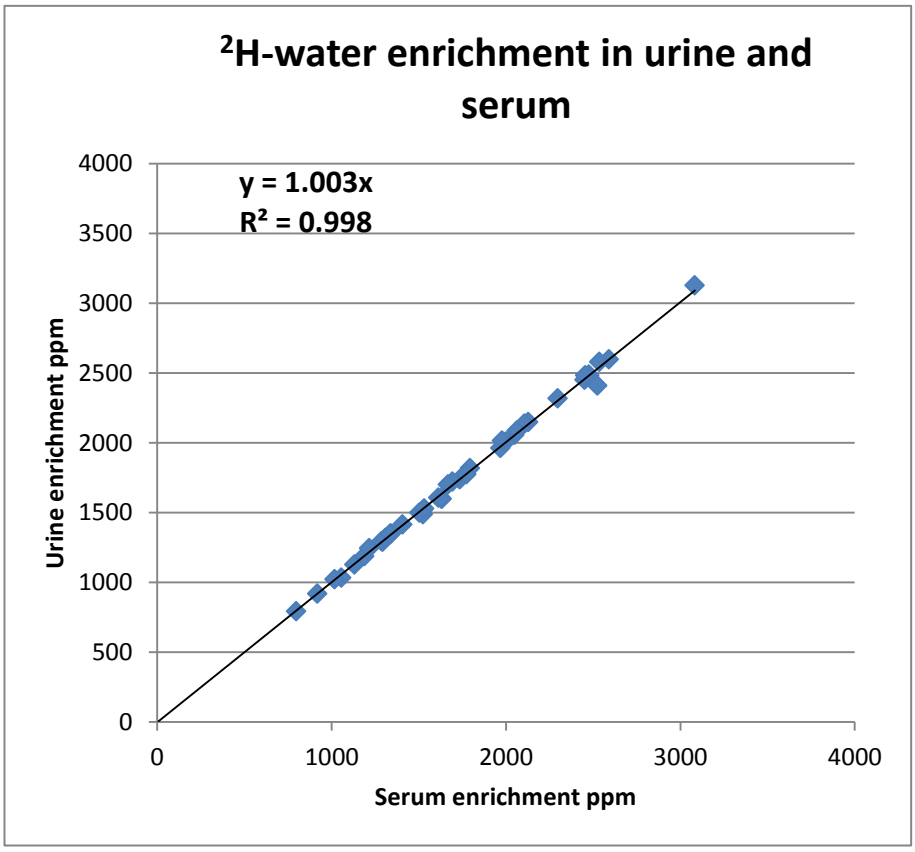

Figure 39 - Comparison of urine versus serum ^{2}H enrichment in paired samples across all time-points in both cancer patients and controls (ppm = parts per million).

10.4.3 Skeletal muscle fractional synthetic rate

When patients were categorised by weight loss there was a trend in quadriceps myofibrillar protein FSR across all three groups (Healthy controls < weight stable patients with cancer < weight losing patients with cancer) (*Jonckheere*-Terpstra trend test p=0.022) Figure 40. Quadriceps FSR was higher in weight-losing patients with cancer (0.073 % per hour) compared with healthy volunteers (0.058% per hour) p=0.03 (Wilcoxon Signed ranks test). There was no significant difference between cancer (0.058% per hour) and control groups (0.067% per hour) overall p=0.079 (Mann-Whitney U test). In patients with cancer, median rectus muscle fractional synthetic rate was less than quadriceps at 0.058% per hour p=0.028 (Wilcoxon Signed ranks test). Skeletal muscle FSR by weight loss group and muscle type is summarised in Table 31.

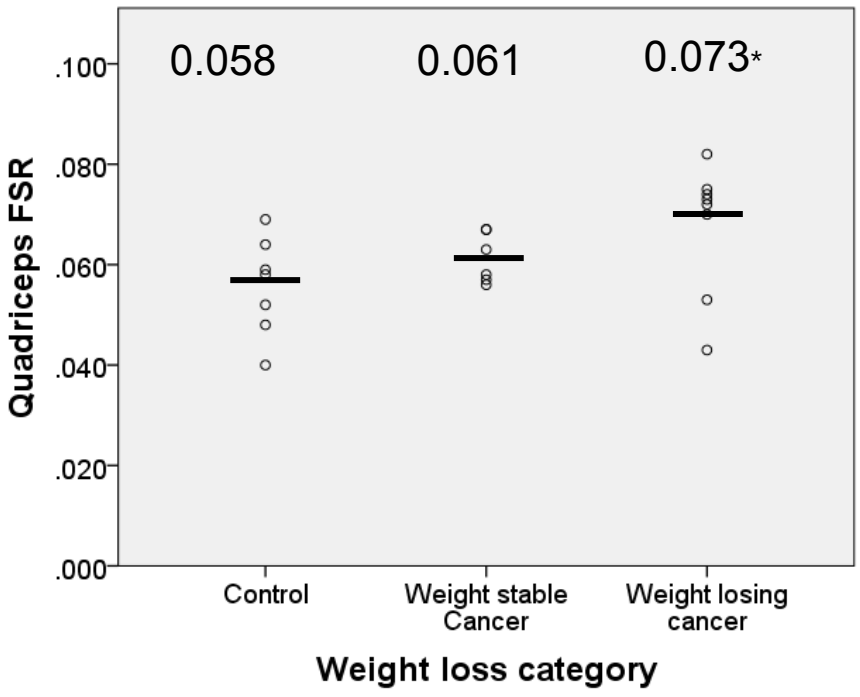

Figure 40 - Quadriceps FSR by weight loss category. Values are median Quadriceps FSR. * p=0.021 weight losing vs controls (Wilcoxon Signed Ranks)

Muscle group	Participant group	Median FSR (%/hr)
Quadriceps	Control (n=7)	0.058
	Weight stable cancer (n=6)	0.061
	Weight losing cancer (n=8)	0.073*
Rectus	Weight stable cancer (n=6)	0.059
	Weight losing cancer (n=8)	0.058

Table 31 - Fractional synthetic rate in rectus and quadriceps in each patient/participant group. Values are median FSR. (* p≤0.05 by Mann-Whitney U test vs control)

Comparison of *quadriceps* and *rectus* FSR within weight loss categories revealed no difference between *quadriceps* and *rectus* in the weight-stable group (p=0.34) but significantly increased in quadriceps in weight-losing patients (p=0.021, Wilcoxon Signed Ranks Test) Post-hoc comparisons revealed no significant associations (Spearman's rho) between quadriceps FSR or rectus FSR with skeletal muscle index (p=0.322, p=0.537), mean Hounsfield units (p=0.583, p=0.625), or the presence of myosteatosis (p=0.544, p=0.856). Sarcopenia was not associated with altered quadriceps FSR (p=0.463) (sarcopenia quadriceps FSR=0.063 %/hr range 0.043-0.082, non-sarcopenic FSR=0.067 %/hr, range 0.058-0.074). However rectus FSR was greater in sarcopenic patients (FSR=0.063 %/hr, range 0.042-0.069) than non-sarcopenic patients (FSR=0.046 %/hr, range 0.036-0.061) (p=0.038, Mann-Whitney U test).

10.4.4 Baseline body composition and pre-op loss of skeletal muscle mass

Pre-operative CT scans were available for all 14 patients with cancer. Sequential pre-operative scans were available in 10 patients with a mean interval time of 78.8 days. Summary body composition measures are seen in Table 32. Of the 14 patients with cancer,

9 were classified as sarcopenic by skeletal muscle index measured from CT as defined by a muscle index <55.5 cm^2/m^2 for men and 38.9cm^2/m^2 for women (60), 7 were classified as myosteatotic as defined by mean HU<41 For BMI<25 or HU<33 For BMI≥25 (245). Median muscle change was -4.0% (range -17.0% to 0.4%). All but one patient with interval CT scans lost muscle during the pre-operative period (Figure 41) median muscle loss was 5.6%. There was no correlation between muscle loss and muscle FSR using either quadriceps or rectus measures (p=0.531, p=0.940, Spearman's rho).

Body composition measures	Median	IQR
Skeletal muscle mass index (cm^2/m^2)	41.7	39.3-47.7
Mean HU	36.3	32.3-38.8
CT-derived Fat Free Mass (kg)	44.8	39.8-51.2
CT-derived Fat Mass	24.6	19.6-27.7
Fat Free Mass (kg; deuterium dilution)	46.3	41.9-49.8
Fat Mass (kg; deuterium dilution)	28.6	24.9-31.4

Table 32 - Summary body composition measures for patients with upper GI cancer derived from CT and deuterium dilution methods

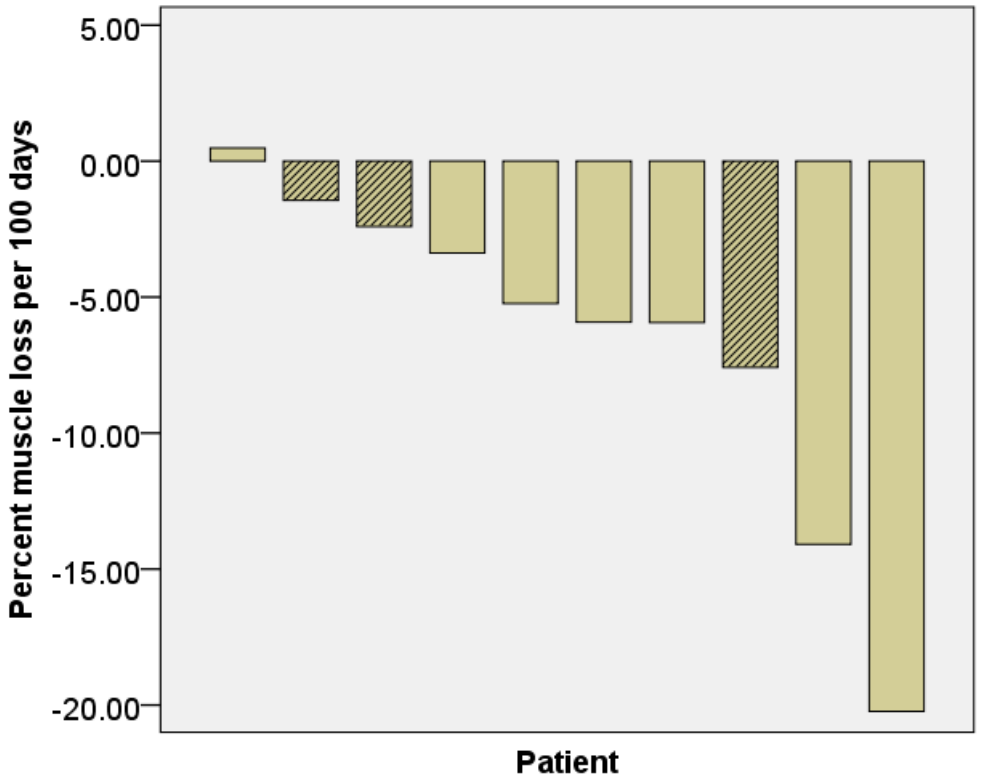

Figure 41 - Pre-operative L3 CT skeletal muscle loss (pre and post neo-adjuvant chemotherapy) in the 10/14 patients in the habitual muscle synthesis study who had 2 sequantial scans (hashed bars = weight-stable patients, plain bars = weight-losing patients)

Comparison of body composition measures by deuterium dilution and by CT analysis were made by conversion of TBW estimates to FFM estimates by the method in paragraph 10.3.5, and conversion of L3 CT skeletal muscle CSA measures to FFM by the formula of Mourtzakis (186). Comparison was made by Bland-Altman analysis. The mean difference for FFM between CT and deuterium derived measures was 1.2 kg with limits of agreement -6.4 to 8.7. For FM the mean difference was 2.0 with limits of agreement of -7.4 to 11.5. When plotted on a Bland-Altman plot, there was no evidence of heterodasticity in the FFM comparison (Figure 42), however in the FM comparison the differences were greatest at the extremes of body fatness (Figure 43).

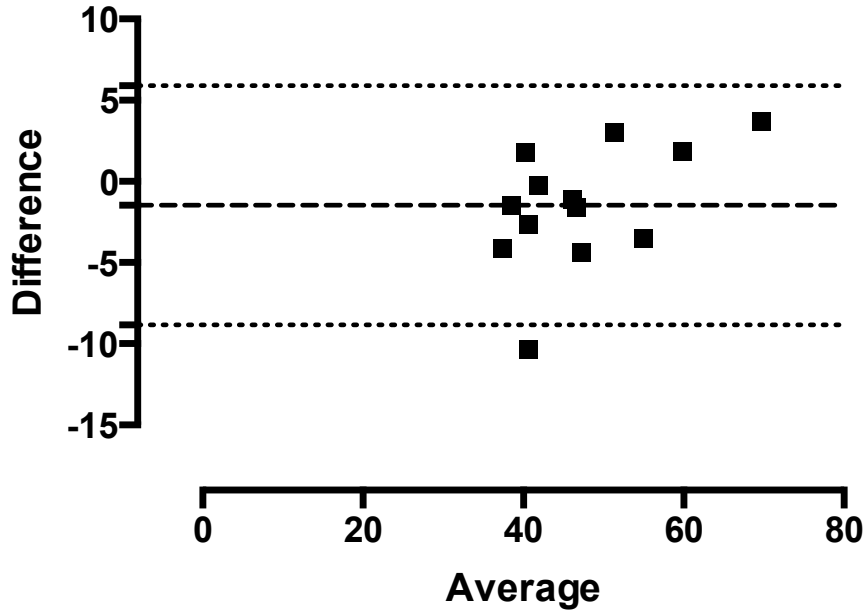

Figure 42 - Bland Altman-plot of FFM CT vs deuterium dilution methods in patients with upper GI cancer. Plot of mean against mean difference

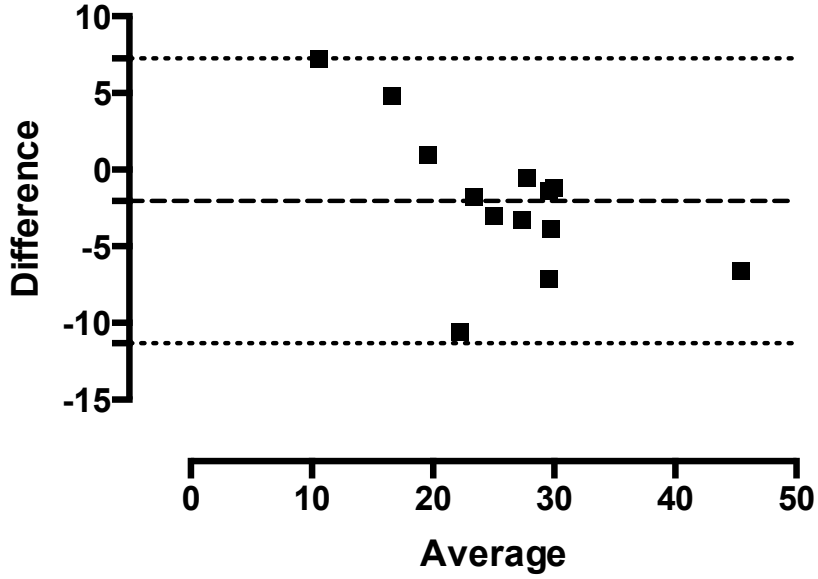

Figure 43 - Bland-Altman plot of FM CT vs deuterium dilution methods in patients with upper GI cancer. Plot of mean against mean difference

10.4.5 Myofibrillar protein synthesis and breakdown

Skeletal muscle FBR was not different between weight stable (n=3, FBR -0.056%hr, range -0.049 to -0.067) and weight losing patients with cancer (n=7, FBR -0.061, range -0.037 to -0.075) (p=0.833, Mann-Whitney U). Skeletal muscle mass estimated from deuterium dilution in only those cancer patients who underwent serial CT scans is given in Table 33. Loss of muscle mass as revealed by CT scans enabled FBR data to be calculated in the patients in comparison with the control subjects, who were assumed to have stable muscle mass (thus, FSR=FBR). These early stage cancer patients showed similar muscle mass to controls and similar level of relative (FSR) and absolute myofibrillar protein synthesis (Table 33). In the cancer patients, myofibrillar protein breakdown was just 1.2 g/day (2.9%) greater than synthesis.

	Cancer (n=10)		Control (n=7)	
	Median	IQR	Median	IQR
Body weight (kg)	71.0	66.8 - 80	70.4	67.1 - 80.8
Skeletal muscle mass (kg)	20.2	18.6 - 22.5	19.8	18.9 – 25.3
Myofibrillar protein synthesis (g/day)	41.1	38.2 – 41.8	37.2	34.0 – 45.4
Myofibrillar protein breakdown (g/day)	42.4	39.1 – 42.8	37.2	34.0 – 45.4

Table 33 - Skeletal muscle mass (kg), absolute myofibrillar protein synthesis and absolute myofibrillar protein breakdown (g/day). Cancer patients with serial CT scans are included (n=10; comprising 7 weight losing and 3 weight stable subjects). Muscle mass was estimated at the time of consuming deuterium oxide. Control subjects (n=7) were assumed to have stable muscle mass. Protein kinetics were derived from quadriceps biopsy data.

10.5 Discussion

10.5.1 Skeletal muscle fractional synthetic rate in cancer

This study found that skeletal muscle fractional synthetic rate was greater in weight-losing patients with cancer than weight-stable patients with cancer or healthy controls. Although the observed differences between groups were small and are not likely to represent a biologically significant variation, this study suggests that the hypothesis that muscle wasting in cancer is caused by a marked reduction in synthetic rate is likely to be incorrect. This study is the first to measure skeletal muscle fractional synthetic rate in patients and volunteers during their normal daily routine over a period of time that incorporates the normal cycles associated with feeding/fasting and activity/rest. Two studies that compare directly skeletal muscle fractional synthetic rate by primed constant infusion of isotope tracer have shown that skeletal muscle FSR may be reduced in fed patients with cancer (62) or may be unchanged but with a blunted response to the normally anabolic stimulus of feeding (amino acid infusion) (333). As a result it would be expected that any reduction in FSR in the patients with cancer would be more apparent during this protocol than during an infusion protocol as the oral tracer design incorporates the potentially cumulative anabolic effect of up around 21 meals over the course of the one week protocol. As a result there appears to be a contradiction between the results of the current study and those of the previous infusion tracer studies. Consideration should be given to the potential for methodological differences to account for these different outcomes. It is known that calculated FSR differs depending on the tracer used during infusion methodologies (340). Absolute values for myofibrillar protein synthesis in the control groups in this study (0.058 %/hr) were consistent with measurements made from healthy controls in previous studies. These values have been reported as 0.031 %/hr (resting, fasted) (341), 0.043 %/hr resting increasing to ~0.06%/hr after exercise (223) although the reported ranges of myofibrillar FSR at rest are known to be variable between studies ranging from 0.031 to 0.066 %/hr (219). Comparison of the values in the patients

with cancer are comparable with recent studies where FSR is in the region of 0.006 to 0.007 %/hr (128). It appears unlikely that the choice of tracer itself would result in a dramatically different finding in this situation. Other aspects of the design of the two previous studies differ significantly from the current study. One key element present in the infusion methods is the relative inactivity of the participants who were instructed not to exercise for 72 hours prior to participation and were then required to lie supine for 120mins during the study period. In contrast, participants in the current study were encouraged to continue their everyday activity during the study period. Both healthy volunteers and patients consisted of relatively active individuals and the results may reflect a normal overall response to activity in the presence or absence of cancer. No measurement of activity levels was made during the course of this study, however one potential advantage of the method is that with the addition of ^{18}O to the deuterium oxide dose, energy expenditure may be calculated using a doubly labelled water protocol (342) in future studies.

An alternative explanation for the different findings between the current and previous studies may require the development of an alternate model of the demonstrated blunted anabolic response. Conventionally FSR may be considered to occur at a basal rate representing un-stimulated muscle turnover with periodic rises occurring in response to feeding or exercise. If plotted in a hypothetical model (Figure 44) the responses to three meals during the course of the day would be seen as three peaks in FSR. The area under the line represents the total muscle synthesis occurring over the course of the 24 hour period and this area under the line can be represented as an integrated 24 hour measure of habitual FSR as measured by the oral tracer method. In cachexia an anabolic block could result in a simple reduction in FSR during feeding, resulting in a reduction in habitual FSR in keeping with the original hypothesis.

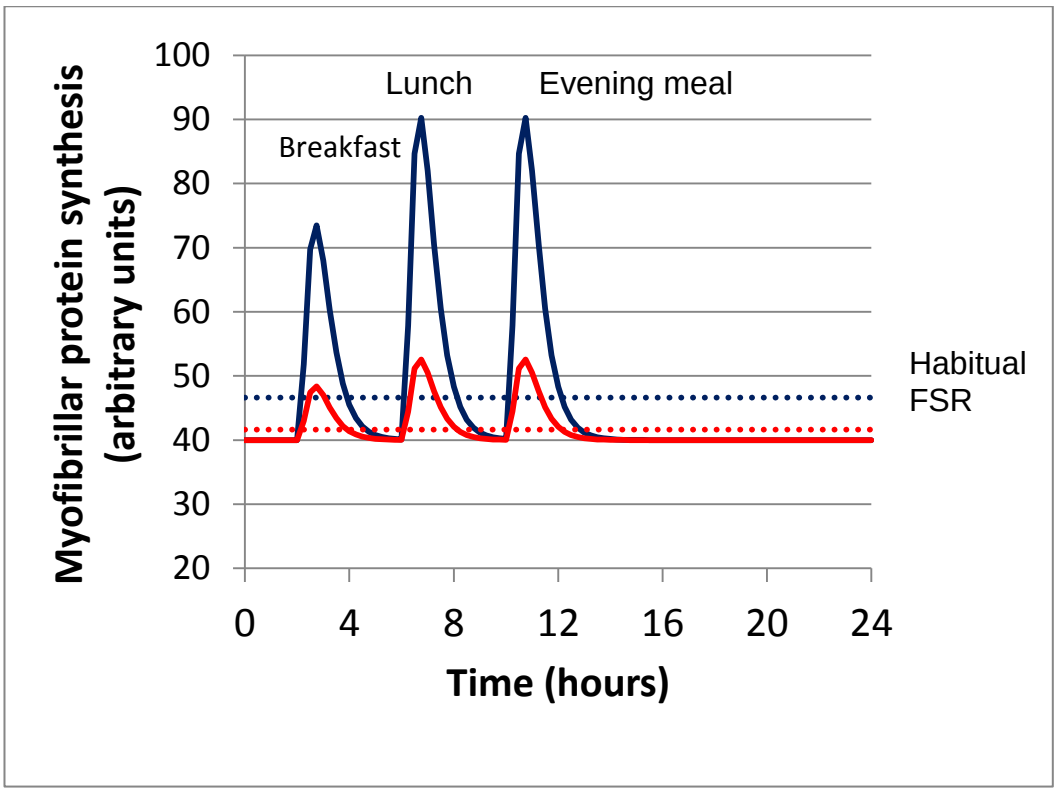

Figure 44 – Conventional hypothetical model of patterns of muscle synthesis over 24 hours. Solid blue line = healthy FSR, dotted blue line = healthy 24 hour habitual FSR, solid red = line cachexia FSR, dotted red line = cachexia 24 hour habitual FSR

Alternatively an anabolic block could result in alteration of muscle protein synthesis kinetics. Instead of a reduced FSR peak with feeding the response may be blunted or prolonged Figure 45. In this model the area under the curve is identical for both the healthy control group and the cancer cachexia group resulting in an identical measure of habitual skeletal muscle FSR.

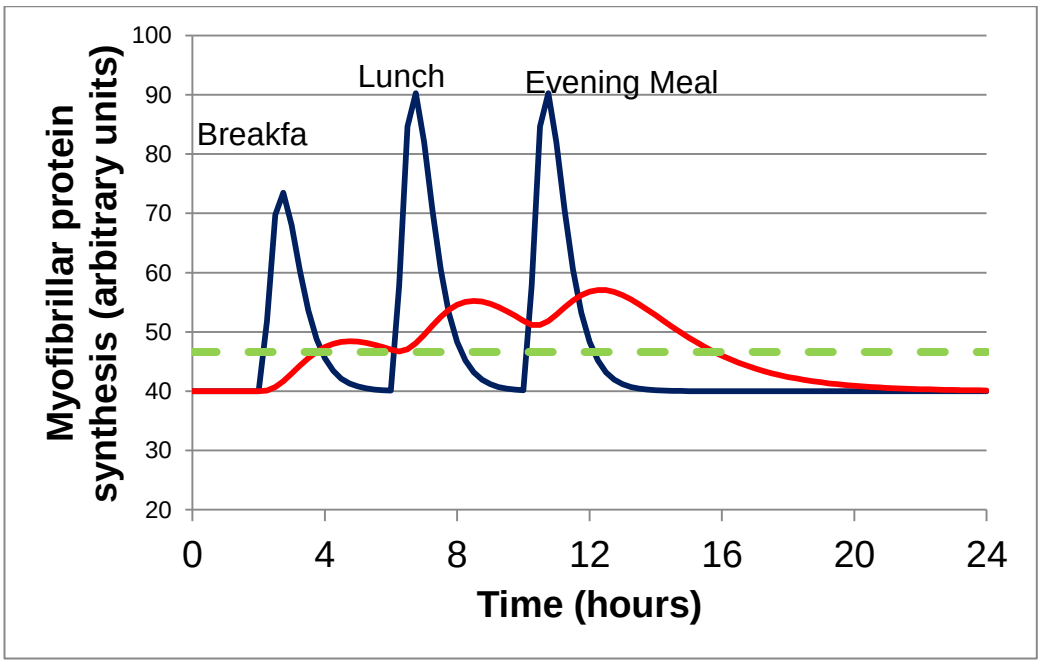

Figure 45 - Alternate hypothetical model of patterns of muscle synthesis over 24 hours. Solid blue line = healthy FSR, solid red = line cachexia FSR, dotted green line = healthy and cachexia habitual 24 hours FSR

To demonstrate this in patients with cancer cachexia would require the use of a traditional IV labelled tracer infusion study with serial biopsies over the course of several hours such as previously performed to demonstrate the duration of response to feeding in health (43). Such a study results in significant discomfort and may be difficult to justify in frail cachectic patients with cancer.

10.5.1 Comparison of muscle groups

Different rates of muscle protein synthesis were observed in the two muscle groups biopsied. This finding is consistent with the differences seen in regional cross sectional measures of muscle mass described in chapters 6 and 7. It is also consistent with previous direct measures of FSR in different muscle groups where triceps FSR differed from Quadriceps FSR by ~15% in healthy individuals (341). Similar to the previous study, the size of the difference in

FSR between quadriceps and rectus is small and the clinical significance of the finding is uncertain. It does demonstrate the importance of comparing only similar muscle groups in studies of muscle wasting as different muscle types are likely to respond differently to anabolic and catabolic stimuli.

10.5.2 Interaction between skeletal muscle synthesis and breakdown

Although skeletal muscle breakdown was not measured during this study, serial CT scans demonstrated a reduction in skeletal muscle truncal cross sectional area in the period leading up to muscle biopsy in all but one patient. The implication of this finding is that this loss in skeletal muscle is likely to be due to increased degradation. This is consistent with direct measures of skeletal muscle degradation using arterio-venous difference methodology where increased degradation has been found in patients with cancer compared to controls (333). Skeletal muscle synthetic and degradative pathways are closely interdependent, conventionally this interdependence is understood to reduce synthesis when degradation is increased and to inhibit degradative pathways in response to muscle synthetic pathway stimulation (343). However this interaction appears to be more complex, even in health where increased muscle breakdown is seen in response to the anabolic stimulus of resistance or endurance exercise (30). As such it is possible that the changes seen in cachectic muscle reflect a process of deranged skeletal muscle remodelling where synthesis is necessarily increased but overwhelmed by increased muscle degradation. Alternatively the increased synthesis could be the result of an inadequate compensatory mechanism to counteract the pathological muscle breakdown. Supporting evidence from previous studies for the existence of an increased skeletal muscle FSR in situations of muscle loss and a mechanism for this exists. Increased skeletal muscle FSR in the presence of a net loss of muscle protein occurs in murine models of muscle wasting after denervation over one to 14 days (344-348) with degradation being the main determinant of muscle loss. The mechanism for an increase in

muscle synthesis during net protein loss could be through stimulation of protein synthesis via mTORC1. This protein complex, normally associated with the maintenance of muscle mass and muscle hypertrophy is activated by the increase in amino acids released as a result of increased protein breakdown by the proteasome (348).

10.5.3 Impact of cancer on muscle mass

The effect of cancer on muscle mass is demonstrated by serial CT scans in this group of patients. The median muscle loss was 5.6% per 100 days in the group overall. It is possible to estimate the absolute effect of this on muscle mass in an individual. In an average 70kg individual of approximately 40% muscle mass with 12% of this being myofibrillar protein (349) then daily myofibrillar protein loss is equivalent to a loss of 1.8g per day. Rectus skeletal muscle myofibrillar synthesis is 0.058% per hour or 1.39% per day. This is equivalent to 47g of myofibrillar protein synthesised per day. Comparison of the size of these values reveals that the rate of muscle loss represents 2.5% of total daily skeletal muscle turnover. Whether increased or decreased, the difference between myofibrillar synthesis and breakdown can only be around this value of 2.5%. It is unsurprising therefore that its measurement is difficult.

10.5.4 Study limitations

There are a number of potential limitations to this study and the results should be interpreted with consideration given to these.

10.5.4.1 Patient selection

The overall numbers of patients and volunteers in the study is small with 7 healthy volunteers and 14 patients with cancer completing the protocol, resulting in small groups for comparison. This difficulty in recruiting suitable patients and volunteers has also been

present in the two previous tracer studies of healthy volunteers and patients with cancer where the overall numbers included were 7 controls and 5 patients (62) and 8 controls and 13 patients (333). One benefit of the novel protocol developed for this study was the reduction in burden on the participant by reducing the biopsies required and eliminating the intravenous infusion with the aim of reducing the number of potential volunteers who decline to participate or drop out after recruitment. In future studies using this protocol it will be possible to reduce the blood sampling giving a protocol with a single blood sample, daily urine collection and a single muscle biopsy. The small numbers resulted in groups that did not appear to fit the normal distribution with respect to FSR and were not matched for age. Both these problems were also present in the recent infusion study (333) in the current study the patient group were older than the volunteer group and so it is unlikely that a difference between the groups is masked by the small age difference as older individuals are likely to have a reduced FSR or reduced response to anabolic stimuli (350, 351).

10.5.4.2 Study method

This study used a novel protocol for the measurement of skeletal muscle FSR and consideration should be given to possible sources of error resulting from this. As a newly developed method, it was not known at the outset whether the method would have sufficient sensitivity to distinguish between two small groups. Since development of this method two other studies have used an oral deuterium tracer method to measure skeletal muscle fractional synthetic rate. These studies in healthy individuals used a regular daily doing regime demonstrating an increase in myofibrillar FSR with resistance exercise (227) in young individuals (n=12) and no additional increase with post exercise protein supplementation in older people (n=16) (228). These studies demonstrate the ability of an endogenous labelling protocol to describe differences in FSR in small group studies.

Possible sources of error in the method may arise from contamination of the myofibrillar sample from labelled amino acids from non-myofibrillar sources such as collagen or

sarcoplasmic proteins resulting in an artificially low or high myofibrillar FSR respectively. Due to the anticipated low levels of enrichment, care was taken during this protocol to ensure no such contamination occurred. The myofibrillar isolation protocol was chosen to ensure repeated washing of the myofibrils to eliminate sarcoplasmic contamination. An additional advantage of the protocol is the low levels of precursor ^{2}H and long protocol compared to the high levels of intracellular labelled amino acids associated with an infusion protocol. This low ratio acts to reduce the risk of contamination of the presumed myofibrillar fraction with labelled amino acids from serum or sarcoplasm. Contamination with collagen proteins is equally unlikely; this can be demonstrated by the amino-acid profile obtained during analysis of the myofibrillar component. Approximately 30% of amino acids in collagen are proline and the absence of high levels in the final sample is reassuring that no contamination or minimal contamination has occurred.

10.6 Conclusion

Myofibrillar skeletal muscle FSR measured in free living individuals over the period of one week is not reduced in patients with cancer compared to healthy volunteers. The impaired response to anabolic stimuli seen in short term infusion studies does not result in reduced muscle synthesis during normal activity over longer periods of time.

11 General Discussion

This thesis examines the changes in muscularity that occur in patients with upper GI cancer. It assesses the use of cross sectional imaging as a means of measuring muscle mass and changes in muscle mass. Cross sectional imaging-derived body composition anaylsis is of particular interest as a non-invasive measure that is often readily available as part of a patient's clinical assessment and thus does not increase the burden of investigation on the patient. The thesis also describes the development of a direct measure of muscle synthesis that is designed to have a reduced burden on the patient / participant and provide a measure representative of the muscle synthetic rate that occurs during normal everyday activity.

Each chapter contains a discussion of the main findings, this section summarises the findings and places them into context of the overall themes of the thesis.

Chapter 3 begins by defining the need for direct measures of muscle mass at all time-points of interest. Here it was not possible to estimate accurately pre-illness whole body muscularity using anthropometric measures with the degree of precision necessary to be able to identify reliably clear differences between individuals or between different time-points in the same individual. These findings are consistent with previous studies comparing measured and estimated muscle mass (162, 249). As error existed both in the CT-derived data whole body estimate and in the anthropometrically-derived data estimate, a second comparison was made with the direct measure of cross sectional area of muscle using an anthropometrically derived estimate of cross sectional area from a Canadian cohort of patients. This method also resulted in broad limits of agreement adding support to the hypothesis that wide variations in body composition make anthropometric-based estimates of muscle or lean mass to be of limited use in individuals or small group comparisons. In conclusion there was no reliable means to estimate pre-illness muscularity and therefore a direct measure of muscle mass

and/or body composition is required. This difficulty underlies biomarker discovery in cancer cachexia, particularly in relation to body composition as it is difficult to compare an individual who presents with cancer cachexia with any measure in their pre-illness state. As a result, cachexia research defines the presence of low muscle mass by the use of "cut-offs" defining points below which there is a worse prognosis.

Analysis of these cut-offs forms the focus of Chapter 4. Recent cachexia and sarcopenia definitions include measures of low muscle mass as a defining characteristic. As muscle mass may be measured by a variety of means a broad definition is given that sarcopenia values should be less that 2SD of the mean of a normal healthy young group. Chapter 4 sets out to define a value for low muscle mass/sarcopenia (i.e. <2SD of muscle mass observed in healthy 30 yr olds) as measured by single slice quadriceps MRI and then to compare this definition with appendicular skeletal muscle mass derived from DXA in a group of older individuals. Whilst it was possible to define quadriceps area cut-off with MRI, there was a significant difference in the proportion of elderly subjects classified as sarcopenic when compared with established DXA cut off values. This is likely to be as a result of the young reference population sampled as this was a small group and may not be representative of the population as a whole. However, it may reflect a real difference in the young population between the North American Baumgartner DXA population and those in the Scottish cohort. In the context of cancer cachexia this would mean that the application of cut-offs are unlikely to provide a reliable biomarker for the identification of a wasting cachectic process in individual patients where the cut-off value was derived in a different population. Ideally, population-specific cut-offs should be developed to define cachexia. However, to date these population studies do not exist. In the absence of functional or outcome data associated with the quadriceps cut-off developed in the present thesis it would be inappropriate to claim this as a new sarcopenia cut-off value. Further study could be performed to assess the validity of the new cut off applied to patients with cancer or the elderly with prospective evaluation for

patient focussed outcomes such as survival and quality of life. Such study is beyond the scope of this thesis. Alternative approaches to the development of sarcopenia or cachexia biomarkers are considered in the following Chapter

Chapter 5 investigates the possibility of development of a urinary biomarker for muscle wasting in cancer. Whilst CT provides a gold standard measure of muscle mass it is not an ideal biomarker for cachexia associated muscle wasting as single slice cut-offs may lack specificity due to wide intra-individual variation in muscularity in health and due to the requirement for repeated scanning if it is to be used to monitor progression of disease or reversibility with treatment. Analysis of the urinary proteome was performed in an attempt to define abnormal muscle by analysis of urine and therefore obviate the need for CT based diagnosis of muscle wasting and provide a means for non-invasive monitoring of progress or reversibility. The proteome based model had poor specificity, however the finding that a fragment with a m/z consistent with the up-regulation of Agrin was of interest. This marker has also been found in a group of patients with sarcopenia (285) suggesting that the potential urinary markers identified warrant further investigation in patients with cancer. The poor specificity of the model could be related to the muscle characteristic (Hounsfield units) used, whilst myosteatosis has been identified as being associated with impaired function and outcome, its relationship with cancer cachexia is assumed rather than proven. Further longitudinal study comparing progression of myosteatosis with established markers of cachexia such as progressive weight loss or muscle loss would more clearly define the role of myosteatosis in cancer cachexia. The markers proposed in Chapter 5 would currently be best further evaluated against sequential measures of muscle mass to determine their value in defining muscle loss over time.

The following three Chapters go on to investigate the use of cross sectional imaging as a measure of muscle wasting in cancer cachexia. Chapter 6 compared regional measures of muscle mass with different functional measures. The two body regions investigated (trunk

and lower limb) had different associations with different functional measurements. This finding indicates that all measures of muscle mass are not equal and loss of different muscles may have different consequences for patient function. Whilst (as expected) around 40% of the variance in quadriceps strength/power could be explained by quadriceps mass, truncal muscle mass was better correlated with complex measures of body movement.

Chapter 7 and 8 attempt to characterise the regional changes in muscle mass that occur during treatments for cancer. Here it is shown that truncal muscle CSA falls during neo-adjuvant chemotherapy for upper GI cancer using serial CT scans. Changes in muscle CSA however were not seen in in the arms and legs of patients with cancer undergoing cancer resection. Despite this, these chapters show the loss of muscle mass experienced by these patients pre-operatively and demonstrate the ability of serial cross sectional imaging techniques to quantify this muscle loss. They also illustrate the reversibility of muscle wasting with effective cancer treatment. Here the post-operative phase scans that at seven months the muscle lost in the immediate preoperative period has been regained. These Chapters also illustrate the practical difficulty in obtaining serial cross sectional investigations to fully describe changes in muscle mass and point towards the need for a direct measure of muscle synthesis by a means that places a minimal burden on the patient participant.

The final two Chapters develop a novel method for measuring muscle synthesis. This measure was initially tested in a small group of healthy volunteers. It was possible to obtain a measure of skeletal muscle synthesis over a period of one to two weeks using and oral tracer method. The method uses a single oral bolus and a single biopsy and provides a measure of "habitual" muscle synthesis in free living individuals who are able to continue their normal activities during the study period. The final Chapter applies this novel method in combination with measures of cross sectional muscle area from serial CT scans to investigate skeletal muscle synthesis and loss in a comparison of healthy volunteers and

patients with cancer. It was hypothesised that weight losing cancer patients would show a reduction in muscle synthetic rate. Previously, short term measures of muscle synthesis have demonstrated a blunting of the anabolic response to feeding (333) and examination of the transcriptome in patients with cancer had shown a down regulation of around 1800 genes in sequential muscle biopsies (64) suggesting a reduction in muscle turnover. Unexpectedly, the results in the present study showed no difference between patients with cancer and healthy controls and suggested that FSR may even be increased in weight-losing patients with cancer. Importantly these patients had measures of muscularity from serial CT scans providing a robust measure of muscle loss. This allowed calculation of the net muscle loss in the context of the continual muscle synthesis that appears to be maintained in cancer cachexia. Whether the observed rise in FSR in weight losing patients with cancer is a genuine effect is uncertain as the numbers of patients in each group are small, however the results appear to exclude the possibility of a significant fall in skeletal muscle FSR. The absolute mass of muscle lost in the patients studied would require only a 2-3% discrepancy between muscle synthesis and degradation in cancer and it is unlikely that direct estimation of degredation rates would detect such change.

11.1 Final conclusions

This thesis has explored muscle wasting in cancer cachexia and its assessment by means that minimise the burden on the patient or participant. The final conclusions are

- Direct measures of muscularity are required and cannot be inferred from simple anthropometric measurements or be provided by surrogate biomarkers such as urinary peptides

- The use of different measures of muscle mass may result in variation in the classification of individuals as sarcopenic, and different regional measures of muscle mass may have different implications for the functional ability of a patient.
- Serial cross sectional imaging measures provide a sensitive measure of muscle wasting in patients with cancer. The use of routine CT scans provides a measure that is both reliable and convenient for the patient and researcher but is restricted to time-points selected by clinical indication.
- Habitual skeletal muscle fractional synthetic rate can be measured by the use of a novel oral tracer method.
- Skeletal muscle fractional synthetic rate is not significantly reduced in patients with cancer compared to controls

Bibliography

1. Rassier DE, MacIntosh BR, Herzog W. Length dependence of active force production in skeletal muscle. J Appl Physiol. 1999;86(5):1445-57.

2. Spargo E, Pratt OE, Daniel PM. Metabolic functions of skeletal muscles of man, mammals, birds and fishes: a review. J R Soc Med. 1979;72(12):921-5.

3. Wolfe RR. The underappreciated role of muscle in health and disease. Am J Clin Nutr. 2006;84(3):475-82.

4. Zurlo F, Nemeth PM, Choksi RM, Sesodia S, Ravussin E. Whole-body energy metabolism and skeletal muscle biochemical characteristics. Metabolism. 1994;43(4):481-6.

5. Chevalier S, Burgess SC, Malloy CR, Gougeon R, Marliss EB, Morais JA. The greater contribution of gluconeogenesis to glucose production in obesity is related to increased whole-body protein catabolism. Diabetes. 2006;55(3):675-81.

6. Janssen I. The epidemiology of sarcopenia. Clin Geriatr Med. 2011;27(3):355-63.

7. Phillips SM, Glover EI, Rennie MJ. Alterations of protein turnover underlying disuse atrophy in human skeletal muscle. J Appl Physiol. 2009;107(3):645-54.

8. Skipworth RJ, Stewart GD, Ross JA, Guttridge DC, Fearon KC. The molecular mechanisms of skeletal muscle wasting: implications for therapy. Surgeon. 2006;4(5):273-83.

9. Glass DJ. Skeletal muscle hypertrophy and atrophy signaling pathways. Int J Biochem Cell Biol. 2005;37(10):1974-84.

10. Fearon KC, Glass DJ, Guttridge DC. Cancer cachexia: mediators, signaling, and metabolic pathways. Cell Metab. 2012;16(2):153-66.

11. Lai KM, Gonzalez M, Poueymirou WT, Kline WO, Na E, Zlotchenko E, et al. Conditional activation of akt in adult skeletal muscle induces rapid hypertrophy. Mol Cell Biol. 2004;24(21):9295-304.

12. Glass DJ. PI3 kinase regulation of skeletal muscle hypertrophy and atrophy. Curr Top Microbiol Immunol. 2010;346:267-78.

13. Sandri M, Sandri C, Gilbert A, Skurk C, Calabria E, Picard A, et al. Foxo transcription factors induce the atrophy-related ubiquitin ligase atrogin-1 and cause skeletal muscle atrophy. Cell. 2004;117(3):399-412.

14. Murton AJ, Constantin D, Greenhaff PL. The involvement of the ubiquitin proteasome system in human skeletal muscle remodelling and atrophy. Biochim Biophys Acta. 2008;1782(12):730-43.

15. Lokireddy S, McFarlane C, Ge X, Zhang H, Sze SK, Sharma M, et al. Myostatin induces degradation of sarcomeric proteins through a Smad3 signaling mechanism during skeletal muscle wasting. Mol Endocrinol. 2011;25(11):1936-49.

16. Lokireddy S, Mouly V, Butler-Browne G, Gluckman PD, Sharma M, Kambadur R, et al. Myostatin promotes the wasting of human myoblast cultures through promoting ubiquitin-proteasome pathway-mediated loss of sarcomeric proteins. Am J Physiol Cell Physiol. 2011;301(6):C1316-24.

17. McFarlane C, Hui GZ, Amanda WZ, Lau HY, Lokireddy S, Xiaojia G, et al. Human myostatin negatively regulates human myoblast growth and differentiation. Am J Physiol Cell Physiol. 2011;301(1):C195-203.

18. Penna F, Costamagna D, Pin F, Camperi A, Fanzani A, Chiarpotto EM, et al. Autophagic Degradation Contributes to Muscle Wasting in Cancer Cachexia. Am J Pathol. 2013.

19. Grumati P, Bonaldo P. Autophagy in Skeletal Muscle Homeostasis and in Muscular Dystrophies. Cells. 2012;1(3):325-45.

20. Ogata T, Oishi Y, Higuchi M, Muraoka I. Fasting-related autophagic response in slow- and fast-twitch skeletal muscle. Biochem Biophys Res Commun. 2010;394(1):136-40.

21. O'Leary MF, Vainshtein A, Carter HN, Zhang Y, Hood DA. Denervation-induced mitochondrial dysfunction and autophagy in skeletal muscle of apoptosis-deficient animals. Am J Physiol Cell Physiol. 2012;303(4):C447-54.

22. Masiero E, Agatea L, Mammucari C, Blaauw B, Loro E, Komatsu M, et al. Autophagy is required to maintain muscle mass. Cell Metab. 2009;10(6):507-15.

23. Lira VA, Okutsu M, Zhang M, Greene NP, Laker RC, Breen DS, et al. Autophagy is required for exercise training-induced skeletal muscle adaptation and improvement of physical performance. FASEB J. 2013.

24. Sakuma K, Yamaguchi A. Sarcopenia and cachexia: the adaptations of negative regulators of skeletal muscle mass. J Cachexia Sarcopenia Muscle. 2012;3(2):77-94.

25. Chesley A, MacDougall JD, Tarnopolsky MA, Atkinson SA, Smith K. Changes in human muscle protein synthesis after resistance exercise. J Appl Physiol. 1992;73(4):1383-8.

26. DeVol DL, Rotwein P, Sadow JL, Novakofski J, Bechtel PJ. Activation of insulin-like growth factor gene expression during work-induced skeletal muscle growth. Am J Physiol. 1990;259(1 Pt 1):E89-95.

27. O'Neil TK, Duffy LR, Frey JW, Hornberger TA. The role of phosphoinositide 3-kinase and phosphatidic acid in the regulation of mammalian target of rapamycin following eccentric contractions. J Physiol. 2009;587(Pt 14):3691-701.

28. Durham WJ, Miller SL, Yeckel CW, Chinkes DL, Tipton KD, Rasmussen BB, et al. Leg glucose and protein metabolism during an acute bout of resistance exercise in humans. J Appl Physiol. 2004;97(4):1379-86.

29. Dreyer HC, Fujita S, Cadenas JG, Chinkes DL, Volpi E, Rasmussen BB. Resistance exercise increases AMPK activity and reduces 4E-BP1 phosphorylation and protein synthesis in human skeletal muscle. J Physiol. 2006;576(Pt 2):613-24.

30. Biolo G, Maggi SP, Williams BD, Tipton KD, Wolfe RR. Increased rates of muscle protein turnover and amino acid transport after resistance exercise in humans. Am J Physiol. 1995;268(3 Pt 1):E514-20.

31. MacDougall JD, Gibala MJ, Tarnopolsky MA, MacDonald JR, Interisano SA, Yarasheski KE. The time course for elevated muscle protein synthesis following heavy resistance exercise. Can J Appl Physiol. 1995;20(4):480-6.

32. Wolfe RR. Skeletal muscle protein metabolism and resistance exercise. J Nutr. 2006;136(2):525S-8S.

33. Hudelmaier M, Wirth W, Himmer M, Ring-Dimitriou S, Sänger A, Eckstein F. Effect of exercise intervention on thigh muscle volume and anatomical cross-sectional areas--quantitative assessment using MRI. Magn Reson Med. 2010;64(6):1713-20.

34. Howarth KR, Moreau NA, Phillips SM, Gibala MJ. Coingestion of protein with carbohydrate during recovery from endurance exercise stimulates skeletal muscle protein synthesis in humans. J Appl Physiol. 2009;106(4):1394-402.

35. Harber MP, Konopka AR, Jemiolo B, Trappe SW, Trappe TA, Reidy PT. Muscle protein synthesis and gene expression during recovery from aerobic exercise in the fasted and fed states. Am J Physiol Regul Integr Comp Physiol. 2010;299(5):R1254-62.

36. Sheffield-Moore M, Yeckel CW, Volpi E, Wolf SE, Morio B, Chinkes DL, et al. Postexercise protein metabolism in older and younger men following moderate-intensity aerobic exercise. Am J Physiol Endocrinol Metab. 2004;287(3):E513-22.

37. Walrand S, Guillet C, Salles J, Cano N, Boirie Y. Physiopathological mechanism of sarcopenia. Clin Geriatr Med. 2011;27(3):365-85.

38. Bennet WM, Connacher AA, Scrimgeour CM, Smith K, Rennie MJ. Increase in anterior tibialis muscle protein synthesis in healthy man during mixed amino acid infusion: studies of incorporation of [1-13C]leucine. Clin Sci (Lond). 1989;76(4):447-54.

39. Miller SL, Tipton KD, Chinkes DL, Wolf SE, Wolfe RR. Independent and combined effects of amino acids and glucose after resistance exercise. Med Sci Sports Exerc. 2003;35(3):449-55.

40. Volpi E, Kobayashi H, Sheffield-Moore M, Mittendorfer B, Wolfe RR. Essential amino acids are primarily responsible for the amino acid stimulation of muscle protein anabolism in healthy elderly adults. Am J Clin Nutr. 2003;78(2):250-8.

41. Crozier SJ, Kimball SR, Emmert SW, Anthony JC, Jefferson LS. Oral leucine administration stimulates protein synthesis in rat skeletal muscle. J Nutr. 2005;135(3):376-82.

42. Glynn EL, Fry CS, Drummond MJ, Timmerman KL, Dhanani S, Volpi E, et al. Excess leucine intake enhances muscle anabolic signaling but not net protein anabolism in young men and women. J Nutr. 2010;140(11):1970-6.

43. Bohé J, Low JF, Wolfe RR, Rennie MJ. Latency and duration of stimulation of human muscle protein synthesis during continuous infusion of amino acids. J Physiol. 2001;532(Pt 2):575-9.

44. Rennie MJ, Bohé J, Wolfe RR. Latency, duration and dose response relationships of amino acid effects on human muscle protein synthesis. J Nutr. 2002;132(10):3225S-7S.

45. Hughes VA, Frontera WR, Roubenoff R, Evans WJ, Singh MA. Longitudinal changes in body composition in older men and women: role of body weight change and physical activity. Am J Clin Nutr. 2002;76(2):473-81.

46. Zadik Z, Chalew SA, McCarter RJ, Meistas M, Kowarski AA. The influence of age on the 24-hour integrated concentration of growth hormone in normal individuals. J Clin Endocrinol Metab. 1985;60(3):513-6.

47. Vermeulen A, Kaufman JM, Giagulli VA. Influence of some biological indexes on sex hormone-binding globulin and androgen levels in aging or obese males. J Clin Endocrinol Metab. 1996;81(5):1821-6.

48. Paddon-Jones D, Short KR, Campbell WW, Volpi E, Wolfe RR. Role of dietary protein in the sarcopenia of aging. Am J Clin Nutr. 2008;87(5):1562S-6S.

49. Buford TW, Cooke MB, Manini TM, Leeuwenburgh C, Willoughby DS. Effects of age and sedentary lifestyle on skeletal muscle NF-kappaB signaling in men. J Gerontol A Biol Sci Med Sci. 2010;65(5):532-7.

50. Marzetti E, Leeuwenburgh C. Skeletal muscle apoptosis, sarcopenia and frailty at old age. Exp Gerontol. 2006;41(12):1234-8.

51. Volpi E, Sheffield-Moore M, Rasmussen BB, Wolfe RR. Basal muscle amino acid kinetics and protein synthesis in healthy young and older men. JAMA. 2001;286(10):1206-12.

52. Walker DK, Dickinson JM, Timmerman KL, Drummond MJ, Reidy PT, Fry CS, et al. Exercise, amino acids, and aging in the control of human muscle protein synthesis. Med Sci Sports Exerc. 2011;43(12):2249-58.

53. Klitgaard H, Mantoni M, Schiaffino S, Ausoni S, Gorza L, Laurent-Winter C, et al. Function, morphology and protein expression of ageing skeletal muscle: a cross-sectional study of elderly men with different training backgrounds. Acta Physiol Scand. 1990;140(1):41-54.

54. Symons TB, Sheffield-Moore M, Mamerow MM, Wolfe RR, Paddon-Jones D. The anabolic response to resistance exercise and a protein-rich meal is not diminished by age. J Nutr Health Aging. 2011;15(5):376-81.

55. Koopman R, Verdijk L, Manders RJ, Gijsen AP, Gorselink M, Pijpers E, et al. Co-ingestion of protein and leucine stimulates muscle protein synthesis rates to the same extent in young and elderly lean men. Am J Clin Nutr. 2006;84(3):623-32.

56. Pennings B, Koopman R, Beelen M, Senden JM, Saris WH, van Loon LJ. Exercising before protein intake allows for greater use of dietary protein-derived amino acids for de novo muscle protein synthesis in both young and elderly men. Am J Clin Nutr. 2011;93(2):322-31.

57. Gray C, MacGillivray TJ, Eeley C, Stephens NA, Beggs I, Fearon KC, et al. Magnetic resonance imaging with k-means clustering objectively measures whole muscle volume compartments in sarcopenia/cancer cachexia. Clin Nutr. 2011;30(1):106-11.

58. Mcmillan DC, Watson WS, Preston T, Mcardle CS. Lean body mass changes in cancer patients with weight loss. Clin Nutr. 2000;19(6):403-6.

59. Fearon K, Strasser F, Anker SD, Bosaeus I, Bruera E, Fainsinger RL, et al. Definition and classification of cancer cachexia: an international consensus. Lancet Oncol. 2011;12(5):489-95.

60. Baracos VE, Reiman T, Mourtzakis M, Gioulbasanis I, Antoun S. Body composition in patients with non-small cell lung cancer: a contemporary view of cancer cachexia with the use of computed tomography image analysis. Am J Clin Nutr. 2010;91(4):1133S-7S.

61. Tan BH, Birdsell LA, Martin L, Baracos VE, Fearon KC. Sarcopenia in an overweight or obese patient is an adverse prognostic factor in pancreatic cancer. Clin Cancer Res. 2009;15(22):6973-9.

62. Emery PW, Edwards RH, Rennie MJ, Souhami RL, Halliday D. Protein synthesis in muscle measured in vivo in cachectic patients with cancer. Br Med J (Clin Res Ed). 1984;289(6445):584-6.

63. Lundholm K, Bennegård K, Edén E, Svaninger G, Emery PW, Rennie MJ. Efflux of 3-methylhistidine from the leg in cancer patients who experience weight loss. Cancer Res. 1982;42(11):4807-11.

64. Gallagher IJ, Stephens NA, MacDonald AJ, Skipworth RJ, Husi H, Greig CA, et al. Suppression of skeletal muscle turnover in cancer cachexia: evidence from the transcriptome in sequential human muscle biopsies. Clin Cancer Res. 2012;18(10):2817-27.

65. Buford TW, Anton SD, Judge AR, Marzetti E, Wohlgemuth SE, Carter CS, et al. Models of accelerated sarcopenia: critical pieces for solving the puzzle of age-related muscle atrophy. Ageing Res Rev. 2010;9(4):369-83.

66. Preston T, Slater C, McMillan DC, Falconer JS, Shenkin A, Fearon KC. Fibrinogen synthesis is elevated in fasting cancer patients with an acute phase response. J Nutr. 1998;128(8):1355-60.

67. Rolland Y, Abellan van Kan G, Gillette-Guyonnet S, Vellas B. Cachexia versus sarcopenia. Curr Opin Clin Nutr Metab Care. 2011;14(1):15-21.

68. Decramer M, Gosselink R, Troosters T, Verschueren M, Evers G. Muscle weakness is related to utilization of health care resources in COPD patients. Eur Respir J. 1997;10(2):417-23.

69. Winter Y, Schepelmann K, Spottke AE, Claus D, Grothe C, Schröder R, et al. Health-related quality of life in ALS, myasthenia gravis and facioscapulohumeral muscular dystrophy. J Neurol. 2010;257(9):1473-81.

70. Roubenoff R. Sarcopenia and its implications for the elderly. Eur J Clin Nutr. 2000;54 Suppl 3:S40-7.

71. Janssen I, Shepard DS, Katzmarzyk PT, Roubenoff R. The healthcare costs of sarcopenia in the United States. J Am Geriatr Soc. 2004;52(1):80-5.

72. Svenson KL, Lundqvist G, Wide L, Hällgren R. Impaired glucose handling in active rheumatoid arthritis: relationship to the secretion of insulin and counter-regulatory hormones. Metabolism. 1987;36(10):940-3.

73. Fearon K, Evans WJ, Anker SD. Myopenia-a new universal term for muscle wasting. J Cachexia Sarcopenia Muscle. 2011;2(1):1-3.

74. de Rekeneire N, Visser M, Peila R, Nevitt MC, Cauley JA, Tylavsky FA, et al. Is a fall just a fall: correlates of falling in healthy older persons. The Health, Aging and Body Composition Study. J Am Geriatr Soc. 2003;51(6):841-6.

75. Rosenberg IH. Summary comments. The American Journal of Clinical Nutrition. 1989;50(5):1231-3.

76. Morley JE, Abbatecola AM, Argiles JM, Baracos V, Bauer J, Bhasin S, et al. Sarcopenia with limited mobility: an international consensus. J Am Med Dir Assoc. 2011;12(6):403-9.

77. Flynn MA, Nolph GB, Baker AS, Martin WM, Krause G. Total body potassium in aging humans: a longitudinal study. Am J Clin Nutr. 1989;50(4):713-7.

78. Baumgartner RN, Koehler KM, Gallagher D, Romero L, Heymsfield SB, Ross RR, et al. Epidemiology of sarcopenia among the elderly in New Mexico. Am J Epidemiol. 1998;147(8):755-63.

79. Gillette-Guyonnet S, Nourhashemi F, Andrieu S, Cantet C, Albarède JL, Vellas B, et al. Body composition in French women 75+ years of age: the EPIDOS study. Mech Ageing Dev. 2003;124(3):311-6.

80. Skelton DA, Greig CA, Davies JM, Young A. Strength, power and related functional ability of healthy people aged 65-89 years. Age Ageing. 1994;23(5):371-7.

81. Frontera WR, Hughes VA, Lutz KJ, Evans WJ. A cross-sectional study of muscle strength and mass in 45- to 78-yr-old men and women. J Appl Physiol. 1991;71(2):644-50.

82. Visser M, Newman AB, Nevitt MC, Kritchevsky SB, Stamm EB, Goodpaster BH, et al. Reexamining the sarcopenia hypothesis. Muscle mass versus muscle strength. Health, Aging, and Body Composition Study Research Group. Ann N Y Acad Sci. 2000;904:456-61.

83. Ochi M, Tabara Y, Kido T, Uetani E, Ochi N, Igase M, et al. Quadriceps sarcopenia and visceral obesity are risk factors for postural instability in the middle-aged to elderly population. Geriatr Gerontol Int. 2010;10(3):233-43.

84. Janssen I, Heymsfield SB, Ross R. Low relative skeletal muscle mass (sarcopenia) in older persons is associated with functional impairment and physical disability. J Am Geriatr Soc. 2002;50(5):889-96.

85. Jankowski CM, Gozansky WS, Van Pelt RE, Schenkman ML, Wolfe P, Schwartz RS, et al. Relative contributions of adiposity and muscularity to physical function in community-dwelling older adults. Obesity (Silver Spring). 2008;16(5):1039-44.

86. Rolland Y, Lauwers-Cances V, Cristini C, Abellan van Kan G, Janssen I, Morley JE, et al. Difficulties with physical function associated with obesity, sarcopenia, and sarcopenic-obesity in community-dwelling elderly women: the EPIDOS (EPIDemiologie de l'OSteoporose) Study. Am J Clin Nutr. 2009;89(6):1895-900.

87. Szulc P, Beck TJ, Marchand F, Delmas PD. Low skeletal muscle mass is associated with poor structural parameters of bone and impaired balance in elderly men--the MINOS study. J Bone Miner Res. 2005;20(5):721-9.

88. Pichard C, Kyle UG, Morabia A, Perrier A, Vermeulen B, Unger P. Nutritional assessment: lean body mass depletion at hospital admission is associated with an increased length of stay. Am J Clin Nutr. 2004;79(4):613-8.

89. Cosquéric G, Sebag A, Ducolombier C, Thomas C, Piette F, Weill-Engerer S. Sarcopenia is predictive of nosocomial infection in care of the elderly. Br J Nutr. 2006;96(5):895-901.

90. Lang T, Cauley JA, Tylavsky F, Bauer D, Cummings S, Harris TB, et al. Computed tomographic measurements of thigh muscle cross-sectional area and attenuation coefficient predict hip fracture: the health, aging, and body composition study. J Bone Miner Res. 2010;25(3):513-9.

91. Lang T, Koyama A, Li C, Li J, Lu Y, Saeed I, et al. Pelvic body composition measurements by quantitative computed tomography: association with recent hip fracture. Bone. 2008;42(4):798-805.

92. Cawthon PM, Fox KM, Gandra SR, Delmonico MJ, Chiou CF, Anthony MS, et al. Do muscle mass, muscle density, strength, and physical function similarly influence risk of hospitalization in older adults? J Am Geriatr Soc. 2009;57(8):1411-9.

93. Newman AB, Kupelian V, Visser M, Simonsick EM, Goodpaster BH, Kritchevsky SB, et al. Strength, but not muscle mass, is associated with mortality in the health, aging and body composition study cohort. J Gerontol A Biol Sci Med Sci. 2006;61(1):72-7.

94. Cesari M, Pahor M, Lauretani F, Zamboni V, Bandinelli S, Bernabei R, et al. Skeletal muscle and mortality results from the InCHIANTI Study. J Gerontol A Biol Sci Med Sci. 2009;64(3):377-84.

95. Szulc P, Munoz F, Marchand F, Chapurlat R, Delmas PD. Rapid loss of appendicular skeletal muscle mass is associated with higher all-cause mortality in older men: the prospective MINOS study. Am J Clin Nutr. 2010;91(5):1227-36.

96. Blum D, Omlin A, Fearon K, Baracos V, Radbruch L, Kaasa S, et al. Evolving classification systems for cancer cachexia: ready for clinical practice? Support Care Cancer. 2010;18(3):273-9.

97. Fearon K, Strasser F, Anker SD, Bosaeus I, Bruera E, Fainsinger RL, et al. Definition and classification of cancer cachexia: an international consensus. Lancet Oncol. 2011.

98. de Graaf SS, Meeuwsen-van der Roest WP, Schraffordt Koops H, Zijlstra WG. Dissociation of body weight and lean body mass during cancer chemotherapy. Eur J Cancer Clin Oncol. 1987;23(6):731-7.

99. Heymsfield SB, McManus CB. Tissue components of weight loss in cancer patients. A new method of study and preliminary observations. Cancer. 1985;55(1 Suppl):238-49.

100. Cohn SH, Gartenhaus W, Sawitsky A, Rai K, Zanzi I, Vaswani A, et al. Compartmental body composition of cancer patients by measurement of total body nitrogen, potassium, and water. Metabolism. 1981;30(3):222-9.

101. Liedman B, Andersson H, Bosaeus I, Hugosson I, Lundell L. Changes in body composition after gastrectomy: results of a controlled, prospective clinical trial. World J Surg. 1997;21(4):416-20; discussion 20-1.

102. Prado CM, Baracos VE, McCargar LJ, Reiman T, Mourtzakis M, Tonkin K, et al. Sarcopenia as a determinant of chemotherapy toxicity and time to tumor progression in metastatic breast cancer patients receiving capecitabine treatment. Clin Cancer Res. 2009;15(8):2920-6.

103. Weber MA, Krakowski-Roosen H, Schröder L, Kinscherf R, Krix M, Kopp-Schneider A, et al. Morphology, metabolism, microcirculation, and strength of skeletal muscles in cancer-related cachexia. Acta Oncol. 2009;48(1):116-24.

104. Copland L, Rothenberg E, Ellegård L, Hyltander A, Bosaeus I. Muscle mass and exercise capacity in cancer patients after major upper gastrointestinal surgery. e-SPEN, the European e-Journal of Clinical Nutrition and Metabolism. 2010;5(6):e265-e71.

105. Prado CM, Lieffers JR, McCargar LJ, Reiman T, Sawyer MB, Martin L, et al. Prevalence and clinical implications of sarcopenic obesity in patients with solid tumours of the respiratory and gastrointestinal tracts: a population-based study. Lancet Oncol. 2008;9(7):629-35.

106. Prado CM, Baracos VE, McCargar LJ, Mourtzakis M, Mulder KE, Reiman T, et al. Body composition as an independent determinant of 5-fluorouracil-based chemotherapy toxicity. Clin Cancer Res. 2007;13(11):3264-8.

107. Antoun S, Birdsell L, Sawyer MB, Venner P, Escudier B, Baracos VE. Association of skeletal muscle wasting with treatment with sorafenib in patients with advanced renal cell carcinoma: results from a placebo-controlled study. J Clin Oncol. 2010;28(6):1054-60.

108. Awad S, Tan BH, Cui H, Bhalla A, Fearon KC, Parsons SL, et al. Marked changes in body composition following neoadjuvant chemotherapy for oesophagogastric cancer. Clin Nutr. 2011.

109. Liu CJ, Latham NK. Progressive resistance strength training for improving physical function in older adults. Cochrane Database Syst Rev. 2009(3):CD002759.

110. Verdijk LB, Gleeson BG, Jonkers RA, Meijer K, Savelberg HH, Dendale P, et al. Skeletal muscle hypertrophy following resistance training is accompanied by a fiber type-specific increase in satellite cell content in elderly men. J Gerontol A Biol Sci Med Sci. 2009;64(3):332-9.

111. Slivka D, Raue U, Hollon C, Minchev K, Trappe S. Single muscle fiber adaptations to resistance training in old (>80 yr) men: evidence for limited skeletal muscle plasticity. Am J Physiol Regul Integr Comp Physiol. 2008;295(1):R273-80.

112. Kryger AI, Andersen JL. Resistance training in the oldest old: consequences for muscle strength, fiber types, fiber size, and MHC isoforms. Scand J Med Sci Sports. 2007;17(4):422-30.

113. Frontera WR, Hughes VA, Krivickas LS, Kim SK, Foldvari M, Roubenoff R. Strength training in older women: early and late changes in whole muscle and single cells. Muscle Nerve. 2003;28(5):601-8.

114. Raguso CA, Kyle U, Kossovsky MP, Roynette C, Paoloni-Giacobino A, Hans D, et al. A 3-year longitudinal study on body composition changes in the elderly: role of physical exercise. Clin Nutr. 2006;25(4):573-80.

115. Volpi E, Mittendorfer B, Wolf SE, Wolfe RR. Oral amino acids stimulate muscle protein anabolism in the elderly despite higher first-pass splanchnic extraction. Am J Physiol. 1999;277(3 Pt 1):E513-20.

116. Tieland M, Borgonjen-Van den Berg KJ, van Loon LJ, de Groot LC. Dietary protein intake in community-dwelling, frail, and institutionalized elderly people: scope for improvement. Eur J Nutr. 2012;51(2):173-9.

117. O'Connell MD, Roberts SA, Srinivas-Shankar U, Tajar A, Connolly MJ, Adams JE, et al. Do the effects of testosterone on muscle strength, physical function, body composition, and quality of life persist six months after treatment in intermediate-frail and frail elderly men? J Clin Endocrinol Metab. 2011;96(2):454-8.

118. Rolland Y, Onder G, Morley JE, Gillette-Guyonet S, Abellan van Kan G, Vellas B. Current and future pharmacologic treatment of sarcopenia. Clin Geriatr Med. 2011;27(3):423-47.

119. Rolland Y, Dupuy C, Abellan van Kan G, Gillette S, Vellas B. Treatment strategies for sarcopenia and frailty. Med Clin North Am. 2011;95(3):427-38, ix.

120. Galvão DA, Newton RU. Review of exercise intervention studies in cancer patients. J Clin Oncol. 2005;23(4):899-909.

121. Barber MD, Fearon KC. Tolerance and incorporation of a high-dose eicosapentaenoic acid diester emulsion by patients with pancreatic cancer cachexia. Lipids. 2001;36(4):347-51.

122. Barber MD, Ross JA, Voss AC, Tisdale MJ, Fearon KC. The effect of an oral nutritional supplement enriched with fish oil on weight-loss in patients with pancreatic cancer. Br J Cancer. 1999;81(1):80-6.

123. Fearon KC, Von Meyenfeldt MF, Moses AG, Van Geenen R, Roy A, Gouma DJ, et al. Effect of a protein and energy dense N-3 fatty acid enriched oral supplement on loss of weight and lean tissue in cancer cachexia: a randomised double blind trial. Gut. 2003;52(10):1479-86.

124. Murphy RA, Mourtzakis M, Chu QS, Baracos VE, Reiman T, Mazurak VC. Nutritional intervention with fish oil provides a benefit over standard of care for weight and skeletal muscle mass in patients with nonsmall cell lung cancer receiving chemotherapy. Cancer. 2011;117(8):1775-82.

125. Fearon KC, Barber MD, Moses AG, Ahmedzai SH, Taylor GS, Tisdale MJ, et al. Double-blind, placebo-controlled, randomized study of eicosapentaenoic acid diester in patients with cancer cachexia. J Clin Oncol. 2006;24(21):3401-7.

126. Ries A, Trottenberg P, Elsner F, Stiel S, Haugen D, Kaasa S, et al. A systematic review on the role of fish oil for the treatment of cachexia in advanced cancer: an EPCRC cachexia guidelines project. Palliat Med. 2012;26(4):294-304.

127. Dewey A, Baughan C, Dean T, Higgins B, Johnson I. Eicosapentaenoic acid (EPA, an omega-3 fatty acid from fish oils) for the treatment of cancer cachexia. Cochrane Database Syst Rev. 2007(1):CD004597.

128. Deutz NE, Safar A, Schutzler S, Memelink R, Ferrando A, Spencer H, et al. Muscle protein synthesis in cancer patients can be stimulated with a specially formulated medical food. Clin Nutr. 2011;30(6):759-68.

129. Mantovani G. Randomised phase III clinical trial of 5 different arms of treatment on 332 patients with cancer cachexia. Eur Rev Med Pharmacol Sci. 2010;14(4):292-301.

130. Madeddu C, Dessì M, Panzone F, Serpe R, Antoni G, Cau MC, et al. Randomized phase III clinical trial of a combined treatment with carnitine + celecoxib ± megestrol acetate for patients with cancer-related anorexia/cachexia syndrome. Clin Nutr. 2012;31(2):176-82.

131. Mantovani G, Madeddu C, Macciò A. Drugs in development for treatment of patients with cancer-related anorexia and cachexia syndrome. Drug Des Devel Ther. 2013;7:645-56.

132. Greig CA, Johns N, Gray C, Macdonald A, Stephens NA, Skipworth RJ, et al. Phase I/II trial of formoterol fumarate combined with megestrol acetate in cachectic patients with advanced malignancy. Support Care Cancer. 2014.

133. Group. BDW. Biomarkers and surrogate endpoints: preferred definitions and conceptual framework. Clin Pharmacol Ther. 2001;69(3):89-95.

134. Stephens NA, Gallagher IJ, Rooyackers O, Skipworth RJ, Tan BH, Marstrand T, et al. Using transcriptomics to identify and validate novel biomarkers of human skeletal muscle cancer cachexia. Genome Med. 2010;2(1):1.

135. Weber MA, Kinscherf R, Krakowski-Roosen H, Aulmann M, Renk H, Künkele A, et al. Myoglobin plasma level related to muscle mass and fiber composition: a clinical marker of muscle wasting? J Mol Med (Berl). 2007;85(8):887-96.

136. Nedergaard A, Karsdal MA, Sun S, Henriksen K. Serological muscle loss biomarkers: an overview of current concepts and future possibilities. J Cachexia Sarcopenia Muscle. 2013;4(1):1-17.

137. Wang ZM, Pierson RN, Heymsfield SB. The five-level model: a new approach to organizing body-composition research. Am J Clin Nutr. 1992;56(1):19-28.

138. Ellis KJ. Human body composition: in vivo methods. Physiol Rev. 2000;80(2):649-80.

139. Eknoyan G. Adolphe Quetelet (1796-1874)--the average man and indices of obesity. Nephrol Dial Transplant. 2008;23(1):47-51.

140. Keys A, Fidanza F, Karvonen MJ, Kimura N, Taylor HL. Indices of relative weight and obesity. J Chronic Dis. 1972;25(6):329-43.

141. Gallagher D, Visser M, Sepúlveda D, Pierson RN, Harris T, Heymsfield SB. How useful is body mass index for comparison of body fatness across age, sex, and ethnic groups? Am J Epidemiol. 1996;143(3):228-39.

142. Ellis KJ. Selected body composition methods can be used in field studies. J Nutr. 2001;131(5):1589S-95S.

143. Oreopoulos A, Fonarow GC, Ezekowitz JA, McAlister FA, Sharma AM, Kalantar-Zadeh K, et al. Do Anthropometric Indices Accurately Reflect Directly Measured Body Composition in Men and Women With Chronic Heart Failure?

144. BROZEK J, GRANDE F, ANDERSON JT, KEYS A. DENSITOMETRIC ANALYSIS OF BODY COMPOSITION: REVISION OF SOME QUANTITATIVE ASSUMPTIONS. Ann N Y Acad Sci. 1963;110:113-40.

145. Heymsfield SB, Wang J, Kehayias J, Heshka S, Lichtman S, Pierson RN. Chemical determination of human body density in vivo: relevance to hydrodensitometry. Am J Clin Nutr. 1989;50(6):1282-9.

146. Bakker HK, Struikenkamp RS. Biological variability and lean body mass estimates. Hum Biol. 1977;49(2):187-202.

147. Biaggi RR, Vollman MW, Nies MA, Brener CE, Flakoll PJ, Levenhagen DK, et al. Comparison of air-displacement plethysmography with hydrostatic weighing and bioelectrical impedance analysis for the assessment of body composition in healthy adults. Am J Clin Nutr. 1999;69(5):898-903.

148. Vescovi JD, Zimmerman SL, Miller WC, Hildebrandt L, Hammer RL, Fernhall B. Evaluation of the BOD POD for estimating percentage body fat in a heterogeneous group of adult humans. European Journal Of Applied Physiology. 2001;85(3-4):326-32.

149. Brodie D, Moscrip V, Hutcheon R. Body composition measurement: a review of hydrodensitometry, anthropometry, and impedance methods. Nutrition. 1998;14(3):296-310.

150. Heymsfield SB, Wang Z, Baumgartner RN, Ross R. Human body composition: advances in models and methods. Annu Rev Nutr. 1997;17:527-58.

151. Edelman IS, Olney JM, James AH, Brooks L, Moore FD. Body Composition: Studies in the Human Being by the Dilution Principle. Science. 1952;115(2991):447-54.

152. Wang Z, Deurenberg P, Wang W, Pietrobelli A, Baumgartner RN, Heymsfield SB. Hydration of fat-free body mass: review and critique of a classic body-composition constant. Am J Clin Nutr. 1999;69(5):833-41.

153. Siervo M, Faber P, Gibney ER, Lobley GE, Elia M, Stubbs RJ, et al. Use of the cellular model of body composition to describe changes in body water compartments after total fasting, very low calorie diet and low calorie diet in obese men. Int J Obes (Lond). 2010;34(5):908-18.

154. Kyle UG, Bosaeus I, De Lorenzo AD, Deurenberg P, Elia M, Gómez JM, et al. Bioelectrical impedance analysis--part I: review of principles and methods. Clin Nutr. 2004;23(5):1226-43.

155. statement NC. Bioelectrical impedance analysis in body composition measurement: National Institutes of Health Technology Assessment Conference Statement. Am J Clin Nutr. 1996;64(3 Suppl):524S-32S.

156. Slater C, Preston T. A simple prediction of total body water to aid quality control in isotope dilution studies in subjects 3-87 years of age. Isotopes Environ Health Stud. 2005;41(2):99-107.

157. Kyle UG, Bosaeus I, De Lorenzo AD, Deurenberg P, Elia M, Manuel Gómez J, et al. Bioelectrical impedance analysis-part II: utilization in clinical practice. Clin Nutr. 2004;23(6):1430-53.

158. Sun SS, Chumlea WC, Heymsfield SB, Lukaski HC, Schoeller D, Friedl K, et al. Development of bioelectrical impedance analysis prediction equations for body composition with the use of a multicomponent model for use in epidemiologic surveys. Am J Clin Nutr. 2003;77(2):331-40.

159. Steiner MC, Barton RL, Singh SJ, Morgan MD. Bedside methods versus dual energy X-ray absorptiometry for body composition measurement in COPD. Eur Respir J. 2002;19(4):626-31.

160. Deurenberg P, Weststrate JA, Hautvast JG, van der Kooy K. Is the bioelectrical-impedance method valid? Am J Clin Nutr. 1991;53(1):179-81.

161. Forbes GB, Simon W, Amatruda JM. Is bioimpedance a good predictor of body-composition change? Am J Clin Nutr. 1992;56(1):4-6.

162. Boddy K, King PC, Hume R, Weyers E. The relation of total body potassium to height, weight, and age in normal adults. J Clin Pathol. 1972;25(6):512-7.

163. Mattsson S, Thomas BJ. Development of methods for body composition studies. Phys Med Biol. 2006;51(13):R203-28.

164. Knight GS, Beddoe AH, Streat SJ, Hill GL. Body composition of two human cadavers by neutron activation and chemical analysis. Am J Physiol. 1986;250(2 Pt 1):E179-85.

165. Modlesky CM, Lewis RD, Yetman KA, Rose B, Rosskopf LB, Snow TK, et al. Comparison of body composition and bone mineral measurements from two DXA instruments in young men. Am J Clin Nutr. 1996;64(5):669-76.

166. Abate N, Burns D, Peshock RM, Garg A, Grundy SM. Estimation of adipose tissue mass by magnetic resonance imaging: validation against dissection in human cadavers. J Lipid Res. 1994;35(8):1490-6.

167. Val-Laillet D, Blat S, Louveau I, Malbert CH. A computed tomography scan application to evaluate adiposity in a minipig model of human obesity. Br J Nutr. 2010;104(11):1719-28.

168. Positano V, Christiansen T, Santarelli MF, Ringgaard S, Landini L, Gastaldelli A. Accurate segmentation of subcutaneous and intermuscular adipose tissue from MR images of the thigh. J Magn Reson Imaging. 2009;29(3):677-84.

169. Liu J, Fox CS, Hickson DA, May WD, Hairston KG, Carr JJ, et al. Impact of abdominal visceral and subcutaneous adipose tissue on cardiometabolic risk factors: the Jackson Heart Study. J Clin Endocrinol Metab. 2010;95(12):5419-26.

170. Guiu B, Petit JM, Bonnetain F, Ladoire S, Guiu S, Cercueil JP, et al. Visceral fat area is an independent predictive biomarker of outcome after first-line bevacizumab-based treatment in metastatic colorectal cancer. Gut. 2010;59(3):341-7.

171. Prado CM, Lima IS, Baracos VE, Bies RR, McCargar LJ, Reiman T, et al. An exploratory study of body composition as a determinant of epirubicin pharmacokinetics and toxicity. Cancer Chemother Pharmacol. 2011;67(1):93-101.

172. Visser M, Kritchevsky SB, Goodpaster BH, Newman AB, Nevitt M, Stamm E, et al. Leg muscle mass and composition in relation to lower extremity performance in men and women aged 70 to 79: the health, aging and body composition study. J Am Geriatr Soc. 2002;50(5):897-904.

173. Keller A, Gunderson R, Reikerås O, Brox JI. Reliability of computed tomography measurements of paraspinal muscle cross-sectional area and density in patients with chronic low back pain. Spine (Phila Pa 1976). 2003;28(13):1455-60.

174. Boesch C, Slotboom J, Hoppeler H, Kreis R. In vivo determination of intra-myocellular lipids in human muscle by means of localized 1H-MR-spectroscopy. Magn Reson Med. 1997;37(4):484-93.

175. Fiatarone MA, Marks EC, Ryan ND, Meredith CN, Lipsitz LA, Evans WJ. High-intensity strength training in nonagenarians. Effects on skeletal muscle. JAMA. 1990;263(22):3029-34.

176. Nelson ME, Fiatarone MA, Layne JE, Trice I, Economos CD, Fielding RA, et al. Analysis of body-composition techniques and models for detecting change in soft tissue with strength training. Am J Clin Nutr. 1996;63(5):678-86.

177. Prado CM, Birdsell LA, Baracos VE. The emerging role of computerized tomography in assessing cancer cachexia. Curr Opin Support Palliat Care. 2009;3(4):269-75.

178. Strandberg S, Wretling ML, Wredmark T, Shalabi A. Reliability of computed tomography measurements in assessment of thigh muscle cross-sectional area and attenuation. BMC Med Imaging. 2010;10:18.

179. Hicks GE, Simonsick EM, Harris TB, Newman AB, Weiner DK, Nevitt MA, et al. Cross-sectional associations between trunk muscle composition, back pain, and physical function in the health, aging and body composition study. J Gerontol A Biol Sci Med Sci. 2005;60(7):882-7.

180. Mitsiopoulos N, Baumgartner RN, Heymsfield SB, Lyons W, Gallagher D, Ross R. Cadaver validation of skeletal muscle measurement by magnetic resonance imaging and computerized tomography. J Appl Physiol. 1998;85(1):115-22.

181. Gallagher D, Kuznia P, Heshka S, Albu J, Heymsfield SB, Goodpaster B, et al. Adipose tissue in muscle: a novel depot similar in size to visceral adipose tissue. Am J Clin Nutr. 2005;81(4):903-10.

182. Irving BA, Weltman JY, Brock DW, Davis CK, Gaesser GA, Weltman A. NIH ImageJ and Slice-O-Matic computed tomography imaging software to quantify soft tissue. Obesity (Silver Spring). 2007;15(2):370-6.

183. Gronemeyer SA, Steen RG, Kauffman WM, Reddick WE, Glass JO. Fast adipose tissue (FAT) assessment by MRI. Magn Reson Imaging. 2000;18(7):815-8.

184. Berker D, Koparal S, Işik S, Paşaoğlu L, Aydin Y, Erol K, et al. Compatibility of different methods for the measurement of visceral fat in different body mass index strata. Diagn Interv Radiol. 2010;16(2):99-105.

185. Boettcher M, Machann J, Stefan N, Thamer C, Häring HU, Claussen CD, et al. Intermuscular adipose tissue (IMAT): association with other adipose tissue compartments and insulin sensitivity. J Magn Reson Imaging. 2009;29(6):1340-5.

186. Mourtzakis M, Prado CM, Lieffers JR, Reiman T, McCargar LJ, Baracos VE. A practical and precise approach to quantification of body composition in cancer patients using computed tomography images acquired during routine care. Appl Physiol Nutr Metab. 2008;33(5):997-1006.

187. Beneke R, Neuerburg J, Bohndorf K. Muscle cross-section measurement by magnetic resonance imaging. Eur J Appl Physiol Occup Physiol. 1991;63(6):424-9.

188. Hudash G, Albright JP, McAuley E, Martin RK, Fulton M. Cross-sectional thigh components: computerized tomographic assessment. Med Sci Sports Exerc. 1985;17(4):417-21.

189. Positano V, Gastaldelli A, Sironi AM, Santarelli MF, Lombardi M, Landini L. An accurate and robust method for unsupervised assessment of abdominal fat by MRI. J Magn Reson Imaging. 2004;20(4):684-9.

190. Lönn L, Starck G, Alpsten M, Ekholm S, Sjöström L. Determination of tissue volumes. A comparison between CT and MR imaging. Acta Radiol. 1999;40(3):314-21.

191. Bonekamp S, Ghosh P, Crawford S, Solga SF, Horska A, Brancati FL, et al. Quantitative comparison and evaluation of software packages for assessment of abdominal adipose tissue distribution by magnetic resonance imaging. Int J Obes (Lond). 2008;32(1):100-11.

192. Positano V, Cusi K, Santarelli MF, Sironi A, Petz R, Defronzo R, et al. Automatic correction of intensity inhomogeneities improves unsupervised assessment of abdominal fat by MRI. J Magn Reson Imaging. 2008;28(2):403-10.

193. Arif H, Racette SB, Villareal DT, Holloszy JO, Weiss EP. Comparison of methods for assessing abdominal adipose tissue from magnetic resonance images. Obesity (Silver Spring). 2007;15(9):2240-4.

194. Shen W, Punyanitya M, Wang Z, Gallagher D, St-Onge MP, Albu J, et al. Total body skeletal muscle and adipose tissue volumes: estimation from a single abdominal cross-sectional image. J Appl Physiol. 2004;97(6):2333-8.

195. Lee SJ, Janssen I, Heymsfield SB, Ross R. Relation between whole-body and regional measures of human skeletal muscle. Am J Clin Nutr. 2004;80(5):1215-21.

196. Cotofana S, Hudelmaier M, Wirth W, Himmer M, Ring-Dimitriou S, Sänger AM, et al. Correlation between single-slice muscle anatomical cross-sectional area and muscle volume in thigh extensors, flexors and adductors of perimenopausal women. Eur J Appl Physiol. 2010;110(1):91-7.

197. Morse CI, Degens H, Jones DA. The validity of estimating quadriceps volume from single MRI cross-sections in young men. Eur J Appl Physiol. 2007;100(3):267-74.

198. Levine JA, Abboud L, Barry M, Reed JE, Sheedy PF, Jensen MD. Measuring leg muscle and fat mass in humans: comparison of CT and dual-energy X-ray absorptiometry. J Appl Physiol. 2000;88(2):452-6.

199. Miljkovic I, Zmuda JM. Epidemiology of myosteatosis. Curr Opin Clin Nutr Metab Care. 2010;13(3):260-4.

200. Goodpaster BH, Kelley DE, Thaete FL, He J, Ross R. Skeletal muscle attenuation determined by computed tomography is associated with skeletal muscle lipid content. J Appl Physiol. 2000;89(1):104-10.

201. Brandberg J, Lonn L, Bergelin E, Sjostrom L, Forssell-Aronsson E, Starck G. Accurate tissue area measurements with considerably reduced radiation dose achieved by patient-specific CT scan parameters. Br J Radiol. 2008;81(970):801-8.

202. Goodpaster BH, Thaete FL, Kelley DE. Thigh adipose tissue distribution is associated with insulin resistance in obesity and in type 2 diabetes mellitus. Am J Clin Nutr. 2000;71(4):885-92.

203. Seki Y, Ohue M, Sekimoto M, Takiguchi S, Takemasa I, Ikeda M, et al. Evaluation of the technical difficulty performing laparoscopic resection of a rectosigmoid carcinoma: visceral fat reflects technical difficulty more accurately than body mass index. Surg Endosc. 2007;21(6):929-34.

204. Potretzke AM, Schmitz KH, Jensen MD. Preventing overestimation of pixels in computed tomography assessment of visceral fat. Obes Res. 2004;12(10):1698-701.

205. Armao D, Guyon JP, Firat Z, Brown MA, Semelka RC. Accurate quantification of visceral adipose tissue (VAT) using water-saturation MRI and computer segmentation: preliminary results. J Magn Reson Imaging. 2006;23(5):736-41.

206. Broderick BJ, Dessus S, Grace PA, Olaighin G. Technique for the computation of lower leg muscle bulk from magnetic resonance images. Med Eng Phys. 2010;32(8):926-33.

207. Eng CM, Abrams GD, Smallwood LR, Lieber RL, Ward SR. Muscle geometry affects accuracy of forearm volume determination by magnetic resonance imaging (MRI). J Biomech. 2007;40(14):3261-6.

208. Leroy-Willig A. Skeletal muscle measurements by MRI. J Appl Physiol. 1999;86(3):1097-8.

209. Carraro F, Stuart CA, Hartl WH, Rosenblatt J, Wolfe RR. Effect of exercise and recovery on muscle protein synthesis in human subjects. Am J Physiol. 1990;259(4 Pt 1):E470-6.

210. Rennie MJ, Smith K, Watt PW. Measurement of human tissue protein synthesis: an optimal approach. Am J Physiol. 1994;266(3 Pt 1):E298-307.

211. Garlick PJ, McNurlan MA, Essén P, Wernerman J. Measurement of tissue protein synthesis rates in vivo: a critical analysis of contrasting methods. Am J Physiol. 1994;266(3 Pt 1):E287-97.

212. Davis TA, Reeds PJ. Of flux and flooding: the advantages and problems of different isotopic methods for quantifying protein turnover in vivo : II. Methods based on the incorporation of a tracer. Curr Opin Clin Nutr Metab Care. 2001;4(1):51-6.

213. McNurlan MA, Essen P, Heys SD, Buchan V, Garlick PJ, Wernerman J. Measurement of protein synthesis in human skeletal muscle: further investigation of the flooding technique. Clin Sci (Lond). 1991;81(4):557-64.

214. Garlick PJ, Wernerman J, McNurlan MA, Essen P, Lobley GE, Milne E, et al. Measurement of the rate of protein synthesis in muscle of postabsorptive young men by injection of a 'flooding dose' of [1-13C]leucine. Clin Sci (Lond). 1989;77(3):329-36.

215. Smith K, Barua JM, Watt PW, Scrimgeour CM, Rennie MJ. Flooding with L-[1-13C]leucine stimulates human muscle protein incorporation of continuously infused L-[1-13C]valine. Am J Physiol. 1992;262(3 Pt 1):E372-6.

216. Smith K, Downie S, Barua JM, Watt PW, Scrimgeour CM, Rennie MJ. Effect of a flooding dose of leucine in stimulating incorporation of constantly infused valine into albumin. Am J Physiol. 1994;266(4 Pt 1):E640-4.

217. Smith K, Reynolds N, Downie S, Patel A, Rennie MJ. Effects of flooding amino acids on incorporation of labeled amino acids into human muscle protein. Am J Physiol. 1998;275(1 Pt 1):E73-8.

218. Tessari P, Tsalikian E, Schwenk WF, Nissen SL, Haymond MW. Effects of [15N]leucine infused at low rates on leucine metabolism in humans. Am J Physiol. 1985;249(1 Pt 1):E121-30.

219. Smith GI, Patterson BW, Mittendorfer B. Human muscle protein turnover--why is it so variable? J Appl Physiol. 2011;110(2):480-91.

220. Elia M, Carter A, Bacon S, Winearls CG, Smith R. Clinical usefulness of urinary 3-methylhistidine excretion in indicating muscle protein breakdown. Br Med J (Clin Res Ed). 1981;282(6261):351-4.

221. Marliss EB, Wei CN, Dietrich LL. The short-term effects of protein intake on 3-methylhistidine excretion. Am J Clin Nutr. 1979;32(8):1617-21.

222. Zhang XJ, Chinkes DL, Sakurai Y, Wolfe RR. An isotopic method for measurement of muscle protein fractional breakdown rate in vivo. Am J Physiol. 1996;270(5 Pt 1):E759-67.

223. Kumar V, Atherton P, Smith K, Rennie MJ. Human muscle protein synthesis and breakdown during and after exercise. J Appl Physiol. 2009;106(6):2026-39.

224. Busch R, Kim YK, Neese RA, Schade-Serin V, Collins M, Awada M, et al. Measurement of protein turnover rates by heavy water labeling of nonessential amino acids. Biochim Biophys Acta. 2006;1760(5):730-44.

225. Moses AW, Slater C, Preston T, Barber MD, Fearon KC. Reduced total energy expenditure and physical activity in cachectic patients with pancreatic cancer can be modulated by an energy and protein dense oral supplement enriched with n-3 fatty acids. Br J Cancer. 2004;90(5):996-1002.

226. Gasier HG, Riechman SE, Wiggs MP, Previs SF, Fluckey JD. A comparison of 2H2O and phenylalanine flooding dose to investigate muscle protein synthesis with acute exercise in rats. Am J Physiol Endocrinol Metab. 2009;297(1):E252-9.

227. Gasier HG, Fluckey JD, Previs SF, Wiggs MP, Riechman SE. Acute resistance exercise augments integrative myofibrillar protein synthesis. Metabolism. 2012;61(2):153-6.

228. Robinson MM, Turner SM, Hellerstein MK, Hamilton KL, Miller BF. Long-term synthesis rates of skeletal muscle DNA and protein are higher during aerobic training in older humans than in sedentary young subjects but are not altered by protein supplementation. FASEB J. 2011;25(9):3240-9.

229. Gasier HG, Fluckey JD, Previs SF. The application of 2H2O to measure skeletal muscle protein synthesis. Nutr Metab (Lond). 2010;7:31.

230. Greig CA, Young A, Skelton DA, Pippet E, Butler FM, Mahmud SM. Exercise studies with elderly volunteers. Age Ageing. 1994;23(3):185-9.

231. Bohannon RW. Sit-to-stand test for measuring performance of lower extremity muscles. Percept Mot Skills. 1995;80(1):163-6.

232. Csuka M, McCarty DJ. Simple method for measurement of lower extremity muscle strength. Am J Med. 1985;78(1):77-81.

233. Podsiadlo D, Richardson S. The timed "Up & Go": a test of basic functional mobility for frail elderly persons. J Am Geriatr Soc. 1991;39(2):142-8.

234. Creel GL, Light KE, Thigpen MT. Concurrent and construct validity of scores on the Timed Movement Battery. Phys Ther. 2001;81(2):789-98.

235. Harridge SD, Kryger A, Stensgaard A. Knee extensor strength, activation, and size in very elderly people following strength training. Muscle Nerve. 1999;22(7):831-9.

236. Todd G, Gorman RB, Gandevia SC. Measurement and reproducibility of strength and voluntary activation of lower-limb muscles. Muscle Nerve. 2004;29(6):834-42.

237. Arden NK, Spector TD. Genetic influences on muscle strength, lean body mass, and bone mineral density: a twin study. J Bone Miner Res. 1997;12(12):2076-81.

238. Solaro RJ, Pang DC, Briggs FN. The purification of cardiac myofibrils with Triton X-100. Biochim Biophys Acta. 1971;245(1):259-62.

239. Laemmli UK. Cleavage of structural proteins during the assembly of the head of bacteriophage T4. Nature. 1970;227(5259):680-5.

240. Bradford MM. A rapid and sensitive method for the quantitation of microgram quantities of protein utilizing the principle of protein-dye binding. Anal Biochem. 1976;72:248-54.

241. Gundry RL, White MY, Murray CI, Kane LA, Fu Q, Stanley BA, et al. Preparation of proteins and peptides for mass spectrometry analysis in a bottom-up proteomics workflow. Curr Protoc Mol Biol. 2009;Chapter 10:Unit10.25.

242. Fearon KC, Falconer JS, Slater C, McMillan DC, Ross JA, Preston T. Albumin synthesis rates are not decreased in hypoalbuminemic cachectic cancer patients with an ongoing acute-phase protein response. Ann Surg. 1998;227(2):249-54.

243. Preston T, Small AC. Improved measurement of protein synthesis in human subjects using 2H-phenylalanine isotopomers and gas chromatography/mass spectrometry. Rapid Commun Mass Spectrom. 2010;24(5):549-53.

244. Collins J, Noble S, Chester J, Coles B, Byrne A. The assessment and impact of sarcopenia in lung cancer: a systematic literature review. BMJ Open. 2014;4(1):e003697.

245. Martin L, Birdsell L, Macdonald N, Reiman T, Clandinin MT, McCargar LJ, et al. Cancer Cachexia in the Age of Obesity: Skeletal Muscle Depletion Is a Powerful Prognostic Factor, Independent of Body Mass Index. J Clin Oncol. 2013.

246. Larsson I, Lindroos AK, Peltonen M, Sjöström L. Potassium per kilogram fat-free mass and total body potassium: predictions from sex, age, and anthropometry. Am J Physiol Endocrinol Metab. 2003;284(2):E416-23.

247. Hume R, Weyers E. Relationship between total body water and surface area in normal and obese subjects. J Clin Pathol. 1971;24(3):234-8.

248. Wang Z, Heo M, Lee RC, Kotler DP, Withers RT, Heymsfield SB. Muscularity in adult humans: proportion of adipose tissue-free body mass as skeletal muscle. Am J Hum Biol. 2001;13(5):612-9.

249. Wang Z, Zhu S, Wang J, Pierson RN, Heymsfield SB. Whole-body skeletal muscle mass: development and validation of total-body potassium prediction models. Am J Clin Nutr. 2003;77(1):76-82.

250. Lee RC, Wang Z, Heo M, Ross R, Janssen I, Heymsfield SB. Total-body skeletal muscle mass: development and cross-validation of anthropometric prediction models. Am J Clin Nutr. 2000;72(3):796-803.

251. Baumgartner RN, Waters DL, Gallagher D, Morley JE, Garry PJ. Predictors of skeletal muscle mass in elderly men and women. Mech Ageing Dev. 1999;107(2):123-36.

252. Newman AB, Kupelian V, Visser M, Simonsick E, Goodpaster B, Nevitt M, et al. Sarcopenia: alternative definitions and associations with lower extremity function. J Am Geriatr Soc. 2003;51(11):1602-9.

253. Faul F, Erdfelder E, Lang AG, Buchner A. G*Power 3: a flexible statistical power analysis program for the social, behavioral, and biomedical sciences. Behav Res Methods. 2007;39(2):175-91.

254. Szulc P, Beck TJ, Marchand F, Delmas PD. Low skeletal muscle mass is associated with poor structural parameters of bone and impaired balance in elderly men--the MINOS study. J Bone Miner Res. 2005;20(5):721-9.

255. Bunout D, de la Maza MP, Barrera G, Leiva L, Hirsch S. Association between sarcopenia and mortality in healthy older people. Australas J Ageing. 2011;30(2):89-92.

256. Lieffers JR, Bathe OF, Fassbender K, Winget M, Baracos VE. Sarcopenia is associated with postoperative infection and delayed recovery from colorectal cancer resection surgery. Br J Cancer. 2012;107(6):931-6.

257. Srikanthan P, Hevener AL, Karlamangla AS. Sarcopenia exacerbates obesity-associated insulin resistance and dysglycemia: findings from the National Health and Nutrition Examination Survey III. PLoS One. 2010;5(5):e10805.

258. Cruz-Jentoft AJ, Baeyens JP, Bauer JM, Boirie Y, Cederholm T, Landi F, et al. Sarcopenia: European consensus on definition and diagnosis: Report of the European Working Group on Sarcopenia in Older People. Age Ageing. 2010;39(4):412-23.

259. MacDonald AJ, Greig CA, Baracos V. The advantages and limitations of cross-sectional body composition analysis. Curr Opin Support Palliat Care. 2011;5(4):342-9.

260. Fearon KC. Cancer cachexia and fat-muscle physiology. N Engl J Med. 2011;365(6):565-7.

261. Skipworth RJ, Stewart GD, Dejong CH, Preston T, Fearon KC. Pathophysiology of cancer cachexia: much more than host-tumour interaction? Clin Nutr. 2007;26(6):667-76.

262. Russell ST, Tisdale MJ. Mechanism of attenuation of skeletal muscle atrophy by zinc-alpha2-glycoprotein. Endocrinology. 2010;151(10):4696-704.

263. Johnen H, Lin S, Kuffner T, Brown DA, Tsai VW, Bauskin AR, et al. Tumor-induced anorexia and weight loss are mediated by the TGF-beta superfamily cytokine MIC-1. Nat Med. 2007;13(11):1333-40.

264. Stephens NA, Skipworth RJ, Macdonald AJ, Greig CA, Ross JA, Fearon KC. Intramyocellular lipid droplets increase with progression of cachexia in cancer patients. J Cachexia Sarcopenia Muscle. 2011;2(2):111-7.

265. Beasley LE, Koster A, Newman AB, Javaid MK, Ferrucci L, Kritchevsky SB, et al. Inflammation and race and gender differences in computerized tomography-measured adipose depots. Obesity (Silver Spring). 2009;17(5):1062-9.

266. Ross R, Goodpaster B, Kelley D, Boada F. Magnetic resonance imaging in human body composition research. From quantitative to qualitative tissue measurement. Ann N Y Acad Sci. 2000;904:12-7.

267. Visser M, Goodpaster BH, Kritchevsky SB, Newman AB, Nevitt M, Rubin SM, et al. Muscle mass, muscle strength, and muscle fat infiltration as predictors of incident mobility limitations in well-functioning older persons. J Gerontol A Biol Sci Med Sci. 2005;60(3):324-33.

268. Delmonico MJ, Harris TB, Visser M, Park SW, Conroy MB, Velasquez-Mieyer P, et al. Longitudinal study of muscle strength, quality, and adipose tissue infiltration. Am J Clin Nutr. 2009;90(6):1579-85.

269. Delmonico MJ, Harris TB, Lee JS, Visser M, Nevitt M, Kritchevsky SB, et al. Alternative definitions of sarcopenia, lower extremity performance, and functional impairment with aging in older men and women. J Am Geriatr Soc. 2007;55(5):769-74.

270. Hicks GE, Simonsick EM, Harris TB, Newman AB, Weiner DK, Nevitt MA, et al. Trunk muscle composition as a predictor of reduced functional capacity in the health, aging and body composition study: the moderating role of back pain. J Gerontol A Biol Sci Med Sci. 2005;60(11):1420-4.

271. Kushnir MM, Mrozinski P, Rockwood AL, Crockett DK. A depletion strategy for improved detection of human proteins from urine. J Biomol Tech. 2009;20(2):101-8.

272. Caffrey RE. A review of experimental design best practices for proteomics based biomarker discovery: focus on SELDI-TOF. Methods Mol Biol. 2010;641:167-83.

273. Jr GW, Cazares LH, Leung SM, Nasim S, Adam BL, Yip TT, et al. Proteinchip(R) surface enhanced laser desorption/ionization (SELDI) mass spectrometry: a novel protein biochip technology for detection of prostate cancer biomarkers in complex protein mixtures. Prostate Cancer Prostatic Dis. 1999;2(5/6):264-76.

274. Husi H, Stephens N, Cronshaw A, MacDonald A, Gallagher I, Greig C, et al. Proteomic analysis of urinary upper gastrointestinal cancer markers. Proteomics Clin Appl. 2011;5(5-6):289-99.

275. Kelley DE, Slasky BS, Janosky J. Skeletal muscle density: effects of obesity and non-insulin-dependent diabetes mellitus. Am J Clin Nutr. 1991;54(3):509-15.

276. Goodpaster BH, Thaete FL, Kelley DE. Composition of skeletal muscle evaluated with computed tomography. Ann N Y Acad Sci. 2000;904:18-24.

277. Goodpaster BH, Carlson CL, Visser M, Kelley DE, Scherzinger A, Harris TB, et al. Attenuation of skeletal muscle and strength in the elderly: The Health ABC Study. J Appl Physiol. 2001;90(6):2157-65.

278. Hosokawa M, Kashiwaya K, Eguchi H, Ohigashi H, Ishikawa O, Furihata M, et al. Over-expression of cysteine proteinase inhibitor cystatin 6 promotes pancreatic cancer growth. Cancer Sci. 2008;99(8):1626-32.

279. Farges MC, Balcerzak D, Fisher BD, Attaix D, Béchet D, Ferrara M, et al. Increased muscle proteolysis after local trauma mainly reflects macrophage-associated lysosomal proteolysis. Am J Physiol Endocrinol Metab. 2002;282(2):E326-35.

280. Salminen A, Kihlström M. Lysosomal changes in mouse skeletal muscle during the repair of exercise injuries. Muscle Nerve. 1985;8(4):269-79.

281. Wen D, Corina K, Chow EP, Miller S, Janmey PA, Pepinsky RB. The plasma and cytoplasmic forms of human gelsolin differ in disulfide structure. Biochemistry. 1996;35(30):9700-9.

282. Rao J, Li N. Microfilament actin remodeling as a potential target for cancer drug development. Curr Cancer Drug Targets. 2004;4(4):345-54.

283. Huzé C, Bauché S, Richard P, Chevessier F, Goillot E, Gaudon K, et al. Identification of an agrin mutation that causes congenital myasthenia and affects synapse function. Am J Hum Genet. 2009;85(2):155-67.

284. Bentzinger CF, Barzaghi P, Lin S, Ruegg MA. Overexpression of mini-agrin in skeletal muscle increases muscle integrity and regenerative capacity in laminin-alpha2-deficient mice. FASEB J. 2005;19(8):934-42.

285. Hettwer S, Dahinden P, Kucsera S, Farina C, Ahmed S, Fariello R, et al. Elevated levels of a C-terminal agrin fragment identifies a new subset of sarcopenia patients. Exp Gerontol. 2013;48(1):69-75.

286. Brenner M, Johnson AB, Boespflug-Tanguy O, Rodriguez D, Goldman JE, Messing A. Mutations in GFAP, encoding glial fibrillary acidic protein, are associated with Alexander disease. Nat Genet. 2001;27(1):117-20.

287. Notturno F, Capasso M, DeLauretis A, Carpo M, Uncini A. Glial fibrillary acidic protein as a marker of axonal damage in chronic neuropathies. Muscle Nerve. 2009;40(1):50-4.

288. Watson CJ, Ledwidge MT, Phelan D, Collier P, Byrne JC, Dunn MJ, et al. Proteomic analysis of coronary sinus serum reveals leucine-rich α2-glycoprotein as a novel biomarker of ventricular dysfunction and heart failure. Circ Heart Fail. 2011;4(2):188-97.

289. Zong WX. Histone, H1.2: another housekeeping protein that kills. Cancer Biol Ther. 2004;3(1):42-3.

290. DeFreitas JM, Beck TW, Stock MS, Dillon MA, Sherk VD, Stout JR, et al. A comparison of techniques for estimating training-induced changes in muscle cross-sectional area. J Strength Cond Res. 2010;24(9):2383-9.

291. Fukunaga T, Miyatani M, Tachi M, Kouzaki M, Kawakami Y, Kanehisa H. Muscle volume is a major determinant of joint torque in humans. Acta Physiol Scand. 2001;172(4):249-55.

292. Maughan RJ, Watson JS, Weir J. Strength and cross-sectional area of human skeletal muscle. J Physiol. 1983;338:37-49.

293. Payette H, Hanusaik N, Boutier V, Morais JA, Gray-Donald K. Muscle strength and functional mobility in relation to lean body mass in free-living frail elderly women. Eur J Clin Nutr. 1998;52(1):45-53.

294. Hasselager R, Gögenur I. Core muscle size assessed by perioperative abdominal CT scan is related to mortality, postoperative complications, and hospitalization after major abdominal surgery: a systematic review. Langenbecks Arch Surg. 2014;399(3):287-95.

295. Martin L, Birdsell L, Macdonald N, Reiman T, Clandinin MT, McCargar LJ, et al. Cancer cachexia in the age of obesity: skeletal muscle depletion is a powerful prognostic factor, independent of body mass index. J Clin Oncol. 2013;31(12):1539-47.

296. Heymsfield SB, Adamek M, Gonzalez MC, Jia G, Thomas DM. Assessing skeletal muscle mass: historical overview and state of the art. J Cachexia Sarcopenia Muscle. 2014;5(1):9-18.

297. Stephens NA, Gray C, MacDonald AJ, Tan BH, Gallagher IJ, Skipworth RJ, et al. Sexual dimorphism modulates the impact of cancer cachexia on lower limb muscle mass and function. Clin Nutr. 2012;31(4):499-505.

298. Lord SR, Murray SM, Chapman K, Munro B, Tiedemann A. Sit-to-stand performance depends on sensation, speed, balance, and psychological status in addition to strength in older people. J Gerontol A Biol Sci Med Sci. 2002;57(8):M539-43.

299. Schlicht J, Camaione DN, Owen SV. Effect of intense strength training on standing balance, walking speed, and sit-to-stand performance in older adults. J Gerontol A Biol Sci Med Sci. 2001;56(5):M281-6.

300. Anker SD, Swan JW, Volterrani M, Chua TP, Clark AL, Poole-Wilson PA, et al. The influence of muscle mass, strength, fatigability and blood flow on exercise capacity in cachectic and non-cachectic patients with chronic heart failure. Eur Heart J. 1997;18(2):259-69.

301. Millington PJ, Myklebust BM, Shambes GM. Biomechanical analysis of the sit-to-stand motion in elderly persons. Arch Phys Med Rehabil. 1992;73(7):609-17.

302. Karatas M, Cetin N, Bayramoglu M, Dilek A. Trunk muscle strength in relation to balance and functional disability in unihemispheric stroke patients. Am J Phys Med Rehabil. 2004;83(2):81-7.

303. Helbostad JL, Sturnieks DL, Menant J, Delbaere K, Lord SR, Pijnappels M. Consequences of lower extremity and trunk muscle fatigue on balance and functional tasks in older people: a systematic literature review. BMC Geriatr. 2010;10:56.

304. Suri P, Kiely DK, Leveille SG, Frontera WR, Bean JF. Trunk muscle attributes are associated with balance and mobility in older adults: a pilot study. PM R. 2009;1(10):916-24.

305. Berman RS, Harrison LE, Pearlstone DB, Burt M, Brennan MF. Growth hormone, alone and in combination with insulin, increases whole body and skeletal muscle protein kinetics in cancer patients after surgery. Ann Surg. 1999;229(1):1-10.

306. Yamada M, Maruta K, Shiojiri Y, Takeuchi S, Matsuo Y, Takaba T. Atrophy of the abdominal wall muscles after extraperitoneal approach to the aorta. J Vasc Surg. 2003;38(2):346-53.

307. Yu W, Seo BY, Chung HY. Postoperative body-weight loss and survival after curative resection for gastric cancer. Br J Surg. 2002;89(4):467-70.

308. Basse L, Raskov HH, Hjort Jakobsen D, Sonne E, Billesbølle P, Hendel HW, et al. Accelerated postoperative recovery programme after colonic resection improves physical performance, pulmonary function and body composition. Br J Surg. 2002;89(4):446-53.

309. Morlion BJ, Stehle P, Wachtler P, Siedhoff HP, Köller M, König W, et al. Total parenteral nutrition with glutamine dipeptide after major abdominal surgery: a randomized, double-blind, controlled study. Ann Surg. 1998;227(2):302-8.

310. Yuill KA, Richardson RA, Davidson HI, Garden OJ, Parks RW. The administration of an oral carbohydrate-containing fluid prior to major elective upper-gastrointestinal surgery preserves skeletal muscle mass postoperatively--a randomised clinical trial. Clin Nutr. 2005;24(1):32-7.

311. Reardon K, Galea M, Dennett X, Choong P, Byrne E. Quadriceps muscle wasting persists 5 months after total hip arthroplasty for osteoarthritis of the hip: a pilot study. Intern Med J. 2001;31(1):7-14.

312. Fouladiun M, Körner U, Bosaeus I, Daneryd P, Hyltander A, Lundholm KG. Body composition and time course changes in regional distribution of fat and lean tissue in unselected cancer patients on palliative care--correlations with food intake, metabolism, exercise capacity, and hormones. Cancer. 2005;103(10):2189-98.

313. Bachmann J, Heiligensetzer M, Krakowski-Roosen H, Büchler MW, Friess H, Martignoni ME. Cachexia worsens prognosis in patients with resectable pancreatic cancer. J Gastrointest Surg. 2008;12(7):1193-201.

314. Pescatello LS, Kelsey BK, Price TB, Seip RL, Angelopoulos TJ, Clarkson PM, et al. The muscle strength and size response to upper arm, unilateral resistance training among adults who are overweight and obese. J Strength Cond Res. 2007;21(2):307-13.

315. Prado CM, Bekaii-Saab T, Doyle LA, Shrestha S, Ghosh S, Baracos VE, et al. Skeletal muscle anabolism is a side effect of therapy with the MEK inhibitor: selumetinib in patients with cholangiocarcinoma. Br J Cancer. 2012;106(10):1583-6.

316. Murphy RA, Wilke MS, Perrine M, Pawlowicz M, Mourtzakis M, Lieffers JR, et al. Loss of adipose tissue and plasma phospholipids: relationship to survival in advanced cancer patients. Clin Nutr. 2010;29(4):482-7.

317. Lieffers JR, Mourtzakis M, Hall KD, McCargar LJ, Prado CM, Baracos VE. A viscerally driven cachexia syndrome in patients with advanced colorectal cancer: contributions of organ and tumor mass to whole-body energy demands. Am J Clin Nutr. 2009;89(4):1173-9.

318. Ferriolli E, Skipworth RJ, Hendry P, Scott A, Stensteth J, Dahele M, et al. Physical activity monitoring: a responsive and meaningful patient-centered outcome for surgery, chemotherapy, or radiotherapy? J Pain Symptom Manage. 2012;43(6):1025-35.

319. Attaix D, Baracos VE, Pichard C. Muscle wasting: a crosstalk between protein synthesis and breakdown signalling. Curr Opin Clin Nutr Metab Care. 2012;15(3):209-10.

320. Abstracts of the 6th cachexia conference, milan, Italy, december 8-10, 2011. J Cachexia Sarcopenia Muscle. 2011;2(4):209-61.

321. Han HQ, Mitch WE. Targeting the myostatin signaling pathway to treat muscle wasting diseases. Curr Opin Support Palliat Care. 2011;5(4):334-41.

322. Gardner JL, Turner SM, Bautista A, Lindwall G, Awada M, Hellerstein MK. Measurement of liver collagen synthesis by heavy water labeling: effects of profibrotic toxicants and antifibrotic interventions. Am J Physiol Gastrointest Liver Physiol. 2007;292(6):G1695-705.

323. Previs SF, Mahsut A, Kulick A, Dunn K, Andrews-Kelly G, Johnson C, et al. Quantifying cholesterol synthesis in vivo using (2)H(2)O: enabling back-to-back studies in the same subject. J Lipid Res. 2011;52(7):1420-8.

324. Previs SF, Fatica R, Chandramouli V, Alexander JC, Brunengraber H, Landau BR. Quantifying rates of protein synthesis in humans by use of 2H2O: application to patients with end-stage renal disease. Am J Physiol Endocrinol Metab. 2004;286(4):E665-72.

325. Balagopal P, Nair KS, Stirewalt WS. Isolation of myosin heavy chain from small skeletal muscle samples by preparative continuous elution gel electrophoresis: application to measurement of synthesis rate in human and animal tissue. Anal Biochem. 1994;221(1):72-7.

326. Hasten DL, Morris GS, Ramanadham S, Yarasheski KE. Isolation of human skeletal muscle myosin heavy chain and actin for measurement of fractional synthesis rates. Am J Physiol. 1998;275(6 Pt 1):E1092-9.

327. Preston T, Slater C. Mass spectrometric analysis of stable-isotope-labelled amino acid tracers. Proc Nutr Soc. 1994;53(2):363-72.

328. Berthold HK, Hachey DL, Reeds PJ, Thomas OP, Hoeksema S, Klein PD. Uniformly 13C-labeled algal protein used to determine amino acid essentiality in vivo. Proc Natl Acad Sci U S A. 1991;88(18):8091-5.

329. Jim S, Jones V, Ambrose SH, Evershed RP. Quantifying dietary macronutrient sources of carbon for bone collagen biosynthesis using natural abundance stable carbon isotope analysis. Br J Nutr. 2006;95(6):1055-62.

330. Rachdaoui N, Austin L, Kramer E, Previs MJ, Anderson VE, Kasumov T, et al. Measuring proteome dynamics in vivo: as easy as adding water? Mol Cell Proteomics. 2009;8(12):2653-63.

331. Dodson S, Baracos VE, Jatoi A, Evans WJ, Cella D, Dalton JT, et al. Muscle wasting in cancer cachexia: clinical implications, diagnosis, and emerging treatment strategies. Annu Rev Med. 2011;62:265-79.

332. Padrão AI, Oliveira P, Vitorino R, Colaço B, Pires MJ, Márquez M, et al. Bladder cancer-induced skeletal muscle wasting: disclosing the role of mitochondria plasticity. Int J Biochem Cell Biol. 2013.

333. Williams JP, Phillips BE, Smith K, Atherton PJ, Rankin D, Selby AL, et al. Effect of tumor burden and subsequent surgical resection on skeletal muscle mass and protein turnover in colorectal cancer patients. Am J Clin Nutr. 2012;96(5):1064-70.

334. Johns N, Stephens NA, Preston T. Muscle protein kinetics in cancer cachexia. Curr Opin Support Palliat Care. 2012;6(4):417-23.

335. Fearon KC, Hansell DT, Preston T, Plumb JA, Davies J, Shapiro D, et al. Influence of whole body protein turnover rate on resting energy expenditure in patients with cancer. Cancer Res. 1988;48(9):2590-5.

336. Glass RE, Fern EB, Garlick PJ. Whole-body protein turnover before and after resection of colorectal tumours. Clin Sci (Lond). 1983;64(1):101-8.

337. van Marken Lichtenbelt WD, Westerterp KR, Wouters L. Deuterium dilution as a method for determining total body water: effect of test protocol and sampling time. Br J Nutr. 1994;72(4):491-7.

338. SCHLOERB PR, FRIIS-HANSEN BJ, EDELMAN IS, SOLOMON AK, MOORE FD. The measurement of total body water in the human subject by deuterium oxide dilution; with a consideration of the dynamics of deuterium distribution. J Clin Invest. 1950;29(10):1296-310.

339. Pace N, Rathbun EN. Studies on body composition III. The body water and chemically combined nitrogen content in relation to fat content. Journal of Biological Chemistry. 1945;158(3):685-91.

340. Smith GI, Villareal DT, Mittendorfer B. Measurement of human mixed muscle protein fractional synthesis rate depends on the choice of amino acid tracer. Am J Physiol Endocrinol Metab. 2007;293(3):E666-71.

341. Mittendorfer B, Andersen JL, Plomgaard P, Saltin B, Babraj JA, Smith K, et al. Protein synthesis rates in human muscles: neither anatomical location nor fibre-type composition are major determinants. J Physiol. 2005;563(Pt 1):203-11.

342. Schoeller DA, van Santen E. Measurement of energy expenditure in humans by doubly labeled water method. J Appl Physiol. 1982;53(4):955-9.

343. Sandri M. Protein breakdown in muscle wasting: Role of autophagy-lysosome and ubiquitin-proteasome. Int J Biochem Cell Biol. 2013.

344. Argadine HM, Hellyer NJ, Mantilla CB, Zhan WZ, Sieck GC. The effect of denervation on protein synthesis and degradation in adult rat diaphragm muscle. J Appl Physiol. 2009;107(2):438-44.

345. Goldspink DF. The effects of denervation on protein turnover of rat skeletal muscle. Biochem J. 1976;156(1):71-80.

346. Buse MG, McMaster J, Buse J. The effect of denervation and insulin on protein synthesis in the isolated rat diaphragm. Metabolism. 1965;14(11):1220-32.

347. Turner LV, Garlick PJ. The effect of unilateral phrenicectomy on the rate of protein synthesis in rat diaphragm in vivo. Biochim Biophys Acta. 1974;349(1):109-13.

348. Quy PN, Kuma A, Pierre P, Mizushima N. Proteasome-dependent activation of mammalian target of rapamycin complex 1 (mTORC1) is essential for autophagy suppression and muscle remodeling following denervation. J Biol Chem. 2013;288(19):13639.

349. Chapter 2 gross and elemental content of reference man. Annals of the ICRP/ICRP Publication. 1975;23(0):273-334.

350. Proctor DN, Balagopal P, Nair KS. Age-related sarcopenia in humans is associated with reduced synthetic rates of specific muscle proteins. J Nutr. 1998;128(2 Suppl):351S-5S.

351. Balagopal P, Rooyackers OE, Adey DB, Ades PA, Nair KS. Effects of aging on in vivo synthesis of skeletal muscle myosin heavy-chain and sarcoplasmic protein in humans. Am J Physiol. 1997;273(4 Pt 1):E790-800.

Appendices

Appendix 1 – Health questionnaire

Studies of Human Performance: Health Questionnaire

Name:

Address:

Date of Birth:

Telephone no.:

If the answer is YES to any of the following questions, please give some details including dates where possible.

Have you any history of heart trouble?

(such as heart attack, angina, valve disease, palpitations, pains in chest, dizzy spells)

Have you any history of problems with blood vessels?

(such as thrombosis, embolus, claudication, aneurysm, dizzy spells, stroke, blood clots)

_

Have you any history of chest problems?

(bronchitis, asthma or wheezy chest)

Have you ever smoked?

(if YES please state whether you are a current or ex-smoker and how much)

Do you suffer from diabetes?

(if YES please state if insulin dependent)

Have you any history of major illness now or in the last 20 years?

(such as rheumatoid arthritis, blood disorders, cancer)

Have you any history of emotional or psychiatric problems?

Do you suffer from osteoarthritis?

(if YES please state joints affected and indicate mild, moderate or severe and any medication regularly taken)

Have you broken or fractured any bones? If so, when?

Do you have any problems with your bones?

(osteoporosis, loss of height)

Have you any history of back problems? If so, when did they start and do they still affect you in any way?

Have you had any surgery on your joints? If so, when?

Do you suffer from high blood pressure?

Have you had any acute illness in the last six months?

(such as influenza, recurrent sore-throat, bronchitis)

Please state any medication, prescribed or over the counter, regularly taken for any condition

Name of medication How often medication is taken

Have you been in hospital in the last 5 years? If so, why and for how long?

Do you have any physical disabilities?

(such as visual or hearing problems)

Is there any other illness or condition that affects your general health or interferes with your mobility?

Approximately how tall are you?

Approximately how much do you weigh?

Your Doctor's Name:

Your Doctor's Address:

Thank you for completing this questionnaire